

**Design, synthesis and pharmacological evaluation
of non-peptidergic ligands for the human
CXCR3 receptor**

Stefania Storelli

The research described in this thesis was performed at the Leiden/Amsterdam Center for Drug Research, Division of Medicinal Chemistry, Department of Pharmacology, Vrije Universiteit Amsterdam, De Boelelaan 1083, 1081 HV Amsterdam, The Netherlands

This research was financially supported by the **Nederlandse Organisatie voor Wetenschappelijk Onderzoek (NWO)**

© All rights reserved. No part of this thesis may be reproduced, in any form or by any means, without the prior written permission from the author.

VRIJE UNIVERSITEIT

**Design, synthesis and pharmacological evaluation of
non-peptidergic ligands for the human CXCR3 receptor**

ACADEMISCH PROEFSCHRIFT

ter verkrijging van de graad Doctor aan
de Vrije Universiteit Amsterdam,
op gezag van de rector magnificus
prof.dr. L.M. Bouter,
in het openbaar te verdedigen
ten overstaan van de promotiecommissie
van de faculteit der Exacte Wetenschappen
op dinsdag 2 november 2010 om 13.45 uur
in het auditorium van de universiteit,
De Boelelaan 1105

door

Stefania Storelli

geboren te San Severo, Italië

promotoren: prof.dr. R. Leurs
prof.dr. H.Timmerman
copromotoren: dr. I.J.P. de Esch
dr. M. Wijtmans

*For knowledge comes slowly, and when it comes, it is often at
great personal expense.*
(The New York Trilogy, Paul Auster)

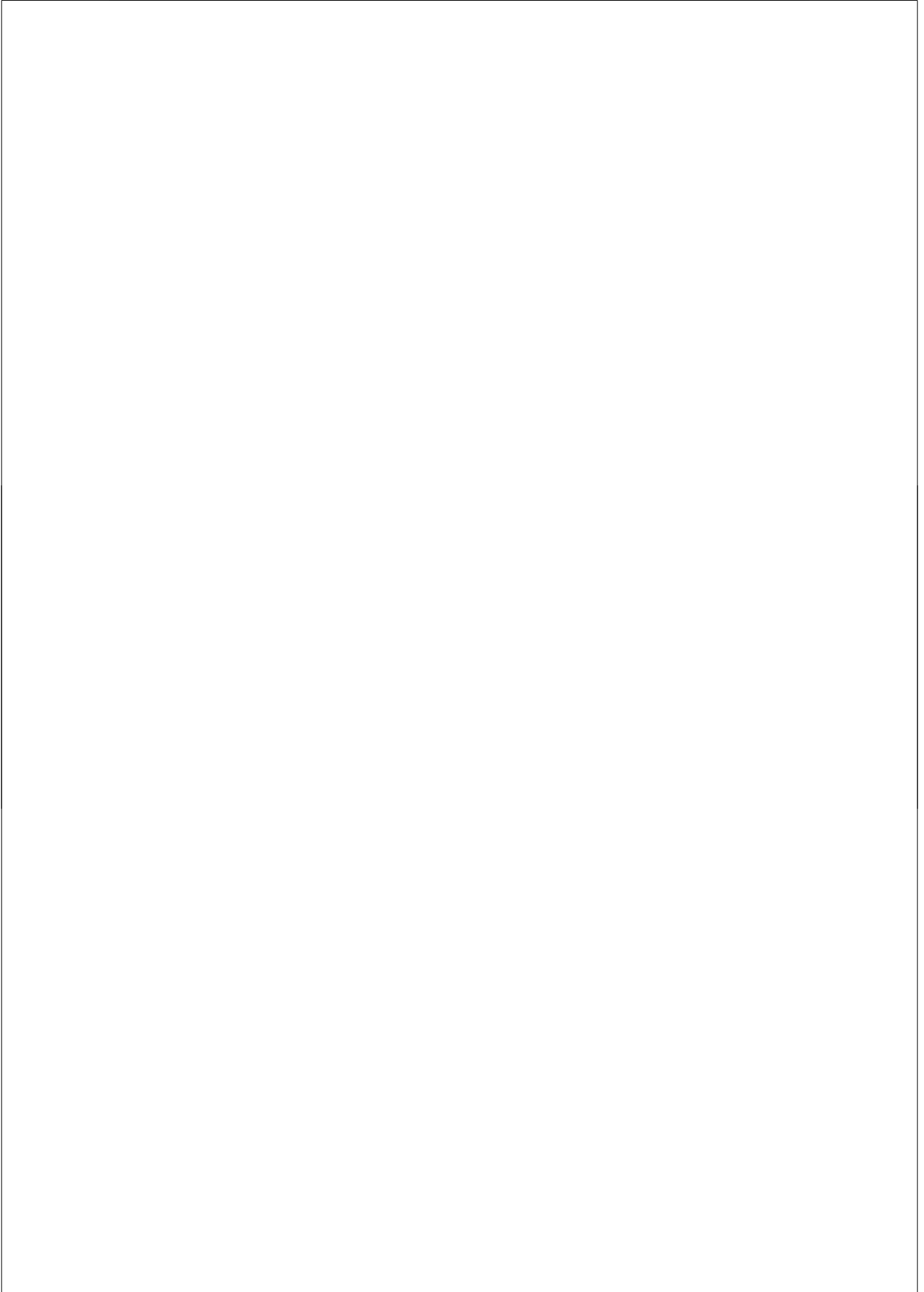
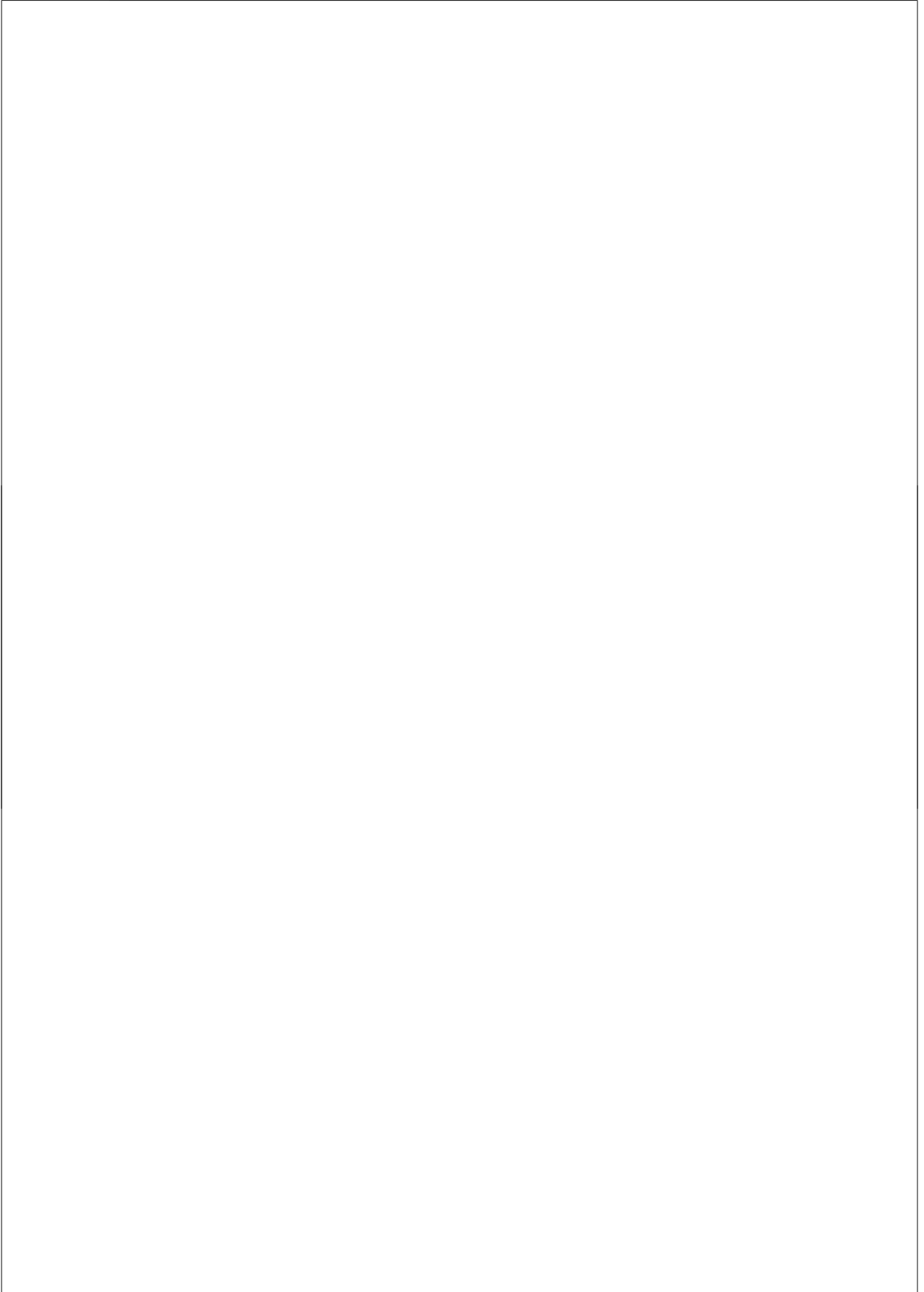


Table of contents

Chapter 1	Introduction: a review on CXCR3, small CXCR3 ligands and their clinical potential	1
Chapter 2	Scope of this thesis	31
Chapter 3	Synthesis and structure-activity relationship of 3-phenyl-3 <i>H</i> -quinazolin-4-one derivatives as CXCR3 chemokine receptor antagonists	33
Chapter 4	Synthesis and structure-activity relationships of 3 <i>H</i> -quinazolin-4-ones and 3 <i>H</i> -pyrido[2,3- <i>d</i>]pyrimidin-4-ones as CXCR3 receptor antagonists	57
Chapter 5	Imidazolium compounds as CXCR3 ligands	81
Chapter 6	Non-competitive antagonism and inverse agonism as mechanism of action of non-peptidergic antagonists at primate and rodent CXCR3 chemokine receptors	101
Chapter 6	Preliminary investigations into bivalent ligands for CXCR3	127
Summary		141
Samenvatting		145
Acknowledgments		151



Chapter 1

Introduction: a review on CXCR3, small CXCR3 ligands and their clinical potential

Abstract

The CXCR3 chemokine receptor was discovered in 1996 and has been shown to play an important role in several diseases, most of which are related to inflammation. This chapter describes in detail the development of small CXCR3 ligands and their therapeutic potential. Classes of CXCR3 antagonists with strikingly variable core structures have emerged. Some of these compounds have confirmed the beneficial role of CXCR3 antagonism in animal models of disease. One of the compounds, AMG 487, progressed to Phase II clinical trials but has been withdrawn due to lack of efficacy. New antagonist classes are being developed in order to reveal the full therapeutic potential of CXCR3.

Introduction

Chemokines are peptides of 70 to 90 amino acids in length which exert important signaling functions in the body. Chemokines are classified into two main subfamilies based on whether the first two of four conserved cysteines are adjacent (CC) or separated by one amino acid (CXC).¹ The chemokine peptides signal via membrane-bound chemokine receptors, whose nomenclature is based on the class of chemokines they bind, i.e. CC or CXC chemokine receptors (CCR and CXCR, respectively). The first chemokine receptor was reported in 1991 after the discovery that the chemokine interleukin-8 (now named CXCL8) binds to a class A G protein-coupled receptor (GPCR).^{2,3} Chemokine receptors show less than 30% homology with all other known GPCRs and are major modulators in the immune system where they affect e.g. migration of leukocytes. Besides their role in inflammatory processes, the role of chemokine receptors in organogenesis, angiogenesis and the central nervous system, but also in metastasis and growth of tumor cells has become apparent.^{4,5} Therapeutic interest in chemokine receptors boosted in 1996 with the finding that chemokine receptors CXCR4 and CCR5 are coreceptors for human immunodeficiency virus (HIV).⁶⁻⁹ Several chemokine receptors have since attracted interest from the drug discovery community.¹⁰⁻¹² This review will describe one of the promising emerging drug targets of this class, namely the CXCR3 receptor, and will outline all CXCR3-associated medicinal chemistry disclosed to date in scientific and patent literature.

CXCR3 and peptidergic ligands

The CXCR3 chemokine receptor was discovered in 1996 during a search for T lymphocyte-specific chemokine receptors. A novel cDNA was isolated from a human CD4+ T cell library and the encoded GPCR proved to have affinity for chemokines.¹³ A truncated version of this clone, with an incomplete coding sequence, was already isolated in 1995.¹⁴ CXCR3 consists of 368 amino acids which, as with all GPCRs, are oriented in a typical seven-transmembrane α -helical topology. This is illustrated in detail by the 2D snakeplot in Figure 1. Typical structural motifs for GPCRs such as the conserved DRY motif and the NPxxYX_{5,6}F motif at the cytoplasmic ends of transmembrane domains 3 and 7 respectively are present, as well as cysteine residues in the first and second extracellular loops.¹⁵ Similar to most receptors of the chemokine subfamily of GPCRs,¹⁶ CXCR3 has additional cysteine residues in the aminoterminal and third extracellular loop. The threonine and serine residues in the intracellular carboxyl-tail are potential sites for phosphorylation by receptor kinases.^{13,17}

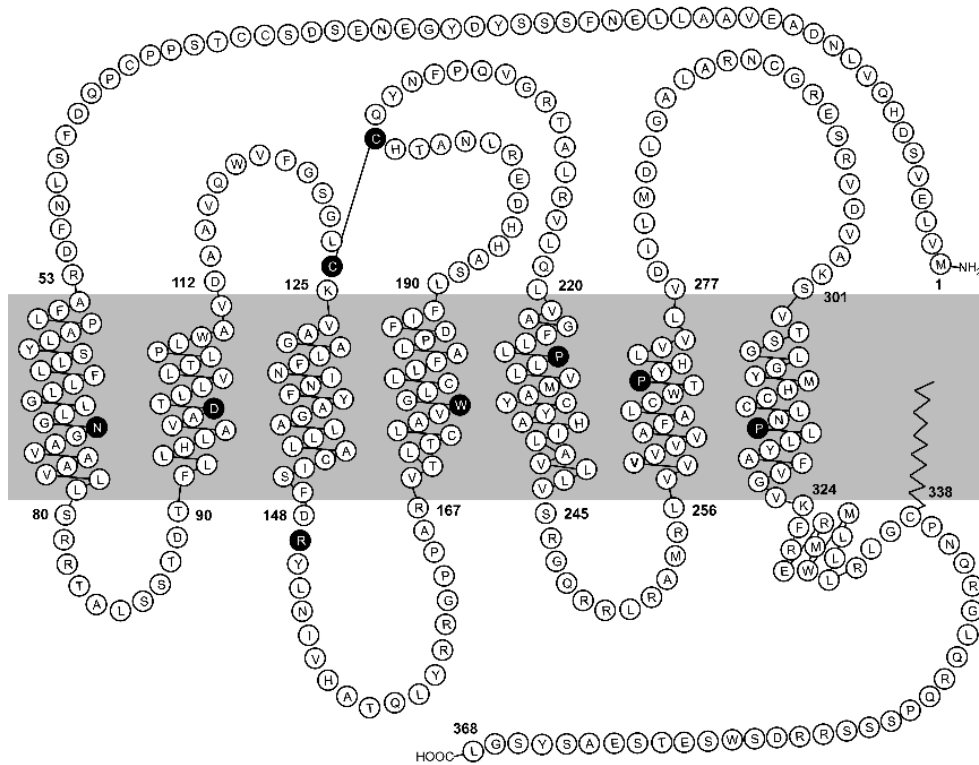


Figure 1. Snakeplot of CXCR3. The typical seven-transmembrane α -helical topology of GPCRs is shown, with an additional proposed helix (helix 8) in the membrane proximal part of the intracellular carboxyl-terminus, based on the structure of rhodopsin. Residues that are highly conserved between GPCRs of class A are shown as black residues.¹⁵ These residues are N1.50, D2.50, R3.50 in the DRY motif, W4.50, P5.50, P6.50 in the WxP motif and P7.50 in the NPxxYx5,6F motif. In this GPCR numbering according to Ballesteros and Weinstein, the first number refers to the transmembrane helix and the second number indicates the position of the most conserved residue, which is assigned position 50 in that helix. Residues N-terminal from the most conserved residue at position 50 are designated with lower numbers, e.g. Asp¹⁴⁸ is assigned D3.49 etc. The use of this Ballesteros-Weinstein numbering simplifies the identification of residues at similar positions between different GPCRs. The presumed disulfide bond between cysteines in the first and second extracellular loops is shown, as well as potential palmitoylation of the cysteine in the carboxy-terminus that anchors helix 8 to the membrane.

Activated Th1 lymphocytes express high levels of CXCR3, but the receptor is also found on blood T cells and on a small proportion of B cells and natural killer cells.^{13,18,19} CXCR3 binds the endogenous CXC chemokines CXCL9, CXCL10 and CXCL11, which before the introduction of the systematic nomenclature¹ were called monokine induced by interferon-gamma (Mig), interferon-gamma inducible 10-kD protein (IP-10) and

interferon-inducible T cell alpha chemoattractant/interferon-gamma-inducible protein 9 (I-TAC/IP-9), respectively.^{13,20-23} Additionally, CXCL13 has been reported to bind and, at high concentrations, activate CXCR3.²⁴ Chemokine CXCL4 was shown to bind a splice variant of CXCR3 with an extended amino-terminus called CXCR3-B²⁵, and recently also the original CXCR3 (CXCR3-A) has been reported to mediate CXCL4-induced responses at high concentrations.²⁶ CXCR3 activates pertussis toxin-sensitive G proteins of the G α_i class upon activation by chemokines, and mediates chemotaxis, calcium flux and activation of kinases such as p44/p42 MAPK and Akt.^{13,17,27}

While it is common for chemokines to bind several chemokine receptors, this promiscuity is usually restricted to receptors of the same class, i.e. CXC chemokines generally bind only to CXC receptors. An intriguing exception may be found for CXCR3: agonists of CCR3, e.g. CCL13 and CCL11, bind with high affinity to CXCR3.^{21,28} In one study CCL11 blocked CXCR3 activation,²¹ although two other studies did not confirm this finding.^{28,29} This leaves the question open if CCR3 ligands are true endogenous antagonists of CXCR3 in vivo, or that they may interfere with CXCR3 signalling through other means.

CXCL9, CXCL10 and CXCL11 are all CXCR3 agonists with CXCL11 having the highest potency and efficacy.^{13,20-23,30} Typically, the NH₂-terminus of chemokines is important for receptor activation. After binding of a chemokine to the NH₂-terminus and extracellular loops of a chemokine receptor, the NH₂-terminus of the chemokine is believed to interact with yet to be identified domains of the receptor, resulting in activation.^{31,32} Consequently, deletion or addition of only a few NH₂-terminal amino acids of the chemokine often changes it from an agonist into an antagonist.³²⁻³⁴ Indeed, NH₂-terminal truncation of CXCL11 (CXCL11 4-73) barely affects CXCR3 binding affinity, but results in complete loss of agonist activity.³⁵ Similarly, when the first five amino acids of CXCL10 are deleted and a methionine is added, a potent CXCR3 antagonist is obtained.³⁶ Interestingly, the endogenous CXCR3 ligands can be processed in vivo by cellular proteases to give chemokines with modified activity. After NH₂-terminal proteolytic processing of CXCL10 and CXCL11 by CD26 (dipeptidyl peptidase IV), the chemokine metabolites lose their CXCR3-mediated chemotactic activity and calcium signalling, while retaining their ability to bind to CXCR3 albeit with reduced affinity.^{37,38} CD26-processed CXCL10 inhibits chemotactic responses of CXCR3-expressing cells towards intact CXCL10, illustrating that NH₂-terminal processing of CXCL10 produces a natural CXCR3 antagonist.³⁸

CXCR3 as a potential drug target

The general "druggability" of chemokine receptors remains a subject of discussion. Despite the reputation of GPCRs as popular drug targets³⁹ no antagonists targeting any chemokine receptors have reached the market yet except for HIV entry inhibitors.¹¹ On one hand, this may be due to the relatively recent discovery of chemokine receptors. On the other hand, there has been ongoing discussion about the applicability of such antagonists considering the redundancy of the chemokine system. The notion that most chemokine receptors bind more than one chemokine and most chemokines bind to several chemokine receptors clearly complicates the prediction of the therapeutic effects of chemokine receptor antagonists. It is therefore encouraging that specific roles for various chemokine receptors in disease models are emerging.⁴⁰ Indeed, based on the upregulated expression of CXCR3 and its ligands, CXCR3 has been implicated in a variety of inflammatory diseases. These include multiple sclerosis,⁴¹ rheumatoid arthritis,¹⁸ atherosclerosis,⁴² chronic obstructive pulmonary disease,⁴³ inflammatory bowel disease,⁴⁴ inflammatory skin diseases^{22,45} such as psoriasis,⁴⁶ hepatitis C infected liver,⁴⁷ sarcoidosis,⁴⁸ and SARS.^{49,50} CXCR3 also appears to be a key factor in the rejection of donor organs after transplantation.^{51,52} Moreover, CXCR3 appears to play an important role in metastasis of melanoma and colon cancer cells to the lymph nodes and in metastasis of breast cancer cells to the lung.⁵³⁻⁵⁵ Last, for certain HIV virus strains and isolates, CXCR3 may act as a coreceptor.⁵⁶

Various preclinical approaches have been used to confirm the therapeutic potential of the CXCR3 receptor system: (1) the generation of CXCR3 knockout (KO) mice, (2) targeting CXCR3 or its endogenous ligands by antibodies, (3) inhibiting CXCR3 by means of protein-based antagonists, and (4) targeting CXCR3 by small molecules. The first three approaches will be briefly highlighted below, while approach (4) is the topic of the next section.

Use of CXCR3-KO mice

CXCR3-KO (CXCR3^{-/-}) mice appear phenotypically normal in the unchallenged host,^{51,57,58} although a deficiency in NK cells in the lung and peripheral blood has been reported. Moreover, a reduction of natural killer (NK) and NK T cells in the liver is observed, indicating that CXCR3 is required for NK and NK T cell homeostasis.⁵⁹ In murine models of transplant rejection, CXCR3^{-/-} mice showed delayed acute or chronic rejection of cardiac allografts⁵¹ or pancreatic island allografts.⁶⁰ In some cases, allografts were even maintained chronically in CXCR3^{-/-} mice, especially in combination with the

immunosuppressive drug cyclosporine A.⁵¹ Using CXCR3^{-/-} mice, it was shown that CXCR3 is involved in skin wound healing, although CXCR3 is not a critical factor.⁵⁷ Antagonism of CXCR3 signalling is suggested to leave less scarring of the skin, whereas agonism of CXCR3 may result in more rapid maturation of the skin compartments.⁵⁷ Studies on CXCR3^{-/-} mice also revealed that CXCR3 plays a critical role in the positioning of effector T cells at sites of viral inflammation in the brain⁵⁸ and in limiting lung fibrosis following lung injury.⁵⁹

Targeting of CXCR3 or its endogenous ligands by antibodies

CXCL10-antibodies attenuate chronic experimental colitis by blocking cellular trafficking and protecting intestinal epithelial cells, a finding relevant in diseases like ulcerative colitis.⁶¹ Notably, a Phase II clinical trial has been launched to investigate a CXCL10 antibody (MDX1100) in treating ulcerative colitis.⁶² In addition, similar to the CXCR3^{-/-} models mentioned above, the use of an antibody directed against either CXCR3 or CXCL10 significantly prolongs allograft survival, sometimes even with administration taking place several days after the transplantation.^{51,60,63-65} Moreover, an antibody directed against CXCR3 not only reduced T cell recruitment to inflamed arthritic joints in a rat model of arthritis, but also prevented weight loss by the animals and decreased the severity of arthritis in general.⁶⁶ The CXCL10 antibody MDX1100 (vide supra) will also be investigated in a Phase II trial for rheumatoid arthritis.⁶² Last, a CXCL10-antibody suppressed metastasis of melanoma cells to the lymph nodes in mice.⁵³

Although targeting of one or more of the CXCR3 ligands with antibodies appeared beneficial in certain models,⁶⁷ targeting CXCR3 appears a more straightforward way to treat the condition since this abrogates the effects of all three chemokines at the same time. Indeed, deletion of either CXCL9 or CXCL10 alone in a mouse model of obliterative bronchiolitis did not affect T-cell recruitment into the allograft, whereas deletion of CXCR3 did.⁶⁸

Targeting of CXCR3 by protein antagonists

The strategic use of protein-based antagonists (e.g. chemokine analogs) has confirmed some of the key roles presented so far. In a mouse model for skin inflammation, CXCL11-based antagonists reduced swelling of the skin in response to a sensitizer.⁶⁹ Such antagonists also inhibited neuroinflammation in mice implanted with the neurotoxic CXCR3-binder SDF(5-67).⁷⁰ Administration of CXCL10-based protein antagonists to mice

reduced the progression of autoimmune sialadenitis, which relates to the inflammation of the salivary glands as observed in Sjögren's syndrome.³⁶

Targeting of CXCR3 by non-peptidergic CXCR3-antagonists

Figure 2 shows that publications on small CXCR3 ligands first emerged around 2002 with increases occurring over subsequent years. As there is only a handful of speculative therapeutic indications for CXCR3 agonists (*vide supra*), virtually all the reports deal with antagonists. The CXCR3 antagonist area has been reviewed before.^{71, 72} The current review provides the developments in this area up to early 2008. Below, all known classes of CXCR3-antagonists will be discussed with accompanying medicinal chemistry and available (pre)clinical data. In all cases, affinity or activity numbers are accompanied by the reference chemokine and/or the type of assay used (if reported) and, unless specified, human CXCR3 was used in these assays.

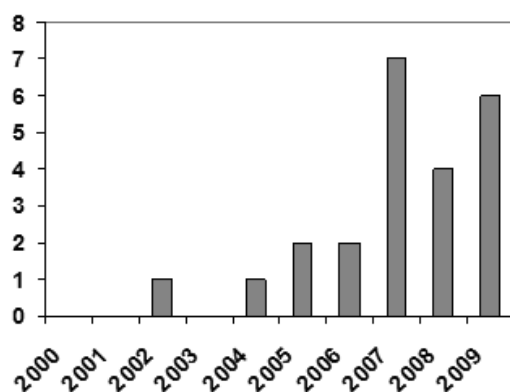


Figure 2: The number of publications that has appeared on structure-activity studies of small CXCR3 ligands per year. Numbers were obtained by detailed searches with SciFinder Scholar and PubMed and do not include conference reports. Date of acceptance was used.

TAK-779 and naturally occurring non-peptidergic antagonists

Besides the frequently used method of screening corporate collections, two other venues have afforded CXCR3 hits. First, the known CCR5-ligand TAK-779 (**1**)¹⁰ attracted some interest from the CXCR3 community as it proved to bind mouse CXCR3 as well ($IC_{50}=369$ nM, ^{125}I -CXCL10).⁷³ However, despite showing efficacy in rodent models involving CXCR3, CCR5 and CCR2,⁷⁴⁻⁷⁷ the moderate affinity of TAK-779 for CXCR3 and its poor selectivity profile have rendered it only of limited value to CXCR3 research as a whole. Secondly, various natural products were found to bind CXCR3. Merck performed a screen (^{125}I -

CXCL10) on a library consisting of extracts from microbial, plant and marine sources.⁷⁸ A highly diverse set of hits was picked up, including sugar-derivatised steroid **2** (IC_{50} =470 nM) and dipyridinium salt **3** (IC_{50} =690 nM).

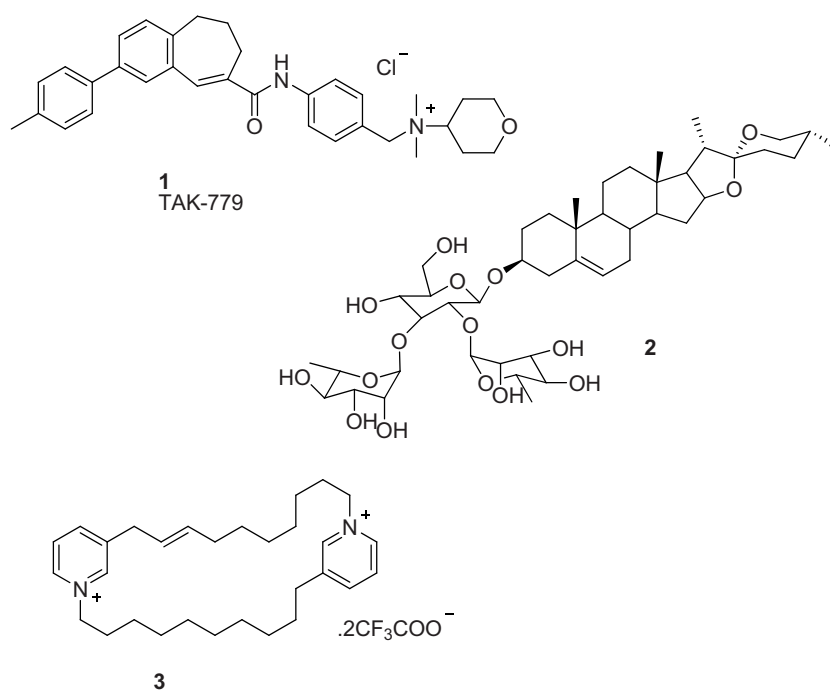


Figure 3. Structures of TAK-779 and some naturally occurring binders.

(Aza)quinazolinones – from bench to clinical trials

The companies Chemocentryx and Tularik, later acquired by Amgen, teamed up to develop small (aza)quinazolinone-based CXCR3 antagonists leading to an array of patents with the first one appearing in 2001.^{79,80} Compound **4** was retrieved as a moderate hit (IC_{50} =250 nM, ¹²⁵I-CXCL10) from a High Throughput Screening (HTS) campaign, but it displayed unacceptable pharmacokinetic properties.⁸¹ Studies on **4** identified the decanoyl and dimethylamino group as major metabolic culprits.⁸¹ However, replacement of the decanoyl chain in **4** by other hydrophobic groups initially led to compromised affinity.^{81,82} Later, it was discovered that a biphenylmethylene group (**6**) or an isostere with a *p*-CF₃ (**7**) or *p*-OCF₃ group (**8**) could be successfully introduced.⁸¹ With improved hit **7** in hand, the dimethylamino-group was investigated. Other groups, such as a 3-pyridylmethyl (**9**) and 2-ethoxyethyl (**10**), served as effective substitutes.⁸¹ In

many compounds, the 4-F group be successfully exchanged for a 4-CN group.⁸⁰ For example, applying such an exchange on compound **9** gave maintained affinity,⁸¹ whereas for **4** it was found to give a three-fold boost in affinity (i.e. **5**, VUF5834).⁸² The affinity of **9** could be improved further by substituting the 4-F atom by a propargyl or ethoxy group.^{80,81} Eventually, the pharmacokinetically more attractive 4-ethoxy substituent was combined with the CF₃O-substituted phenylacetamide moiety to deliver **11** (*IC*₅₀=6 nM, ¹²⁵I-CXCL10). While seeking an increase in polarity of compound **11**, an N-atom was introduced in the Ph-ring of the quinazolinone to give azaquinazolinone **12** (*IC*₅₀=8 nM, ¹²⁵I-CXCL10).^{80,81} Compound **12**, dubbed AMG 487, contains one chiral centre which has the (R)-configuration. This configuration is important for affinity, since the (S)-enantiomer is less efficient.⁸³ AMG 487 is currently the most studied member of the azaquinazolinone class. In addition, a more active 4-F,3-CF₃ analogue (**13**, NBI-74330) from the same patent⁸⁰ was independently studied by researchers from Neurocrine and UCB (*K*_i=1.5 nM, ¹²⁵I-CXCL10).^{84,85}

The (pre)clinical properties of NBI-74330 and AMG 487 have been extensively studied. NBI-74330 inhibits CXCL11 in [³⁵S]-GTP γ S binding (*IC*₅₀=10.8 nM), Ca²⁺ mobilization (*IC*₅₀=7 nM) and chemotaxis (*IC*₅₀=3.9 nM).⁸⁴ The antagonism of human CXCR3 is non-competitive, i.e. the maximum signal induced by CXCL11 (*E*_{max}) was dose-dependently reduced by NBI-74330 with notable reductions already visible at 3 nM ([³⁵S]-GTP γ S). Our group has confirmed non-competitive antagonism on human CXCR3 by NBI-74330, amongst other antagonists.⁸⁶ Non-competitive antagonism for NBI-74330 is also reported on murine CXCR3 (*pA*₂=8.35, CXCL11, [³⁵S]-GTP γ S), but in a less pronounced manner.⁸⁵ Here, NBI-74330 induced a rightshift in the *EC*₅₀ at low and high concentrations, but only a significant reduction in *E*_{max} at high concentrations (1 μ M).

Like NBI-74330, the structurally related AMG 487 exhibits non-competitive antagonism.⁸⁶ It inhibits CXCR3-mediated cell migration (*IC*₅₀= 15 nM, CXCL11) as well as Ca²⁺ mobilization (*IC*₅₀=5 nM, CXCL11).⁸¹ Interestingly, in addition to this antagonism of the original CXCR3 (CXCR3-A), AMG 487 also inhibits CXCL4 and CXCL11-mediated responses through the alternatively spliced variant CXCR3-B.²⁶ The compound displays a greater than 1000-fold selectivity for CXCR3 versus a panel of other receptors, including 11 chemokine receptors.⁸⁷ Compared to initial HTS hit **4**, AMG 487 has lower clearance (1.6 and 1.1 L/h/kg, 0.5-1.0 mg/kg i.v. in rats and dogs, respectively) and an improved bioavailability (12-57 and 85 %, 2.0-2.5 mg/kg orally in rats and dogs, respectively).⁸¹ The safety profile of AMG 487, as assessed by various genotoxicity and cardiotoxicity assays, revealed no major concerns.⁸³ The two main metabolic pathways for AMG 487 involve CYP3A4-mediated oxidation of the pyridine N-atom to the N-oxide (**14**) and de-ethylation to phenol **15**. Metabolite **14** efficiently binds CXCR3 (*IC*₅₀=6 nM, ¹²⁵I-CXCL10)⁸³ and has also been patented.⁸⁸ The Area-Under-the-Curve (AUC) ratio of **14** vs

AMG 487 varies from 0.03 to 0.6 in various animal studies.⁸³ Recent studies on analogue NBI-74330 have shown that this ratio also depends on the mode of administration. Higher exposure of NBI-74330 over N-oxide was achieved by oral dosing, while subcutaneous (s.c.) dosing led to about equivalent exposures.⁸⁵ It may be expected that similar dependences on administration hold true for AMG 487.

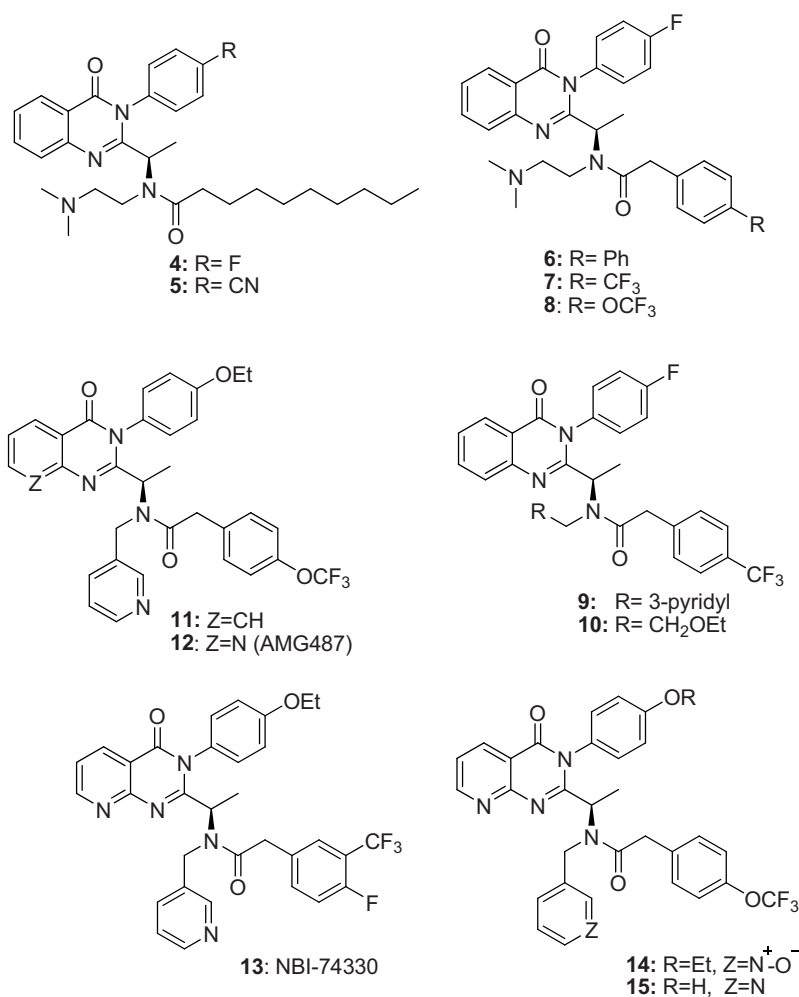


Figure 4. Structures of first generation (aza)quinazolinones and some metabolites.

Studies with NBI-74330 and AMG 487 in animal models reveal that this azaquinazolinone class of CXCR3 antagonists bears clinical promise in a variety of diseases. The ability of AMG 487 to inhibit inflammatory cell migration *in vivo* was confirmed in a mouse model of bleomycin-induced cellular recruitment, where AMG 487 significantly reduced

infiltration of macrophages and lymphocytes into the lungs with infiltration levels being as low as in CXCR3-KO mice (3 mg/kg sc).⁸³ In a mouse model for idiopathic pneumonia syndrome (IPS), AMG 487 reduced recruitment of donor T cells to the lung after allogeneic stem cell transplantation, leading to improved survival rates.⁸⁹ Likewise, reductions in inflammation, pannus formation and cartilage damage were observed upon administering AMG 487 at doses up to 50 mg/kg s.c. in mouse collagen-induced arthritis models.⁹⁰ Interestingly, NBI-74330 gave rise to reduction in lesion formation in models for atherosclerosis by the inhibition of effector cell migration to the atherosclerotic plaque and by regulating the local immune response.⁹¹ Last, as outlined earlier, metastasis of breast cancer was identified as a possible therapeutic area. This was substantiated by the inhibiting effect of AMG 487 on lung metastasis in a murine model for metastatic breast cancer.⁵⁴

The preclinical studies convincingly paved the way for clinical studies on two inflammation-related diseases: psoriasis and rheumatoid arthritis. In 2003, results of a Phase I trial on AMG 487 were disclosed. The compound was assessed for safety and pharmacokinetics in 30 healthy males in a randomized, double blind, placebo-controlled dose-escalation study. Generally, the compound was well tolerated and adverse events were mild to moderate (25 to 1100 mg doses).⁹² In a subsequent Phase IIa trial, patients suffering from psoriasis received 50 or 200 mg of AMG 487 or placebo orally once a day for 28 days. Disappointingly, no significant differences in the endpoints (Psoriasis Severity Index or Physician Global Assessment scores) were seen between patient groups. It was speculated that this lack of clinical efficacy may result from high variability in drug exposure.⁹³ Metabolic studies with healthy humans provided a plausible explanation for such variability.⁹⁴ Of key relevance were the two metabolites **15** and **14**, the latter being formed through CYP3A4. The studies revealed that **15** was a relatively potent (5 μ M) and time-dependent inhibitor of CYP3A4, leading in turn to variable formation of the major metabolite **14**. In 2004, it was announced that Phase II trials with AMG 487 on patients with rheumatoid arthritis were to be initiated.⁹⁵ The current status of these trials is unknown.

It comes therefore as no surprise that the latest lead optimisation efforts on AMG 487 have aimed at replacing the metabolically liable pyridine ring, ethoxy group and azaquinazolinone core.⁹⁶⁻⁹⁸ The described N-oxidation can be blocked through replacement of the pyridine ring by a sulphone-group. Likewise, metabolic de-ethylation can be circumvented by replacing the ethoxy group with a cyano-group.^{97,98} Changing the azaquinazolinone bicyclic core for a wide variety of heterocyclic groups (**16**) was tolerated and sometimes beneficial, leading to the hypothesis that the rigid bicyclic core serves as a scaffold to hold the adjacent groups in the correct orientations.⁹⁸ These structural replacements differentially affected binding to plasma proteins and the overall

effects had to be balanced. This led to the identification of **17** which compared to AMG 487 had similar affinity but reduced clearance (0.24 L/h/kg, 0.5 mg/kg i.v. in rat).⁹⁸ However, compounds in this class of pyrido[1,2-*a*]pyrimidin-4-ones appear to suffer from CYP-induction mediated by the Pregnane X receptor. It was reported that optimisation to structure **18** could counteract this unwanted effect.⁹⁶ Another effective replacement of the azaquinazolinone core is an imidazole group (**19**) substituted at the 4-position (R^2) with a lipophilic group.⁹⁷ Although affinities could be kept in the low nM range within this class, it presented its own metabolic hurdle: substantial addition of glutathione to the imidazole ring. This was elegantly overcome by installing electron-withdrawing groups on the 5-position of the imidazole ring (R^1 in **19**) as exemplified by compound **20** ($IC_{50} = 18$ nM, ^{125}I -CXCL10), although clearance levels remained inferior to those of **17** (**20**: 2.2 L/h/kg, 0.5 mg/kg i.v. in rat).

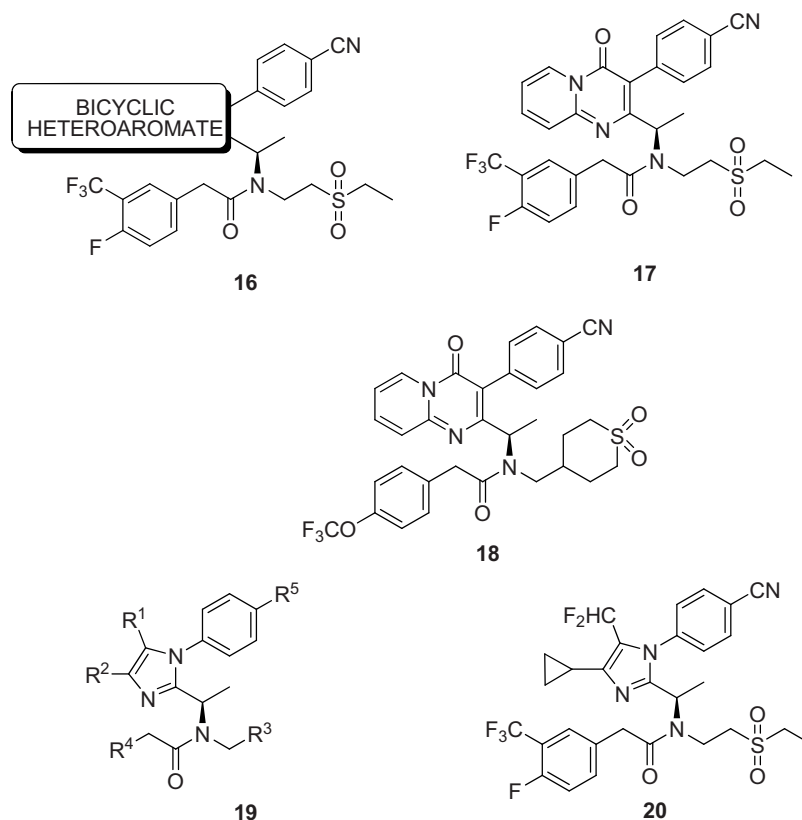


Figure 5. Structures of later-generation compounds based on the (aza)quinazolinones.

Piperazinyl piperidines

Schering-Plough has filed many patents describing a piperazinyl piperidine-scaffold flanked by a substituted benzyl unit and a polar headgroup (general structure **21**). Notably, many compounds of this class have subnanomolar affinities (e.g., **22**, **23**, **24**: $K_i=0.2$ nM, ^{125}I -CXCL10).⁹⁹⁻¹⁰¹ Upon inspection of the best compounds, the (S)-configuration of the ethyl-substituted carbon is maintained and R^1 and/or R^2 in **21** are often halogens or halogenated groups, suggesting crucial roles for these moieties. No functional data has been disclosed.

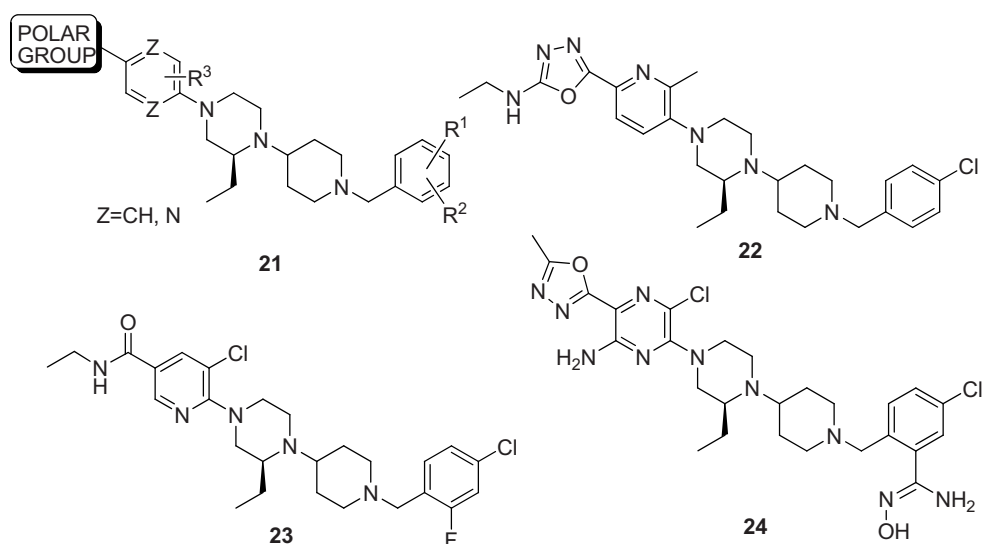


Figure 6. Structures of piperazinyl piperidines.

1-Aryl-3-piperidin-4-yl-ureas

UCB has designed CXCR3 antagonists based on an initial rigid piperidinyl-urea scaffold (general structure **25**). A HTS campaign using a FLIPR-based calcium flux assay led to the identification of hit **26** ($K_i=110$ nM, $[^{35}\text{S}]\text{-GTP}\gamma\text{S}$). This compound was reported to have poor solubility (0.1 $\mu\text{g}/\text{mL}$).¹⁰² Replacement of the cyclooctenyl ring by a variety of highly lipophilic substituents mostly afforded K_i values higher than 10 μM . A fortunate exception was the naturally occurring (-)-myrtenyl group which gave a compound with

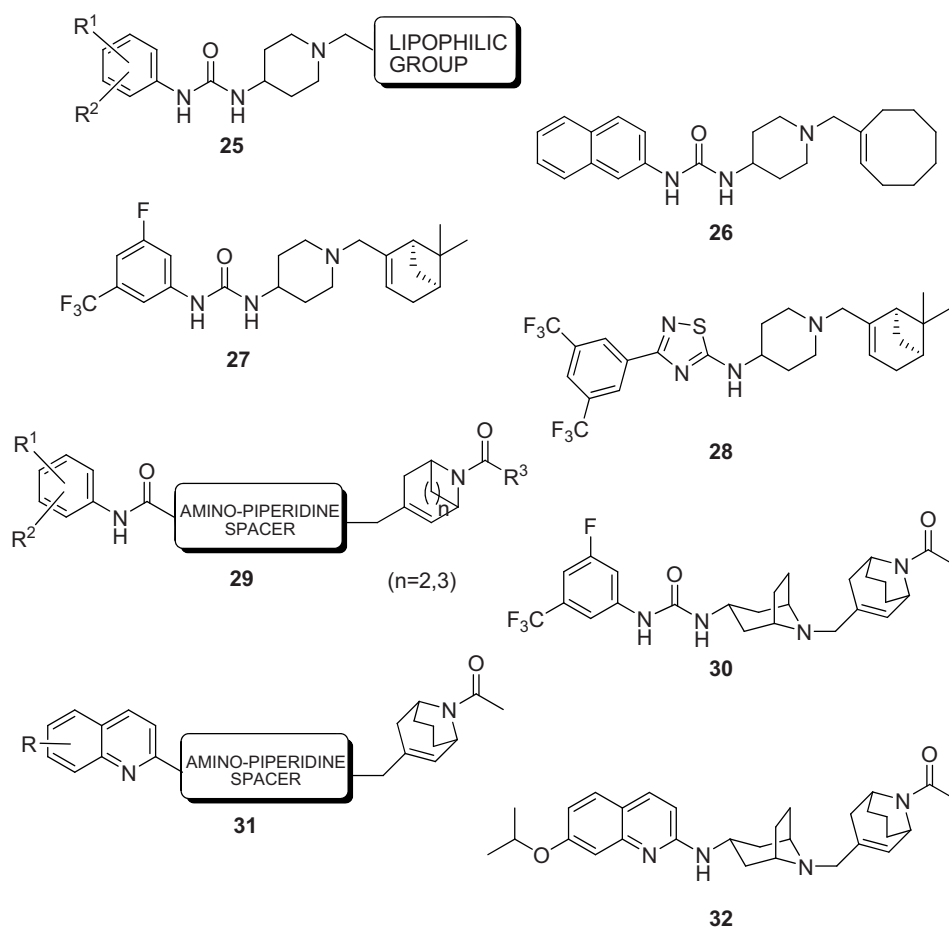


Figure 7. Structures of rigid piperidinyl-ureas and later-generation compounds.

similar affinity as **26**.¹⁰² With the (-)myrtenyl group in place, extensive structural variation of the aromatic group was performed in order to optimise affinity and drug-like properties. Several compounds were identified that had better affinities ($[^{35}\text{S}]\text{-GTP}\gamma\text{S}$) and improved physicochemical properties compared to hit **26**. This can be clearly illustrated by compound **27** ($K_i=16$ nM, solubility 23 $\mu\text{g}/\text{mL}$). N-Methylation of **27** to a quaternary ammonium salt was allowed for CXCR3 interaction while it further increased solubility. However, the resulting compounds suffered from reduced membrane permeability.^{102,103} In order to improve the in vivo pharmacokinetic properties of **27**, two approaches were followed. In the first approach, the urea group was replaced by a hydantoin or imidazolinone group as well as by a modelling-inspired switch to a benzazole or aryl azole.¹⁰⁴ None of these alternative linkers surpassed **27** in affinity, but

several gave increased microsomal stability and low CYP inhibition. For example, **28** displayed low clearance (2.8 mL/min/kg) and a long plasma half-life (5.4 h). A second and seemingly more successful approach focused on the spacer and (-)myrtenyl group in **27**.¹⁰⁵ Hundred compounds with myrtenyl-replacements were prepared, revealing a terminal piperidinyl-amide (**29**) as an entry into pharmacokinetically more favourable compounds. Subsequent modelling studies suggested that a homotropanyl-amide would spatially better resemble the myrtenyl group in **27** than an unsubstituted piperidinyl-amide in **29**. Concomitant focus was placed on preventing the central amino-piperidine unit from being oxidised in vivo. Interestingly, modelling revealed that, once again, a tropanyl unit would do just that by bridging the ring. Thus, an exo-tropanyl central core and homotropanyl peripheral unit were combined to deliver **30**. Compared to **27**, this compound is slightly more potent ($K_i = 7$ nM, [³⁵S]-GTP γ S) but is cleared less rapidly (7 μ L/min/mg), boosts a similar solubility (40 μ g/mL) and has a high bioavailability (70 %). Notably, a high selectivity for CXCR3 in a panel of 50 receptors was disclosed for **30**.¹⁰⁵ With the novel (homo)tropanyl-type structural elements at hand, replacement of the urea group was revisited.¹⁰⁶ This resulted in the discovery of quinoline-based antagonists (**31**). Compared to **30**, one isopropoxy-substituted member (**32**) has comparable affinity ($K_i = 5$ nM, [³⁵S]-GTP γ S) and higher solubility (1280 μ g/mL at pH=6.5), but at the same time an increased propensity to bind plasma proteins. Quinoline **32** was tested for its in vivo properties where it showed good oral availability ($t_{1/2} = 7.6$ h, 30 mg/kg p.o in mice) and dose-related inhibition of CXCR3 internalisation.⁸⁵ At 100 mg/kg, an effect on CXCR3 internalisation was observed up to 24 h post-dose.

4-N-aryl-[1,4]diazepane-ureas

Pharmacopeia researchers screened over 4 million compounds (90 libraries)¹⁰⁷ using a FLIPR-based calcium mobilization assay.^{108,109} This HTS screen led to the discovery of various antagonist scaffolds.¹⁰⁸ The general structure of one disclosed class is represented by **33**. The phenethyl substituent benefits from halogen substitutions, most particularly a 3,5-dichloro pattern. A similar preference for a 3-chloro (but also 3-fluoro) substituent was observed for the benzamide moiety. Replacement of the azepane spacer or the urea unit by different groups led to a dramatic drop in affinity. The combined SAR studies resulted in the discovery of **34** as a potent CXCR3 antagonist ($IC_{50} = 60$ nM, CXCL11, Ca²⁺).¹⁰⁸ The compound was capable of inhibiting chemotaxis ($IC_{50} \sim 100$ nM, CXCL11). No cytotoxicity at 100 μ M was observed while high selectivity over 14 other GPCRs was noted.

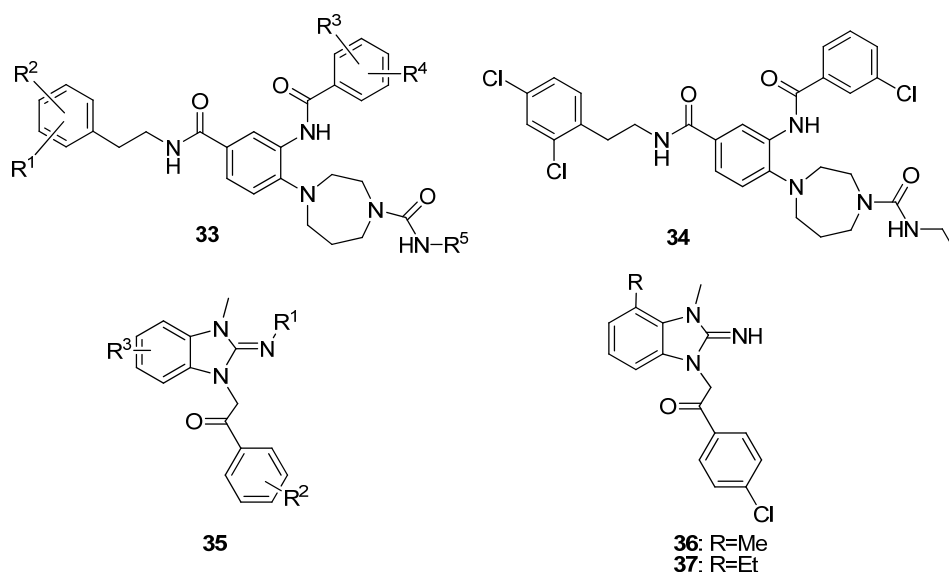


Figure 8. Structures of 4-N-aryl-[1,4]diazepane-ureas and 2-imino-benzimidazoles.

2-Imino-benzimidazoles

Researchers from Abbott Laboratories recently disclosed 2-imino-benzimidazoles as CXCR3 antagonists.^{110,111} The initial HTS hit, a substituted 2-acetyl-1*H*-benzo[*d*]imidazole, as well as several first-generation derivatives gave reasonable affinities ($IC_{50}=2 - 20 \mu M$, ^{125}I -CXCL10) but suffered from solubility problems in aqueous buffer. This complicated the pharmacology as it gave apparent partial antagonism. A strategic substitution of the 2-acetyl-benzimidazole core by a 3-methyl-2-imino-benzimidazole moiety (general structure **35**) afforded not only much improved solubility but also higher affinities. Variation of the benzophenone substituent (R^2) in this scaffold showed that 4-halo substituents gave submicromolar affinities. Upon selection of the 4-Cl group, the effect of ring substituents at the benzimidazole core (R^3) was investigated. The most notable improvements in affinity resulted from installing small, apolar substituents at the C4 position (**36**: $IC_{50}=100$ nM, **37**: $IC_{50}=30$ nM / ^{125}I -CXCL10). Whereas this represented an 8- and 27-fold boost in affinity for **36** and **37** compared to the unsubstituted counterpart ($R=H$), the corresponding boost in functional antagonism was an interesting 113- and 129-fold, respectively (**36**: $IC_{50}=80$ nM, **37**: $IC_{50}=70$ nM / CXCL10, Ca^{2+}). Compound **36** was evaluated for its *in vivo* pharmacokinetic properties, where it showed a $t_{1/2}$ of 4.9 h and a bioavailability of 57 % upon oral dosing in mice (10 mg/kg).

Bipiperidines

Researchers from Janssen have devised compounds centered around the 3,4'-bipiperidine scaffold (**38**).^{112,113} One of the N-termini was linked to an amide or urea group (3,4'-bipiperidine-amides and -ureas), or carbonyl groups were included in one of the piperidine rings (3,4'-bipiperidine-2,6-diones). The scaffolds were decorated by Ph-rings, with ring halogenation often appearing to be a privileged manipulation. Exemplary compounds from all three series are represented by structures (R)-**39**, **40** and (R)-**41** (IC₅₀=79, 50 and 32 nM, CXCL11, [³⁵S]-GTP_γS). Within this class of compounds, the (R)-configuration seems generally preferred, which can be deduced from selected affinities of (S)-isomers reported in the same patents ((S)-**39**: IC₅₀=251 nM, (S)-**41** IC₅₀=6310 nM).^{112,113} Two piperidine rings were also the essence of a patent filed by Amgen, but there the connection was established through a spiro-fusion (**42**). This novel scaffold was discovered after a screening of Amgen's chemical library.¹¹⁴ The compounds were decorated with a fused indole and halogenated aromatic rings. Compounds **43-45** all had IC₅₀ values < 500 nM as reported in the patent.¹¹⁵

Ergolines

A rather unusual type of CXCR3 antagonist was patented by Novartis (**46**).¹¹⁶ Replacement of the N-Me group of LSD by an N-phenylcarbamate moiety afforded compound **47**. It exerts good binding (IC₅₀=54 nM, ¹²⁵I-CXCL11) and blocks Ca²⁺ mobilization (IC₅₀=18 nM, CXCL11) as well as chemotaxis (IC₅₀=74 nM, CXCL11). Slight improvements could be achieved by certain replacements of the diethylamide moiety. For example, morpholine-containing compound **48** has an IC₅₀ of 23 nM (¹²⁵I-CXCL11) but otherwise similar functional properties as **47**. This class of compounds successfully reduced vessel wall remodelling after allotransplantation in murine models.¹¹⁶ This is to our knowledge the first SAR report on ergoline-type compounds for a chemokine receptor, although these are known as promiscuous GPCR ligands, binding on e.g. various dopamine-, serotonin- and adrenergic-receptors.¹¹⁷

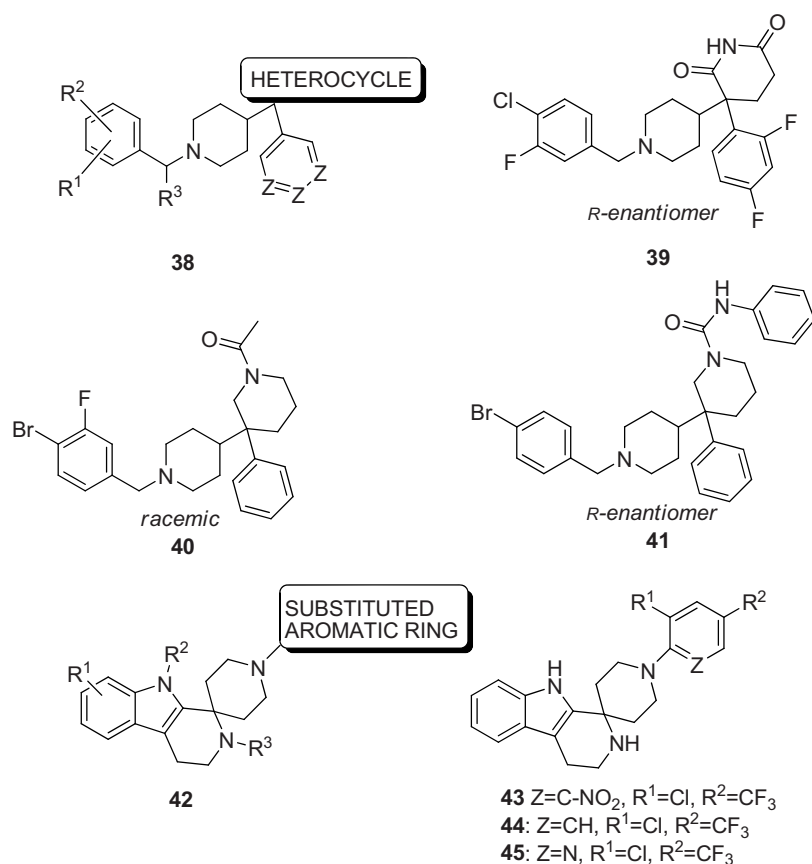


Figure 9. Structures of various bipiperidines.

Various

A handful of additional different scaffolds for CXCR antagonists have been disclosed in patents but often with little pharmacological data. As a result, no clear SAR can be deduced. To offer the reader the fullest overview possible, we show here the general structure of these scaffolds as deduced from inspecting of all structures.

Charged imidazolium salts (**49**) were reported by SmithKlineBeecham researchers.¹¹⁸ One such compound (**50**) has a K_i -value of 251 nM (¹²⁵I-CXCL10).⁸⁶ This group also disclosed camphor-containing antagonists of structure **51**, which had potencies up to 10 nM (CXCL10, Ca²⁺).¹¹⁹ Three patents from Merck describe a substituted piperidinylamide linked by its C-4 position to a substituted Ph-ring through a heteroaromatic spacer such as a thiazole or pyridine (**52**).¹²⁰⁻¹²² Reported IC₅₀ values were as low as 0.5 nM (CXCL10, chemotaxis).

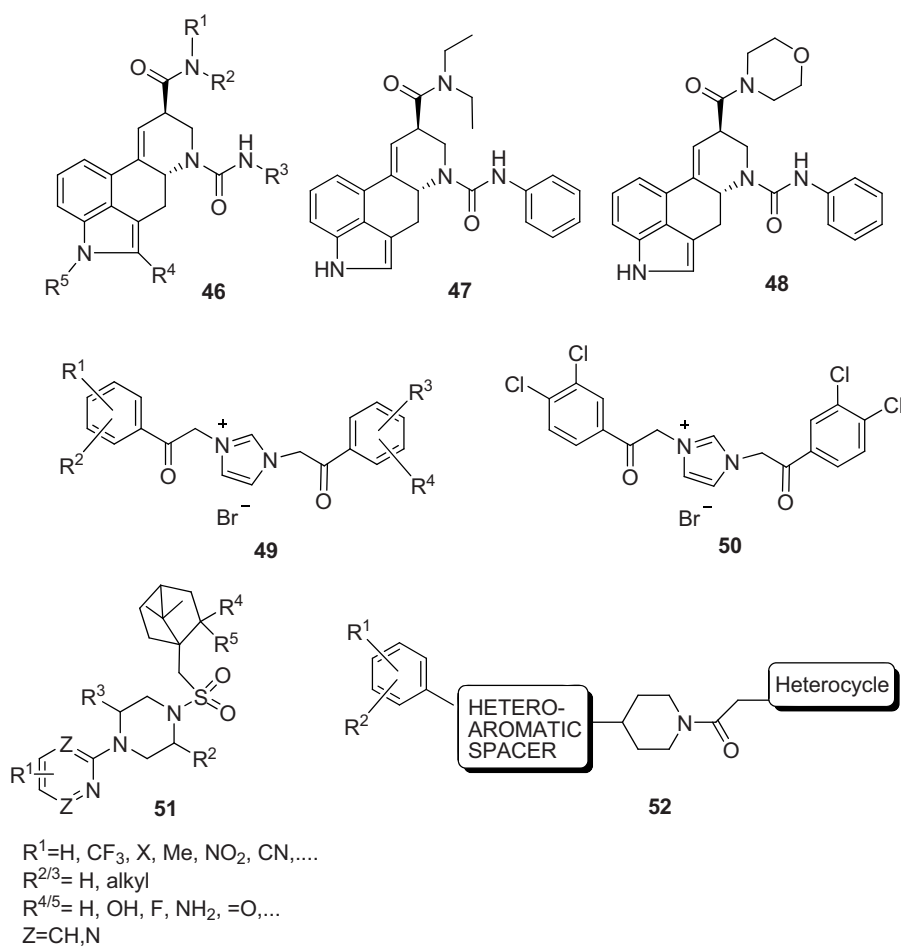


Figure 10. Structures of ergolines, imidazolium salts and various other scaffolds.

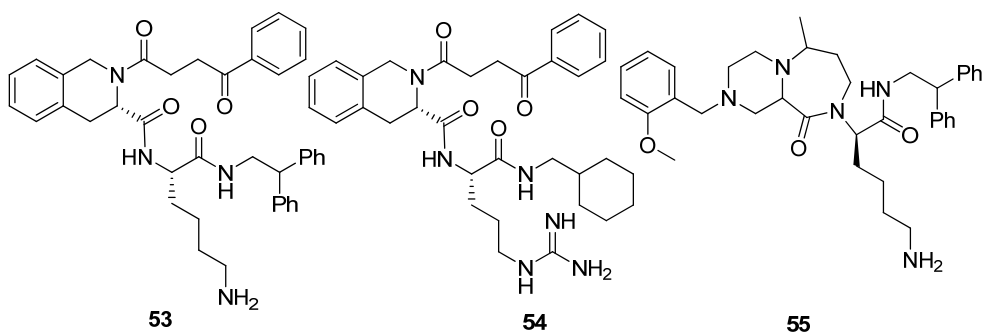


Figure 11. Structures of CXCR3 agonists.

Non-peptidergic CXCR3-agonists

Intuitively, development of agonists for inflammatory chemokine receptors does not seem attractive from a therapeutic point of view.¹²³ However, CXCR3 may offer an intriguing exception. One study suggests that CXCR3 agonism is beneficial in skin wound healing (vide supra).⁵⁷ Moreover, the CXCR3 agonists CXCL9,¹²⁴ CXCL10¹²⁵ and CXCL11¹²⁶ have been shown to possess anti-tumor activity, which is attributed to the recruitment of leukocytes by these chemokines. Therefore, topical application of a CXCR3 agonist may have beneficial effects in these specific cases.

In itself the task of designing a small non-peptidergic activator for any chemokine receptor seems daunting. Nevertheless, a handful of agonists for chemokine receptors other than CXCR3 has already been found in recent years.¹²⁷⁻¹²⁹ CXCR3 agonists were disclosed by researchers from PharmacoPeia in 2006. In an HTS screen for antagonists of a pool of more than 4 millions compounds, they identified a few CXCR3 agonist chemotypes.¹⁰⁹ Three exemplary compounds (**53-55**) were described in detail.¹⁰⁹ All three show structural similarities: a basic amino acid, a hydrophobic group and an N-containing bicyclic unit. Notable differences include the lack of a benzopropione unit in **55** and the opposite stereochemistry of the amino acid in **55** compared to **53** and **54**. Compounds **53-55** activate CXCR3 (EC_{50} =3.3, 1.1 and 1.7 μ M, respectively / Ca^{2+} influx) with high efficacies (120, 120 and 100 % of that of CXCL11, respectively). Activation by the agonists was dose-dependently inhibited by antagonist **34**, indicating specific CXCR3-mediated effects. This was further illustrated by lack of binding to a panel of GPCRs, including six chemokine receptors. Importantly, **54** and **55** were able to stimulate chemotaxis of T-cells in vitro (no results for **53** disclosed).

Modulation of CXCR3 by non-peptidergic ligands. General considerations.

Structural elements

The diversity amongst the CXCR3 antagonists described in this review is quite high and a general pharmacophore model seems difficult to construct. Indeed, to date no such models have been proposed in the public domain. Basic or charged groups are often thought to be beneficial for chemokine receptor affinity. While a good deal of the discussed antagonists possesses permanent charges or basic groups poised for protonation at pH 7.4, more and more emerging ligands lack a highly basic group (see **18**, **34** and **47**). Also of importance is that non-competitive CXCR3 antagonism occurs in a structurally diverse set of compounds.⁸⁴⁻⁸⁶ Given the huge structural and spatial differences between the small antagonists and large chemokine, their binding sites are

likely different. Precedence for such differential binding of chemokine ligands can be found for e.g. TAK-779, which was shown to bind CCR5 in a cavity between transmembrane helices 1, 2, 3, and 7 rather than at the extracellular domain.¹³⁰ Lastly, CXCR3 antagonists of different structural classes have been shown to act as inverse agonists at a constitutively active mutant of CXCR3, namely CXCR3 N3.35A.⁸⁶

A recurring and highly important issue in drug research is the translation of animal models to human studies. Chemokine research represents no exception to this. In fact, mouse knock-in models for e.g. CXCR2 have been specifically constructed to circumvent problems related to species-differences.¹³¹ Another illustration involves TAK-779, which has a 100-fold higher affinity for human CCR5 than for mouse CCR5, complicating interpretation of the results from murine studies.^{73,132} A careful inspection of all available results on CXCR3 points towards some species differences, caused by differences in the protein sequence of CXCR3 from various species. Compound **27** has affinities of 16 and 227 nM for human and murine CXCR3 ($[^{35}\text{S}]\text{-GTP}\gamma\text{S}$),¹⁰² respectively, whereas some compounds of the related later-stage tropanyl class reveal a 3-4 fold preference for human CXCR3.¹⁰⁵ A systematic study on other antagonist classes (AMG 487, NBI-74330, **5** and **50**) shows a similar 4-fold higher affinity for human and rhesus macaque CXCR3 compared to rat or mouse CXCR3.⁸⁶ Clearly, there is a slight CXCR3 species difference but it is believed that it does not represent a serious hurdle for future CXCR3 drug discovery efforts.

(Pre)clinical effects

Inhibiting the recruitment of inflammatory cells is at the heart of the clinical rationale for developing CXCR3 antagonists. Animal models using AMG 487 and NBI-74330 suggest that this rationale bears fruit. That is, CXCR3-related therapeutic effects have been observed in a general model for in vivo recruitment of inflammatory cells⁸³ as well as in more specific models for idiopathic pneumonia syndrome,⁸⁹ arthritis⁹⁰ and atherosclerosis.⁹¹ Unfortunately, no beneficial effect was observed with AMG 487 in Phase IIa trials on psoriasis. This clinical failure may have been due to pharmacokinetic rather than pharmacodynamic properties. Clinical promise of CXCR3 antagonism therefore remains to be confirmed by newer generations of compounds.

Conclusion

This review has dealt with the different aspects of CXCR3 as a drug target with emphasis on the potential of small, non-peptidergic ligands to therapeutically modulate the receptor. After a relatively slow start, more and more ligand classes are steadily disclosed by the drug discovery community. The structural variability amongst these classes is strikingly high. One quest for antagonists has left researchers with the first series of small molecule CXCR3 agonists, which will undoubtedly prove useful as research tools. For the antagonists, the highest affinities are found for the piperazinyl piperidines of Schering-Plough. In contrast, the best described series are the 1-aryl-3-piperidin-4-yl-ureas from UCB and most notably the Amgen class represented by AMG 487 and NBI-74330. Positive preclinical results with the latter two CXCR3 antagonists have strengthened the therapeutic expectations for CXCR3 antagonism. Unfortunately, a Phase IIa clinical trial with AMG 487 has been halted. Since this may have been due to unacceptable variability in drug exposure, it is clear that this failure is not a falsification of CXCR3 as a drug target per se. Indeed, clinical promise for the CXCR3 system is illustrated by the recent announcement of two Phase II clinical trials investigating a CXCL10 antibody in treating ulcerative colitis and rheumatoid arthritis.⁶² In all, CXCR3 target validation in humans still remains the ultimate and elusive goal and it is expected that ongoing medicinal chemistry efforts will soon shed more light on the therapeutic use of small CXCR3 ligands.

Acknowledgments

We thank Danny Scholten for providing the Snake Plot.

References

- (1) Murphy, P. M.; Baggiolini, M.; Charo, I. F.; Hebert, C. A.; Horuk, R.; Matsushima, K.; Miller, L. H.; Oppenheim, J. J.; Power, C. A. International union of pharmacology. XXII. Nomenclature for chemokine receptors. *Pharmacol. Rev.*, **2000**, *52*, 145-176.
- (2) Murphy, P.; Tiffany, H. Cloning of complementary DNA encoding a functional human interleukin-8 receptor. *Science*, **1991**, *253*, 1280-1283.
- (3) Holmes, W.; Lee, J.; Kuang, W.; Rice, G.; Wood, W. Structure and functional expression of a human interleukin-8 receptor. *Science*, **1991**, *253*, 1278-1280.
- (4) Biber, K.; de Jong, E. K.; van Weering, H. R.; Boddeke, H. W. Chemokines and their receptors in central nervous system disease. *Curr. Drug Targets*, **2006**, *7*, 29-46.
- (5) Zlotnik, A. Chemokines and cancer. *Int. J. Cancer*, **2006**, *119*, 2026-2029.
- (6) Alkhatib, G.; Combadiere, C.; Broder, C. C.; Feng, Y.; Kennedy, P. E.; Murphy, P. M.; Berger, E. A. CC CKR5: A RANTES, MIP-1alpha, MIP-1beta Receptor as a Fusion Cofactor for Macrophage-Tropic HIV-1. *Science*, **1996**, *272*, 1955-1958.
- (7) Deng, H.; Liu, R.; Ellmeier, W.; Choe, S.; Unutmaz, D.; Burkhart, M.; Marzio, P. D.; Marmon, S.; Sutton, R. E.; Hill, C. M.; Davis, C. B.; Peiper, S. C.; Schall, T. J.; Littman, D. R.; Landau, N. R. Identification of a major co-receptor for primary isolates of HIV-1. *Nature*, **1996**, *381*, 661-666.
- (8) Dragic, T.; Litwin, V.; Allaway, G. P.; Martin, S. R.; Huang, Y.; Nagashima, K. A.; Cayanan, C.; Maddon, P. J.; Koup, R. A.; Moore, J. P.; Paxton, W. A. HIV-1 entry into CD4+ cells is mediated by the chemokine receptor CC-CKR-5. *Nature*, **1996**, *381*, 667-673.
- (9) Feng, Y.; Broder, C. C.; Kennedy, P. E.; Berger, E. A. HIV-1 Entry Cofactor: Functional cDNA Cloning of a Seven-Transmembrane, G Protein-Coupled Receptor. *Science*, **1996**, *272*, 872-877.
- (10) Baba, M.; Nishimura, O.; Kanzaki, N.; Okamoto, M.; Sawada, H.; Iizawa, Y.; Shiraishi, M.; Aramaki, Y.; Okonogi, K.; Ogawa, Y.; Meguro, K.; Fujino, M. A small-molecule, nonpeptide CCR5 antagonist with highly potent and selective anti-HIV-1 activity. *Proc. Natl. Acad. Sci. USA*, **1999**, *96*, 5698-5703.
- (11) Este, J. A.; Telenti, A. HIV entry inhibitors. *Lancet*, **2007**, *370*, 81-88.
- (12) Wells, T. N. C.; Power, C. A.; Shaw, J. P.; Proudfoot, A. E. I. Chemokine blockers - therapeutics in the making? *Trends Pharmacol. Sci.*, **2006**, *27*, 41-47.
- (13) Loetscher, M.; Gerber, B.; Loetscher, P.; Jones, S. A.; Piali, L.; Clark-Lewis, I.; Baggiolini, M.; Moser, B. Chemokine receptor specific for IP10 and mig: structure, function, and expression in activated T-lymphocytes. *J. Exp. Med.*, **1996**, *184*, 963-969.
- (14) Marchese, A.; Heiber, M.; Nguyen, T.; Heng, H. H. Q.; Saldivia, V. R.; Cheng, R.; Murphy, P. M.; Tsui, L. C.; Shi, X. M.; Gregor, P.; George, S. R.; Odowd, B. F.; Docherty, J. M. Cloning and Chromosomal Mapping of 3 Novel Genes, Gpr9, Gpr10, and Gpr14 Encoding Receptors Related to Interleukin-8, Neuropeptide-Y, and Somatostatin Receptors. *Genomics*, **1995**, *29*, 335-344.
- (15) Gether, U. Uncovering molecular mechanisms involved in activation of G protein-coupled receptors. *Endocr. Rev.*, **2000**, *21*, 90-113.
- (16) Ai, L. S.; Liao, F. Mutating the four extracellular cysteines in the chemokine receptor CCR6 reveals their differing roles in receptor trafficking, ligand binding, and signaling. *Biochemistry*, **2002**, *41*, 8332-8341.
- (17) Colvin, R. A.; Campanella, G. S. V.; Sun, J. T.; Luster, A. D. Intracellular domains of CXCR3 that mediate CXCL9, CXCL10, and CXCL11 function. *J. Biol. Chem.*, **2004**, *279*, 30219-30227.
- (18) Qin, S.; Rottman, J. B.; Myers, P.; Kassam, N.; Weinblatt, M.; Loetscher, M.; Koch, A. E.; Moser, B.; Mackay, C. R. The chemokine receptors CXCR3 and CCR5 mark subsets of T cells associated with certain inflammatory reactions. *J. Clin. Invest.*, **1998**, *101*, 746-754.

- (19) Bonecchi, R.; Bianchi, G.; Bordignon, P. P.; D'Ambrosio, D.; Lang, R.; Borsatti, A.; Sozzani, S.; Allavena, P.; Gray, P. A.; Mantovani, A.; Sinigaglia, F. Differential expression of chemokine receptors and chemotactic responsiveness of type 1 T helper cells (Th1s) and Th2s. *J. Exp. Med.*, **1998**, *187*, 129-134.
- (20) Cole, K. E.; Strick, C. A.; Paradis, T. J.; Ogborne, K. T.; Loetscher, M.; Gladue, R. P.; Lin, W.; Boyd, J. G.; Moser, B.; Wood, D. E.; Sahagan, B. G.; Neote, K. Interferon-inducible T cell alpha chemoattractant (I-TAC): a novel non-ELR CXC chemokine with potent activity on activated T cells through selective high affinity binding to CXCR3. *J. Exp. Med.*, **1998**, *187*, 2009-2021.
- (21) Weng, Y.; Siciliano, S. J.; Waldburger, K. E.; Sirotina-Meisher, A.; Staruch, M. J.; Daugherty, B. L.; Gould, S. L.; Springer, M. S.; DeMartino, J. A. Binding and functional properties of recombinant and endogenous CXCR3 chemokine receptors. *J. Biol. Chem.*, **1998**, *273*, 18288-18291.
- (22) Tensen, C. P.; Flier, J.; Van Der Raaij-Helmer, E. M.; Sampat-Sardjoepersad, S.; Van Der Schors, R. C.; Leurs, R.; Scheper, R. J.; Boorsma, D. M.; Willemze, R. Human IP-9: A keratinocyte-derived high affinity CXC-chemokine ligand for the IP-10/Mig receptor (CXCR3). *J. Invest. Dermatol.*, **1999**, *112*, 716-722.
- (23) Loetscher, M.; Loetscher, P.; Brass, N.; Meese, E.; Moser, B. Lymphocyte-specific chemokine receptor CXCR3: regulation, chemokine binding and gene localization. *Eur. J. Immunol.*, **1998**, *28*, 3696-3705.
- (24) Jenh, C. H.; Cox, M. A.; Hipkin, W.; Lu, T.; Pugliese-Sivo, C.; Gonsiorek, W.; Chou, C. C.; Narula, S. K.; Zavodny, P. J. Human B cell-attracting chemokine 1 (BCA-1; CXCL13) is an agonist for the human CXCR3 receptor. *Cytokine*, **2001**, *15*, 113-121.
- (25) Lasagni, L.; Francalanci, M.; Annunziato, F.; Lazzeri, E.; Giannini, S.; Cosmi, L.; Sagrinati, C.; Mazzinghi, B.; Orlando, C.; Maggi, E.; Marra, F.; Romagnani, S.; Serio, M.; Romagnani, P. An alternatively spliced variant of CXCR3 mediates the inhibition of endothelial cell growth induced by IP-10, Mig, and I-TAC, and acts as functional receptor for platelet factor 4. *J. Exp. Med.*, **2003**, *197*, 1537-1549.
- (26) Mueller, A.; Meiser, A.; McDonagh, E. M.; Fox, J. M.; Petit, S. J.; Xanthou, G.; Williams, T. J.; Pease, J. E. CXCL4-induced migration of activated T lymphocytes is mediated by the chemokine receptor CXCR3. *J. Leukocyte Biol.*, **2008**, *83*, 875-882.
- (27) Smit, M. J.; Verdijk, P.; van der Raaij-Helmer, E. M. H.; Navis, M.; Hensbergen, P. J.; Leurs, R.; Tensen, C. P. CXCR3-mediated chemotaxis of human T cells is regulated by a G(i)- and phospholipase C-dependent pathway and not via activation of MEK/p44/p42 MAPK nor Akt/PI-3 kinase. *Blood*, **2003**, *102*, 1959-1965.
- (28) Xanthou, G.; Duchesnes, Cécile, E.; Williams, Timothy, J.; Pease, James, E. CCR3 functional responses are regulated by both CXCR3 and its ligands CXCL9, CXCL10 and CXCL11. *Eur. J. Immunol.*, **2003**, *33*, 2241-2250.
- (29) Loetscher, P.; Pellegrino, A.; Gong, J.-H.; Mattioli, I.; Loetscher, M.; Bardi, G.; Baggiolini, M.; Clark-Lewis, I. The Ligands of CXC Chemokine Receptor 3, I-TAC, Mig, and IP10, Are Natural Antagonists for CCR3. *J. Biol. Chem.*, **2001**, *276*, 2986-2991.
- (30) Cox, M. A.; Jenh, C. H.; Gonsiorek, W.; Fine, J.; Narula, S. K.; Zavodny, P. J.; Hipkin, R. W. Human interferon-inducible 10-kDa protein and human interferon-inducible T cell alpha chemoattractant are allotropic ligands for human CXCR3: Differential binding to receptor states. *Mol. Pharmacol.*, **2001**, *59*, 707-715.
- (31) Fernandez, E. J.; Lolis, E. Structure, function, and inhibition of chemokines. *Annu. Rev. Pharmacol. Toxicol.*, **2002**, *42*, 469-499.
- (32) Rajagopalan, L.; Rajarathnam, K. Structural basis of chemokine receptor function—a model for binding affinity and ligand selectivity. *Biosci. Rep.*, **2006**, *26*, 325-339.
- (33) Moser, B.; Dewald, B.; Barella, L.; Schumacher, C.; Baggiolini, M.; Clark-Lewis, I. Interleukin-8 antagonists generated by N-terminal modification. *J. Biol. Chem.*, **1993**, *268*, 7125-7128.

- (34) Proudfoot, A. E.; Power, C. A.; Hoogewerf, A. J.; Montjovent, M. O.; Borlat, F.; Offord, R. E.; Wells, T. N. Extension of recombinant human RANTES by the retention of the initiating methionine produces a potent antagonist. *J. Biol. Chem.*, **1996**, *271*, 2599-2603.
- (35) Clark-Lewis, I.; Mattioli, I.; Gong, J. H.; Loetscher, P. Structure-function relationship between the human chemokine receptor CXCR3 and its ligands. *J. Biol. Chem.*, **2003**, *278*, 289-295.
- (36) Hasegawa, H.; Inoue, A.; Kohno, M.; Muraoka, M.; Miyazaki, T.; Terada, M.; Nakayama, T.; Yoshie, O.; Nose, M.; Yasukawa, M. Antagonist of interferon-inducible protein 10/CXCL10 ameliorates the progression of autoimmune sialadenitis in MRL/lpr mice. *Arthritis Rheum.*, **2006**, *54*, 1174-1183.
- (37) Hensbergen, P. J.; van der Raaij-Helmer, E. M. H.; Dijkman, R.; van der Schors, R. C.; Werner-Felmayer, G.; Boorsma, D. M.; Scheper, R. J.; Willemze, R.; Tensen, C. P. Processing of natural and recombinant CXCR3-targeting chemokines and implications for biological activity. *Eur. J. Biochem.*, **2001**, *268*, 4992-4999.
- (38) Proost, P.; Schutyser, E.; Menten, P.; Struyf, S.; Wuyts, A.; Opdenakker, G.; Detheux, M.; Parmentier, M.; Durinx, C.; Lambeir, A.-M.; Neyts, J.; Liekens, S.; Maudgal, P. C.; Billiau, A.; Van Damme, J. Amino-terminal truncation of CXCR3 agonists impairs receptor signaling and lymphocyte chemotaxis, while preserving antiangiogenic properties. *Blood*, **2001**, *98*, 3554-3561.
- (39) Lundstrom, K. Structural biology of G protein-coupled receptors. *Bioorg. Med. Chem. Lett.*, **2005**, *15*, 3654-3657.
- (40) Power, C. A. Knock out models to dissect chemokine receptor function in vivo. *J. Immunol. Methods*, **2003**, *273*, 73-82.
- (41) Sorensen, T. L.; Tani, M.; Jensen, J.; Pierce, V.; Lucchinetti, C.; Folcik, V. A.; Qin, S.; Rottman, J.; Sellebjerg, F.; Strieter, R. M.; Frederiksen, J. L.; Ransohoff, R. M. Expression of specific chemokines and chemokine receptors in the central nervous system of multiple sclerosis patients. *J. Clin. Invest.*, **1999**, *103*, 807-815.
- (42) Mach, F.; Sauty, A.; Iarossi, A. S.; Sukhova, G. K.; Neote, K.; Libby, P.; Luster, A. D. Differential expression of three T lymphocyte-activating CXC chemokines by human atheroma-associated cells. *J. Clin. Invest.*, **1999**, *104*, 1041-1050.
- (43) Saetta, M.; Mariani, M.; Panina-Bordignon, P.; Turato, G.; Buonsanti, C.; Baraldo, S.; Bellettato, C. M.; Papi, A.; Corbetta, L.; Zuin, R.; Sinigaglia, F.; Fabbri, L. M. Increased expression of the chemokine receptor CXCR3 and its ligand CXCL10 in peripheral airways of smokers with chronic obstructive pulmonary disease. *Am. J. Respir. Crit. Care Med.*, **2002**, *165*, 1404-1409.
- (44) Yuan, Y. H.; ten Hove, T.; The, F. O.; Slors, J. F.; van Deventer, S. J.; te Velde, A. A. Chemokine receptor CXCR3 expression in inflammatory bowel disease. *Inflamm. Bowel Dis.*, **2001**, *7*, 281-286.
- (45) Flier, J.; Boorsma, D. M.; van Beek, P. J.; Nieboer, C.; Stoof, T. J.; Willemze, R.; Tensen, C. P. Differential expression of CXCR3 targeting chemokines CXCL10, CXCL9, and CXCL11 in different types of skin inflammation. *J. Pathol.*, **2001**, *194*, 398-405.
- (46) Rottman, J. B.; Smith, T. L.; Ganley, K. G.; Kikuchi, T.; Krueger, J. G. Potential role of the chemokine receptors CXCR3, CCR4, and the integrin alpha E beta 7 in the pathogenesis of psoriasis vulgaris. *Lab. Invest.*, **2001**, *81*, 335-347.
- (47) Shields, P. L.; Morland, C. M.; Salmon, M.; Qin, S.; Hubscher, S. G.; Adams, D. H. Chemokine and chemokine receptor interactions provide a mechanism for selective T cell recruitment to specific liver compartments within hepatitis C-infected liver. *J. Immunol.*, **1999**, *163*, 6236-6243.
- (48) Agostini, C.; Cassatella, M.; Zambello, R.; Trentin, L.; Gasperini, S.; Perin, A.; Piazza, F.; Siviero, M.; Facco, M.; Dziejman, M.; Chilosi, M.; Qin, S.; Luster, A. D.; Semenzato, G. Involvement of the IP-10 chemokine in sarcoid granulomatous reactions. *J. Immunol.*, **1998**, *161*, 6413-6420.
- (49) Glass, W. G.; Subbarao, K.; Murphy, B.; Murphy, P. M. Mechanisms of host defense following severe acute respiratory syndrome-coronavirus (SARS-CoV) pulmonary infection of mice. *J. Immunol.*, **2004**, *173*, 4030-4039.

- (50) Danesh, A.; Seneviratne, C.; Cameron, C.; Banner, D.; Devries, M.; Kelvin, A.; Xu, L.; Ran, L.; Bosinger, S.; Rowe, T.; Czub, M.; Jonsson, C.; Cameron, M.; Kelvin, D. Cloning, expression and characterization of ferret CXCL10. *Mol. Immunol.*, **2008**, *45*, 1288-1297.
- (51) Hancock, W. W.; Lu, B.; Gao, W.; Csizmadia, V.; Faia, K.; King, J. A.; Smiley, S. T.; Ling, M.; Gerard, N. P.; Gerard, C. Requirement of the chemokine receptor CXCR3 for acute allograft rejection. *J. Exp. Med.*, **2000**, *192*, 1515-1520.
- (52) Inston, N.; Drayson, M.; Ready, A.; Cockwell, P. Serial Changes in the Expression of CXCR3 and CCR5 on Peripheral Blood Lymphocytes Following Human Renal Transplantation. *Exp. Clin. Transplant.*, **2007**, *5*, 638-642.
- (53) Kawada, K.; Sonoshita, M.; Sakashita, H.; Takabayashi, A.; Yamaoka, Y.; Manabe, T.; Inaba, K.; Minato, N.; Oshima, M.; Taketo, M. M. Pivotal role of CXCR3 in melanoma cell metastasis to lymph nodes. *Cancer Res.*, **2004**, *64*, 4010-4017.
- (54) Walser, T. C.; Rifat, S.; Ma, X. R.; Kundu, N.; Ward, C.; Goloubeva, O.; Johnson, M. G.; Medina, J. C.; Collins, T. L.; Fulton, A. M. Antagonism of CXCR3 inhibits lung metastasis in a murine model of metastatic breast cancer. *Cancer Res.*, **2006**, *66*, 7701-7707.
- (55) Kawada, K.; Hosogi, H.; Sonoshita, M.; Sakashita, H.; Manabe, T.; Shimahara, Y.; Sakai, Y.; Takabayashi, A.; Oshima, M.; Taketo, M. M. Chemokine receptor CXCR3 promotes colon cancer metastasis to lymph nodes. *Oncogene*, **2007**, *26*, 4679-4688.
- (56) Hatse, S.; Huskens, D.; Princen, K.; Vermeire, K.; Bridger, G. J.; De Clercq, E.; Rosenkilde, M. M.; Schwartz, T. W.; Schols, D. Modest human immunodeficiency virus coreceptor function of CXCR3 is strongly enhanced by mimicking the CXCR4 ligand binding pocket in the CXCR3 receptor. *J. Virol.*, **2007**, *81*, 3632-3639.
- (57) Yates, C. C.; Whaley, D.; Kulasekeran, P.; Hancock, W. W.; Lu, B.; Bodnar, R.; Newsome, J.; Hebda, P. A.; Wells, A. Delayed and deficient dermal maturation in mice lacking the CXCR3 ELR-negative CXC chemokine receptor. *Am. J. Pathol.*, **2007**, *171*, 484-495.
- (58) Christensen, J. E.; Nansen, A.; Moos, T.; Lu, B.; Gerard, C.; Christensen, J. P.; Thomsen, A. R. Efficient T-cell surveillance of the CNS requires expression of the CXC chemokine receptor 3. *J. Neurosci.*, **2004**, *24*, 4849-4858.
- (59) Jiang, D.; Liang, J.; Hodge, J.; Lu, B.; Zhu, Z.; Yu, S.; Fan, J.; Gao, Y.; Yin, Z.; Homer, R.; Gerard, C.; Noble, P. W. Regulation of pulmonary fibrosis by chemokine receptor CXCR3. *J. Clin. Invest.*, **2004**, *114*, 291-299.
- (60) Baker, M. S.; Chen, X.; Rotramel, A. R.; Nelson, J. J.; Lu, B.; Gerard, C.; Kanwar, Y.; Kaufman, D. B. Genetic deletion of chemokine receptor CXCR3 or antibody blockade of its ligand IP-10 modulates posttransplantation graft-site lymphocytic infiltrates and prolongs functional graft survival in pancreatic islet allograft recipients. *Surgery*, **2003**, *134*, 126-133.
- (61) Suzuki, K.; Kawauchi, Y.; Palaniyandi, S. S.; Veeraveedu, P. T.; Fujii, M.; Yamagiwa, S.; Yoneyama, H.; Han, G. D.; Kawachi, H.; Okada, Y.; Ajioka, Y.; Watanabe, K.; Hosono, M.; Asakura, H.; Aoyagi, Y.; Narumi, S. Blockade of interferon-gamma-inducible protein-10 attenuates chronic experimental colitis by blocking cellular trafficking and protecting intestinal epithelial cells. *Pathol. Int.*, **2007**, *57*, 413-420.
- (62) Pien, H. Presented at the 26th Annual JP Morgan Healthcare Conference (San Francisco, CA), Jan 7 - 10, **2008**.
- (63) Schnickel, G. T.; Hsieh, G. R.; Garcia, C.; Shefizadeh, A.; Fishbein, M. C.; Ardehali, A. Role of CXCR3 and CCR5 in allograft rejection. *Transplant. Proc.*, **2006**, *38*, 3221-3224.
- (64) Hancock, W. W.; Gao, W.; Csizmadia, V.; Faia, K. L.; Shemmeri, N.; Luster, A. D. Donor-derived IP-10 initiates development of acute allograft rejection. *J. Exp. Med.*, **2001**, *193*, 975-980.
- (65) Zhang, Z.; Kaptanoglu, L.; Haddad, W.; Ivancic, D.; Alnadjim, Z.; Hurst, S.; Tishler, D.; Luster, A. D.; Barrett, T. A.; Fryer, J. Donor T cell activation initiates

- small bowel allograft rejection through an IFN-gamma-inducible protein-10-dependent mechanism. *J. Immunol.*, **2002**, *168*, 3205-3212.
- (66) Mohan, K.; Issekutz, T. B. Blockade of chemokine receptor CXCR3 inhibits T cell recruitment to inflamed joints and decreases the severity of adjuvant arthritis. *J. Immunol.*, **2007**, *179*, 8463-8469.
- (67) Belperio, J. A.; Keane, M. P.; Burdick, M. D.; Lynch, J. P., 3rd; Xue, Y. Y.; Li, K.; Ross, D. J.; Strieter, R. M. Critical role for CXCR3 chemokine biology in the pathogenesis of bronchiolitis obliterans syndrome. *J. Immunol.*, **2002**, *169*, 1037-1049.
- (68) Medoff, B. D.; Wain, J. C.; Seung, E.; Jackobek, R.; Means, T. K.; Ginns, L. C.; Farber, J. M.; Luster, A. D. CXCR3 and its ligands in a murine model of obliterative bronchiolitis: regulation and function. *J. Immunol.*, **2006**, *176*, 7087-7095.
- (69) Proudfoot, A.; Kosco-Vilbois, M. Novel antagonists of CXCR3-binding CXC chemokines. *WO03106488* **2003**.
- (70) Vergote, D.; Butler, G. S.; Ooms, M.; Cox, J. H.; Silva, C.; Hollenberg, M. D.; Jhamandas, J. H.; Overall, C. M.; Power, C. Proteolytic processing of SDF-1 alpha reveals a change in receptor specificity mediating HIV-associated neurodegeneration. *Proc. Natl. Acad. Sci. USA*, **2006**, *103*, 19182-19187.
- (71) Medina, J. C.; Johnson, M. G.; Collins, T. L. CXCR3 antagonists. *Annu. Rep. Med. Chem.*, **2005**, *40*, 215-225.
- (72) Collins, T. L.; Johnson, M. G.; Medina, J. C. in *Chemokine Biology-Basic Research and Clinical Application, Vol.2* (Eds.: K. Neote, K., G. L. Letts, B. Moser), *Birkhauser Verlag Publishers*, **2007**, 79.
- (73) Gao, P.; Zhou, X. Y.; Yashiro-Ohtani, Y.; Yang, Y. F.; Sugimoto, N.; Ono, S.; Nakanishi, T.; Obika, S.; Imanishi, T.; Egawa, T.; Nagasawa, T.; Fujiwara, H.; Hamaoka, T. The unique target specificity of a nonpeptide chemokine receptor antagonist: selective blockade of two Th1 chemokine receptors CCR5 and CXCR3. *J. Leukocyte Biol.*, **2003**, *73*, 273-280.
- (74) Akashi, S.; Sho, M.; Kashizuka, H.; Hamada, K.; Ikeda, N.; Kuzumoto, Y.; Tsurui, Y.; Nomi, T.; Mizuno, T.; Kanehiro, H.; Hisanaga, M.; Ko, S.; Nakajima, Y. A novel small-molecule compound targeting CCR5 and CXCR3 prevents acute and chronic allograft rejection. *Transplantation*, **2005**, *80*, 378-384.
- (75) Akahori, T.; Sho, M.; Kashizuka, H.; Nomi, T.; Kanehiro, H.; Nakajima, Y. A novel CCR5/CXCR3 antagonist protects intestinal ischemia/reperfusion injury. *Transplant. Proc.*, **2006**, *38*, 3366-3368.
- (76) Tokuyama, H.; Ueha, S.; Kurachi, M.; Matsushima, K.; Moriyasu, F.; Blumberg, R. S.; Kakimi, K. The simultaneous blockade of chemokine receptors CCR2, CCR5 and CXCR3 by a non-peptide chemokine receptor antagonist protects mice from dextran sodium sulfate-mediated colitis. *Int. Immunol.*, **2005**, *17*, 1023-1034.
- (77) Suzuki, Y.; Hamada, K.; Nomi, T.; Ito, T.; Sho, M.; Kai, Y.; Nakajima, Y.; Kimura, H. A small-molecule compound targeting CCR5 and CXCR3 prevents the development of asthma. *Eur. Respir. J.*, **2007**, DOI: 10.1183/09031936.00111507.
- (78) Ondeyka, J. G.; Herath, K. B.; Jayasuriya, H.; Polishook, J. D.; Bills, G. F.; Dombrowski, A. W.; Mojena, M.; Koch, G.; DiSalvo, J.; DeMartino, J.; Guan, Z.; Nanakorn, W.; Morenberg, C. M.; Balick, M. J.; Stevenson, D. W.; Slattery, M.; Borris, R. P.; Singh, S. B. Discovery of structurally diverse natural product antagonists of chemokine receptor CXCR3. *Mol. Diversity*, **2005**, *9*, 123-129.
- (79) Schall, T. J.; Dairaghi, D. J.; McMaster, B. E. Compounds and methods for modulating CXCR3 function. *WO0116114* **2001**.
- (80) Medina, J. C.; Johnson, M. G.; Li, A.; Liu, J.; Huang, A. X.; Zhu, L.; Marcus, A. P. CXCR3 antagonists. *WO02083143* **2002**.
- (81) Johnson, M.; Li, A.-R.; Liu, J.; Fu, Z.; Zhu, L.; Miao, S.; X. Wang; Q. Xu; A. Huang; A. Marcus; F. Xu; K. Ebsworth; E. Sablan; J. Danao; J. Kumer; D. Dairaghi; C. Lawrence; T. Sullivan; G. Tonn; T. Schall; Collins, T.; Medina, J. Discovery and optimization of a series of quinazolinone-derived antagonists of CXCR3. *Bioorg. Med. Chem. Lett.*, **2007**, *17*, 3339-3343.

- (82) Storelli, S.; Verdijk, P.; Verzijl, D.; Timmerman, H.; van de Stolpe, A. C.; Tensen, C. P.; Smit, M. J.; De Esch, I. J. P.; Leurs, R. Synthesis and structure-activity relationship of 3-phenyl-3H-quinazolin-4-one derivatives as CXCR3 chemokine receptor antagonists. *Bioorg. Med. Chem. Lett.*, **2005**, *15*, 2910-2913.
- (83) Johnson, M. G. Presented at the XIXth International Symposium on Medicinal Chemistry (Istanbul, Turkey), Aug 29 - Sep 2, **2006**.
- (84) Heise, C. E.; Pahuja, A.; Hudson, S. C.; Mistry, M. S.; Putnam, A. L.; Gross, M. M.; Gottlieb, P. A.; Wade, W. S.; Kiankarimi, M.; Schwarz, D.; Crowe, P.; Zlotnik, A.; Alleva, D. G. Pharmacological characterization of CXCR3 chemokine receptor 3 ligands and a small molecule antagonist. *J. Pharmacol. Exp. Ther.*, **2005**, *313*, 1263-1271.
- (85) Jopling, L.; Watt, G.; Fisher, S.; Birch, H.; Coggon, S.; Christie, M. Analysis of the pharmacokinetic/pharmacodynamic relationship of a small molecule CXCR3 antagonist, NBI-74330, using a murine CXCR3 internalization assay. *Br. J. Pharmacol.*, **2007**, *152*, 1260-1271.
- (86) Verzijl, D.; Storelli, S.; Scholten, D.; Bosch, L.; Reinhart, T. A.; Strebblow, D. N.; Tensen, C. P.; Fitzsimons, C. P.; Zaman, G. J. R.; Pease, J. E.; De Esch, I. J. P.; Smit, M. J.; Leurs, R. Non-competitive antagonism and inverse agonism as mechanism of action of non-peptidergic antagonists at primate and rodent CXCR3 chemokine receptors. *J. Pharmacol. Exp. Ther.*, **2008**, *325*, 544-555.
- (87) Collins, T. L. Presented at Inflammation 2003 - Sixth World Congress (Vancouver, Canada), Aug 2 - 6, **2003**.
- (88) Collins, T. L.; Johnson, M. G.; Ma, J.; Medina, J. C.; Miao, S.; Schneider, M.; Tonn, G. R. CXCR3 antagonists. *WO2004075863*, **2004**.
- (89) Deurloo, D. T.; Chaudhary, M. N.; Olkiewicz, K. M.; Silva, I. A.; Choi, S. W.; Liu, C.; Collins, T. L.; Sullivan, T. J.; Cooke, K. R. A Small Molecular Weight Antagonist Of Cxcr3 Reduces The Severity Of Experimental Idiopathic Pneumonia Syndrome And Improves Survival Following Allogeneic Stem Cell Transplantation. *Biol. Blood Marrow Trans.*, **2007**, *13*, 105-105.
- (90) Medina, J. Discovery and Development of the CXCR3 Antagonist T487 as Therapy for TH1 Mediated Immune Disorders. Presented at the 29th National Medicinal Chemistry Symposium (Madison, Wisconsin), June 27 - July 1, **2004**.
- (91) van Wanrooij, E. J.; De Jager, S. C.; van Es, T.; de Vos, P.; Birch, H. L.; Owen, D. A.; Watson, R. J.; Biessen, E. A.; Chapman, G. A.; van Berkel, T. J.; Kuiper, J. CXCR3 Antagonist NBI-74330 Attenuates Atherosclerotic Plaque Formation in LDL Receptor-Deficient Mice. *Arterioscler. Thromb. Vasc. Biol.*, **2008**, *28*, 251-257.
- (92) Floren, L. C. Presented at Inflammation 2003 - Sixth World Congress (Vancouver, Canada), Aug 2 - 6, **2003**.
- (93) Berry, K.; Friedrich, M.; Kersey, K.; Stempien, M.; Wagner, F.; van Lier, J.; Sabat, R.; Wolk, K. Evaluation of T0906487, a CXCR3 antagonist, in a phase 2a psoriasis trial. *Inflammation Res.*, **2004**, *Suppl. 53*, pS222.
- (94) Tonn, G. R.; Wong, S. G.; Wong, S. C.; Ye, Q.; M. Schneider; Ma, J. An Inhibitory Metabolite Implicated In The Time-Dependent Increase In AMG 487 Exposures In Healthy Human Subjects Following Multiple Oral Dosing. *Drug Metab. Rev.*, **2006**, *38*, 102-103.
- (95) David V. Goeddel. Tularik expects to begin a Phase 2 study of T487 in patients with rheumatoid arthritis in the first quarter of this year. Presented at the 22nd Annual JP Morgan Healthcare Conference (San Francisco, CA), January 14, **2004**.
- (96) Duquette, J.; Du, X.; Chan, J.; Lemon, B.; Collins, T.; Tonn, G.; Medina, J.; Chen, X. Pyrido[1,2-a]pyrimidin-4-ones as potent CXCR3 antagonists. Presented at the 234th ACS National Meeting (Boston, MA), Aug 19-23, **2007**.
- (97) Du, X.; Chen, X.; Mihalic, J.; Deignan, J.; Duquette, J.; Li, A.-R.; Lemon, B.; Ma, J.; Miao, S.; Ebsworth, K.; Sullivan, T. J.; Tonn, G.; Collins, T.; Medina, J. Design and optimisation of imidazole derivatives as potent CXCR3 antagonists. *Bioorg. Med. Chem. Lett.*, **2008**, *18*, 608-613.
- (98) Li, A.-R.; Johnson, M. G.; Liu, J.; Chen, X.; Du, X.; Mihalic, J. T.; Deignan, J.; Gustin, D. J.; Duquette, J.; Fu, Z.; Zhu, L.; Marcus, A. P.; Bergeron, P.; McGee, L.

- R.; Danao, J.; Sullivan, T.; Ma, J.; Tang, L.; Tonn, G.; Collins, T.; Medina, J. C. Optimisation of the heterocyclic core of the quinazolinone-derived CXCR3 antagonists. *Bioorg. Med. Chem. Lett.*, **2008**, *18*, 688-693.
- (99) Rosenblum, S. B.; Kozlowski, J. A.; Shih, N.-Y.; McGuinness, B. F.; Hobbs, D. W. Heterocyclic Substituted Pyridine Compounds With CXCR3 Antagonist Activity. *WO2007109238*, **2007**.
- (100) McGuinness, B. F.; Rosenblum, S. F.; Kozlowski, J. A.; Anilkumar, G. N.; Kim, S. H.; Shih, N.-Y.; Jenh, C.-H.; Zavodny, P. J.; Hobbs, D. W.; Dong, G.; Shao, Y.; Zawacki, L. G.; Yang, C.; Carroll, C. D. Pyridyl and Phenyl Substituted Piperazine-Piperidines With CXCR3 Antagonist Activity. *WO2006088919*, **2006**.
- (101) Kim, S. H.; Anilkumar, G. N.; Wong, M. K. C.; Zeng, Q.; Rosenblum, S. B.; Kozlowski, J. A.; Shao, Y.; McGuinness, B. F.; Hobbs, D. W. Heterocyclic substituted piperazines with CXCR3 antagonist activity. *WO2006088837*, **2006**.
- (102) Allen, D. R.; Bolt, A.; Chapman, G. A.; Knight, R. L.; Meissner, J. W. G.; Owen, D. A.; Watson, R. J. Identification and structure-activity relationships of 1-aryl-3-piperidin-4-yl-urea derivatives as CXCR3 receptor antagonists. *Bioorg. Med. Chem. Lett.*, **2007**, *17*, 697-701.
- (103) Watson, R. J.; Meissner, J. W. G.; Owen, D. A. Cyclic Quaternary Amino Derivatives As Modulators Of Chemokine Receptors. *WO2004094381*, **2004**.
- (104) Watson, R. J.; Allen, D. R.; Birch, H. L.; Chapman, G. A.; Hannah, D. R.; Knight, R. L.; Meissner, J. W. G.; Owen, D. A.; Thomas, E. J. Development of CXCR3 antagonists. Part 2: Identification of 2-amino(4-piperidinyl)azoles as potent CXCR3 antagonists. *Bioorg. Med. Chem. Lett.*, **2007**, *17*, 6806-6810.
- (105) Watson, R. J.; Allen, D. R.; Birch, H. L.; Chapman, G. A.; Galvin, F. C.; Jopling, L. A.; Knight, R. L.; Meier, D.; Oliver, K.; Meissner, J. W.; Owen, D. A.; Thomas, E. J.; Tremayne, N.; Williams, S. C. Development of CXCR3 Antagonists. Part 3: Tropenyl and homotropenyl-piperidine urea derivatives. *Bioorg. Med. Chem. Lett.*, **2008**, *18*, 147-151.
- (106) Knight, R. L.; Allen, D. R.; Birch, H. L.; Chapman, G. A.; Galvin, F. C.; Jopling, L. A.; Lock, C. J.; Meissner, J. W. G.; Owen, D. A.; Raphy, G.; Watson, R. J.; Williams, S. C. Development of CXCR3 Antagonists, Part 4: Discovery of 2-amino-(4-tropinyl) quinolines. *Bioorg. Med. Chem. Lett.*, **2008**, *18*, 629-633.
- (107) Ohlmeyer, M. H. J.; Swanson, R. N.; Dillard, L. W.; Reader, J. C.; Asouline, G.; Kobayashi, R.; Wigler, M.; Still, W. C. Complex Synthetic Chemical Libraries Indexed with Molecular Tags. *Proc. Natl. Acad. Sci. USA*, **1993**, *90*, 10922-10926.
- (108) Cole, A. G.; Stroke, I. L.; Brescia, M. R.; Simhadri, S.; Zhang, J. J.; Hussain, Z.; Snider, M.; Haskell, C.; Ribeiro, S.; Appell, K. C.; Henderson, I.; Webb, M. L. Identification and initial evaluation of 4-N-aryl-[1,4]diazepane ureas as potent CXCR3 antagonists. *Bioorg. Med. Chem. Lett.*, **2006**, *16*, 200-203.
- (109) Stroke, I. L.; Cole, A. G.; Simhadri, S.; Brescia, M. R.; Desai, M.; Zhang, J. J.; Merritt, J. R.; Appell, K. C.; Henderson, I.; Webb, M. L. Identification of CXCR3 receptor agonists in combinatorial small-molecule libraries. *Biochem. Biophys. Res. Commun.*, **2006**, *349*, 221-228.
- (110) Hayes, M. E.; Wallace, G. A.; Grongsaard, P.; Bischoff, A.; George, D. M.; Miao, W.; McPherson, M. J.; Stoffel, R. H.; Green, D. W.; Roth, G. P. Discovery of small molecule benzimidazole antagonists of the chemokine receptor CXCR3. *Bioorg. Med. Chem. Lett.*, **2008**, *18*, 1573-1576.
- (111) Roth, G.; Wallace, G. A.; George, D. M.; Grongsaard, P.; Hayes, M.; Breinlinger, E. C. 2-Imino-Benzimidazoles. *WO2007084728*, **2007**.
- (112) Coesemans, E.; Bongartz, J. A. M.; Van Lommen, G. R. E. Piperidine derivatives as CXCR3 receptor antagonists. *WO2007090836*, **2007**.
- (113) Coesemans, E.; Bongartz, J. A. M.; Van Lommen, G. R. E.; Van Wauwe, J. P. F.; Buntinx, M. Piperidine derivatives as CXCR3 receptor antagonists. *WO2007090826*, **2007**.
- (114) Zhu, L.; Xu, F.; Collins, T. L.; Medina, J. C. Discovery and optimization of a series of 2,3,4,9-tetrahydro-1H-pyrido[3,4-b]indole derivatives as CXCR3 antagonists. Presented at the 231st ACS National Meeting (Atlanta, GA), March 26-30 **2006**.

- (115) Collins, T.; Medina, J. C.; Xu, F.; Zhu, L. CXCR3 Antagonists. *WO2007062175*, **2007**.
- (116) Baenteli, R.; Glickman, F.; Kovarik, J.; Lewis, I.; Streiff, M.; Thoma, G.; Zerwes, H.-G. Ergoline Derivatives And Their Use As Chemokine Receptor Ligands. *WO2006128658*, **2006**.
- (117) Millan, M. J.; Maiofiss, L.; Cussac, D.; Audinot, V.; Boutin, J. A.; Newman-Tancredi, A. Differential actions of antiparkinson agents at multiple classes of monoaminergic receptor. I. A multivariate analysis of the binding profiles of 14 drugs at 21 native and cloned human receptor subtypes. *J. Pharmacol. Exp. Ther.*, **2002**, *303*, 791-804.
- (118) Axten, J. M.; Foley, J. J.; Kingsbury, W. D.; Sarau, H. M. Imidazolium CXCR3 Inhibitors. *WO03101970*, **2003**.
- (119) Busch-Petersen, J.; Jin, J.; Graybill, T. L.; Kiesow, T.; Rivero, R. A.; Wang, F.; Wang, Y. Camphor-Derived CXCR3 Antagonists. *WO2007076318*, **2007**.
- (120) Adams, A. D.; Green, A. I.; Szweczyk, J. W. Thiazole Derivatives As CXCR3 Receptor Modulators. *WO2007064553*, **2007**.
- (121) Samuel, R.; Santini, C. 2-Arylthiazole Derivatives As CXCR3 Receptor Modulators. *WO2007070433*, **2007**.
- (122) Adams, A. D.; Santini, C. Pyridine, Pyrimidine and Pyrazine Derivatives As CXCR3 Receptor Modulators. *WO2007100610*, **2007**.
- (123) Ali, S.; O'Boyle, G.; Mellor, P.; Kirby, J. A. An apparent paradox: Chemokine receptor agonists can be used for anti-inflammatory therapy. *Mol. Immunol.*, **2007**, *44*, 1477-1482.
- (124) Sgadari, C.; Farber, J. M.; Angiolillo, A. L.; Liao, F.; TeruyaFeldstein, J.; Burd, P. R.; Yao, L.; Gupta, G.; Kanegane, C.; Tosato, G. Mig, the monokine induced by interferon-gamma, promotes tumor necrosis in vivo. *Blood*, **1997**, *89*, 2635-2643.
- (125) Luster, A. D.; Leder, P. Ip-10, a -C-X-C- Chemokine, Elicits a Potent Thymus-Dependent Antitumor Response in-Vivo. *J. Exp. Med.*, **1993**, *178*, 1057-1065.
- (126) Hensbergen, P. J.; Wijnands, P. G. J. T. B.; Schreurs, M. W. J.; Scheper, R. J.; Willemze, R.; Tensen, C. P. The CXCR3 targeting chemokine CXCL11 has potent antitumor activity in vivo involving attraction of CD8(+) T lymphocytes but not inhibition of angiogenesis. *J. Immunother.*, **2005**, *28*, 343-351.
- (127) Haskell, C. A.; Horuk, R.; Liang, M.; Rosser, M.; Dunning, L.; Islam, I.; Kremer, L.; Gutierrez, J.; Marquez, G.; Martinez, C.; Biscione, M. J.; Doms, R. W.; Ribeiro, S. Identification and characterization of a potent, selective nonpeptide agonist of the CC chemokine receptor CCR8. *Mol. Pharmacol.*, **2006**, *69*, 309-316.
- (128) Anderskewitz, R.; Bauer, R.; Bodenbach, G.; Gester, D.; Gramlich, B.; Morschhauser, G.; Birke, F. W. Pyrrolidinoquinazolines - a novel class of CCR3 modulators. *Bioorg. Med. Chem. Lett.*, **2005**, *15*, 669-673.
- (129) Saita, Y.; Kodama, E.; Orita, M.; Kondo, M.; Miyazaki, T.; Sudo, K.; Kajiwara, K.; Matsuoka, M.; Shimizu, Y. Structural basis for the interaction of CCR5 with a small molecule, functionally selective CCR5 agonist. *J. Immunol.*, **2006**, *177*, 3116-3122.
- (130) Dragic, T.; Trkola, A.; Thompson, D. A. D.; Cormier, E. G.; Kajumo, F. A.; Maxwell, E.; Lin, S. W.; Ying, W. W.; Smith, S. O.; Sakmar, T. P.; Moore, J. P. A binding pocket for a small molecule inhibitor of HIV-1 entry within the transmembrane helices of CCR5. *Proc. Natl. Acad. Sci. USA*, **2000**, *97*, 5639-5644.
- (131) Mihara, K.; Smit, M. J.; Krajnc-Franken, M.; Gossen, J.; Rooseboom, M.; Dokter, W. Human CXCR2 (hCXCR2) takes over functionalities of its murine homolog in hCXCR2 knockin mice. *Eur. J. Immunol.*, **2005**, *35*, 2573-2582.
- (132) Saita, Y.; Kondo, M.; Shimizu, Y. Species selectivity of small-molecular antagonists for the CCR5 chemokine receptor. *Int. Immunopharmacol.*, **2007**, *7*, 1528-1534.

Chapter 2

Scope of this thesis

The gene for the chemokine receptor CXCR3 was first cloned in 1996. The protein was identified as the endogenous receptor for the chemokines CXCL9, CXCL10 and CXCL11. Over the years, potential implications of CXCR3 in a variety of inflammatory diseases and in cancer have been studied and clarified to a certain extent. Recently, some controversy regarding the role of CXCR3 in transplant rejection has emerged. Nevertheless, it is thought that CXCR3 inhibition represents an appealing target for developing new classes of compounds that may be used both as pharmacological tools and as potential new drugs.

As described in chapter 1, the only compound that is currently known to have progressed to Phase II clinical trials (AMG 487) showed a lack of efficacy in that setting and hence did not proceed to the next development stages. Therefore, there is a need for new antagonist classes that may aid in fully clarifying the therapeutic potential of CXCR3.

In 2002, at the start of the studies described in this PhD thesis, many publications on the role of CXCR3 and its biogenic ligands CXCL9, CXCL10 and CXCL11 were already available describing e.g. expression studies. However, very little was disclosed on the design and synthesis of small non-peptidergic ligands for CXCR3 (see Figure 2 in Chapter 1), and the only known information was restricted to a few patent reports.

The aim of the research described in the following chapters was to synthesize and pharmacologically evaluate structurally diverse antagonistic ligands for CXCR3 in order to obtain a better understanding of the structural requirements necessary for antagonism on this receptor. Several approaches were followed, including classical SAR studies, pharmacophore models and the concept of bivalent ligands.

Chapter 3 describes the synthesis and pharmacological evaluation of a series of 3-phenyl-3*H*-quinazolin-4-one derivatives for their action as CXCR3 antagonists. A CXCR3 antagonist abstracted from a patent was used as the starting point for the development of high-affinity CXCR3 antagonists. The use of SAR studies led to the identification of a compound with 3 times higher affinity.

Chapter 4 reports on the synthesis and structure activity relationship of 3*H*-pyrido[2,3-*d*]pyrimidin-4-ones and their link with the 3-phenyl-3*H*-quinazolin-4-one series described in Chapter 3. The evaluation of the afforded class of compounds confirmed NBI-74330 as

Chapter 2

a highly efficient, nanomolar CXCR3 antagonist and set the stage for a deeper pharmacological evaluation of this important tool (Chapter 6).

In chapter 5, the synthesis of a series of imidazolium compounds and their affinities at CXCR3 are reported. This new class of compounds was identified after a pharmacophore model development and an optimization of a database screening, followed by a 'merging' approach with a patented CXCR3 ligand scaffold.

Chapter 6 deals with the molecular mechanism of action of diverse small molecule antagonists at the CXCR3 receptor. Additionally, this chapter reports on the behaviour of small CXCR3 ligands at species different from human. Also, a constitutively active mutant of CXCR3 was used which led to the identification of inverse agonistic properties of these small molecules.

In chapter 7, preliminary steps towards the use of dimeric ligands for CXCR3 are illustrated. This was based on the emerging concept of receptor dimerization. Bivalent derivatives of the 3*H*-pyrido[2,3-*d*]pyrimidin-4-ones series (Chapter 4) as well as of the 3-phenyl-3*H*-quinazolin-4-one series (Chapter 3) have been synthesized and evaluated for their affinity and antagonistic activity at CXCR3.

Chapter 3

Synthesis and structure-activity relationship of 3-phenyl-3H-quinazolin-4-one derivatives as CXCR3 chemokine receptor antagonists

Adapted from:

*Stefania Storelli, Pauline Verdijk, Dennis Verzijl, Henk Timmerman, Andrea C. van de Stolpe, Cornelis P. Tensen, Martine J. Smit, Iwan J. P. De Esch and Rob Leurs
Bioorg. Med. Chem. Lett. 2005, 15, 2910 – 2913*

Abstract

A series of 3-phenyl-3H-quinazolin-4-ones has been synthesized and tested for affinity and activity at the chemokine CXCR3 receptor using radioligand binding. The most potent compound, decanoic acid {1-[3-(4-cyano-phenyl)-4-oxo-3,4-dihydroquinazolin-2-yl]-ethyl}-(2-dimethylamino-ethyl)-amide (**1d**), has been further evaluated in functional assays with CXCR3-expressing cells. Compound **1d** efficiently inhibited CXCR3 induced phospholipase C activity and calcium mobilization. Moreover, in CXCR3 expressing human primary T cells, **1d** completely abrogated CXCR3-mediated actin polymerization and chemotaxis, while migration towards CXCR4-ligand CXCL12 was not affected. Compound **1d** is a useful tool for further characterization of the CXCR3 receptor.

Introduction

Chemokines constitute a superfamily of small secreted proteins that attract and activate a variety of cell types. They are classified by structure according to the number and spacing of conserved cysteine residues into four major groups (CC, CXC, CX3C and XC).^{1,2} Chemokine receptors are defined by their ability to signal on binding of one or more members of the chemokine superfamily of chemotactic cytokines. All of them belong to the family of G protein-coupled receptors (GPCRs).^{3,4}

The chemokine receptor CXCR3 is mainly expressed on activated T cells and natural killer cells and binds CXCL9 (monokine induced by IFN- γ ; Mig), CXCL10 (IFN- γ -inducible protein 10; IP10) and CXCL11 (IFN- γ -inducible T cell α -chemoattractant; I-TAC/IP9).⁵⁻⁹ Exposure of cells expressing CXCR3 to CXCL9, CXCL10 and CXCL11 leads to the activation of phospholipase C (PLC) followed by an increase of intracellular calcium via activation of G_i proteins.^{10,11} Furthermore the agonists binding to CXCR3 expressed on human T cells determines a rapid and transient increase in filamentous actin (F-actin) and chemotaxis towards the chemotactic gradient.^{10,11} Increased expression of CXCR3-targeting chemokines is observed in chronic inflammatory diseases (rheumatoid arthritis,^{12,13} multiple sclerosis,¹⁴ hepatitis C-infected liver,¹⁵ atherosclerosis¹⁶ and chronic skin reactions^{10,17,18}) and is associated with the infiltration of CXCR3-positive T-cells.

The involvement of CXCR3 in the pathophysiology of the Th1-type diseases suggests that CXCR3 may serve as a new molecular target for anti-inflammatory therapies.^{19,20}

For further characterization of the receptor and for validating CXCR3 as a viable drug target, the development of small, non-peptidergic CXCR3 ligands is essential. In patent literature, it has been suggested that decanoic acid (2-dimethylamino-ethyl)-{1-[3-(4-fluoro-phenyl)-4-oxo-3,4-dihydro-quinazolin-2-yl]-ethyl}-amide (**1c**) (Figure 1) is a CXCR3 ligand with micromolar affinity.²¹

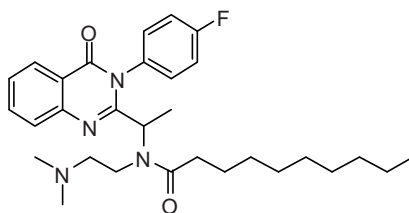


Figure 1. Structure of decanoic acid (2-dimethylamino-ethyl)-{1-[3-(4-fluoro-phenyl)-4-oxo-3,4-dihydro-quinazolin-2-yl]-ethyl}-amide (**1c**)

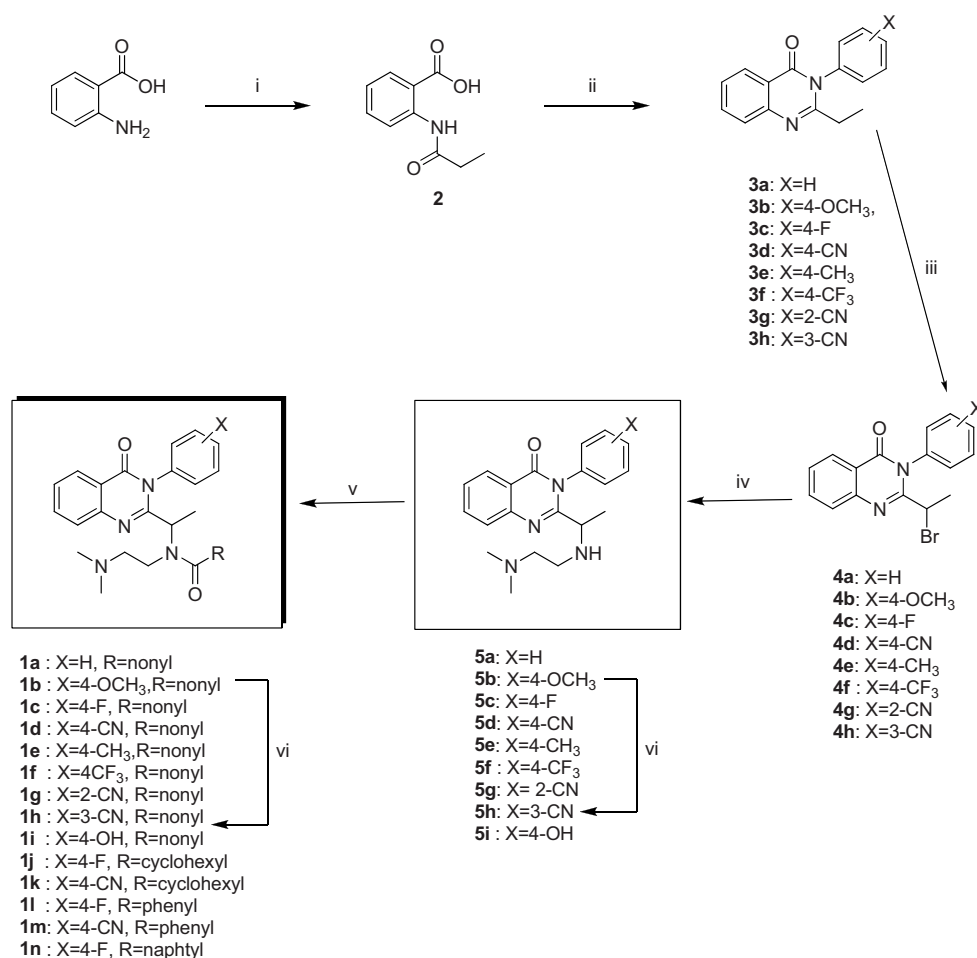
We set out to explore the SAR of this compound. More specifically, the role of the nonyl chain of lead structure (**1c**) was investigated. In addition, the 4-phenyl ring substituent effect on the biological activity was evaluated.²²

Chemistry

The 3-phenyl-3-*H*-quinazolin-4-ones **1a-n** were prepared according to Scheme 1. Reaction of 2-amino-benzoic acid with propionyl chloride gave 2-propionylamino-benzoic acid (**2**) (76% yield). Treatment of this intermediate with phosphorus trichloride and the appropriate substituted aniline gave compounds **3a-h** in moderate to good yields (35-75%). Reaction with bromine gave the intermediates **4a-h** (60-80% yields) that were used for the subsequent reaction with the commercially available *N,N*-dimethyl-ethylene-diamine. The crude oils were readily purified by flash chromatography giving the corresponding key derivatives **5a-h** (5-80% yields). Reaction with decanoyl, cyclohexanecarbonyl, benzoyl or naphthalene-1-carbonyl chloride afforded compound **1a-h** and **1j-n** (15-85 % yields). The methoxy group of **5b** and **1b** was converted to a hydroxy moiety by treatment with boron tribromide^{23,24} to give compounds **5i** and **1i**, respectively, in low isolated yields (10-15%).

Pharmacology

The affinities of compounds **1a-n**, **5a-f** and **5i** for CXCR3 were assayed by testing their ability to displace [¹²⁵I]CXCL10 from HEK-293 cells expressing the human CXCR3 receptor.²⁵ Follow-up pharmacological studies on selected compounds were aimed at inspecting functional activities on CXCR3 in more detail. Toward this end, antagonistic effects of a compound were measured in four different CXCR3-based functional assays: (1) CXCL11-induced phospholipase C activity (2) CXCL11-induced increase of intracellular [Ca²⁺] (3) CXCL11-induced actin polymerization (4) CXCL11-induced chemotaxis of activated T cells.



Scheme 1. Reagents: i) CH₃CH₂COCl, DMF; ii) PCl₃, substituted anilines, toluene; iii) Br₂, CH₃COOH, CH₃COONa; iv) H₂N(CH₂)₂N(CH₃)₂, EtOH, reflux; v) RCOCl, Et₃N, 1,4-dioxane, vi) BBr₃, DCM.

Results and conclusions

In patent literature, compound **1c** has been reported as CXCR3 antagonist in the micromolar range.²¹ We confirmed this result in our binding assay where **1c** showed an IC₅₀ value of 3.2 μM. The importance of the nonyl chain of **1c** was investigated by its removal (**5a-i**) or substitution with different hydrophobic moieties (**1j-n**). These modifications result in a total loss of affinity (Figure 2), suggesting an important role of the flexible aliphatic chain.

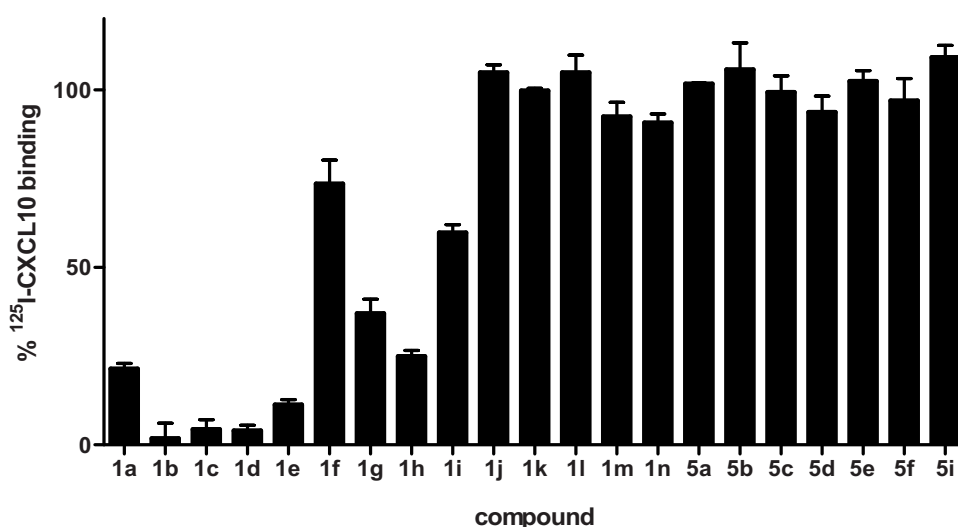


Figure 2. Displacement of [¹²⁵I]-CXCL10 binding to CXCR3. The binding experiments were carried out on HEK-293 cells expressing the human CXCR3 receptor. The compounds **1a-n**, **5a-f** and **5i** (10 μ M) were tested for their ability to displace [¹²⁵I]CXCL10. Error bars show standard error of the mean.

The role of the *para*-fluoro atom of the phenyl ring in the lead compound **1c** was also studied (Table 1). The presence of appropriate substituents is required for affinity at CXCR3, since the unsubstituted analogue (**1a**) is five times less potent (IC_{50} = 15 μ M) than the lead compound (**1c**). Substituents with different electronic and lipophilic properties resulted in ligands with altered affinities for the CXCR3 receptor. The *para*-methoxy and *para*-methyl derivatives (**1b** and **1e**) showed the same degrees of affinity as the prototype, **1c**, whereas the *para*-cyano derivative, **1d**, was 3 fold more potent than **1c**. In fact within this series **1d** is the only compound to show submicromolar affinity. Shifting the cyano substituent from the *para*- to the *ortho*- or *meta*- position caused a large decrease in CXCR3 affinity (IC_{50} = 10 μ M for **1g** and 5.8 μ M for **1h**, respectively). Replacement of the 4-fluoro atom of **1c** by a 4-CF₃ (**1f**) or 4-OH (**1i**) group is not allowed for activity.

Compound **1d** (VUF5834) has the highest affinity for CXCR3 in the [¹²⁵I]CXCL10 binding assay and was therefore tested in different functional assays.

The effect of **1d** on CXCL11- and CXCL10-mediated processes was studied in different signaling assays in human CXCR3 expressing cells and its effects were compared to the analogue without nonyl chain **5d**. Agonist binding to CXCR3 results in the activation of phospholipase C (PLC) via G α_i proteins.¹¹ The effect of **1d** on CXCL11-induced PLC activity was determined by measuring the production of [³H]-inositol phosphates ([³H]-

Table 1. IC₅₀ values of the compounds **1a-i** for their displacement of [¹²⁵I]CXCL10 binding to CXCR3

<i>Compound</i>	R	X	IC₅₀ (μM)^a
1a	nonyl	H	15 (10-20)
1b	nonyl	4-OCH ₃	3.3 (2.2-4.4)
1c	nonyl	4-F	3.2 (2.3-4.2)
1d	nonyl	4-CN	0.93 (0.74-1.1)
1e	nonyl	4-CH ₃	3.1 (2.0-4.1)
1f	nonyl	4-CF ₃	> 100
1g	nonyl	2-CN	10 (8.6-12)
1h	nonyl	3-CN	5.8 (5.1-6.5)
1i	nonyl	4-OH	> 100

^a The binding experiments were carried out on HEK-293 cells expressing the human CXCR3 receptor. The compounds were tested for their ability to displace [¹²⁵I]CXCL10. The values are represented as the mean and the interval of the IC₅₀ (μM) values of at least three independent experiments

IPx) in COS-7-CXCR3 cells. A 10 minute preincubation of COS-7-CXCR3 cells with **1d** inhibited CXCR3-mediated phosphatidylinositol (PI) turnover in a dose-dependent manner (IC₅₀ [10 nM CXCL11]: 6 μM), while **5d** had no effect on this process (Figure 3). Inositol trisphosphate (IP₃), one of the products of PLC activity, induces an increase in intracellular [Ca²⁺] concentrations, by mobilizing [Ca²⁺] from intracellular stores and activating the influx of [Ca²⁺] from the extracellular environment.^{9,10,26} Stimulation of the human CXCR3 receptor with 10 nM CXCL11 resulted in a rapid increase of intracellular [Ca²⁺], which returned thereafter to baseline levels (Figure 4). Pre-incubation of the cells with 10 μM of **1d**, 10 minutes prior to chemokine stimulation completely abrogated the CXCL11-induced [Ca²⁺] increase, while **5d** had no effect (Figure 4). These data demonstrate that compound **1d** can efficiently block CXCL11-induced PI turnover and CXCR3-mediated calcium release.

A consequence of agonist binding to CXCR3 on human T cells is the fast and transient increase of F-actin which is therefore considered one of the earliest measurable biological response. Nevertheless, the following binding of chemoattractants^{10,11} to their receptor is considered as an early sign of lymphocyte migration.²⁷⁻²⁹

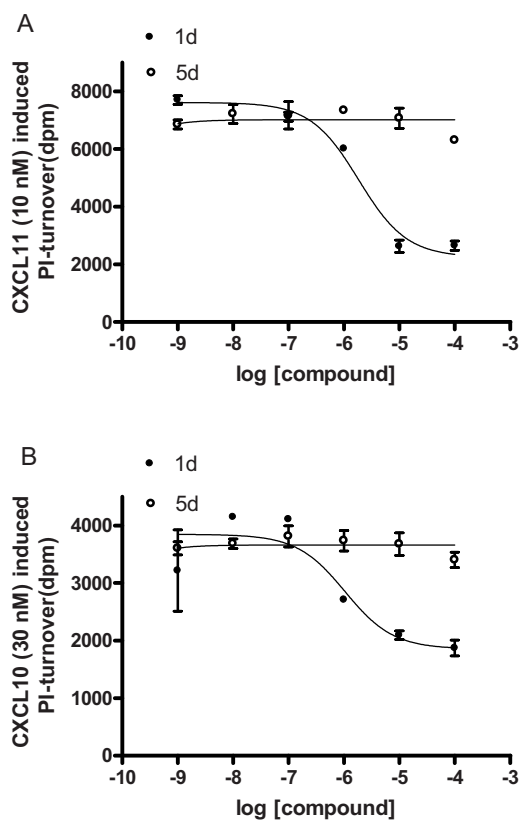


Figure 3. Compound 1d abrogates CXCR3-mediated IP3 production. Effect of **1d** and **5d** on CXCR3-mediated PLC activity by CXCL11 (**A**) and CXCL10 (**B**). PLC activity was measured by the production of [³H]IPx from radioactive labeled inositol in COS-7-CXCR3.

We investigated the effect of **1d** on both CXCR3-induced actin polymerization and migration of human activated T cells. CXCR3-induced increase in actin filaments was completely abrogated in the presence of 1 μ M of **1d** (figure 5) whereas **5d** had no effect on CXCR3-agonist induced actin polymerization, indicating that inhibition was dependent on receptor binding.

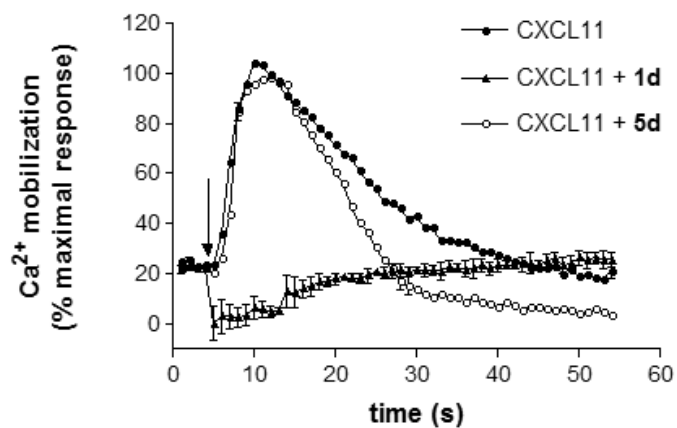


Figure 4. Compound 1d abrogates CXCR3-mediated $[Ca^{2+}]$ mobilization. Effect of compounds **1d** and **5d** ($10 \mu\text{M}$) on the CXCL11 (10 nM) induced Ca^{2+} mobilization in HEK-293-CXCR3 cells. Compounds were added 10 min prior to chemokine stimulation with CXCL11 (indicated by the arrow). The experiment is representative of two independent experiments performed in triplicate defines the maximal response as maximal Ca^{2+} concentration induced. Error bars show standard error of the mean.

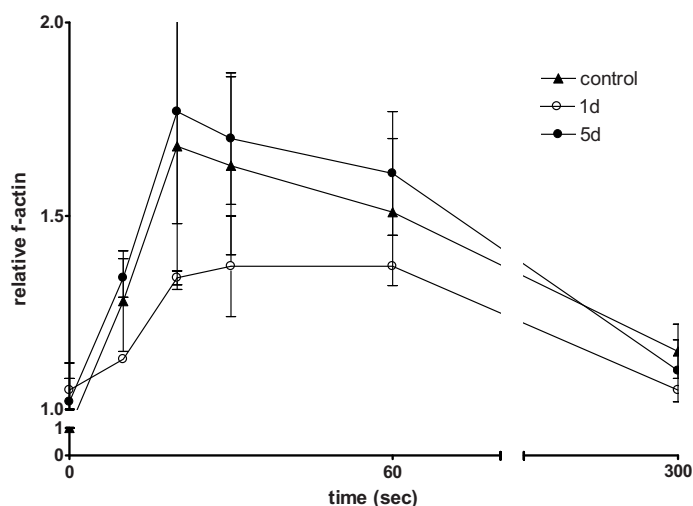


Figure 5. Compound 1d inhibits CXCR3-mediated actin polymerization. Human T cells were isolated from peripheral blood and activated with PHA and IL-2. Actin polymerization in response to CXCL11 was measured in the presence or absence of $1 \mu\text{M}$ of **1d** or **5d**. Results are representative for 3 donors. Error bars show the standard error of the mean.

Subsequently we studied the effect of both **1d** and **5d** on CXCR3-mediated chemotaxis. Migration of activated T cells towards CXCR3-ligands CXCL11 and CXCL10 was dose-dependently inhibited by preincubation with **1d** and not by **5d** (Figure 6A). Compound **1d** inhibited T cell migration induced by 30 nM CXCL11 with an IC₅₀ of 0.5 μM.

Furthermore we studied the **1d** effect on T cell migration towards CXCR4-ligand CXCL12 (30 nM). Compound **1d** did not affect the migration of activated T cells to CXCR4-agonist CXCL12 formerly known as SDF-1 α (Figure 6B), indicating that **1d** acts specifically on CXCR3-mediated migration. Basal migration in the absence of chemoattractants was not changed by **1d**, demonstrating that motility of the cells was not affected.

Conclusions

We have described the SAR of a series of 3-phenyl-3*H*-quinazolin-4-one derivatives for their action as CXCR3 antagonists. Compound **1d** has the highest affinity for the human CXCR3 receptor and is able to effectively inhibit CXCR3 mediated IP3 production and calcium mobilization in cells expressing the human CXCR3. Furthermore compound **1d** abrogates CXCR3 mediated actin polymerization and chemotaxis of human T cells representing therefore a valuable tool for future lead optimization programs.

Experimental section

Chemistry

General. All the reactions were performed under an atmosphere of dry nitrogen. ¹H NMR spectra were recorded on a Bruker AC-200 (200 MHz) spectrometer. Mass spectra were recorded on a Finnigan MAT-90 mass spectrometer. Chromatography was performed on J.T.Baker silica gel for flash chromatography. THF was freshly distilled from LiAlH₄ and DMF was dried on molecular sieves.

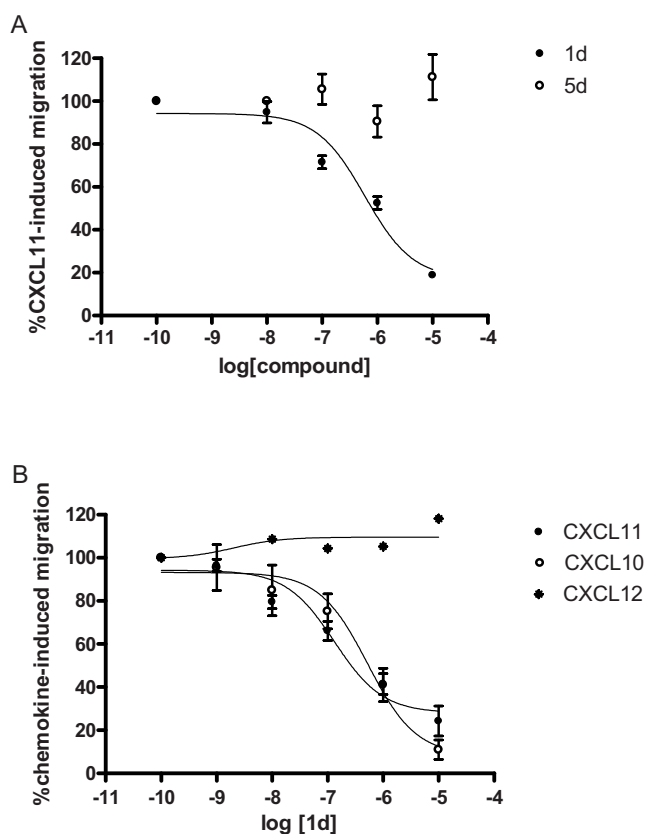


Figure 6. Compound 1d inhibits CXCR3-mediated chemotaxis of human T cells. **A)** Dose-response effect of **1d** and **5d** on chemotaxis of activated T cells induced by 30 nM of CXCL11. **B)** Dose-response effect of **1d** on CXCL11-, CXCL10- and CXCL12-induced chemotaxis (all 30 nM) of activated T cells. Results are representative for 3 donors. Error bars show the standard deviation.

2-Propionylamino-benzoic acid (**2**)

Anthranilic acid (68.6 g, 0.50 mol) was dissolved in N,N-dimethylformamide (250 mL). Propionyl chloride (47.6 mL, 0.55 mol) was added dropwise at such a rate that the temperature of the mixture remained below 40 °C. The product began to precipitate after about one half of the acid chloride was added, and the suspension was stirred vigorously at room temperature for an additional three hours after the addition was completed. The resulting mixture was poured into water (2.0 L) and stirred for an additional two hours. The precipitated product was collected by filtration, washed with water and dried in a vacuum oven at 40 °C under reduced pressure. This afforded 73.03 g (76%) of white

crystals. ¹H NMR (CDCl₃) δ: 1.25 (t, 3H), 2.55 (q, 2H), 6.75 (brs, 1H), 7.07-7.14 (m, 1H), 7.55-7.59 (m, 1H), 8.02-8.14 (m, 1H), 8.72-8.76 (m, 1H), 10.98 (s, 1H).

2-Ethyl-3-phenyl-3*H*-quinazolin-4-one (3a)

To a suspension of 2-propionylamino-benzoic acid (**2**) (3.00 g, 12.52 mmol) and aniline (1.41 mL, 15.52 mmol) in toluene was added dropwise phosphorus chloride (0.96 mL, 6.98 mmol). The resulting suspension was heated to reflux for 8 hours. After cooling to r.t., a saturated sodium carbonate solution was added and the mixture was stirred vigorously until all solid was dissolved. The toluene was removed *in vacuo* and the resulting solid was collected by filtration, rinsed with water, dried and recrystallized from isopropyl alcohol. This afforded 2.74 g (71%) of the desired compound as a white solid. ¹H NMR (CDCl₃) δ: 1.21 (t, 3H), 2.43 (q, 2H), 7.10-7.31 (m, 2H), 7.33-7.61 (m, 4H), 7.62-7.83 (m, 2H), 8.13-8.30 (m, 1H).

2-Ethyl-3-(4-methoxy-phenyl)-3*H*-quinazolin-4-one (3b)

The same procedure as for **3a** was applied, using **2** (8.00 g, 41.41 mmol) and *p*-anisidine (5.10 g, 41.41 mmol). The desired compound was obtained as a white powder (5.49 g, 47%). ¹H NMR (CDCl₃) δ: 1.18 (t, 3H), 2.44 (q, 2H), 4.38 (s, 3H), 6.96-7.18 (m, 4H), 7.35-7.51 (m, 1H), 7.61-7.82 (m, 2H), 8.19-8.34 (m, 1H).

2-Ethyl-3-(4-fluoro-phenyl)-3*H*-quinazolin-4-one (3c)

The same procedure as for **3a** was applied, using 4-fluoroaniline (1.72 g, 15.52 mmol). The desired compound was obtained as a beige powder (3.32 g, 75%). ¹H NMR (CDCl₃) δ: 1.21 (t, 3H), 2.43 (q, 2H), 7.21-7.24 (m, 4H), 7.41-7.49 (m, 1H), 7.68-7.80 (m, 2H), 8.22-8.26 (m, 1H).

4-(2-Ethyl-4-oxo-4*H*-quinazolin-3-yl)benzotrile (3d)

The same procedure as for **3a** was applied, using 4-aminobenzotrile (1.83 g, 15.52 mmol). The desired compound was obtained as a white powder (1.50 g, 35%). ¹H NMR (CDCl₃) δ: 1.18 (t, 3H), 2.34 (q, 2H), 7.30-7.55 (m, 3H), 7.60-7.95 (m, 4H), 8.21-8.29 (m, 1H).

2-Ethyl-3-*p*-tolyl-3*H*-quinazolin-4-one (3e)

The same procedure as for **3a** was applied, using *p*-toluidine (1.66 g, 15.52 mmol). The desired compound was obtained as a yellow oil (2.86 g, 70%). ¹H NMR (CDCl₃) δ: 1.23 (t, 3H), 2.22-2.58 (m = s+q, 5H), 6.88-7.49 (m, 5H), 7.61-7.82 (m, 2H), 8.18-8.29 (m, 1H).

2-Ethyl-3-(4-trifluoromethyl-phenyl)-3H-quinazolin-4-one (3f)

The same procedure as for **3a** was applied, using 4-aminobenzotrifluoride (2.53 mL, 15.52 mmol). The desired compound was obtained as a white powder (2.22 g, 42%). ¹H NMR (CDCl₃) δ: 1.16 (t, 3H), 2.39 (q, 2H), 7.25-7.53 (m, 3H), 7.62-7.95 (m, 4H), 8.16-8.41 (m, 1H).

2-(2-Ethyl-4-oxo-4H-quinazolin-3-yl)-benzonitrile (3g)

The same procedure as for **3a** was applied, using antranilonitrile (1.83 g, 15.52 mmol). The desired compound was obtained as a white powder (1.50 g, 35%). ¹H NMR (CDCl₃) δ: 1.30 (t, 3H), 2.41 (q, 2H), 7.32-7.54 (m, 2H), 7.58-87.99 (m, 5H), 8.27-8.31 (m, 1H).

3-(2-Ethyl-4-oxo-4H-quinazolin-3-yl)-benzonitrile (3h)

The same procedure as for **3a** was applied, using 3-aminobenzonitrile (1.83 g, 15.52 mmol). The desired compound was obtained as a white powder (2.10 g, 50%). ¹H NMR (CDCl₃) δ: 1.20 (t, 3H), 2.38 (q, 2H), 7.39-7.87 (m, 7H), 8.28-8.33 (m, 1H).

2-(1-Bromo-ethyl)-3-phenyl-3H-quinazolin-4-one (4a)

To a mixture of **3a** (2.55 g, 10.21 mmol), anhydrous sodium acetate (1.02 g) and glacial acetic acid (15 mL) at 40 °C, a bromine (0.82 mL, 10.21 mmol) solution in acetic acid was added over a period of 3 hours. After the addition was completed the mixture was poured into water (300 mL) and stirred at room temperature for about 2 hours. The precipitate was isolated by filtration, washed with warm water to remove the trace of the acetic acid, then rinsed with a small amount of isopropyl alcohol and dried to provide the desired compound (1.95 g, 58%) as a yellow solid. ¹H NMR (CDCl₃) δ: 2.01 (d, 3H), 4.52 (q, 1H), 7.00-7.18 (m, 1H), 7.32-7.63, (m, 5H), 7.65-7.82 (m, 2H), 8.22-8.29 (m, 1H).

2-(1-Bromo-ethyl)-3-(4-methoxy-phenyl)-3H-quinazolin-4-one (4b)

This was carried out analogously to the preparation of **4a**, using **3b** (5.33 g, 19.00 mmol). The desired compound was obtained as a pale yellow solid (4.03 g, 59%). ¹H NMR (CDCl₃) δ: 2.02 (d, 3H), 3.38 (s, 3H), 4.60 (q, 1H), 6.91-7.11 (m, 3H), 7.35-7.57 (m, 2H), 7.75-7.80 (m, 2H), 8.18-8.23 (m, 1H).

2-(1-Bromo-ethyl)-3-(4-fluoro-phenyl)-3H-quinazolin-4-one (4c)

This was carried out analogously to the preparation of **4a**, using **3c** (2.03 g, 7.56 mmol). The desired compound was obtained as a pale grey solid (2.20 g, 84%). ¹H NMR (CDCl₃) δ: 2.04 (d, 3H), 4.53 (q, 1H), 7.15-7.32 (m, 3H), 7.47-7.58 (m, 2H), 7.78-7.80 (m, 2H), 8.25-8.29 (m, 1H).

4-[2-(1-Bromo-ethyl)-4-oxo-4*H*-quinazolin-3-yl]- benzonitrile (4d)

This was carried out analogously to the preparation of **4a**, using **3d** (1.50 g, 5.45 mmol). The desired compound was obtained as a pale yellow solid (1.39 g, 72%). ¹H NMR (CDCl₃) δ: 2.02 (d, 3H), 4.40 (q, 1H), 7.25-7.35 (m, 1H), 7.45-7.65 (m, 1H), 7.70-7.95(m, 5H), 8.20-8.24 (m, 1H).

2-(1-Bromo-ethyl)-3-*p*-tolyl-3*H*-quinazolin-4-one (4e)

This was carried out analogously to the preparation of **4a**, using **3e** (2.70 g, 10.21 mmol). The desired compound was obtained as an off white solid (2.69 g, 77%). ¹H NMR (CDCl₃) δ: 2.04 (d, 3H), 2.44 (s, 3H), 4.58 (q, 1H), 6.94-7.09 (m, 1H), 7.30-7.58 (m, 4H), 7.68-7.72 (m, 3H), 8.27-8.31 (d, 1H).

2-(1-Bromo-ethyl)-3-(4-trifluoromethyl-phenyl)-3*H*-quinazolin-4-one (4f)

This was carried out analogously to the preparation of **4a**, using **3f** (2.20 g, 7.56 mmol). The desired compound was obtained as a white solid (2.11 g, 70%). ¹H NMR (CDCl₃) δ: 2.09 (d, 3H), 4.49 (q, 1H), 7.28-7.34 (m, 1H), 7.38-7.56 (m, 1H), 7.58-7.89 (m, 5H), 8.20-8.24 (m, 1H).

2-[2-(1-Bromo-ethyl)-4-oxo-4*H*-quinazolin-3-yl]-benzonitrile (4g)

This was carried out analogously to the preparation of **4a**, using **3g** (1.50 g, 5.45 mmol). The desired compound was obtained as a pale yellow solid (1.52 g, 79%). ¹H NMR (CDCl₃) δ: 1.98-2.18 (m, 3H), 4.35 (q, 0.7H), 4.59 (q, 0.3H), 7.30-7.35 (m, 0.5H), 7.49-7.98 (m, 6.5H), 8.20-8.25 (m, 1H).

3-[2-(1-Bromo-ethyl)-4-oxo-4*H*-quinazolin-3-yl]-benzonitrile (4h)

This was carried out analogously to the preparation of **4a**, using **3h** (2.00 g, 7.26 mmol). The desired compound was obtained as a white solid (2.07 g, 80%). ¹H NMR (CDCl₃) δ: 2.04-2.09 (m, 3H), 4.41 (q, 1H), 7.42-7.58 (m, 2H), 7.63-7.89 (m, 5H), 8.23-8.27 (m, 1H).

2-[1-(2-Dimethylamino-ethylamino)-ethyl]-3-phenyl-3*H*-quinazolin-4-one (5a)

A mixture of compound **4a** (1.90 g, 5.77 mmol) and N,N dimethylethylenediamine (1.01 mL, 9.23 mmol) in 100 mL ethanol was heated to reflux for 18 hours. The ethanol was removed in vacuo and the concentrate dissolved in chloroform and extracted with saturated aqueous sodium bicarbonate solution (3×50 mL). The combined organic extracts were dried over sodium sulphate, filtered and concentrated *in vacuo*. The crude material was purified by flash chromatography on silica gel eluting with methanol/dichloromethane (1:9) to afford the desired compound as a colourless oil (1.23

g, 63%). ^1H NMR (CDCl_3) δ : 1.17 (d, 3H, CH_3CH), 2.09-2.70 (s+m, 10H, $(\text{CH}_3)_2\text{N}$, $\text{NCH}_2\text{CH}_2\text{N}$), 3.34 (q, 1H, CH_3CH), 4.25 (brs, 1H, NH), 7.03-7.19 (m, 2H), 7.23-7.51, (m, 4H), 7.53-7.72 (m, 2H), 8.09-8.13 (m, 1H); MS(ESI) m/z 337 ($\text{M}+\text{H}$) $^+$. The (+)-tartrate salt of compound **5a** was prepared and subsequently recrystallized from 2-PrOH:EtOH (1:1). ^1H NMR (DMSO) δ : 1.18 (d, 3H), 2.46-2.92 (s+m, 10H), 3.18 (s, 1H), 4.15 (s, 2H), 7.15-7.94 (m, 10H), 8.11-8.13 (m, 1H).

2-[1-(2-Dimethylamino-ethylamino)-ethyl]-3-(4-methoxy-phenyl)-3H-quinazolin-4-one (5b)

This procedure was performed analogously to the synthesis of **5a**, using **4b** (4.00 g, 11.13 mmol). Compound **5b** was obtained as a solid after flash chromatography (2.19 g, 54%). ^1H NMR (CDCl_3) δ : 1.22 (d, 3H, CH_3CH), 2.12-2.64 (s+m, 10H, $(\text{CH}_3)_2\text{N}$, $\text{NCH}_2\text{CH}_2\text{N}$), 2.88 (brs, 1H, NH), 3.52 (q, 1H, CH_3CH), 3.80 (s, 3H, CH_3O), 6.91-7.18 (m, 4H), 7.40-7.51, (m, 1H), 7.59-7.68 (m, 2H), 8.18-8.22 (m, 1H); MS(ESI) m/z 367 ($\text{M}+\text{H}$) $^+$.

2-[1-(2-Dimethylamino-ethylamino)-ethyl]-3-(4-fluoro-phenyl)-3H-quinazolin-4-one (5c)

This procedure was performed analogously to the synthesis of **5a**, using **4c** (2.62 g, 7.55 mmol). Compound **5c** was obtained as a solid after flash chromatography (0.99 g, 37%). ^1H NMR (CDCl_3) δ : 1.20 (d, 3H, CH_3CH), 2.22-2.80 (s+m, 10H, $(\text{CH}_3)_2\text{N}$, $\text{NCH}_2\text{CH}_2\text{N}$), 3.39 (q, 1H, CH_3CH), 4.41 (brs, 1H, NH), 7.00-7.22 (m, 4H), 7.32-7.41 (m, 1H), 7.55-7.77 (m, 2H), 8.11-8.15 (d, 1H); MS(ESI) m/z 355 ($\text{M}+\text{H}$) $^+$.

4-{2-[1-(2-Dimethylamino-ethylamino)-ethyl]-4-oxo-4H-quinazolin-3-yl}-benzotrile (5d)

This procedure was performed analogously to the synthesis of **5a**, using **4d** (1.30 g, 4.49 mmol). Compound **5d** was obtained as a white solid after flash chromatography (1.11 g, 68%). ^1H NMR (CDCl_3) δ : 1.23 (d, 3H, CH_3CH), 2.22 (s, 6H, $(\text{CH}_3)_2\text{N}$), 2.30-2.59 (m, 4H, $\text{NCH}_2\text{CH}_2\text{N}$), 3.31 (q, 1H, CH_3CH), 7.22-7.50, (m, 3H), 7.70-7.86 (m, 4H), 8.20-8.24 (m, 1H); MS(ESI) m/z 362 ($\text{M}+\text{H}$) $^+$.

2-[1-(2-Dimethylamino-ethylamino)-ethyl]-3-*p*-tolyl-3H-quinazolin-4-one (5e)

This procedure was performed analogously to the synthesis of **5a**, using **4e** (2.60 g, 7.57 mmol). Compound **5e** was obtained as a pale yellow solid after flash chromatography (1.71 g, 64%). ^1H NMR (CDCl_3) δ : 1.21 (d, 3H, CH_3CH), 2.18 (s, 6H, $(\text{CH}_3)_2\text{N}$), 2.30-2.70 (s+m, 7H, $\text{NCH}_2\text{CH}_2\text{N}$, $\text{CH}_3\text{-Ar}$), 3.11 (brs, 1H, NH), 3.43 (q, 1H, CH_3CH), 6.98-7.17 (m, 2H), 7.23-7.50 (m, 3H), 7.60-7.79 (m, 2H), 8.19-8.23 (m, 1H); MS(ESI) m/z 351

(M+H)⁺.

2-[1-(2-Dimethylamino-ethylamino)-ethyl]-3-(4-trifluoromethyl-phenyl)-3*H*-quinazolin-4-one (5f)

This procedure was performed analogously to the synthesis of **5a**, using **4f** (2.00 g, 5.04 mmol). Compound **5f** was obtained as a white powder after flash chromatography (1.59 g, 78%). ¹H NMR (CDCl₃) δ: 1.21 (d, 3H, CH₃CH), 2.12 (s, 6H, (CH₃)₂N), 2.21-2.40 (m, 4H, NCH₂CH₂N), 2.81 (brs, 1H, NH), 3.30 (q, 1H, CH₃CH), 7.28-7.48 (m, 3H), 7.58-7.82 (m, 4H), 8.01-8.05 (m, 1H); MS(ESI) m/z 405 (M+H)⁺.

2-{2-[1-(2-Dimethylamino-ethylamino)-ethyl]-4-oxo-4*H*-quinazolin-3-yl}-benzotrile (5g)

This procedure was performed analogously to the synthesis of **5a**, using **4g** (1.50 g, 4.23 mmol). Compound **5g** was obtained as a white powder after flash chromatography (0.07 g, 5%). ¹H NMR (CDCl₃) δ: 1.28 (d, 1.5H, CH₃CH), 1.34 (d, 1.5H, CH₃CH), 2.18 (s, 3H, (CH₃)₂N), 2.24 (s, 3H, (CH₃)₂N), 2.35-2.98 (m, 5H, NCH₂CH₂N+NH), 3.21 (q, 0.5H, CH₃CH), 3.31 (q, 0.5H, CH₃CH), 7.36-7.60 (m, 2H), 7.62-7.88 (m, 5H), 8.22-8.28 (m, 1H); MS(ESI) m/z 362 (M+H)⁺.

3-{2-[1-(2-Dimethylamino-ethylamino)-ethyl]-4-oxo-4*H*-quinazolin-3-yl}-benzotrile (5h)

This procedure was performed analogously to the synthesis of **5a**, using **4h** (2.00 g, 5.65 mmol). Compound **5g** was obtained as a white powder after flash chromatography (0.09 g, 4%). ¹H NMR (CDCl₃) δ: 1.24 (d, 3H, CH₃CH), 2.12 (s, 6H, (CH₃)₂N), 2.32-2.56 (m, 4H, NCH₂CH₂N), 2.62 (brs, 1H, NH), 3.31 (q, 1H, CH₃CH), 7.32-7.88 (m, 7H), 8.16-8.20 (m, 1H); MS(ESI) m/z 362 (M+H)⁺.

2-[1-(2-Dimethylamino-ethylamino)-ethyl]-3-(4-hydroxy-phenyl)-3*H*-quinazolin-4-one (5i)

A boron tribromide solution (1M in dichloromethane, 5.25 mL, 5.46 mmol) was added to a cooled (0°C) solution of **5b** (0.50 g, 1.36 mmol) in anhydrous dichloromethane under nitrogen atmosphere. An orange precipitate formed immediately. The flask was covered with aluminium foil. The mixture was warmed to room temperature and then stirred for 16 hours. All volatiles were removed under reduced pressure and the resulting residue treated with methanol to quench the borate intermediates. The methanol was removed in vacuo, the crude material was treated with a sodium carbonate saturated solution and then extracted with dichloromethane (3x25 mL). The organic phases were dried over magnesium sulphate, filtered and concentrated. The crude material was purified by flash

chromatography on silica gel eluting with DCM/MeOH (7.5:2.5). Fractions containing product were combined to afford **5i** as a white solid (0.23 g, 12%). ¹H NMR (CDCl₃) δ: 1.22 (d, 3H, CH₃CH), 2.11 (s, 6H, (CH₃)₂N), 2.30-2.81 (m, 5H, NCH₂CH₂N+NH), 3.58 (q, 1H, CH₃CH), 5.63 (brs, 1H, Ar-OH, exchangeable with D₂O), 6.58-7.08 (m, 4H), 7.29-7.49 (m, 1H), 7.58-7.79 (m, 2H), 8.12-8.17 (m, 1H); MS(ESI) m/z 353 (M+H)⁺.

Decanoic acid (2-dimethylamino-ethyl)-[1-(4-oxo-3-phenyl-3,4-dihydro-quinazolin-2-yl)-ethyl]-amide (1a)

Compound **5a** (0.34 g, 1.00 mmol) and triethylamine (0.14 mL, 1.00 mmol) were dissolved in 25 mL dioxane. Decanoyl chloride (0.21 mL, 1.00 mmol) was added to the solution. The resulting mixture was stirred at room temperature for 18 hours and then concentrated under reduced pressure. The residue was dissolved in dichloromethane (50 mL) and washed with saturated aqueous Na₂CO₃ solution (50 mL), then twice with water (50 mL). The organic phases were dried over anhydrous Na₂SO₄, filtered and evaporated. The crude material was purified by flash chromatography on silica gel eluting with ethyl acetate/methanol (9:1). This afforded the desired compound (0.31 g, 63%) as a colourless oil. ¹H NMR (CDCl₃) δ: 0.90 (t, 3H), 1.13-1.32 (m, 16H, CH₂), 1.36 (d, 1.2H, CH₃), 1.51 (d, 1.8H, CH₃), 2.01 (s, 2.4H, N(CH₃)₂), 2.13 (s, 3.6H, N(CH₃)₂), 2.18-2.21 (m, 1H, CH₂N), 2.38-2.52 (m, 1H, CH₂N), 3.32-3.57 (m, 2H, CH₂NCO), 4.71 (q, 0.4H, CH), 5.37 (q, 0.6H, CH), 7.35-7.90 (m, 8H), 8.25 (d, 1H); MS(ESI) m/z 492 (M+H)⁺. The compound was obtained as a crystalline material after (+)-tartrate salt formation followed by recrystallization from isopropyl alcohol. ¹H NMR (D₂O) δ: 0.92 (t, 3H), 1.00-1.32 (m, 16H, CH₂), 1.61 (d, 3H, CH₃), 2.35 (s, 5H, N(CH₃)₂), 2.45 (s, 1H, N(CH₃)₂), 3.10-3.18 (m, 2H, CH₂N), 3.53-3.56 (m, 2H, CH₂NCO), 4.62 (s, 4H, 2(CHOH)₂), 5.09 (q, 1H, CH), 7.15-8.00 (m, 8H), 8.10 (d, 1H).

Decanoic acid (2-dimethylamino-ethyl)-{1-[3-(4-methoxy-phenyl)-4-oxo-3,4-dihydro-quinazolin-2-yl]-ethyl}-amide (1b)

The same procedure as for **1a** was applied using **5b** (0.37 g, 1.00 mmol). This afforded **1b** as a colourless oil (0.29 g, 55%). ¹H NMR (CDCl₃) δ: 0.75 (t, 3H), 1.08-1.22 (m, 16H, CH₂), 1.23 (d, 1.2H, CH₃), 1.43 (d, 1.8H, CH₃), 1.83 (s, 4H, N(CH₃)₂), 1.92 (s, 2H, N(CH₃)₂), 2.08-2.22 (m, 1H, CH₂N), 2.23-2.42 (m, 1H, CH₂N), 3.20-3.52 (m, 2H, CH₂NCO), 3.68 (s, 3H, OCH₃), 4.78 (q, 0.4H, CH), 5.25 (q, 0.6H, CH), 7.35-7.90 (m, 7H), 8.25 (d, 1H); MS(ESI) m/z 522 (M+H)⁺. The compound was obtained as a crystalline material after fumarate salt formation followed by recrystallization from isopropyl alcohol. ¹H NMR (DMSO) δ: 0.85 (t, 3H), 1.12-1.32 (m, 16H, CH₂), 1.34 (d, 1.2H, CH₃), 1.46 (d, 1.8H, CH₃), 2.15 (s, 4H, N(CH₃)₂), 2.30 (s, 2H, N(CH₃)₂), 3.28-3.32 (m, 2H, CH₂N), 3.35

(m, 2H, CH₂NCO), 3.80 (s, 3H, OCH₃), 4.78 (q, 0.4H, CH), 5.21 (q, 0.6H, CH), 6.55 (s, 4H, 2(CH=CH)), 6.90-7.90 (m, 7H), 8.25 (d, 1H).

Decanoic acid (2-dimethylamino-ethyl)-{1-[3-(4-fluoro-phenyl)-4-oxo-3,4-dihydro-quinazolin-2-yl]-ethyl}-amide (1c)

The same procedure as for **1a** was applied using **5c** (0.35 g, 1.00 mmol). This afforded **1c** as colourless oil (0.26 g, 51%). ¹H NMR (CDCl₃) δ: 0.80 (t, 3H), 1.08-1.25 (m, 14H, CH₂), 1.38 (d, 0.9H, CH₃) 1.50 (d, 2.1H, CH₃), 1.95 (s, 1.5H, N(CH₃)₂), 2.16 (s, 4.5H, N(CH₃)₂), 2.18-2.30 (m, 1H, CH₂CON), 2.32-2.53 (m, 1H, CH₂CON), 3.22-3.52 (m, 4H, CH₂NCO, CH₂N), 4.74 (q, 0.5H, CH), 5.32 (q, 0.5H, CH), 7.13-7.81 (m, 7H), 8.25 (d, 1H); MS(ESI) m/z 510 (M+H)⁺. The compound was obtained as a crystalline solid after fumarate salt formation followed by recrystallization from isopropyl alcohol. ¹H NMR (DMSO) δ: 0.84 (t, 3H), 0.98-1.38 (m, 14H, CH₂), 1.43 (d, 3H, CH₃), 2.05-2.72 (s+m, 10H, N(CH₃)₂, CH₂CON, CH₂N), 2.98-3.41 (m, 2H, CH₂NCO), 5.22 (q, 1H, CH), 7.15-7.90 (m, 7H), 8.15 (d, 1H).

Decanoic acid {1-[3-(4-cyano-phenyl)-4-oxo-3,4-dihydro-quinazolin-2-yl]-ethyl}-(2-dimethylamino-ethyl)-amide (1d)

The same procedure as for **1a** was applied using **5d** (0.36 g, 1.00 mmol). This afforded **1d** as a white powder (0.33 g, 63%). ¹H NMR (CDCl₃) δ: 0.78 (t, 3H), 1.17-1.23 (m, 16H, CH₂), 1.26 (d, 3H, CH₃) 1.90 (s, 1H, N(CH₃)₂), 2.21 (s, 5H, N(CH₃)₂), 2.29 (m, 2H, CH₂N), 3.28-3.43 (m, 2H, CH₂NCO), 4.66 (q, 0.2H, CH), 5.21 (q, 0.8H, CH), 7.24-7.89 (m, 7H), 8.20 (d, 1H); MS(ESI) m/z 516 (M+H)⁺.

Decanoic acid (2-dimethylamino-ethyl)-[1-(4-oxo-3-*p*-tolyl-3,4-dihydro-quinazolin-2-yl)-ethyl]-amide (1e)

The same procedure as for **1a** using **5e** (0.35 g, 1.00 mmol). This afforded **1e** as colourless oil (0.28 g, 55%). ¹H NMR (CDCl₃) δ: 0.78 (t, 3H), 0.99-1.31 (m, 16H, CH₂), 1.32 (d, 1.0H, CH₃) 1.48 (d, 2.0H, CH₃), 1.95 (s, 3H, N(CH₃)₂), 2.14 (s, 3H, N(CH₃)₂), 2.18-2.22 (m, 2H, CH₂N) 2.41 (s, 3H, Ar-CH₃), 3.22-3.52 (m, 2H, CH₂NCO), 4.78 (q, 0.5H, CH), 5.33 (q, 0.5H, CH), 6.83-7.83 (m, 7H), 8.25 (d, 1H); MS(ESI) m/z 506 (M+H)⁺. The compound was obtained as a crystalline solid after (+)-tartrate salt formation followed by recrystallization from isopropyl alcohol. ¹H NMR (CD₃OD) δ: 0.90 (t, 3H), 1.15-1.40 (m, 16H, CH₂), 1.62 (d, 3H, CH₃), 2.40 (s, 3H, Ar-CH₃), 2.48-2.52 (m, 2H, CH₂N), 2.80 (s, 6H, N(CH₃)₂), 3.45-3.48 (m, 2H, CH₂NCO), 4.45 (s, 4H, 2(CHOH)₂), 5.10 (q, 1H, CH), 7.10-8.10 (m, 7H), 8.25 (d, 1H).

Decanoic acid (2-dimethylamino-ethyl)-{1-[4-oxo-3-(4-trifluoromethyl-phenyl)-3,4-dihydro-quinazolin-2-yl]-ethyl}-amide (1f)

The same procedure as for **1a** was applied using **5f** (0.40 g, 1.00 mmol). This afforded **1f** as a white wax (0.47 g, 84 %). ^1H NMR (CDCl_3) δ : 0.79 (t, 3H), 1.12-1.32 (m, 16H, CH_2), 1.35 (d, 1.5H, CH_3) 1.52 (d, 1.5H, CH_3), 1.90 (s, 2H, $\text{N}(\text{CH}_3)_2$), 2.12 (s, 4H, $\text{N}(\text{CH}_3)_2$), 2.20-2.52 (m, 2H, CH_2N), 3.20-3.52 (m, 2H, CH_2NCO), 4.60 (q, 0.3H, CH), 5.20 (q, 0.7H, CH), 7.21-7.83 (m, 7H), 8.15 (d, 1H); MS(ESI) m/z 560 ($\text{M}+\text{H}$) $^+$.

Decanoic acid {1-[3-(2-cyano-phenyl)-4-oxo-3,4-dihydro-quinazolin-2-yl]-ethyl}-(2-dimethylamino-ethyl)-amide (1g)

The same procedure as for **1a** was applied using **5g** (0.36 g, 1.00 mmol). This afforded **1g** as colourless oil (0.10 g, 20%). ^1H NMR (CDCl_3) δ : 0.80 (t, 3H), 1.08-1.19 (m, 16H, CH_2), 1.39 (d, 3H, CH_3), 2.10 (s, 6H, $\text{N}(\text{CH}_3)_2$), 2.10-2.62 (m, 2H, CH_2N), 3.18-3.35 (m, 1H, CH_2NCO), 3.41-3.55 (m, 1H, CH_2NCO), 5.23 (q, 0.4H, CH), 5.63 (q, 0.6H, CH), 7.31 (d, 1H), 7.43-7.62 (m, 3H), 7.68-7.97 (m, 3H), 8.18-8.31 (m, 1H); MS(ESI) m/z 516 ($\text{M}+\text{H}$) $^+$. The compound was obtained as a crystalline solid after (+)-tartrate salt formation followed by recrystallization from isopropyl alcohol. ^1H NMR (D_2O) δ : 0.88-1.57 (m, 22H) 2.62 (s, 6H, $\text{N}(\text{CH}_3)_2$), 2.99-3.23 (m, 2H, CH_2N), 3.25-3.60 (m, 3H, $\text{CH}_2\text{NCO}+\text{CH}$), 4.50 (s, 4H, $2(\text{CHOH})_2$), 7.30 -8.20 (m, 8H).

Decanoic acid {1-[3-(3-cyano-phenyl)-4-oxo-3,4-dihydro-quinazolin-2-yl]-ethyl}-(2-dimethylamino-ethyl)-amide (1h)

The same procedure as for **1a** was applied using **5h** (0.36 g, 1.00 mmol). This afforded **1h** as colourless oil (0.12g, 26%). ^1H NMR (CDCl_3) δ : 0.80 (t, 3H), 1.12-1.21 (m, 16H, CH_2), 1.34 (d, 3H, CH_3), 2.04 (s, 3H, $\text{N}(\text{CH}_3)_2$), 2.17 (s, 3H, $\text{N}(\text{CH}_3)_2$), 2.19-2.50 (m, 2H, CH_2N), 3.22-3.54 (m, 2H, CH_2NCO), 5.16 (q, 0.5H, CH), 5.38 (q, 0.5H, CH), 7.32-7.98 (m, 7H), 8.20 (d, 1H); MS(ESI) m/z 516 ($\text{M}+\text{H}$) $^+$. The compound was obtained as a crystalline solid after (+)-tartrate salt formation followed by recrystallization from isopropyl alcohol. ^1H NMR (D_2O) δ : 0.80-1.82 (m, 22H), 2.77 (s, 3H, $\text{N}(\text{CH}_3)_2$), 2.83 (s, 3H, $\text{N}(\text{CH}_3)_2$), 3.12-3.30 (m, 2H, CH_2N), 3.63-3.97 (m, 2H, CH_2NCO), 4.45(s, 4H, $2(\text{CHOH})_2$), 5.20 (q, 1H, CH), 7.22 -7.89 (m, 8H).

Decanoic acid (2-dimethylamino-ethyl)-{1-[3-(4-hydroxy-phenyl)-4-oxo-3,4-dihydro-quinazolin-2-yl]-ethyl}-amide (1i)

The same procedure as for **5i** was applied using **1b** (0.53 g, 1.00 mmol). This afforded **1i** as a colorless oil (0.05 g, 10%). ^1H NMR (CDCl_3) δ : 0.84 (t, 3H), 1.12-1.33 (m, 16H, CH_2), 1.38 (d, 1.4H, CH_3) 1.62 (d, 1.6H, CH_3), 2.00 (s, 2.5H, $\text{N}(\text{CH}_3)_2$), 2.22 (s, 3.5H, $\text{N}(\text{CH}_3)_2$), 2.23-2.40 (m, 1H, CH_2N), 2.42-2.63 (m, 1H, CH_2N), 3.33-3.62 (m, 2H,

CH_2NCO), 4.92 (q, 0.4H, CH), 5.15 (s, 1H exchangeable with D_2O , OH), 5.43 (q, 0.6H, CH), 6.68-7.22 (m, 4H), 7.40-7.79 (m, 3H), 8.24 (d, 1H); MS(ESI) m/z 508 (M+H)⁺. The compound was obtained as a crystalline solid after (+)-tartrate salt formation followed by recrystallization from isopropyl alcohol. ¹H NMR (CD_3OD) δ : 0.92 (t, 3H), 1.10-1.32 (m, 16H, CH_2), 1.57 (d, 3H, CH_3), 2.83 (s, 6H, $\text{N}(\text{CH}_3)_2$), 3.12-3.62 (m, 4H, $\text{CH}_2\text{N}+\text{CH}_2\text{NCO}$), 4.40 (s, 4H, $2(\text{CHOH})_2$), 5.40 (q, 1H, CH), 6.68-7.23 (m, 4H), 7.37-7.81 (m, 3H), 8.20 (d, 1H).

Cyclohexanecarboxylic acid (2-dimethylamino-ethyl)-{1-[3-(4-fluoro-phenyl)-4-oxo-3,4-dihydro-quinazolin-2-yl]-ethyl}-amide (1j)

The same procedure as for **1a** was applied using **5c** (0.35 g, 1.00 mmol) and cyclohexane carboxylic acid chloride (0.16 mL, 1mmol). This afforded **1j** as a white solid (0.23 g, 50%). ¹H NMR (CDCl_3) δ : 1.12-1.99 (m, 14H), 2.21 (s, 6H, $\text{N}(\text{CH}_3)_2$), 2.22-2.58 (m, 2H, CH_2N), 3.32-3.70 (m, 2H, CH_2NCO), 4.81 (q, 0.2H, CH), 5.18 (q, 0.8H, CH), 7.08-7.80 (m, 7H), 8.20 (d, 1H); MS(ESI) m/z 466 (M+H)⁺.

Cyclohexanecarboxylic acid {1-[3-(4-cyano-phenyl)-4-oxo-3,4-dihydro-quinazolin-2-yl]-ethyl}-(2-dimethylamino-ethyl)-amide (1k)

The same procedure as for **1a** was applied using **5d** (0.36 g, 1.00 mmol) and cyclohexane carboxylic acid chloride (0.16 mL, 1mmol). This afforded **1k** as a white solid (0.23 g, 49%). ¹H NMR (CDCl_3) δ : 1.11-2.00 (m, 14H), 2.23 (s, 6H, $\text{N}(\text{CH}_3)_2$), 2.18-2.43 (m, 2H, CH_2N), 3.42-3.62 (m, 2H, CH_2NCO), 5.18 (q, 1H, CH), 7.26-7.91 (m, 7H), 8.30 (d, 1H); MS(ESI) m/z 473 (M+H)⁺.

***N*-(2-Dimethylamino-ethyl)-*N*-{1-[3-(4-fluoro-phenyl)-4-oxo-3,4-dihydro-quinazolin-2-yl]-ethyl}-benzamide (1l)**

The same procedure as for **1a** was applied using **5c** (0.36 g, 1.00 mmol) and benzoyl chloride (0.12 mL, 1.00 mmol). This afforded **1l** as a white solid (0.11 g, 24%). ¹H NMR (CDCl_3) δ : 1.49 (d, 3H, CH_3), 1.81 (s, 6H, $\text{N}(\text{CH}_3)_2$), 2.16-2.30 (m, 2H, CH_2N), 3.33-3.45 (m, 2H, CH_2NCO), 5.24 (q, 1H, CH), 7.20-8.01 (m, 12H), 8.30 (d, 1H); MS(ESI) m/z 460 (M+H)⁺.

***N*-{1-[3-(4-Cyano-phenyl)-4-oxo-3,4-dihydro-quinazolin-2-yl]-ethyl}-*N*-(2-dimethylamino-ethyl)-benzamide (1m)**

The same procedure as for **1a** was applied using **5d** (0.36 g, 1.00 mmol) and benzoyl chloride (0.12 mL, 1.00 mmol). This afforded **1m** as a white solid (0.07 g, 15%). ¹H NMR (CDCl_3) δ : 1.43 (d, 3H, CH_3), 1.92 (s, 6H, $\text{N}(\text{CH}_3)_2$), 2.11-2.37 (m, 2H, CH_2N), 3.32-3.55 (m, 2H, CH_2NCO), 5.23 (q, 1H, CH), 6.80-8.11 (m, 12H), 8.20 (d, 1H); MS(ESI) m/z 467 (M+H)⁺.

Naphthalene-1-carboxylic acid (2-dimethylamino-ethyl)-{1-[3-(4-fluorophenyl)-4-oxo-3,4-dihydro-quinazolin-2-yl]-ethyl}-amide (1n)

The same procedure as for **1a** was applied using **5c** (0.36 g, 1.00 mmol) and 1-naphtoyl chloride (0.15 mL, 1.00 mmol). This afforded **1n** as a white solid (0.17 g, 33%). ¹H NMR (CDCl₃) at 100 °C δ: ¹H NMR (CDCl₃) δ: 1.22 (d, 3H, CH₃), 2.00 (s, 6H, N(CH₃)₂), 2.13-2.52 (m, 4H, CH₂N), 3.23-3.42 (CH₂NCO), 5.37 (q, 1H, CH), 7.22-8.25 (m, 15H), 8.88 (d, 1H); MS(ESI) m/z 510 (M+H)⁺.

Pharmacology

Radioligand binding assay

HEK293-CXCR3 cells were grown at 5% CO₂ at 37°C in Dulbecco's modified Eagle's medium supplemented with 10% fetal bovine serum, 250 mg/mL G-418, 50 IU of penicillin per mL, and 50 mg of streptomycin per mL. These cells were seeded in poly-L-Lysine-coated 48-well plates. After 24h, binding was performed on whole cells for 4h at 4°C using approximately 70 pM [¹²⁵I]-labelled CXCL10 (Perkin Elmer Life Science, Boston, USA) in binding buffer (50 mM HEPES [pH 7.4], 1 mM CaCl₂, 5 mM MgCl₂, 0.5% BSA) containing increasing concentrations of the indicated compounds. After incubation, cells were washed three times with ice-cold binding buffer supplemented with 0.5 M NaCl. Subsequently, cells were lysed and counted in a Wallac Compugamma counter.

[Ca²⁺] measurements

CXCL11-induced increases in [Ca²⁺] were quantified by monitoring the fluorescence of Fluo-4 AM-loaded HEK293-CXCR3 cells, using an automated NOVOstar microplate reader (BMG Labtech GmbH, Offenburg, Germany). Cells were loaded in Hanks' balanced salt solution containing 20 mM HEPES, 2.5 mM Probenecid, 2 μM Fluo-4 AM and 0.02 % Pluronic F-127 [pH = 7.4]. Thereafter they were washed three times and fluorescence was measured (1 data point/second, excitation 485 nm, emission 520 nm) for 10 seconds to calculate the mean basal value. Cells were preincubated for 10 min with the indicated compounds (10 μM). After injection of the agonist CXCL11 (10 nM) fluorescence was recorded for 50 seconds. To determine the maximal fluorescence of the system, cells were exposed to Triton X-100 (0.25% [v/v]). Basal and maximal values determined for each well were used to normalize the data. Cells preincubated with compounds **1d** and **5d** show comparable baseline fluorescence to non-treated cells. Results were expressed as percentage of the maximal fluorescence induced by Triton X-100.

[³H]Inositol phosphate production

COS-7 cells were transfected with CXCR3 and Gqi5 chimeric protein.³⁰ 24 h after transfection cells were labeled overnight in inositol free medium (modified Eagle's medium with Earle's salts) supplemented with 2 mM L-glutamine, L-cysteine, L-leucine, L-methionine, L-arginine, glucose, 0.2% bovine serum albumin, and 2 μ Ci/mL *myo*-[2-³H]inositol (Amersham Pharmacia Biotech, Roosendaal, The Netherlands). Subsequently, the labeling medium was aspirated, cells were washed for 10 min with Dulbecco's modified Eagle's medium containing 25 mM HEPES (pH 7.4) and 20 mM LiCl. Cells were preincubated for 10 minutes with/without the indicated compounds and incubated for 2 h in the same medium in the absence or presence of 10 nM CXCL11 or 30 nM CXCL10. The incubation was stopped by aspiration of the medium and addition of cold 10 mM formic acid. After 90 min of incubation on ice, inositol phosphates were isolated by anion exchange chromatography (Dowex AG1-X8 columns, Bio-Rad) and counted by liquid scintillation.

Actin polymerization assay

Cells were resuspended in RPMI-1640 with 0.25% BSA [BSA, fraction V, Sigma] in a concentration of 4×10^6 cells/mL. Indicated compounds were added 10 minutes prior to the stimulation. Chemokines was added in a concentration of 10 nM. At indicated time points, 25 mL of cell suspension was transferred to 25 mL of fixation solution (4 % paraformaldehyde; PFA). Cells were fixed for at least 15 minutes. Thereafter, cells were washed and resuspended in 50 mL of permeabilization reagent (0.1% Triton-X 100). After 10 minutes, cells were washed, blocked with 1% BSA (5 min), washed and incubated with 0.5 mM rhodamine-phalloidin (Molecular Probes, Leiden, The Netherlands) to visualize filamentous actin (F-actin). After 45 minutes, cells were centrifuged and resuspended in PBS with 0.25% BSA. Mean fluorescence intensity was measured by FACS analysis.

Chemotaxis assays

The assay for chemotaxis was performed in 24 well plates (Costar, Cambridge, MA) carrying Transwell permeable supports with 5 μ m pore size polycarbonate membrane. T cells were cultured overnight at 4×10^6 cells/mL in RPMI-1640 containing 0.25% BSA. Cells were incubated with indicated compounds for 10 minutes. Medium alone or supplemented with chemokine and/or indicated compounds was placed in the lower compartment, and cells were loaded onto the inserts at $0.4 \times 10^6/100 \mu$ l. Chambers were incubated for 120 minutes in a 5% CO₂, humidified incubator at 37°C. After the incubation period, numbers of T cells migrating to the lower chamber were counted under a microscope using a hemocytometer. Viability was checked with trypan blue exclusion.

All conditions were tested in at least in triplicate; statistic evaluation was performed using the Student's test.

Acknowledgements

The authors thank Dr. C. Fitzsimons for support with the calcium experiments, R. Oostendorp for the inositol phosphate measurement and Drs. K. Biber and H.W. Boddeke (University of Groningen) for providing the HEK-293 cells expressing CXCR3 receptor. M.J.S. was supported by the Royal Netherlands Academy of Arts and Sciences. S.S. was supported by a NWO-Pioneer grant to R.L.

References

- (1) Zlotnik, A.; Yoshie, O. Chemokines: a new classification system and their role in immunity. *Immunity*, **2000**, *12*, 121-127.
- (2) Rossi, D.; Zlotnik, A. The biology of chemokines and their receptors. *Annu. Rev. Immunol.*, **2000**, *18*, 217-242.
- (3) Zlotnik, A.; Morales, J.; Hedrick, J. A. Recent advances in chemokines and chemokine receptors. *Crit. Rev. Immunol.*, **1999**, *19*, 1-47.
- (4) Murphy, P. M.; Baggiolini, M.; Charo, I. F.; Hebert, C. A.; Horuk, R. et al. International union of pharmacology. XXII. Nomenclature for chemokine receptors. *Pharmacol. Rev.*, **2000**, *52*, 145-176.
- (5) Farber, J. M. A macrophage mRNA selectively induced by gamma-interferon encodes a member of the platelet factor 4 family of cytokines. *Proc. Natl. Acad. Sci. USA*, **1990**, *87*, 5238-5242.
- (6) Cole, K. E.; Strick, C. A.; Paradis, T. J.; Ogborne, K. T.; Loetscher, M. et al. Interferon-inducible T cell alpha chemoattractant (I-TAC): a novel non-ELR CXC chemokine with potent activity on activated T cells through selective high affinity binding to CXCR3. *J. Exp. Med.*, **1998**, *187*, 2009-2021.
- (7) Luster, A. D.; Ravetch, J. V. Biochemical characterization of a gamma interferon-inducible cytokine (IP-10). *J. Exp. Med.*, **1987**, *166*, 1084-1097.
- (8) Clark-Lewis, I.; Mattioli, I.; Gong, J. H.; Loetscher, P. Structure-function relationship between the human chemokine receptor CXCR3 and its ligands. *J. Biol. Chem.*, **2003**, *278*, 289-295.
- (9) Loetscher, M.; Gerber, B.; Loetscher, P.; Jones, S. A.; Piali, L. et al. Chemokine receptor specific for IP10 and mig: structure, function, and expression in activated T-lymphocytes. *J. Exp. Med.*, **1996**, *184*, 963-969.
- (10) Tensen, C. P.; Flier, J.; Van Der Raaij-Helmer, E. M.; Sampat-Sardjoepersad, S.; Van Der Schors, R. C. et al. Human IP-9: A keratinocyte-derived high affinity CXC-chemokine ligand for the IP-10/Mig receptor (CXCR3). *J. Invest. Dermatol.*, **1999**, *112*, 716-722.
- (11) Smit, M. J.; Verdijk, P.; van der Raaij-Helmer, E. M.; Navis, M.; Hensbergen, P. J. et al. CXCR3-mediated chemotaxis of human T cells is regulated by a Gi- and phospholipase C-dependent pathway and not via activation of MEK/p44/p42 MAPK nor Akt/PI-3 kinase. *Blood*, **2003**, *102*, 1959-1965.
- (12) Qin, S.; Rottman, J. B.; Myers, P.; Kassam, N.; Weinblatt, M. et al. The chemokine receptors CXCR3 and CCR5 mark subsets of T cells associated with certain inflammatory reactions. *J. Clin. Invest.*, **1998**, *101*, 746-754.
- (13) Patel, D. D.; Zachariah, J. P.; Whichard, L. P. CXCR3 and CCR5 ligands in rheumatoid arthritis synovium. *Clin. Immunol.*, **2001**, *98*, 39-45.
- (14) Balashov, K. E.; Rottman, J. B.; Weiner, H. L.; Hancock, W. W. CCR5(+) and CXCR3(+) T cells are increased in multiple sclerosis and their ligands MIP-1alpha and IP-10 are expressed in demyelinating brain lesions. *Proc. Natl. Acad. Sci. USA*, **1999**, *96*, 6873-6878.
- (15) Shields, P. L.; Morland, C. M.; Salmon, M.; Qin, S.; Hubscher, S. G. et al. Chemokine and chemokine receptor interactions provide a mechanism for selective T cell recruitment to specific liver compartments within hepatitis C-infected liver. *J. Immunol.*, **1999**, *163*, 6236-6243.
- (16) Mach, F.; Sauty, A.; Iarossi, A. S.; Sukhova, G. K.; Neote, K. et al. Differential expression of three T lymphocyte-activating CXC chemokines by human atheroma-associated cells. *J. Clin. Invest.*, **1999**, *104*, 1041-1050.
- (17) Flier, J.; Boorsma, D. M.; van Beek, P. J.; Nieboer, C.; Stoof, T. J. et al. Differential expression of CXCR3 targeting chemokines CXCL10, CXCL9, and CXCL11 in different types of skin inflammation. *J. Pathol.*, **2001**, *194*, 398-405.
- (18) Flier, J.; Boorsma, D. M.; Bruynzeel, D. P.; Van Beek, P. J.; Stoof, T. J. et al. The CXCR3 activating chemokines IP-10, Mig, and IP-9 are expressed in allergic but not in irritant patch test reactions. *J. Invest. Dermatol.*, **1999**, *113*, 574-578.

- (19) Xie, J. H.; Nomura, N.; Lu, M.; Chen, S. L.; Koch, G. E. et al. Antibody-mediated blockade of the CXCR3 chemokine receptor results in diminished recruitment of T helper 1 cells into sites of inflammation. *J. Leukoc. Biol.*, **2003**, *73*, 771-780.
- (20) Moser, B.; Willmann, K. Chemokines: role in inflammation and immune surveillance. *Ann. Rheum. Dis.*, **2004**, *63*, ii84-ii89.
- (21) Schall, T. J.; Dairaghi, D. J.; McMaster, B.E. Compounds and methods for modulating CXCR3 function. *WO 01/16144 A2*, **2001**.
- (22) Craig, P. N. Interdependence between physical parameters and selection of substituent groups for correlation studies. *J. Med. Chem.*, **1971**, *14*, 680-684.
- (23) Sembiring, S. B.; Colbran, S.B.; Craig, D.C.; Scudder, M.L. Palladium(II) 2-diphenylphosphinoquinone (H₂pqh) complexes: preparation and structures of a novel cluster, [$\text{PdBr}(\text{Hpphq})_4$] $\cdot 2\text{H}_2\text{O}$, and a phosphine-phosphinite complex, *cis*-[$\text{PdBr}_2\{\text{C}_6\text{H}_3(\text{OH})\text{-1,PPH}_2\text{-3,PPH}_2\text{O-4}\}$] $\cdot 2\text{H}_2\text{O}$. *J. Chem. Soc. Dalton Trans.*, **1995**, 3731-3741.
- (24) Mc Omie, J. F. W.; Watts, M.L.; West, D. E. Demethylation of aryl methyl ethers by boron tribromide. *Tetrahedron*, **1968**, *24*, 2289-2292.
- (25) Dijkstra, I. M.; Hulshof, S.; van der Valk, P.; Boddeke, H. W.; Biber, K. Cutting edge: activity of human adult microglia in response to CC chemokine ligand 21. *J. Immunol.*, **2004**, *172*, 2744-2747.
- (26) Rabin, R. L.; Park, M. K.; Liao, F.; Swofford, R.; Stephany, D. et al. Chemokine receptor responses on T cells are achieved through regulation of both receptor expression and signaling. *J. Immunol.*, **1999**, *162*, 3840-3850.
- (27) Voermans, C.; Anthony, E.C.; Mul, E.; van der Schoot, E.; Hordijk, P. SDF-1-induced actin polymerization and migration in human hematopoietic progenitor cells. *Exp. Hematol.*, **2001**, *29*, 1456-1464.
- (28) Tenschler, K.; Metzner, B.; Hofmann, C.; Schopf, E.; Norgauer, J. The monocyte chemotactic protein-4 induces oxygen radical production, actin reorganization, and CD11b up-regulation via a pertussis toxin-sensitive G-protein in human eosinophils. *Biochem. Biophys. Res. Commun.*, **1997**, *240*, 32-35.
- (29) Elsner, J.; Petering, H.; Kluthe, C.; Kimmig, D.; Smolarski, R. et al. Eotaxin-2 activates chemotaxis-related events and release of reactive oxygen species via pertussis toxin-sensitive G proteins in human eosinophils. *Eur. J. Immunol.*, **1998**, *28*, 2152-2158.
- (30) Coward, P., Chan, S.D., Wada, H.G., Humphries, G.M., Conklin, B.R. Chimeric G proteins allow a high-throughput signaling assay of Gi-coupled receptors. *Anal. Biochem.*, **1999**, *270*, 242-248.

Chapter 4

Synthesis and structure-activity relationships of 3*H*-quinazolin-4-ones and 3*H*-pyrido[2,3-*d*]pyrimidin-4-ones as CXCR3 receptor antagonists

Adapted from:

Stefania Storelli, Dennis Verzijl, Jawad Al-Badie, Niels Elders, Leontien Bosch, Henk Timmerman, Martine J. Smit, Iwan J. P. De Esch, and Rob Leurs
Arch. Pharm. Chem. Life Sci. 2007, 340, 281 – 291

Abstract

CXC chemokine receptor-3 (CXCR3) is a G-protein coupled receptor (GPCR) predominantly expressed on activated T lymphocytes that promote Th1 responses. Previously, we described the 3*H*-quinazolin-4-one containing VUF 5834 (decanoic acid {1-[3-(4-cyano-phenyl)-4-oxo-3,4-dihydroquinazolin-2-yl]-ethyl}-(2-dimethylamino-ethyl)-amide) as a small-molecule CXCR3 antagonist with submicromolar affinity and as a lead structure for the development of CXCR3 antagonists. More recently, the related 3*H*-pyrido[2,3-*d*]pyrimidin-4-one compounds AMG 487 and NBI-74330 have been reported as nanomolar CXCR3 antagonists and these ligands are currently under clinical investigation. The aim of this study is to link the structure-activity relationship (SAR) of the previously published class of 3*H*-quinazolin-4-one containing CXCR3 ligands with these novel clinical candidates. From the modification of the lead structure VUF 5834 emerged the importance of the (4-fluoro-3-(trifluoromethyl)phenyl)acetyl and the 3-methylen-pyridine as substituents to improve the affinity at the human CXCR3 receptor, whereas other features are less important. The described molecules serve as tool to investigate the role of the CXCR3 receptor in various inflammatory conditions.

Introduction

Chemokines are a family of small proteins (70–80 aminoacids) secreted by leukocytes or tissue cells that mediate cellular recruitment to sites of inflammation or injury.¹ Depending on the number and spacing of conserved cysteine residues, chemokines are classified into four major groups (CC, CXC, CX3C, and XC).^{2,3} The IFN- γ -inducible CXC chemokines, CXCL9, CXCL10, and CXCL11 interact with CXC chemokine receptor-3 (CXCR3) to exert their functions.⁴ Like all the chemokine receptors, CXCR3 belongs to the superfamily of the G-protein coupled receptors (GPCR).⁵ Activation of CXCR3 via G-proteins of the G_i-type leads to an increase of intracellular calcium and cellular migration.^{6,7} Several studies have shown that levels of CXCL9, CXCL10, and CXCL11 are elevated in various chronic inflammatory diseases such as rheumatoid arthritis,^{8,9} multiple sclerosis,¹⁰ transplant rejection,¹¹ hepatitis C infected liver,¹² atherosclerosis,¹³ chronic skin reactions,^{6,14,15} and chronic obstructive pulmonary disease¹⁶ and are related to the infiltration of CXCR3-positive T-cells. Consequently, it is believed that CXCR3 antagonists provide a therapeutic approach in chronic inflammatory and neoplastic diseases.¹⁷⁻¹⁹

Several classes of CXCR3 antagonists have recently been reported in scientific literature.²⁰⁻²⁵ We²⁴ and others²⁶ have previously described VUF 5834, the decanoic acid {1-[3-(4-cyano-phenyl)-4-oxo-3,4-dihydro-quinazolin-2-yl]-ethyl}-(2-dimethylamino-ethyl)-amide **1a**, as a submicromolar CXCR3 antagonist and we have continued to explore the SAR of this series. During our studies, Amgen Inc. announced that the structural derivative AMG 487 (**2**) was under clinical investigation²⁷, while scientists from Neurocrine Biosciences Inc. described pharmacological evaluation of patent compound NBI-74330 (**3**).²⁸ These ligands are the most potent CXCR3 ligands reported to date, showing affinity values for the human CXCR3 receptor in the nanomolar range. Here, we describe a SAR study in which the previously published 3*H*-quinazolin-4-one scaffold (e.g. VUF 5834, **1a**) and the novel 3*H*-pyrido[2,3-*d*]pyrimidin-4-one scaffold (exemplified by ligands **2** and **3**) are compared. For the structures of reference compounds VUF 5834 (**1a**), AMG 487 (**2**), and NBI-74330 (**3**) see Figure 1.

Chemistry

The 3-phenyl-3*H*-quinazolin-4-one scaffold was constructed as reported earlier (Scheme 1).²⁴ The reaction of 2-amino-benzoic acid with propionyl chloride afforded 2-propionylamino-benzoic acid **5** and treatment of this intermediate with phosphorus trichloride and 4-ethoxyaniline or 4-amino-benzonitrile afforded compounds **6a** and **6b**,

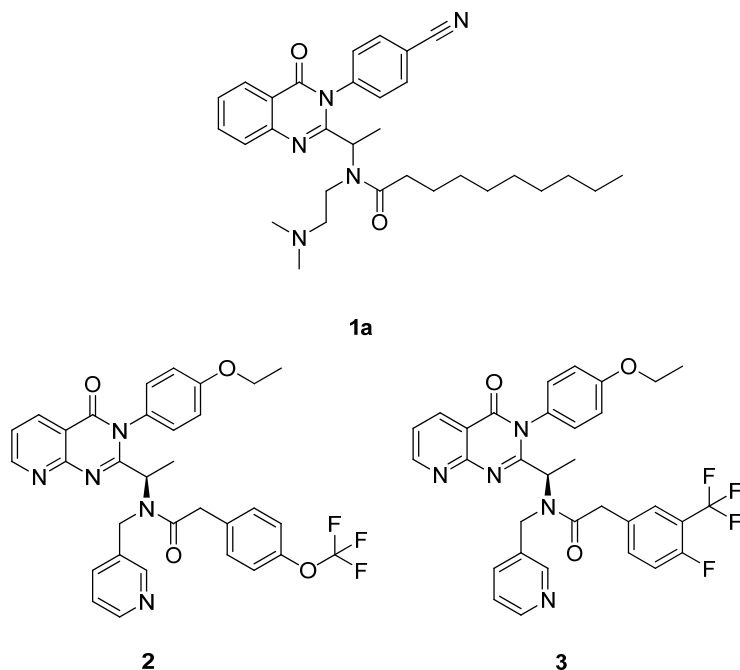
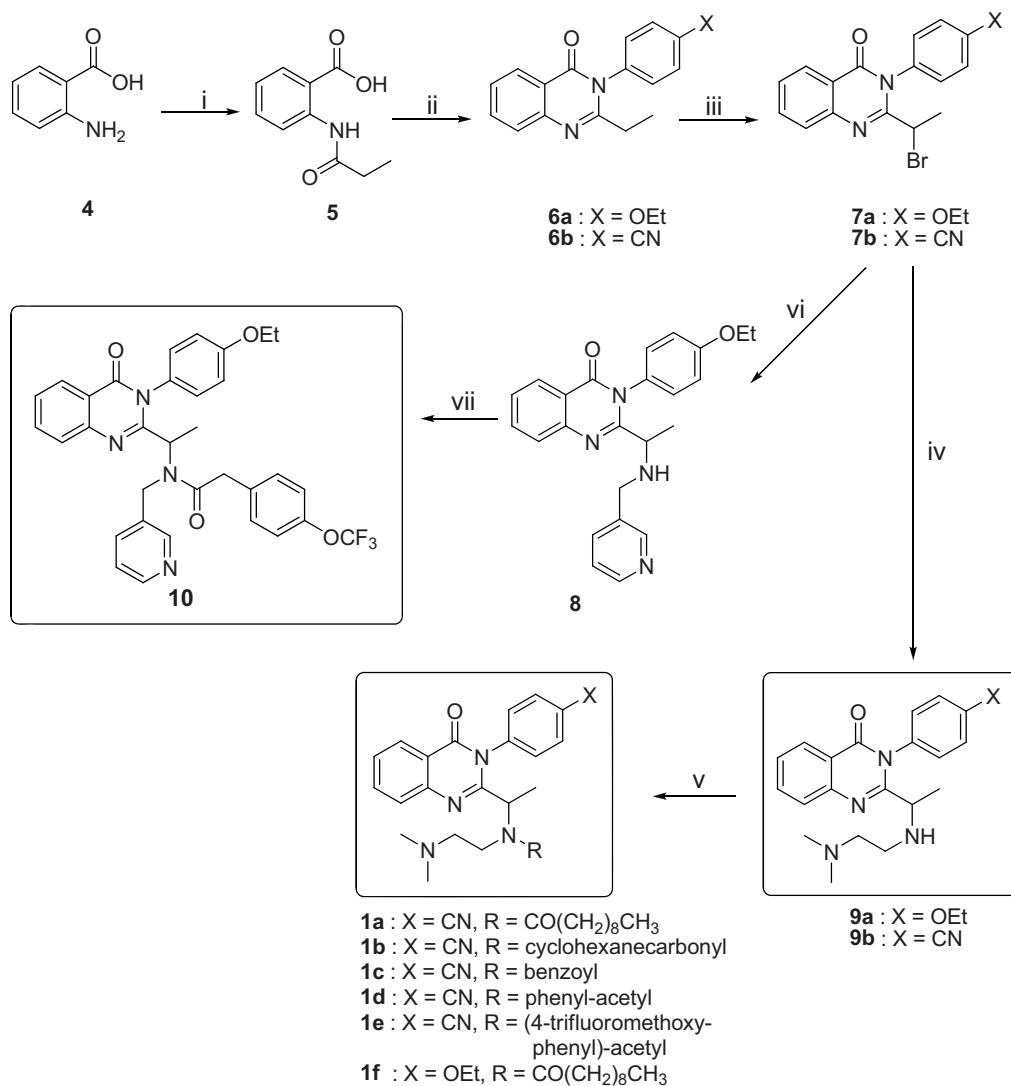


Figure 1. Structures of reference compounds VUF 5834 (**1a**), AMG 487 (**2**) and NBI – 74330 (**3**).

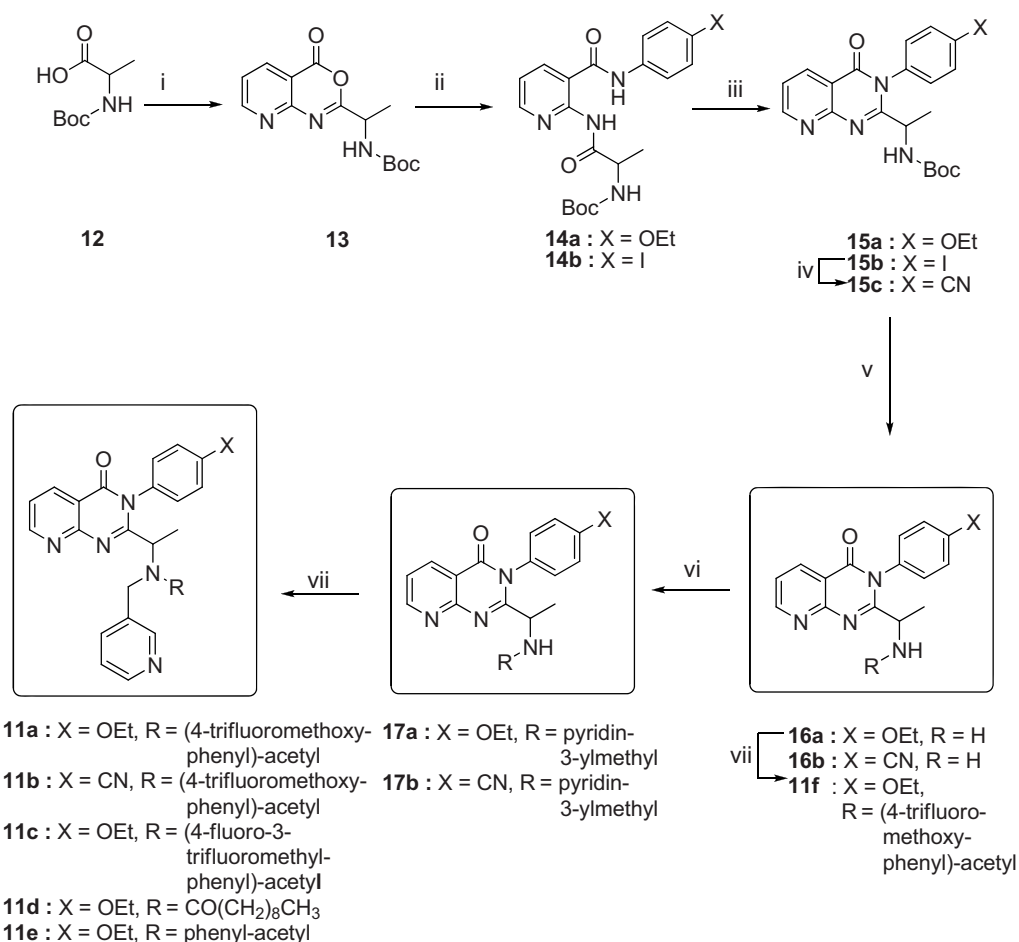
trichloride and 4-ethoxyaniline or 4-amino-benzonitrile afforded compounds **6a** and **6b**, respectively, in moderate yields. Intermediates **7a** and **7b** were obtained in good yields via reaction with bromine and were used for the subsequent reaction with the commercially available *N,N*-dimethylethylene diamine (leading to **9a** and **9b**) or 3-picolylamine (leading to **8**). Reaction of **9a** and **9b** with decanoyl, cyclohexanecarbonyl, benzoyl, or phenylacetyl chloride afforded compound **1a–d** and **1f** whereas compounds **1e** and **10** were obtained via coupling of **8** or **9a**, respectively, with (4-trifluoromethoxyphenyl)-acetic acid and using EDCI as activating agent.

The 3*H*-pyrido[2,3-*d*]pyrimidin-4-one derivatives **11a–f** were prepared according to Scheme 2.²⁶ Boc-*D*-alanine was activated with *iso*-butylchloroformate under basic conditions at -20°C and then allowed to react with 2-aminonicotinic acid leading to **13**. Because of the poor stability of **13**,²⁹ the crude material was immediately reacted with either 4-ethoxy-phenylamine or 4-iodo-phenylamine leading to compound **14a** and **14b**, respectively. Subsequent ring closure afforded compounds **15a** and **15b** in a moderate yield.



Scheme 1. General synthesis of 3H-quinazolin-4-one analogues. **Reagents and conditions:** i) propionyl chloride, DMF, 40 °C; ii) *p*-phenetidine or *p*-amino-benzonitrile, PCl₃, toluene, reflux; iii) Br₂, CH₃COONa, CH₃COOH, 40 °C; iv) H₂N(CH₂)₂N(CH₃)₂, EtOH, reflux; v) acid chloride, NEt₃, dioxane or carboxylic acid, EDCI, DCM, DMF; vi) 3-(aminomethyl)pyridine, NEt₃, DMF, DMF; vii) carboxylic acid, EDCI, DCM.

3*H*-Pyrido[2,3-*d*]pyrimidin-4-ones as CXCR3 receptor antagonists



Scheme 2. General synthesis of 3*H*-pyrido[2,3-*d*]pyrimidin-4-one analogues. **Reagents and conditions:** i) Iso-butylchloroformate, NMM, DCM, -20°C; ii) 4-ethoxy-phenylamine or 4-iodo-phenylamine, -20°C; iii) Iso-butylchloroformate, NMM, DCM, -20°C; iv) Zn (CN)₂, Pd(PPh₃)₄, DMF, 80°C; v) TFA, DCM, rt; vi) 3-pyridinecarboxaldehyde, Na(CH₃COO)₃BH, DCE; vii) acid chloride, NEt₃, dioxane or carboxylic acid, EDCI, DCM, DMF or carboxylic acid, EDCI, HOBT, DIPEA, DCM.

With the aim to obtain the *para*-cyano analogue (in our hand the best substituent of the 3-phenyl-3*H*-quinazolin-4-one series²⁴) of reference compound **2**, intermediate **15b** was treated with zinc cyanide using tetrakis(triphenylphosphine) palladium as catalyst,³⁰ resulting in **15c** in acceptable yield. The Boc protecting group of **15a** and **15c** was cleaved using trifluoroacetic acid and the amines **16a,b** were obtained in excellent yield. Key intermediates **17a** and **17b** were obtained via reductive amination with pyridine-3-

carbaldehyde. Final compounds **11a-c** and **11f** were obtained by coupling the appropriate amine with the corresponding carboxylic acids³¹ whereas for compounds **11d** and **11e** the corresponding acid chlorides were used.

Reference ligands **2** and **3** have been reported as enantiopure compounds using a synthetic strategy very similar to the one outlined here.³² In our hands, however, the synthesis route described in this patent results in racemic mixtures as determined from an absence of e.e. in building blocks **16a,b** (as judged from chiral HPLC). This means that all final compounds **11** are racemic.

Pharmacology

The affinity for the human CXCR3 of all compounds was determined by the displacement of [¹²⁵I]CXCL10 binding to membranes from HEK-293 cells stably expressing the human CXCR3 receptor.

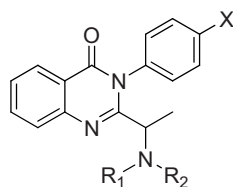
Results and discussion

In this study, we set out to link the SAR of the previously described 3*H*-quinazolin-4-one and the more recent 3*H*-pyrido[2,3-*d*]pyrimidin-4-one CXCR3 ligand classes. In the series of the 3*H*-quinazolin-4-one analogues (**1a-f**, **9b**, **10**, Table 1), proper decoration of the amide group is required to achieve appreciable affinity for the receptor. Previously, we found that the decanoyl chain of **1a** was necessary to obtain micromolar affinity values at CXCR3. Indeed, the absence of the decanoyl chain as in amine **9b** or in the presence of alternative lipophilic acetamide moieties such as cyclohexanecarbonyl **1b**, benzoyl **1c**, or phenylacetyl **1d** resulted in a complete loss of affinity (Table 1). Inspired by the Amgen patent application,³² we subsequently synthesized the 4-trifluoromethoxy-phenyl-acetyl compound **1e** which showed a threefold increase in CXCR3 affinity (Table 1) compared to our lead structure **1a**. Considering that the phenyl-acetyl derivative **1d** does not have affinity for the CXCR3 receptor, the affinity of the 4-trifluoromethoxy-phenylacetyl derivative **1e** is striking. Clearly, the 4-trifluoromethoxy substituent has an enormous effect on the CXCR3 affinity and it seems that this part of the ligands is able to have very specific interaction with the binding site of the receptor.

Next, the influence of the *para*-substitution on the phenyl ring in position 3 of the 3*H*-quinazolin-4-one scaffold was investigated. We previously described the *para*-cyano moiety (as in **1a**) as the best substituent for CXCR3 binding and reported it to be substantially better than a methoxy group in this position.²⁴ Considering the *para*-ethoxyphenyl group in reference compound **2**,³² we synthesized the *para*-ethoxy

substituted analogue for the 3H-quinazolin 4-one series and the resulting ligand **1f** showed a twofold better affinity compared to the *para*-cyano-substituted lead compound **1a**. The difference in affinity between the *para*-methoxyphenyl derivative and the improved *para*-ethoxyphenyl derivative, again illustrates the fine optimization work by Amgen scientists. The subsequent replacement of the *N,N*-ethyldiamine group at R₁ with a pyridin-3-ylmethyl afforded the analogue **10**. With a pK_i value of 7.5, this compound is the most potent CXCR3 antagonist belonging to the 3H-quinazolin-4-one series. Moreover, the development of **10** nicely illustrates the key role of both the R₁ and R₂ substituents at the amino function.

Table 1. pK_i values of the 3H-quinazolin-4-one analogues as determined by the displacement of [¹²⁵I]CXCL10 binding to the human CXCR3 receptor.

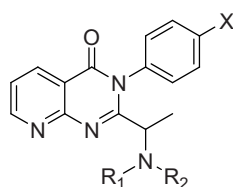


Compound no	X	R ₁	R ₂	pK _i [#]
1a	CN	CH ₂ CH ₂ N(CH ₃) ₂	CO(CH ₂) ₈ CH ₃	6.26±0.25
9b	CN	CH ₂ CH ₂ N(CH ₃) ₂	H	<5
1b	CN	CH ₂ CH ₂ N(CH ₃) ₂	cyclohexanecarbonyl	<5
1c	CN	CH ₂ CH ₂ N(CH ₃) ₂	benzoyl	<5
1d	CN	CH ₂ CH ₂ N(CH ₃) ₂	phenyl-acetyl	<5
1e	CN	CH ₂ CH ₂ N(CH ₃) ₂	(4-Trifluoromethoxy-phenyl)-acetyl	6.71±0.04
1f	OCH ₂ CH ₃	CH ₂ CH ₂ N(CH ₃) ₂	CO(CH ₂) ₈ CH ₃	6.56±0.04
10	OCH ₂ CH ₃	pyridin-3-ylmethyl	(4-Trifluoromethoxy-phenyl)-acetyl	7.45±0.13

[#]The binding experiments were carried out on cell membranes fractions from HEK-293 cells stably expressing the human CXCR3 receptor. The compounds were tested for their ability to displace [¹²⁵I]CXCL10 binding. The values are represented as the mean ± S.E.M. of at least three independent experiments. All compounds are racemic.

Next, we explored if the SAR of the 3*H*-quinazolin-4-ones could be transferred to the new 3*H*-pyrido[2,3-*d*]pyrimidin-4-one scaffold. Comparing the two series (Tables 1 and 2) shows that the introduction of an additional nitrogen atom in the heterocyclic scaffold did not affect the CXCR3 affinity (compare **10** with **11a**). However, the different amino substituents at R₁ and R₂ again had dramatic effects on the CXCR3 affinity. Compound **11d** shows that the decanoyl chain is tolerated, as it is for the 3*H*-quinazolin-4-one series, although only a submicromolar affinity is obtained. In addition, the unsubstituted phenylacetyl analogue **11e** did not have affinity for the CXCR3 receptor, while the slightly more functionalized 4-trifluoromethoxy-phenylacetyl group, as in reference compound **2**, significantly improves affinity. Again, a properly substituted phenyl ring is a key determinant for CXCR3 binding.

Table 2. pK_i values of the 3*H*-pyrido[2,3-*d*]pyrimidin-4-one analogues as determined by the displacement of [¹²⁵I]CXCL10 binding to the human CXCR3 receptor.



Compound no	X	R ₁	R ₂	pK _i [#]
11a	OCH ₂ CH ₃	pyridin-3-ylmethyl	(4-Trifluoromethoxy-phenyl)-acetyl	7.39±0.08
11b	CN	pyridin-3-ylmethyl	(4-Trifluoromethoxy-phenyl)-acetyl	7.39±0.05
11c	OCH ₂ CH ₃	pyridin-3-ylmethyl	(4-Fluoro-3-trifluoromethyl-phenyl)-acetyl	8.13±0.12
11d	OCH ₂ CH ₃	pyridin-3-ylmethyl	CO(CH ₂) ₈ CH ₃	6.47±0.09
11e	OCH ₂ CH ₃	pyridin-3-ylmethyl	phenyl-acetyl	<5
11f	OCH ₂ CH ₃	H	(4-Trifluoromethoxy-phenyl)-acetylH	5.34±0.19
16a	OCH ₂ CH ₃	H	H	<5
17a	OCH ₂ CH ₃	pyridin-3-ylmethyl	H	<5

[#]The binding experiments were carried out on cell membranes fractions from HEK-293 cells stably expressing the human CXCR3 receptor. The compounds were tested for their ability to displace [¹²⁵I]CXCL10 binding. The values are represented as the mean ± S.E.M of at least three independent experiments. All compounds are racemic.

Compound **11c** has a fivefold higher affinity for CXCR3 than **11a**, meaning that in this subset of 3H-pyrido[2,3-d]pyrimidin-4-ones the (4-fluoro-3-trifluoromethyl-phenyl)-acetyl is the best substituent at R₂. These results validate recent disclosures by Amgen Inc. and Neurocrine Biosciences Inc.^{27,28} The presence of both a proper acetamide substituent and the pyridin-3-ylmethyl group are necessary for high CXCR3 affinity. The absence of one of the two (compounds **17a** and **11f**) or both (**16a**) causes a dramatic loss of affinity. Nevertheless, **11f** with (4-trifluoromethoxy-phenyl)-acetyl substituent retains a micromolar affinity for the receptor.

Finally, the influence of the *para*-substituent on the phenyl ring in position 3 of the 3H-pyrido[2,3-d]pyrimidin-4-ones was investigated. Compound **11b** was synthesized to determine the effect of *para*-cyano substitution. For this particular scaffold, the *para*-ethoxy derivative **11a** and *para*-cyano derivative **11b** do not show significant differences in CXCR3 affinity.

Conclusions

This study presents the synthesis and initial SAR of CXCR3 antagonists of the 3H-quinazolin-4-one and 3H-pyrido[2,3-d]pyrimidin-4-one series. These compounds are useful as tools for targeting CXCR3 in a variety of inflammatory models. Moreover, the structural insights obtained may be used in the design of novel CXCR3 antagonists.

Experimental

Chemistry

General procedures. The solvents were dried according to standard procedures. All reactions were performed under an atmosphere of dry nitrogen. ¹H- and ¹³C-NMR spectra were recorded on a Bruker AC-200 (200 MHz; Bruker Bioscience, Billerica, MA, USA) spectrometer. Flash column chromatography was carried out with J. T. Baker silica gel (J. T. Baker, Deventer, The Netherlands). Analytical HPLC-MS analyses were conducted using a Shimadzu LC-8A preparative liquid chromatograph pump system with a Shimadzu SPD-10AV UV-Vis detector set at 254 nm, with the MS detection performed with a Shimadzu LCMS-2010 liquid chromatograph mass spectrometer (Shimadzu, Tokyo, Japan). The analyses were performed using the following two conditions. Condition I: an Xbridge (C18) 5 μm column (100 mm × 4.6 mm), with the following two solvents: solvent A: 10% buffer pH 8 – 90% H₂O; solvent B: 10% aqueous buffer pH 8 –

90% acetonitrile. Flow rate = 2.0 mL/min; gradient from 5% to 90% B in 10 min, then 5 min at 90% B, then 15 min at 5% B. The total run time was 30 min. The buffer-pH 8 is prepared with ammonium bicarbonate in H₂O (0.4% w/v) adjusted to pH 8 with ammonium hydroxide. Condition II: Xbridge (C18) 5 μ m column (100 mm \times 4.6 mm), with the following two solvents: solvent A: 0.1% formic acid – 99.9% H₂O; solvent B: 0.1% formic acid/99.9% acetonitrile. Flow rate = 2.0 mL/ min. Gradient from 5% to 90% B in 10 min, then 5 min at 90% B, then 15 min at 5% B. The total run time was 30 min. Purities calculated are based on RP HPLC-UV peak surface area of the compounds. Chiral HPLC analyses were performed with a CHIRAL CEL OD-H column (4.6 mm \times 250 mm) DAIC 14325, using as eluents 0.05% diethylamine in hexane/isopropyl alcohol (95 : 5). Flow rate = 1.1 mL/min, T = 30°C. High Resolution Electron Impact Ion Mass Spectra (HREIMS) were recorded on a Finnigan MAT 900 mass spectrometer (Thermo Electron Corporation, Bremen, Germany).

2-Propionylamino-benzoic acid (5)

Anthranilic acid (**4**) (68.60 g, 0.50 mol) was dissolved in *N,N*-dimethylformamide (250 mL). Propionyl chloride (47.60 mL, 0.55 mol) was added drop wise at such a rate that the temperature of the mixture remained below 40 °C. The product began to precipitate after about one half of the acid chloride was added, and the suspension was stirred vigorously at room temperature for an additional three hours after the addition was completed. The resulting mixture was poured into water (2.0 L) and stirred for an additional two hours. The precipitated product was collected by filtration, washed with water and dried in a vacuum oven at 40 °C under reduced pressure to afford 73.03 g (76%) of white crystals. ¹H NMR (CDCl₃) δ : 1.25 (t, *J* = 7.6 Hz, 3H), 2.55 (q, *J* = 7.6 Hz, 2H), 6.75 (brs, 1H), 7.07-7.14 (m, 1H), 7.55-7.59 (m, 1H), 8.02-8.14 (m, 1H), 8.72-8.76 (m, 1H), 10.98 (s, 1H).

3-(4-ethoxyphenyl)-2-ethylquinazolin-4(3H)-one (6a)

To a suspension of 2-propionylamino-benzoic acid (3.00 g, 15.52 mmol) and *p*-phenetidine (2.41 g, 15.52 mmol) in toluene was added drop wise phosphorus trichloride (0.61 mL, 6.98 mmol). The resulting suspension was heated to reflux for 8 hours. After cooling to room temperature, a saturated sodium carbonate solution was added and the mixture was stirred vigorously until all solid was dissolved. The solvent was removed *in vacuum* and the resulting solid was collected by filtration, rinsed with water, dried and recrystallized from isopropyl alcohol to afford the desired compound as a white solid. Yield: 2.19 g (48%). ¹H NMR (CDCl₃) δ : 1.20 (t, *J* = 7.4 Hz, 3H), 1.42 (t, *J* = 7.0 Hz, 3H), 2.44 (q, *J* = 7.4 Hz, 2H), 4.10 (q, *J* = 7.0 Hz, 2H), 7.01-7.23 (m, 4H), 7.39-7.58 (m, 1H), 7.62-7.89 (m, 2H), 8.22-8.26 (m, 1H).

4-(2-Ethyl-4-oxoquinazolin-3(4H)-yl)benzotrile (6b)

This was performed analogously to the preparation of **6a**, using *p*-amino-benzotrile (2.22 g, 15.52 mmol). Yield: 1.50 g (35%). ¹H NMR (CDCl₃) δ: 1.18 (t, *J* = 7.4 Hz, 3H), 2.34 (q, *J* = 7.4 Hz, 2H), 7.30-7.55 (m, 3H), 7.60-7.95 (m, 4H), 8.21-8.29 (m, 1H).

2-(1-Bromo-ethyl)-3-(4-ethoxy-phenyl)-3H-quinazolin-4-one (7a)

A mixture of **6a** (2.23 g, 7.56 mmol), anhydrous sodium acetate (756 mg) and glacial acetic acid (10 mL) was warmed 40 °C. A solution of bromine (7.56 mmol) in acetic acid (2 mL) was added over a period of 3 hours. After the addition was completed the mixture was poured into water (150 mL) and stirred at room temperature for about 2 hours. The precipitate product was isolated by filtration, washed with warm water to remove the trace of the acetic acid, then rinsed with a small amount of isopropyl alcohol and dried to provide the desired compound **7a** as a solid. Yield: 2,71 g (96%). ¹H NMR (CDCl₃) δ: 1.44 (t, *J* = 7.0 Hz, 3H), 2.02 (d, *J* = 6.7 Hz, 3H), 4.08 (q, *J* = 7.0 Hz, 2H), 4.61 (q, *J* = 6.7 Hz, 1H), 6.90-7.25 (m, 3H), 7.30-7.55 (m, 2H), 7.75-7.80 (m, 2H), 8.24-8.28 (m, 1H).

4-[2-(1-Bromo-ethyl)-4-oxo-4H-quinazolin-3-yl]-benzotrile (7b)

This was performed analogously to the preparation of **7a**, using **6b** (2.08 g, 7.56 mmol). Yield: 2.34 g (88%). ¹H NMR (CDCl₃) δ: 2.02 (d, *J* = 6.6 Hz, 3H), 4.40 (q, 1H, *J* = 6.6 Hz), 7.25-7.35 (m, 1H), 7.45-7.65 (m, 1H), 7.70-7.95(m, 5H), 8.20-8.24 (m, 1H).

2-[1-(2-Dimethylamino-ethylamino)-ethyl]-3-(4-ethoxy-phenyl)-3H-quinazolin-4-one (9a)

A mixture of **7a** (2.82 g, 7.57 mmol) and *N,N*-dimethylethylendiamine (1.31 mL, 12.11 mmol) in ethanol (100 mL) was heated to reflux for 18 hours. The ethanol was removed *in vacuo* and the concentrate dissolved in chloroform and washed with saturated aqueous sodium bicarbonate (3 × 50 mL) and the combined organic extracts dried over sodium sulfate, filtered and concentrated. The crude material was purified by flash chromatography on silica gel eluting with methanol/dichloromethane (1:9) to afford the desired compound as white solid. Yield: 1.48 g (52%). ¹H NMR (CDCl₃) δ: 1.24 (d, *J* = 6.4 Hz, 3H), 1.43 (t, *J* = 6.9 Hz, 3H), 2.20 (s, 6H), 2.35-2.75 (m, 4H), 3.48 (q, *J* = 6.4 Hz, 1H), 4.07 (q, *J* = 6.9 Hz, 2H), 7.15-7.25, (m, 4H), 7.40-7.55 (m, 1H), 7.55-7.80 (m, 2H), 8.22-8.26 (m, 1H).

4-{2-[1-(2-Dimethylamino-ethylamino)-ethyl]-4-oxo-4H-quinazolin-3-yl}-benzotrile (9b)

This was performed analogously to the preparation of **9a**, using **7b** (2.68 g, 7.56 mmol). Yield: 1.28 g (47%). ¹H NMR (CDCl₃) δ: 1.23 (d, *J* = 6.6 Hz, 3H), 2.22 (s, 6H), 2.30-2.59 (m, 4H), 3.31 (q, *J* = 6.6 Hz, 1H), 7.22-7.50, (m, 3H), 7.70-7.86 (m, 4H), 8.20-8.24 (m, 1H). ¹³C NMR (CDCl₃) δ: 20.87, 44.69, 45.12 (2 C), 54.93, 58.83, 113.55, 117.52, 120.42, 126.88, 127.04, 127.22 (2C), 129.71, 133.60, 133.66, 134.87, 140.66, 147.13, 158.59, 161.92. HREIMS *m/z* 361.18876 (calcd for C₂₁H₂₃N₅O, 361.1903). Anal. RP-HPLC *I*: *t*_R = 10.86 min (purity 100%), *II*: *t*_R = min 9.57 (purity 97%),

3-(4-Ethoxy-phenyl)-2-{1-[(pyridin-3-ylmethyl)-amino]-ethyl}-3H-quinazolin-4-one (8)

A solution of 3-(aminomethyl)pyridine (0.11 mL, 1.07 mmol) and triethylamine (0.15 mL, 1.07 mmol) in DMF (50 mL) was stirred for 0.5 h at room temperature. Then **7a** (0.40 g, 1.07 mmol) was added and the solution was stirred overnight. The reaction mixture was concentrated, dissolved in water and extracted with DCM. The organic layer was washed with water and a saturated aqueous sodium carbonate, then dried, concentrated and purified via flash chromatography (DCM/MeOH, 9.5:0.5) to afford the desired compound as 170 mg (40%) of pale yellow oil. ¹H NMR (CDCl₃) δ: 1.23 (d, *J* = 6.6 Hz, 3H), 1.40 (t, *J* = 7.0 Hz, 3H), 3.48 (q, *J* = 6.6 Hz, 1H), 3.40-3.80 (m, 2H), 4.00 (q, *J* = 7.00 Hz, 2H), 6.75-7.25, (m, 5H), 7.45 (m, 1H), 7.55-7.80 (m, 3H), 8.22-8.26 (m, 1H), 8.35-8.50 (m, 2H).

[1-(4-Oxo-4H-pyrido[2,3-d][1,3]oxazin-2-yl)-ethyl]-carbamic acid tert-butyl ester (13)

N-(*tert*-butoxycarbonyl)-D-alanine (Boc-D-Ala) (5.00 g, 26.43 mmol) was dissolved in dry DCM (350 mL). *N*-methylmorpholine (7.30 mL, 66.07 mmol) was added and the reaction mixture was allowed to stir for 20 min. Iso-butylchloroformate (6.9 mL, 52.85 mmol) was added and the reaction flask was cooled to -20°C. Next, 2-aminonicotinic acid (3.65 g, 26.43 mmol) was added and the reaction mixture was allowed to warm up to room temperature, stirred overnight and then refluxed for 2.5h. The suspension was cooled to room temperature, filtrated and concentrated under reduced pressure. The crude product was used for the next step without any purification.

{1-[3-(4-Ethoxy-phenylcarbamoyle)-pyridin-2-ylcarbamoyle]-ethyl}-carbamic acid tert-butyl ester (14a)

Compound **13** (7.70 g, 26.43 mmol) as crude material was dissolved in dry DCM (250 mL) cooled to -20°C. 4-Ethoxy-phenylamine (3.27 mL, 26.43 mmol) was added and

stirred for 3h. The reaction mixture was allowed to warm up to room temperature overnight, and then washed with 1.0 N hydrochloric acid, saturated aqueous sodium bicarbonate and brine. The organic phase was dried over sodium sulphate, filtered and concentrated in vacuum. The crude product was used for the next step without further purification.

{1-[3-(4-Iodo-phenylcarbamoyl)-pyridin-2-ylcarbamoyl]-ethyl}-carbamic acid tert-butyl ester (14b)

This was performed analogously to the preparation of **14a**, using 4-iodo-phenylamine (5.79 g, 26.43 mmol). The crude product was used for the next step without further purification.

{1-[3-(4-Ethoxy-phenyl)-4-oxo-3,4-dihydro-pyrido[2,3-d]pyrimidin-2-yl]-ethyl}-carbamic acid tert-butyl ester (15a)

A solution containing the crude **14a** (6.69 g, 15.62 mmol) in 50 mL DCM and *N*-methylmorpholine (0.86 mL, 7.81 mmol) was stirred for 20 min at room temperature, then cooled to -20°C. Iso-butylchloroformate (1.01 mL, 7.81 mmol) was added drop wise. The solution was stirred for 3 h and subsequently allowed to warm to room temperature overnight. The reaction mixture was washed with 1.0 N hydrochloric acid, saturated aqueous sodium bicarbonate and brine. The organic phase was dried over sodium sulphate, filtered, concentrated in vacuum to give a dark-yellow oil. This material was dissolved in a small amount of DCM. While stirring, petroleum ether was added. The resulting precipitate was collected by filtration, washed with petroleum ether and dried to afford **15a** as a pale yellow solid. Yield: 3.47 g (64%). ¹H NMR (CDCl₃) δ: 1.17 (d, *J* = 7.00 Hz, 3H), 1.29-1.50 (m, 12H), 4.06 (q, *J* = 7.00 Hz, 2H), 4.61-4.66 (m, 1H), 5.75-5.79 (m, 1H), 7.01-7.44 (m, 5H), 8.56-8.58 (m, 1H), 8.93-8.95 (m, 1H).

{1-[3-(4-Iodo-phenyl)-4-oxo-3,4-dihydro-pyrido[2,3-d]pyrimidin-2-yl]-ethyl}-carbamic acid tert-butyl ester (15b)

This was performed analogously to the preparation of **15a**, using **14b** (6.40 g, 15.62 mmol). Yield: 3.80 g (59%) of a pale yellow solid. ¹H NMR (CDCl₃) δ: 1.28 (d, *J* = 6.77 Hz, 3H), 1.36 (s, 9H), 4.45-4.54 (m, 1H), 5.60-5.73 (m, 1H), 6.97-7.01 (m, 2H), 7.40-7.47 (m, 1H), 7.86-7.96 (m, 1H), 8.56-8.58 (m, 1H), 8.96-8.97 (m, 1H).

{1-[3-(4-Cyano-phenyl)-4-oxo-3,4-dihydro-pyrido[2,3-d]pyrimidin-2-yl]-ethyl}-carbamic acid tert-butyl ester (15c)

To a solution containing **15b** (0.50 g, 1.02 mmol) and zinc cyanide (0.17 g, 1.52 mmol) in DMF (30 mL) was added tetrakis(triphenylphosphine)palladium(0) (0.24 g, 0.2 mmol).

The reaction mixture was heated to 80°C for five hours, diluted with ethyl acetate and filtered through a pad of celite. The filtrate was concentrated under reduced pressure. The residue was diluted with ethyl acetate and washed with saturated aqueous sodium bicarbonate (1×50 mL). The aqueous layer was extracted with ethyl acetate (3×50 mL) and the combined organic layers were concentrated.

The crude material was purified by flash chromatography (ethyl acetate/hexane, 1:1) to afford **15c** as white solid. Yield: 0.24 g (60%). ¹H NMR (CDCl₃) δ: 1.25 (d, *J* = 6.8 Hz, 3H), 1.31 (s, 9H), 4.42-4.44 (m, 1H), 5.53-5.56 (m, 1H), 7.34-7.94 (m, 5H), 8.53-8.55 (m, 1H), 8.93-8.95 (m, 1H)

2-(1-Amino-ethyl)-3-(4-ethoxy-phenyl)-3H-pyrido[2,3-d]pyrimidin-4-one (16a)

Compound **15a** (2.16 g, 5.27 mmol) in DCM (25 mL) was treated with trifluoroacetic acid (8.50 mL) and stirred for four hours at room temperature. The reaction was extracted with hydrochloric acid 1M (3×50 mL), combined water layers were made basic with aqueous NH₄OH solution (25%, pH 9-10) and extracted with DCM (3×150 mL). The combined organic layers were dried over Na₂SO₄ and concentrated to afford 1.64 g of **16a** in quantitative yield as a white solid. ¹H NMR (CDCl₃) δ: 1.31 (d, *J* = 6.6 Hz, 3H), 1.44 (t, *J* = 7.0 Hz, 3H), 1.81 (s, 2H), 3.78 (q, *J* = 6.6 Hz, 1H), 4.07 (q, *J* = 7.0 Hz, 2H), 7.00-7.17 (m, 4H), 7.40-7.42 (m, 1H), 8.55-8.57 (m, 1H), 8.95-8.97 (m, 1H). ¹³C NMR (CDCl₃) δ: 14.61, 22.77, 49.57, 63.71, 115.65, 115.86, 123.55, 124.27, 128.58, 129.03, 132.35, 140.65, 152.15, 156.50, 159.56, 164.54. HREIMS *m/z* 310.14254 (calcd for C₁₇H₁₈N₄O₂, 310.1430). Anal. RP-HPLC *I*: *t_R* = 10.08 min (purity 99%), *II*: *t_R* = min 10.44 (purity 100%). Chiral HPLC: R-enantiomer: *t_R* = 14.91 min, S-enantiomer: *t_R* = 21.78 min. E.e. = 0 %.

4-[2-(1-Amino-ethyl)-4-oxo-4H-pyrido[2,3-d]pyrimidin-3-yl]-benzotrile (16b)

This was performed analogously to the preparation of **16a**, using **15c** (2.06 g, 5.27 mmol). Yield: 1.53 g (100%) of a white solid. ¹H NMR (CDCl₃) δ: 1.31 (d, *J* = 6.6 Hz, 3H), 2.39 (brs, 2H), 3.62 (q, *J* = 6.6 Hz, 1H), 7.23-7.70 (m, 3H), 7.70-7.87 (m, 2H), 8.51-8.53 (m, 1H), 8.96-8.98 (m, 1H). E.e. = 0 %.

3-(4-Ethoxy-phenyl)-2-{1-[(pyridin-3-ylmethyl)-amino]-ethyl}-3H-pyrido[2,3-d]pyrimidin-4-one (17a)

To a solution containing **16a** (3.60 g, 11.60 mmol) in dichloroethane (150 mL) was added 3-pyridinecarboxaldehyde (1.21 mL, 12.76 mmol) followed by sodium triacetoxyborohydride (3.69 g, 17.40 mmol). The reaction was allowed to stir at room temperature overnight. The mixture was diluted with DCM and washed with 1.0 M ammonium hydroxide (1 × 150 mL). The organic phase was dried over magnesium

sulfate, filtered and concentrated to afford a yellow oil that was purified by flash chromatography (DCM/MeOH, 9.5:0.5). A white powder was isolated. Yield: 3.58 g (77%). ¹H NMR (CDCl₃) δ: 1.29 (d, *J* = 6.6 Hz, 3H), 1.41 (t, *J* = 7.0 Hz, 3H), 2.53 (brs, 1H), 3.42-3.80 (q, *J* = 6.6 Hz, 1H), 3.42-3.80 (m, 2H), 4.02 (q, *J* = 7.0 Hz, 2H), 6.80-7.24 (m, 5H), 7.41-7.43 (m, 1H), 7.61-7.63 (m, 1H), 8.41-8.43 (m, 2H), 8.59-8.61 (m, 1H), 8.97-8.99 (m, 1H). ¹³C NMR (CDCl₃) δ: 14.56, 21.32, 48.77, 53.27, 63.68, 115.45, 115.58, 115.99, 122.28, 123.19, 127.46, 128.62, 128.88, 134.83, 135.52, 136.77, 148.36, 149.44, 156.12, 157.51, 159.53, 162.67, 164.66. HREIMS *m/z* 368.16152 (calcd for C₂₃H₂₃N₅O₂ - CH₃, 368.1617). Anal. RP-HPLC *I*: *t_R* = 10.75 min (purity 97%), *II*: *t_R* = min 10.63 (purity 97%).

4-(4-Oxo-2-{1-[(pyridin-3-ylmethyl)-amino]-ethyl}-4H-pyrido[2,3-d]pyrimidin-3-yl)-benzotrile (17b)

This was performed analogously to the preparation of **17a**, using **16b** (3.38 g, 11.60 mmol) Yield: 2.52 g (57%) of a white powder. ¹H NMR (CDCl₃) δ: 1.34 (d, *J* = 6.61 Hz, 3H), 3.35 (q, *J* = 6.61 Hz, 1H), 3.62-3.88 (m, 2H), 7.15-7.32 (m, 2H), 7.33-7.35 (m, 1H), 7.54-7.56 (m, 1H), 7.69-7.71 (m, 2H), 7.84-7.86 (m, 1H), 8.49-8.51 (m, 2H), 8.59-8.61 (m, 1H), 9.00-9.02 (m, 1H).

Decanoic acid {1-[3-(4-cyano-phenyl)-4-oxo-3,4-dihydro-quinazolin-2-yl]-ethyl}-(2-dimethylamino-ethyl)-amide (1a)

To one equivalent of **9b** (0.36 mg, 1.00 mmol) and one equivalent of triethylamine (0.14 mL, 1.00 mmol) dissolved in 25 mL dioxane was added one equivalent of decanoylchloride (0.21 mL, 1.00 mmol). The resulting mixture was stirred at room temperature for 18 hours and concentrated under reduced pressure. The residue was dissolved in dichloromethane and washed with saturated aqueous Na₂CO₃ solution, then twice with water. The organic phases were dried over anhydrous Na₂SO₄ and evaporated. The crude material was purified by flash chromatography with ethyl acetate/methanol (9/1) to afford the desired compound as free bases. Yield 0.18 g (35%). ¹H NMR (CDCl₃) δ: 0.83-0.85 (m, 3H), 1.20-1.22 (m, 16H), 1.34 (d, *J* = 6.9 Hz, 3H), 1.37-1.49 (m, 2H), 1.86-2.19 (m, 7H), 3.30-3.50 (m, 2H), 4.65 (q, 0.2H), 5.18 (q, *J* = 6.9 Hz, 0.8H), 7.33-7.83 (m, 7H), 8.19-8.22 (m, 1H). ¹³C NMR (CDCl₃) δ: 13.94, 16.35, 22.48, 22.23, 29.10, 29.27(2C), 31.67, 30.09, 41.141, 45.33, 45.61(2C), 50.58, 59.69, 113.36, 117.76, 120.66, 126.87, 127.27, 127.44, 129.33, 130.10, 133.28, 133.38, 134.66, 140.14, 146.78, 155.28, 161.89. HREIMS *m/z* 515.32438 (calcd for C₃₁H₄₁N₅O₂, 515.3260). Anal. RP-HPLC *I*: *t_R* = 15.80 min (purity 95%), *II*: *t_R* = min 15.43 (purity 100%), tailing due to the decanoic acid moiety.

Cyclohexanecarboxylic acid {1-[3-(4-cyano-phenyl)-4-oxo-3,4-dihydro-quinazolin-2-yl]-ethyl}-(2-dimethylamino-ethyl)-amide (1b)

This was performed analogously to the preparation of **1a**, using **9b** and cyclohexanoylchloride (0.13 mL, 1.00 mmol). Yield 0.36 g (77%). ¹H NMR (CDCl₃) δ: 1.21-1.56 (m, 6H), 1.63-1.89 (m, 8H), 2.12-2.36 (m, 8H), 3.41-3.59 (m, 2H), 1.86-2.19 (m, 7H), 5.24 (q, *J* = 6.7 Hz, 1H), 7.34-7.83 (m, 7H), 8.19-8.22 (m, 1H). ¹³C NMR (CDCl₃) δ: 16.23, 25.40, 25.52 (2C), 25.61, 41.21, 41.64, 45.66 (2C), 50.18, 60.28, 113.31, 117.84, 120.67, 126.89, 127.40, 129.50, 130.13, 133.26, 133.60, 134.69, 140.10, 146.85, 155.35, 161.88, 176.36. HREIMS *m/z* 471.26212 (calcd for C₂₈H₃₃N₅O₂, 471.2634). Anal. RP-HPLC *I*: *t_R* = 13.19 min (purity 99%), *II*: *t_R* = min 11.22 (purity 100%).

***N*-{1-[3-(4-Cyano-phenyl)-4-oxo-3,4-dihydro-quinazolin-2-yl]-ethyl}-*N*-(2-dimethylamino-ethyl)-benzamide (1c)**

This was performed analogously to the preparation of **1a**, using **9b** and benzoylchloride (0.12 mL, 1.00 mmol). Yield: 0.10 g (22%). ¹H NMR (CDCl₃) δ: 1.47 (d, *J* = 6.8 Hz, 3H), 1.87 (s, 6H), 2.01-2.45 (m, 2H), 3.42-3.57 (m, 2H), 5.21-5.25 (m, 1H), 6.75-7.14 (m, 8H), 7.15-7.95 (m, 4H), 8.12-8.25 (m, 1H). ¹³C NMR (CDCl₃) δ: 18.66, 44.33 (2C), 57.13, 52.35, 58.40, 114.85 (2C), 119.75, 122.05, 127.87, 128.93 (2C), 129.92, 130.28, 130.32, 130.67, 131.64, 133.32, 133.81, 134.33, 134.71, 136.57, 141.03, 147.72, 156.22, 177.85. HREIMS: the compound is not eligible for detecting the mass ion peak. Anal. RP-HPLC *I*: *t_R* = 12.39 min (purity 100%), *II*: *t_R* = min 12.09 (purity 100%).

***N*-{1-[3-(4-Cyano-phenyl)-4-oxo-3,4-dihydro-quinazolin-2-yl]-ethyl}-*N*-(2-dimethylamino-ethyl)-2-phenyl-acetamide (1d)**

This was performed analogously to the preparation of **1a**, using **9b** and phenylacetylchloride (0.13 mL, 1.00 mmol).

Yield: 0.19 g (40%). ¹H NMR (CDCl₃) δ: 1.37 (d, *J* = 7.0 Hz, 3H), 1.77-2.62 (m, 9H), 3.33-4.66 (m, 3H), 5.18 (q, *J* = 7.0 Hz, 1H), 7.12-7.97 (m, 7H), 8.21-8.23 (m, 1H). ¹³C NMR (CDCl₃) δ: 16.23, 40.14, 42.52, 45.64 (2C), 51.01, 59.73, 113.31, 117.76, 120.70, 126.88, 127.02, 127.35, 127.90, 128.03, 128.62, 128.76, 129.30, 130.06, 133.32, 133.81, 134.33, 134.71, 140.00, 146.72, 155.10, 161.85, 171.20. HREIMS *m/z* 479.23178 (calcd for C₂₉H₂₉N₅O₂, 479.2321). Anal. RP-HPLC *I*: *t_R* = 12.83 min (purity 98%), *II*: *t_R* = min 12.31 (purity 99%).

Decanoic acid (2-dimethylamino-ethyl)-{1-[3-(4-ethoxy-phenyl)-4-oxo-3,4-dihydro-quinazolin-2-yl]-ethyl}-amide (1f)

This was performed analogously to the preparation of **1a**, using **9a** (0.38 g, 1.00 mmol) and decanoylchloride (0.21 mL, 1.00 mmol). Yield: 0.23 g (42%). ¹H NMR (CDCl₃) at 27°C δ: 0.78-0.81 (m, 3H), 1.05-1.29 (m, 18H), 1.33-1.50 (m, 4H), 2.11-2.38 (m, 8H), 3.10-3.17 (m, 0.4H), 3.53-3.57 (m, 1.6H), 3.98 (q, *J* = 7.0 Hz, 2H), 4.80 (q, *J* = 7.2 Hz, 0.8H), 5.13 (q, *J* = 7.2 Hz, 0.2H), 6.84-7.15 (m, 3H), 7.25-7.77 (m, 4H), 8.05-8.28 (m, 1H). Peak splitting due to the presence of rotamers, as confirmed by ¹H NMR (DMSO) measurements at 90°C. HREIMS *m/z* 534.35434 (calcd for C₃₂H₄₆N₄O₃, 534.3570). Anal. RP-HPLC *I*: *t_R* = 16.67 min (purity 74%), *II*: *t_R* = min 16.44 (purity 98%), tailing due to the decanoic acid moiety.

Decanoic acid {1-[3-(4-ethoxy-phenyl)-4-oxo-3,4-dihydro-pyrido[2,3-d]pyrimidin-2-yl]-ethyl}-pyridin-3-ylmethyl-amide (11d)

This was performed analogously to the preparation of **1a**, using **17a** (0.40 g, 1.00 mmol) and decanoylchloride (0.21 mL, 1.00 mmol). Yield: 0.22 g (40%). ¹H NMR (CDCl₃) at 27°C δ: 0.80-0.82 (m, 3H), 1.10-1.97 (m, 20H), 2.23-2.30 (m, 2H), 4.01 (q, *J* = 7.0 Hz, 2H), 4.78-5.22 (m, 2.4H), 5.30 (q, *J* = 7.2 Hz, 0.6H), 6.54-6.59 (m, 0.3H), 6.90-8.19 (m, 8H), 8.42-8.55 (m, 1.7H), 8.90-9.01 (m, 1H). Peak splitting due to the presence of rotamers, as confirmed by ¹H NMR (DMSO) measurements at 90°C. HREIMS Not eligible for detecting the ion peak mass. Anal. RP-HPLC *I*: *t_R* = 15.06 min (purity 96%), *II*: *t_R* = min 16.28 (purity 96%), tailing due to the decanoic acid moiety.

N-{1-[3-(4-Ethoxy-phenyl)-4-oxo-3,4-dihydro-pyrido[2,3-d]pyrimidin-2-yl]-ethyl}-2-phenyl-N-pyridin-3-ylmethyl-acetamide (11e)

This was performed analogously to the preparation of **1a**, using **17a** and phenylacetylchloride (0.13 mL, 1.00 mmol). Yield: 0.04 g (8%). ¹H NMR (CDCl₃) at 27°C δ: 1.20 (d, *J* = 7.2 Hz, 2H), 1.40 (t, *J* = 6.9 Hz, 3H), 2.40-2.99 (m, 0.4H), 3.45-3.55 (m, 1.6H), 4.03 (q, *J* = 6.9 Hz, 2H), 4.35-5.17 (m, 2H), 5.35 (q, *J* = 7.2 Hz, 1H), 6.85-7.50 (m, 11H), 7.50-7.75 (m, 1H), 8.25-8.60 (m, 3H), 8.75- 8.92-9.04 (m, 1H). Peak splitting due to the presence of rotamers, as confirmed by ¹H NMR (DMSO) measurements at 90°C. HREIMS *m/z* 519.22551 (calcd for C₃₁H₂₉N₅O₃, 519.2270). Anal. RP-HPLC *I*: *t_R* = 12.16 min (purity 100%), *II*: *t_R* = min 13.22 (purity 100%).

N-{1-[3-(4-Cyano-phenyl)-4-oxo-3,4-dihydro-quinazolin-2-yl]-ethyl}-N-(2-dimethylamino-ethyl)-2-(4-trifluoromethoxy-phenyl)-acetamide (1e)

To one equivalent **9b** (0.36 mg, 1.00 mmol), and one equivalent (4-trifluoromethoxy-phenyl)-acetic acid (0.22 g, 1.00 mmol) dissolved in 25 mL dichloromethane and two

drops *N,N*-dimethylformamide, one equivalent of 1-(3-dimethylaminopropyl)-3-ethylcarbodiimide hydrochloride (EDCI) (0.19 g, 1.00 mmol) was added. The reaction mixture was stirred overnight, then basified with sodium bicarbonate solution and extracted with dichloromethane (3×50 mL). The organic layers were collected, dried over sodium sulfate concentrated and purified by flash chromatography (DCM/methanol, 9.5 : 0.5) to afford the desired compound as free base. Yield: 0.26 g (47%). ¹H NMR (CDCl₃) δ: 1.36 (d, *J* = 7.0 Hz, 3H), 1.88-2.48 (m, 9H), 3.34-4.74 (m, 3H), 5.13 (q, *J* = 7.0 Hz, 1H), 7.07-7.40 (m, 4H), 7.44-7.91 (m, 7H), 8.21-8.23 (m, 1H) ¹³C NMR (CDCl₃) δ: 16.22, 39.39, 42.80, 45.66 (2C), 51.25, 59.93, 113.41, 117.67, 120.69, 121.01, 126.95, 127.29, 128.12, 129.49, 130.26, 131.61 (2C), 132.18, 133.10, 133.32, 133.42, 133.81, 134.75, 135.04, 140.68, 148.00, 155.41, 161.80, 170.96. HREIMS *m/z* 563.21360 (calcd for C₃₀H₂₈F₃N₅O₃, 563.2144). Anal. RP-HPLC *I*: *t_R* = 14.01 min (purity 100%), *II*: *t_R* = min 13.73 (purity 100%).

***N*-{1-[3-(4-Ethoxy-phenyl)-4-oxo-3,4-dihydro-quinazolin-2-yl]-ethyl}-*N*-pyridin-3-ylmethyl-2-(4-trifluoromethoxy-phenyl)-acetamide (10)**

This was performed analogously to the preparation of **1e**, using **8** (0.40 g, 1.00 mmol) and (4-trifluoromethoxy-phenyl)-acetic acid. Yield: 0.35 g (59%). ¹H NMR (CDCl₃) at 27 °C δ: 1.16 (d, *J* = 7.1 Hz, 2H), 1.32-1.41 (m, 5H), 2.56 (dd, *J*₁ = 16.1 Hz, *J*₂ = 40.0 Hz, 0.8H), 3.21-3.78 (m, 1.2H), 3.53-4.06 (m, 2.5H), 4.48 (dd, *J*₁ = 14.8 Hz, *J*₂ = 46.4 Hz, 0.6H), 4.79-5.02 (m, 1.6H), 5.34 (q, *J* = 7.1 Hz, 0.3H), 6.55-5.85 (m, 0.5H), 6.91-7.21 (m, 9H), 7.33-7.56 (m, 3H), 7.64-7.83 (m, 1.5H), 8.11-8.46 (m, 2H). Peak splitting due to the presence of rotamers, as confirmed by ¹H NMR (DMSO) measurements at 90°C. HREIMS *m/z* 602.21506 (calcd for C₃₃H₂₉F₃N₄O₄, 602.2141). Anal. RP-HPLC *I*: *t_R* = 14.53 min (purity 100%), *II*: *t_R* = min 15.36 (purity 100%).

***N*-{1-[3-(4-Cyano-phenyl)-4-oxo-3,4-dihydro-pyrido[2,3-*d*]pyrimidin-2-yl]-ethyl}-*N*-pyridin-3-ylmethyl-2-(4-trifluoromethoxy-phenyl)-acetamide (11b)**

This was performed analogously to the preparation of **1e**, using **17b** (0.40 g, 1.00 mmol) and (4-trifluoromethoxy-phenyl)-acetic acid. Yield: 0.42 g (72%). ¹H NMR (CDCl₃) δ: 1.27 (d, 3H, *J* = 7.2 Hz), 3.50-3.72 (m, 2H), 5.03-5.13 (m, 3H), 7.00-7.19 (m, 5H), 7.23-7.49 (m, 3H), 7.85-7.99 (m, 3H), 8.48-8.56 (m, 3H), 8.99-9.02 (m, 1H). ¹³C NMR (CDCl₃) δ: 16.23, 39.81, 46.69, 52.39, 114.13, 116.24, 117.47, 121.05, 122.77, 123.54(2C), 129.39, 130.15(3C), 130.35(2C), 132.41, 132.98, 133.20, 133.77, 134.10, 136.81, 139.34, 147.20, 148.87, 156.40, 157.07, 161.48, 161.88, 172.77. HREIMS *m/z* 584.17947 (calcd for C₃₁H₂₃F₃N₆O₃, 584.1784). Anal. RP-HPLC *I*: *t_R* = 12.77 min (purity 100%), *II*: *t_R* = min 13.70 (purity 100%).

***N*-{1-[3-(4-Ethoxy-phenyl)-4-oxo-3,4-dihydro-pyrido[2,3-*d*]pyrimidin-2-yl]-ethyl}-*N*-pyridin-3-ylmethyl-2-(4-trifluoromethoxy-phenyl)-acetamide (11a)**

4-(Trifluoromethoxy-phenyl)-acetic acid (0.44 g, 2.00 mmol), 1-(3-dimethylaminopropyl)-3-ethylcarbodiimide hydrochloride (EDCI) (0.38 g, 2.00 mmol), 1-hydroxybenzotriazole hydrate (HOBT) (0.27g, 2.00 mmol) and diisopropylethylamine (DIPEA) (2.27 mL) were stirred in DCM (70 mL). After 30 min **17a** (0.40 g, 1.00 mmol) was added and the reaction mixture was stirred overnight, then extracted with HCl 1M (3×50 mL), basified with ammonia hydroxide 25% solution and extracted with DCM (3×200 mL). The combined organic layers were dried over Na₂SO₄ and concentrated to obtain the crude material that was purified by flash chromatography (EtOAc/EtOH, 9.5:0.5) to afford the desired compounds as free base. Yield: 0.33 g (54%). ¹H NMR (CDCl₃) at 27°C δ: 1.25 (d, *J* = 7.2 Hz, 0.9H), 1.36 (t, *J* = 6.9 Hz, 3H), 1.43 (d, *J* = 7.2 Hz, 2.1H), 2.70 (dd, *J*₁ = 16.0 Hz, *J*₂ = 33.6, 0.6H), 3.59 (dd, *J*₁ = 15.7 Hz, *J*₂ = 13.5H, 1.4H), 4.03 (q, *J* = 6.9 Hz, 2H), 4.57 (dd, *J*₁ = 14.8 Hz, *J*₂ = 107.3Hz, 0.6H), 5.05-5.12 (m, 0.3H), 5.18 (dd, *J*₁ = 18.4 Hz, *J*₂ = 2.9 Hz, 1.4H), 5.37 (q, *J* = 7.2 Hz, 0.7H), 6.70-6.74 (m, 0.3H), 6.85-7.24 (m, 8.5H), 7.36-7.47 (m, 2H), 7.61-7.66 (m, 0.6H), 8.17-8.23 (m, 0.6H), 8.42-8.56 (m, 2H), 8.93-9.04 (m, 1H). Peak splitting due to the presence of rotamers, as confirmed by ¹H NMR (DMSO) measurements at 90 °C. HREIMS *m/z* 603.20902 (calcd for C₃₂H₂₈F₃N₅O₄, 603.2093). Anal. RP-HPLC *I*: *t*_R = 13.38 min (purity 99%), *II*: *t*_R = min 14.65 (purity 99%).

***N*-{1-[3-(4-Ethoxy-phenyl)-4-oxo-3,4-dihydro-pyrido[2,3-*d*]pyrimidin-2-yl]-ethyl}-2-(4-trifluoromethoxy-phenyl)-acetamide (11f)**

This was performed analogously to the preparation of **11a**, using **16a** (0.31 g, 1.00 mmol) and (4-trifluoromethoxy-phenyl)-acetic acid. Yield: 1.64 g (27%). ¹H NMR (CDCl₃) δ: 1.31 (d, *J* = 6.8 Hz, 3H), 1.43 (t, *J* = 7.0 Hz, 3H), 3.53 (s, 2H), 4.04 (q, *J* = 7.0 Hz, 2H), 4.88 (q, *J* = 6.8 Hz, 1H), 6.84 (d, *J* = 7.94 Hz, 1H), 6.99-7.46 (m, 8H), 8.58-8.61 (m, 1H), 8.94-8.97 (m, 1H). ¹³C NMR (CDCl₃) δ: 14.60, 20.01, 42.21, 46.84, 63.67, 115.63, 115.69, 116.27 (2C), 121.01, 122.47, 127.07, 129.04, 129.26 (2C), 130.48, 133.18, 137.02, 155.85, 156.96, 159.79, 162.33, 162.43, 169.74. HREIMS *m/z* 512.16459 (calcd for C₂₆H₂₃F₃N₄O₄, 512.1671). Anal. RP-HPLC *I*: *t*_R = 13.30 min (purity 99%), *II*: *t*_R = min 14.87 (purity 98%).

***N*-{1-[3-(4-Ethoxy-phenyl)-4-oxo-3,4-dihydro-pyrido[2,3-*d*]pyrimidin-2-yl]-ethyl}-2-(4-fluoro-3-trifluoromethyl-phenyl)-acetamide (11c)**

This was performed analogously to the preparation of **11a**, using **17a** (0.40 g, 1.00 mmol) and (4-fluoro-3-trifluoromethyl-phenyl)-acetic acid (0.44 g, 2.00 mmol). Yield: 0.11 g (19%). ¹H NMR (CDCl₃) at 27 °C δ: 1.25 (d, *J* = 7.2 Hz, 2H), 1.39 (t, *J* = 7.0 Hz,

3H), 1.57 (d, $J = 7.2$ Hz, 1H), 2.30-2.95 (m, 0.6H), 3.57 (dd, $J_1 = 16.1$ Hz, $J_2 = 17.9$ Hz, 1.4H), 4.03 (q, $J = 7.0$ Hz, 2H), 4.20-5.23 (m, 2H), 5.05-5.12 (m, 0.3H), 5.33 (q, $J = 7.2$ Hz, 1H), 6.94-7.61 (m, 10H), 8.18-8.57 (m, 3H), 8.20-8.95(m, 1H). Peak splitting due to the presence of rotamers, as confirmed by ^1H NMR (DMSO) measurements at 90 °C. HREIMS m/z 605.20450 (calcd for $\text{C}_{32}\text{H}_{27}\text{F}_4\text{N}_5\text{O}_3$, 605.2050). Anal. RP-HPLC *I*: $t_R = 13.26$ min (purity 99%), *II*: $t_R = 14.45$ min (purity 99%).

[^{125}I]CXCL10 binding to human CXCR3 receptor

Cell membranes from HEK293 cells stably expressing the human CXCR3 receptor were prepared as follows. Cells were washed with cold PBS, detached using cold PBS containing 1 mM EDTA and centrifuged twice at 1500 g for 10 min at 4 °C. The pellet was resuspended in cold membrane buffer (15 mM Tris pH 7.5, 1 mM EGTA, 0.3 mM EDTA, 2 mM MgCl_2) and homogenized by 10 strokes at 1100-1200 rpm using a Teflon-glass homogenizer. The membranes were subjected to two freeze thaw cycles using liquid nitrogen and centrifuged at 40 000 g for 25 min at 4 °C. The pellet was rinsed with cold Tris-sucrose buffer (20 mM Tris pH 7.4, 250 mM sucrose), resuspended in the same buffer and frozen in liquid nitrogen. Protein concentration was determined using a Bio-Rad protein assay. Membranes were incubated in 96 well plates in binding buffer (50 mM HEPES pH 7.4, 1 mM CaCl_2 , 5 mM MgCl_2 , 100 mM NaCl, 0.5% BSA) with approximately 50 pM ^{125}I -CXCL10 (PerkinElmer Life and Analytical Sciences, Boston, MA) and increasing concentrations of antagonists for 2 h at RT. Subsequently, membranes were harvested via filtration through Unifilter GF/C plates (PerkinElmer Life and Analytical Sciences) pretreated with 1% polyethylenimine and washed three times with wash buffer (50 mM HEPES pH 7.4, 1 mM CaCl_2 , 5 mM MgCl_2 , 500 mM NaCl). Radioactivity was measured using a MicroBeta (PerkinElmer Life and Analytical Sciences) counter. Binding data were analyzed using Graphpad Prism.

Acknowledgment

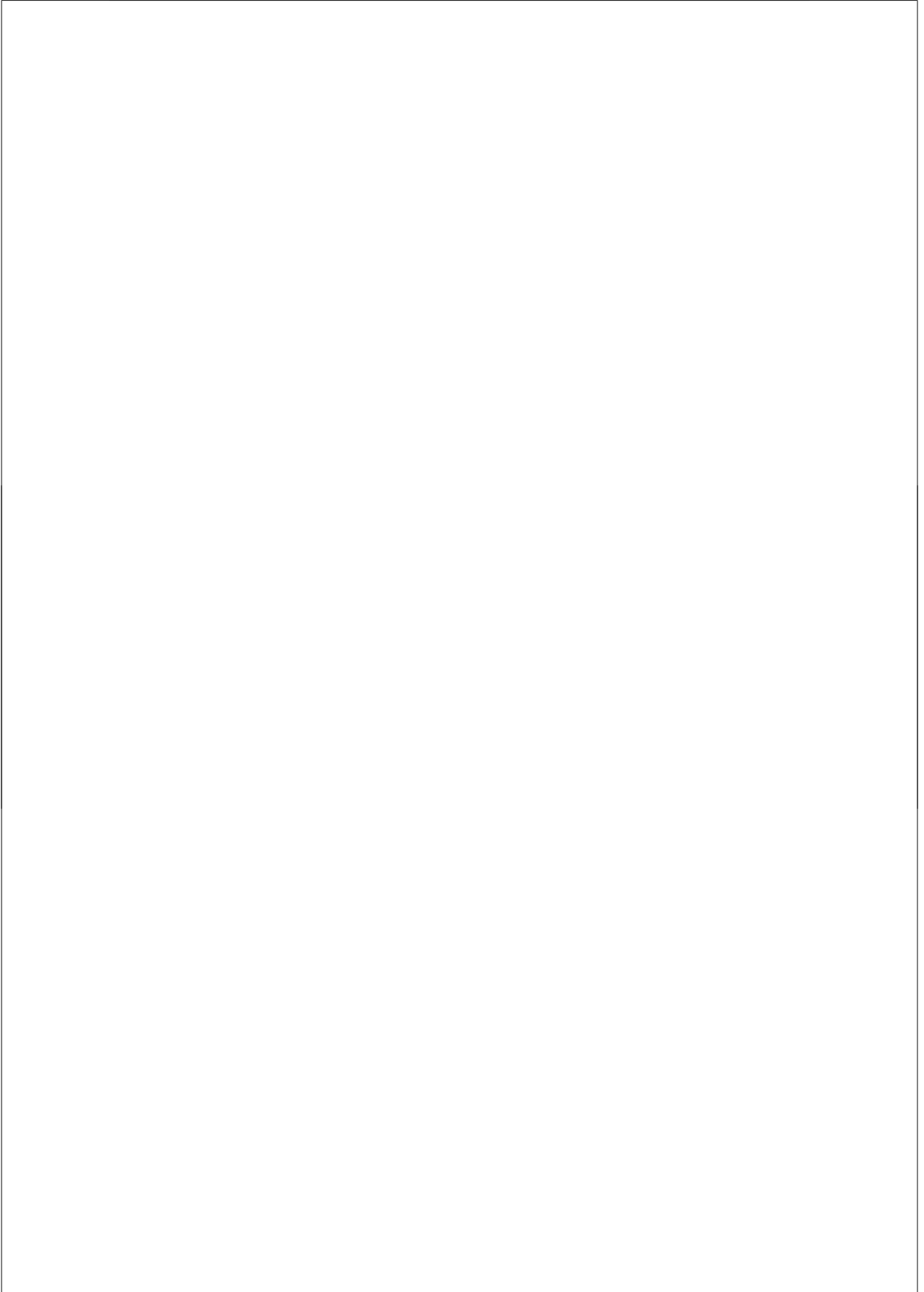
We thank Dr. M. Smoluch, Dr. F. J. De Kanter and Prof. Dr. R. V. Orru (all from the Department of Chemistry and Pharmaceutical Sciences at the Vrije Universiteit Amsterdam) for conducting (HR)MS measurements, for NMR analyses and for constructive help with chiral HPLC analysis, respectively.

References

- (1) Zlotnik, A.; Morales, J.; Hedrick, J. A. Recent advances in chemokines and chemokine receptors. *Crit. Rev. Immunol.*, **1999**, *19*, 1-47.
- (2) Murphy, P. M.; Baggiolini, M.; Charo, I. F.; Hebert, C. A.; Horuk, R.; Matsushima, K.; Miller, L. H.; Oppenheim, J. J.; Power, C. A. International union of pharmacology. XXII. Nomenclature for chemokine receptors. *Pharmacol. Rev.*, **2000**, *52*, 145-176.
- (3) Murphy, P. M. International Union of Pharmacology. XXX. Update on chemokine receptor nomenclature. *Pharmacol. Rev.*, **2002**, *54*, 227-229.
- (4) Clark-Lewis, I.; Mattioli, I.; Gong, J. H.; Loetscher, P. Structure-function relationship between the human chemokine receptor CXCR3 and its ligands. *J. Biol. Chem.*, **2003**, *278*, 289-295.
- (5) Proudfoot, A. E. Chemokine receptors: multifaceted therapeutic targets. *Nat. Rev. Immunol.*, **2002**, *2*, 106-115.
- (6) Tensen, C. P.; Flier, J.; Van Der Raaij-Helmer, E. M.; Sampat-Sardjoepersad, S.; Van Der Schors, R. C.; Leurs, R.; Scheper, R. J.; Boorsma, D. M.; Willemze, R. Human IP-9: A keratinocyte-derived high affinity CXC-chemokine ligand for the IP-10/Mig receptor (CXCR3). *J. Invest. Dermatol.*, **1999**, *112*, 716-722.
- (7) Smit, M. J.; Verdijk, P.; van der Raaij-Helmer, E. M.; Navis, M.; Hensbergen, P. J.; Leurs, R.; Tensen, C. P. CXCR3-mediated chemotaxis of human T cells is regulated by a Gi- and phospholipase C-dependent pathway and not via activation of MEK/p44/p42 MAPK nor Akt/PI-3 kinase. *Blood*, **2003**, *102*, 1959-1965.
- (8) Qin, S.; Rottman, J. B.; Myers, P.; Kassam, N.; Weinblatt, M.; Loetscher, M.; Koch, A. E.; Moser, B.; Mackay, C. R. The chemokine receptors CXCR3 and CCR5 mark subsets of T cells associated with certain inflammatory reactions. *J. Clin. Invest.*, **1998**, *101*, 746-754.
- (9) Patel, D. D.; Zachariah, J. P.; Whichard, L. P. CXCR3 and CCR5 ligands in rheumatoid arthritis synovium. *Clin. Immunol.*, **2001**, *98*, 39-45.
- (10) Balashov, K. E.; Rottman, J. B.; Weiner, H. L.; Hancock, W. W. CCR5(+) and CXCR3(+) T cells are increased in multiple sclerosis and their ligands MIP-1alpha and IP-10 are expressed in demyelinating brain lesions. *Proc. Natl. Acad. Sci. USA*, **1999**, *96*, 6873-6878.
- (11) Hancock, W. W.; Lu, B.; Gao, W.; Csizmadia, V.; Faia, K.; King, J. A.; Smiley, S. T.; Ling, M.; Gerard, N. P.; Gerard, C. Requirement of the chemokine receptor CXCR3 for acute allograft rejection. *J. Exp. Med.*, **2000**, *192*, 1515-1520.
- (12) Shields, P. L.; Morland, C. M.; Salmon, M.; Qin, S.; Hubscher, S. G.; Adams, D. H. Chemokine and chemokine receptor interactions provide a mechanism for selective T cell recruitment to specific liver compartments within hepatitis C-infected liver. *J. Immunol.*, **1999**, *163*, 6236-6243.
- (13) Mach, F.; Sauty, A.; Iarossi, A. S.; Sukhova, G. K.; Neote, K.; Libby, P.; Luster, A. D. Differential expression of three T lymphocyte-activating CXC chemokines by human atheroma-associated cells. *J. Clin. Invest.*, **1999**, *104*, 1041-1050.
- (14) Flier, J.; Boorsma, D. M.; van Beek, P. J.; Nieboer, C.; Stoof, T. J.; Willemze, R.; Tensen, C. P. Differential expression of CXCR3 targeting chemokines CXCL10, CXCL9, and CXCL11 in different types of skin inflammation. *J. Pathol.*, **2001**, *194*, 398-405.
- (15) Flier, J.; Boorsma, D. M.; Bruynzeel, D. P.; Van Beek, P. J.; Stoof, T. J.; Scheper, R. J.; Willemze, R.; Tensen, C. P. The CXCR3 activating chemokines IP-10, Mig, and IP-9 are expressed in allergic but not in irritant patch test reactions. *J. Invest. Dermatol.*, **1999**, *113*, 574-578.
- (16) Saetta, M.; Mariani, M.; Panina-Bordignon, P.; Turato, G.; Buonsanti, C.; Baraldo, S.; Bellettato, C. M.; Papi, A.; Corbetta, L.; Zuin, R.; Sinigaglia, F.; Fabbri, L. M. Increased expression of the chemokine receptor CXCR3 and its ligand CXCL10 in peripheral airways of smokers with chronic obstructive pulmonary disease. *Am. J. Respir. Crit. Care Med.* **2002**, *165*, 1404-1409.

- (17) Proost, P.; Schutyser, E.; Menten, P.; Struyf, S.; Wuyts, A.; Opendakker, G.; Dethoux, M.; Parmentier, M.; Durinx, C.; Lambeir, A. M.; Neyts, J.; Liekens, S.; Maudgal, P. C.; Billiau, A.; Van Damme, J. Amino-terminal truncation of CXCR3 agonists impairs receptor signaling and lymphocyte chemotaxis, while preserving antiangiogenic properties. *Blood*, **2001**, *98*, 3554-3561.
- (18) Romagnani, P.; Lasagni, L.; Annunziato, F.; Serio, M.; Romagnani, S. CXC chemokines: the regulatory link between inflammation and angiogenesis. *Trends. Immunol.* **2004**, *25*, 201-9.
- (19) Walser, T. C.; Rifat, S.; Ma, X.; Kundu, N.; Ward, C.; Goloubeva, O.; Johnson, M. G.; Medina, J. C.; Collins, T. L.; Fulton, A. M. Antagonism of CXCR3 inhibits lung metastasis in a murine model of metastatic breast cancer. *Cancer Res.*, **2006**, *66*, 7701-7707.
- (20) Johnson, M. G., Li, A., Liu, J., Marcus, A. P., Huang, A. X., Medina, J. C. Abstracts of Papers. *231st National Meeting of the American Chemical Society, Atlanta, GA 2006*.
- (21) Akashi, S.; Sho, M.; Kashizuka, H.; Hamada, K.; Ikeda, N.; Kuzumoto, Y.; Tsurui, Y.; Nomi, T.; Mizuno, T.; Kanehiro, H.; Hisanaga, M.; Ko, S.; Nakajima, Y. A novel small-molecule compound targeting CCR5 and CXCR3 prevents acute and chronic allograft rejection. *Transplantation*, **2005**, *80*, 378-384.
- (22) Ondeykal, J. G.; Herath, K. B.; Jayasuriya, H.; Polishook, J. D.; Bills, G. F.; Dombrowski, A. W.; Mojena, M.; Koch, G.; DiSalvo, J.; DeMartino, J.; Guan, Z.; Nanakorn, W.; Morenberg, C. M.; Balick, M. J.; Stevenson, D. W.; Slattery, M.; Borris, R. P.; Singh, S. B. Discovery of structurally diverse natural product antagonists of chemokine receptor CXCR3. *Mol. Divers.*, **2005**, *9*, 123-129.
- (23) Cole, A. G.; Stroke, I. L.; Brescia, M. R.; Simhadri, S.; Zhang, J. J.; Hussain, Z.; Snider, M.; Haskell, C.; Ribeiro, S.; Appell, K. C.; Henderson, I.; Webb, M. L. Identification and initial evaluation of 4-N-aryl-[1,4]diazepane ureas as potent CXCR3 antagonists. *Bioorg. Med. Chem. Lett.*, **2006**, *16*, 200-3.
- (24) Storelli, S.; Verdijk, P.; Verzijl, D.; Timmerman, H.; van de Stolpe, A. C.; Tensen, C. P.; Smit, M. J.; De Esch, I. J.; Leurs, R. Synthesis and structure-activity relationship of 3-phenyl-3H-quinazolin-4-one derivatives as CXCR3 chemokine receptor antagonists. *Bioorg. Med. Chem. Lett.*, **2005**, *15*, 2910-2913.
- (25) Allen, D. R.; Bolt, A.; Chapman, G. A.; Knight, R. L.; Meissner, J. W. G.; Owen, D. A.; Watson, R. J. Identification and structure-activity relationship of 1-aryl-3-piperidin-4-yl urea derivatives as CXCR3 receptor antagonists. *Bioorg Med Chem Lett*, **2007**, *17*, 697-701.
- (26) Schall, T., Dairaghi, D., Mc Master, B.. Compounds and Methods for Modulating CXCR3 function. *WO 01/16144 A2 2001*.
- (27) Johnson, M. G. Potency and PKDM Profile of 2,3-substitued quinazolin-4-ones as CXCR3 antagonists and the discovery of AMG487. *Presentation at the ISMC 2006 in Istanbul, Turkey 2006*.
- (28) Heise, C. E.; Pahuja, A.; Hudson, S. C.; Mistry, M. S.; Putnam, A. L.; Gross, M. M.; Gottlieb, P. A.; Wade, W. S.; Kiankarimi, M.; Schwarz, D.; Crowe, P.; Zlotnik, A.; Alleva, D. G. Pharmacological characterization of CXC chemokine receptor 3 ligands and a small molecule antagonist. *J. Pharmacol. Exp. Ther.*, **2005**, *313*, 1263-1271.
- (29) Errede, L. A.; Oien, H. T.; Yarian, D. R. Acylanthranils. 3. The influence of ring substituents on reactivity and selectivity in the reaction of acylanthranils with amines. *J. Org. Chem.*, **1977**, *42*, 12-18.
- (30) Li, Q.; Li, T.; Woods, K. W.; Gu, W.; Cohen, J.; Stoll, V. S.; Galicia, T.; Hutchins, C.; Frost, D.; Rosenberg, S. H.; Sham, H. L. Benzimidazolones and indoles as non-thiol farnesyltransferase inhibitors based on tipifarnib scaffold: synthesis and activity. *Bioorg. Med. Chem. Lett.*, **1995**, *15*, 2918-2922.
- (31) Palani, A.; Shapiro, S.; Josien, H.; Bara, T.; Clader, J. W.; Greenlee, W. J.; Cox, K.; Strizki, J. M.; Baroudy, B. M. Synthesis, SAR, and biological evaluation of oximino-piperidino-piperidine amides. 1. Orally bioavailable CCR5 receptor antagonists with potent anti-HIV activity. *J. Med. Chem.* **2002**, *45*, 3143-3160.

- (32) Medina, J. C.; Johnshon, M. G.; Li, A.; Liu, J.; Huang, A. X.; Zhu, L., Marcus, A. P., WO/02 083143 A1. **2002**.



Chapter 5

Imidazolium compounds as CXCR3 ligands

Abstract

In our quest to identify new ligands for CXCR3, we created a pharmacophore model based on reported CXCR3 ligands and subsequently screened our in house database. Several imidazole-containing compounds were retrieved as low-affinity hits. A merger approach was then pursued, in which the imidazole-hits were merged with imidazolium salts known from patent literature as CXCR3 binders. Accordingly, we synthesised a series of imidazolium analogues and identified 1-(2-(4-amino-3,5-dichlorophenyl)-2-oxoethyl)-3-(2-(3,4-dichlorophenyl)-2-oxoethyl)-1*H*-imidazol-3-ium bromide (**1m**) having a pK_i value in the submicromolar range as an interesting tool for CXCR3 pharmacological investigations.

Introduction

Chemokines, a group of small (8-14 kDa) proteins belonging to the family of chemotactic cytokines, are known to play an important role in leucocyte activation and migration occurring in various immunomediated diseases¹. These proteins are structurally divided in four groups (CC, CXC, CX3C and XC chemokines) by the number of the conserved cysteine residues. Chemokines exert activity through binding to a subfamily of the GPCRs, the so called chemokine receptor subgroup².

CXCR3, one of the chemokine receptors belonging to the GPCR superfamily, is expressed by epithelial, endothelial and lymphoid cells³. It is very well recognized that CXCR3 is overexpressed on the T helper 1 cells. Also, its ligands are upregulated in various chronic inflammatory diseases (rheumatoid arthritis^{4,5}, inflammatory bowel disease⁶, multiple sclerosis⁷, transplant rejection⁸, hepatitis C-infected liver⁹, atherosclerosis¹⁰, chronic skin reactions¹¹⁻¹³ and chronic obstructive pulmonary disease¹⁴) compared to normal physiologic conditions. Therefore, CXCR3 represents an attractive target for the treatment of inflammatory and autoimmune diseases. Evidence also suggests that CXCR3 may be a worthwhile target to treat cancer.¹⁵⁻¹⁷

While the knowledge of CXCR3 biology has increased in the last decade, the public domain contained relatively little information about small CXCR3 antagonists at the time the work for this thesis started.¹⁸⁻²³ The discovery of new CXCR3 ligands was needed to address both developments of pharmacological tools as well as of lead compounds for new potential drug classes.

This chapter will describe our efforts in the search of novel CXCR3 ligands. At the time of initiation of this work, structural diversity of the known CXCR3 ligands was limited and the known compounds had only moderate affinity for the CXCR3 receptor. Although both issues complicate successful model generation and *in silico* screening efforts, we set out to try rational drug design approaches using the available dataset, nevertheless. To reach our goal, we developed a 3D pharmacophore model based on the lowest energy conformation of VUF 10085/AMG 487 (Figure 1). Using the pharmacophore model, we performed an *in silico* query of our in-house database. The selected compounds were screened *in vitro* for their affinity at CXCR3. Some low-affinity hits were subsequently 'merged' with a scaffold extracted from the patent literature. This led to imidazolium salts showing potential for targeting CXCR3.²⁴

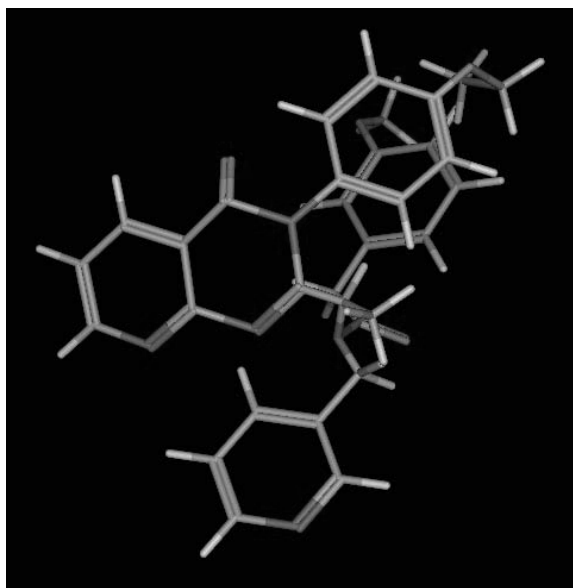
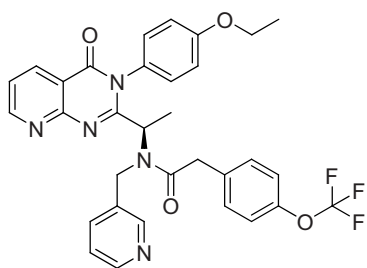


Figure 1. VUF 10085/AMG 487 lowest energy conformation and structure.

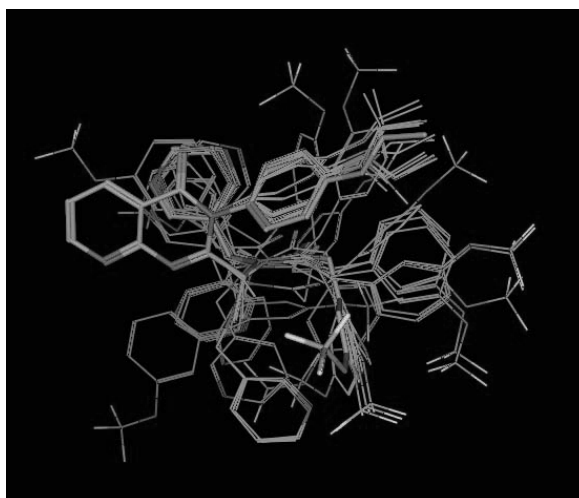
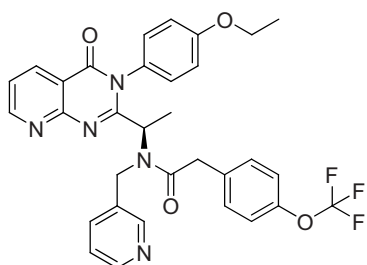


Figure 2. Overlapping of the 20 lowest energy VUF 10085/AMG 487 conformations.

VUF 10085 Conformational Search

Flexible molecules like the CXCR3 reference compound VUF 10085 can adopt many different conformations, but only one (or a selected few) low energy conformer(s) that brings all the important pharmacophoric features in the correct spatial orientation will be responsible for the biological activity.

To assess the conformational space, a stochastic conformational search was performed to generate the different conformers of VUF 10085. Using a stochastic search algorithm was preferred in order to avoid the enormous number of starting conformations generated during a systematic method for conformational analysis. During the conformational analysis, an energy cut off of 7 Kcal/mol was used to prevent the formation of too high-energy conformers. With this method, 53 conformers were generated. As illustrated by the superimposition of the aromatic heterocycles of the 20 lowest energy conformers (Figure 2), the flexibility of VUF 10085 is considerable. For example, key pharmacophoric features (as deduced by the SAR studies that are described in chapter 4) like the pyridine ring and trifluoromethoxybenzene can be positioned in a wide variety of space. Although any of these conformers would serve as a reasonable template for pharmacophore modeling, we selected the lowest energy conformer of VUF 10085 (Figure 1) to define a hypothesis for a pharmacophore model.

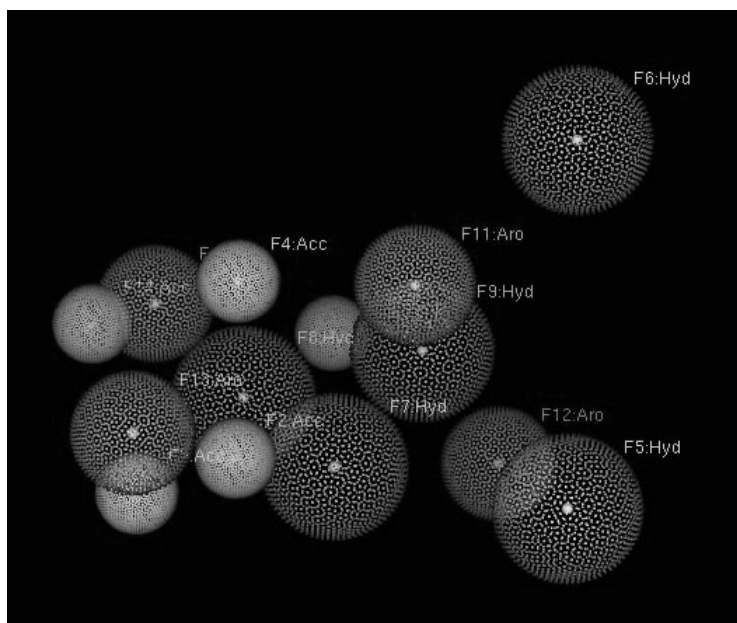


Figure 3. Pharmacophore model generated from the VUF 10085/AMG 487 lowest energy conformations.

Imidazolium compounds as CXCR3 ligands

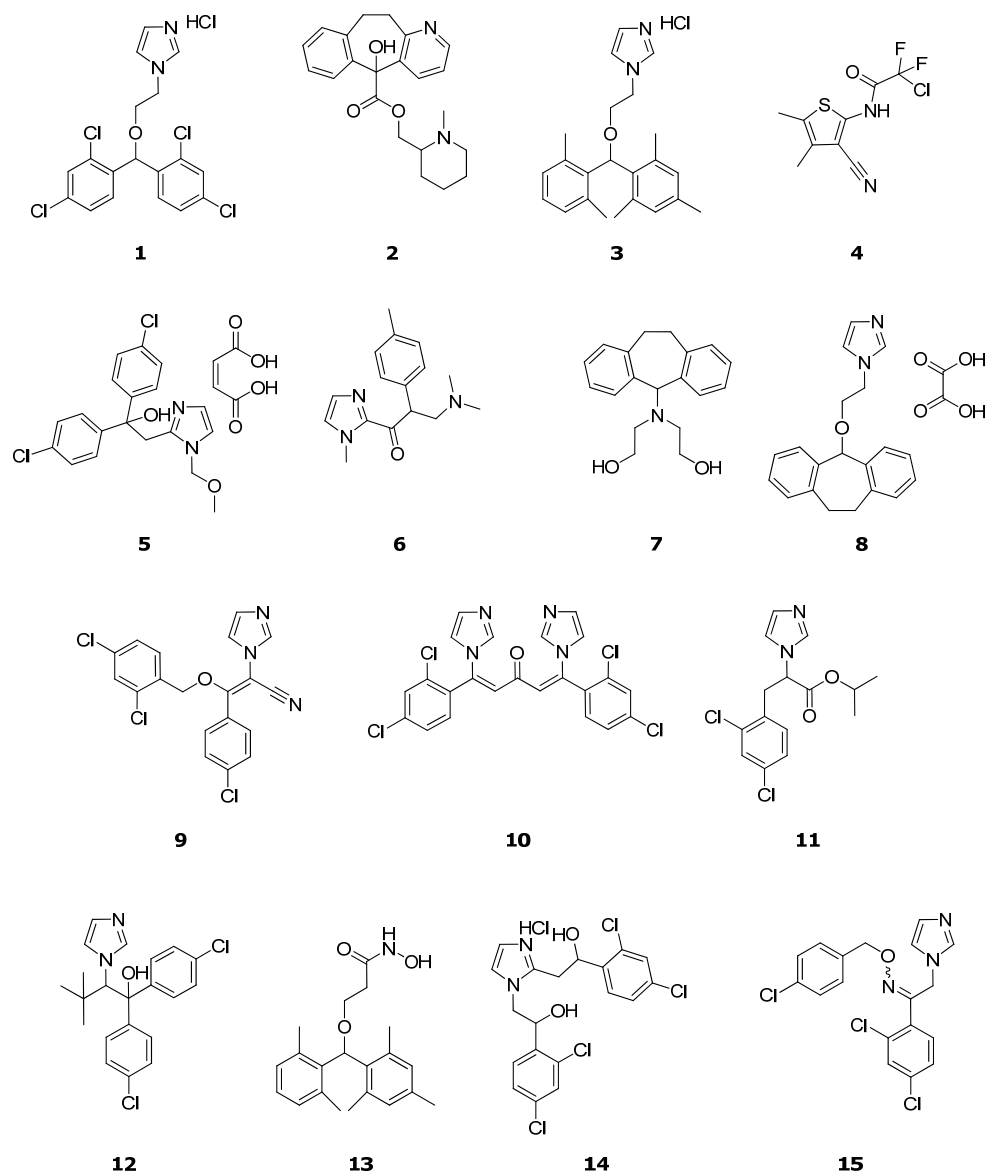


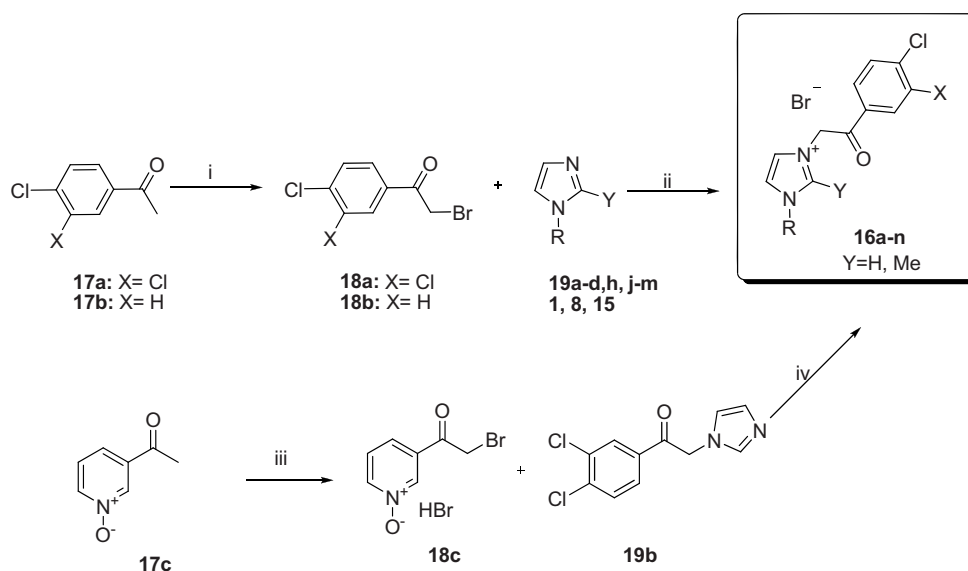
Figure 4. Derivatives resulting from the *in silico* screen of the in-house database. Chiral compounds are racemic and (where applicable) of unknown diastereomeric ratios. Compound **15** is a 20/80 mixture of *cis/trans* isomers.

Pharmacophore query, database screening and chemical modifications

The lowest energy conformation of VUF 10085 was used to generate a pharmacophore query. A total of 14 pharmacophoric points (Figure 3) were selected based on SAR considerations (chapter 4). Starting from this basic "naïve" pharmacophore model, the *in silico* screening of our in-house database (BS/GBR database) did not afford any hit that was able to fulfill all 14 pharmacophoric points, whereas enabling partial match of at least 8 and 7 pharmacophoric points resulted in 13 and 178 hits, respectively. In total, 140 of the 178 selected molecules from the the in-house database were readily available. These were therefore tested at 10^{-5} M concentration for the [125 I]CXCL10 displacement at human CXCR3 receptors on HEK-293 cells membranes stably expressing the receptor. Unfortunately, none of these compounds matched VUF 10085 in terms of affinity, with all showing only a slight affinity or no affinity at all for CXCR3 (data not shown). However, it was observed that most of the hits that showed a slight affinity (**1-15**) contained an imidazole core (Figure 4). Reasoning that the imidazole moieties should be substantially protonated at physiological pH, we noticed a general similarity with compounds from a recent patent application by Smithkline Beecham.²⁴ This patent describes CXCR3 inhibitors with a permanently charged imidazolium core as seen in e.g. 3-benzyl-1-[2-(3,4-dichloro-phenyl)-2-oxo-ethyl]-2-methyl-3*H*-imidazol-1-ium bromide (**16a**) and 1,3-bis-[2-(3,4-dichloro-phenyl)-2-oxo-ethyl]-3*H*-imidazol-1-ium bromide (**16b**). Given that permanently charged compounds are not uncommon binders for CXCR3,^{25,26} we decided to synthesize a small series of compounds in which the patented central imidazolium core was merged with the imidazole compounds identified from our *in silico* screen. Essentially, this opportunistic approach is currently one of the more common fragment optimization strategies in fragment-based drug discovery, as reviewed recently.²⁷ Accordingly, selected imidazole-containing compounds (**1, 8, 15**, see Figure 4 for compound structures) belonging to the *in-house* database were further functionalized with 2-bromo-1-(3,4-dichloro-phenyl)-ethanone or 2-bromo-1-(4-chloro-phenyl)-ethanone moieties. The obtained derivatives (**16e-g, i**) were compared for affinity at human CXCR3 to VUF 10085. Salts **16a** and **16b** were used as references. Furthermore, the importance of the N1 substituent in imidazolium reference compounds **16a** and **16b** has been investigated by its removal (**16j**), substitution with different hydrophobic moieties (**16c, 16d, 16k-m**) or substitution with a more polar group (**16h**). Lastly, the pyridine N-oxide analogue (**16n**) was prepared. This was based on the observation that the main metabolite of VUF 10085, i.e. a pyridine-N-oxide, has high activity.^{28,29}

Chemistry

The synthetic route for compounds **16a-n** is highlighted in Scheme 1. 2-Bromo-1-(3,4-dichloro-phenyl)-ethanone (**18a**) and 2-bromo-1-(4-chloro-phenyl)-ethanone (**18b**) were obtained by bromination of 1-(3,4-dichloro-phenyl)-ethanone (**17a**) and 1-(4-chloro-phenyl)-ethanone (**17b**), respectively, in acetic acid. Compounds **19b-d** were synthesized through substitution on imidazole by **18a**, **18b** and 2-bromo-4'-phenylacetophenone, respectively. The addition of **18a** or **18b** to the appropriate imidazole derivative (**1,8,15,19a-d,19h,19j-m**) afforded final compounds (**16a-m**). Yields varied from high to low (90-30%). Intermediate **18c** was obtained by bromination of acetylpyridine N-oxide (**17c**). The addition of 3-(2-bromoacetyl)pyridine-1-oxide hydrobromide (**18c**) to 1-(3,4-dichlorophenyl)-2-(1H-imidazol-1-yl)ethanone (**19b**) in the presence of base resulted in final compound **16n**.



Scheme 1. Synthesis of compounds **16a-n**. **Reagent and conditions.** (i) Br₂, CH₃COOH; (ii) CH₃CN or DMF, rt; (iii) Br₂, CHCl₃, reflux. (iv) CH₃CN, DIPEA, rt.

Pharmacology

The affinity for human CXCR3 of compounds was determined by the displacement of [¹²⁵I]CXCL10 binding to membranes from HEK-293 cells stably expressing the human CXCR3 receptor. Affinity was measured either in a single-point test or in a full-concentration curve.

Results and Discussion

Aiming to obtain a new class of CXCR3 inhibitors different from the 3*H*-quinazolin-4-ones and 3*H*-pyrido[2,3-*d*]pyrimidin-4-ones CXCR3 described in Chapters 3 and 4¹⁹, we developed a pharmacophore model based on the most active compound known at the time, VUF 10085. According to this model, we performed a screening of the *in-house* database. A total of 140 compounds were tested at a single concentration of 10 μ M for their affinities at human CXCR3 by assessing the [¹²⁵I] CXCL10 displacement. Although none of the screened compounds showed encouraging affinities for CXCR3, it was noted that an imidazole was a commonly found moiety amongst the low-affinity hits. Inspired by a Smithkline Beecham patent on imidazolium salts,²⁴ we decided to perform a merger and further expand some of our imidazole hits to imidazolium compounds. Together with a subsequent exploratory SAR study, these efforts led to **16a-n**. These compounds were tested on human CXCR3. The pK_i values for **16a-n** are summarized in Table 1.

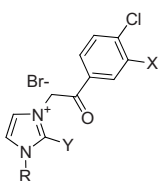
Compounds **16a** and **16b** were previously disclosed in a patent as CXCR3 antagonists.²⁴ In our hands, these compounds showed affinity values in the micromolar range (pK_i = 5.81 and 6.35 respectively). The affinity value of VUF 10085 is in the nanomolar range (pK_i = 7.39)¹⁹. Comparing **16b** to **16a**, the presence of a 1-(3,4-dichloro-phenyl)-ethanone unit instead of a benzyl in N1 and the removal of the methyl in position 2 of the imidazole ring afforded a compound (**16b**), three times higher than **16a** in terms of affinity but ten times lower than VUF 10085.

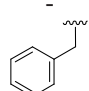
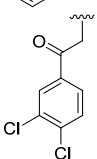
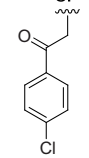
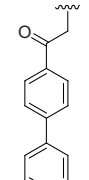
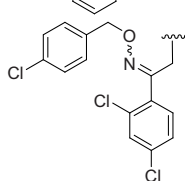
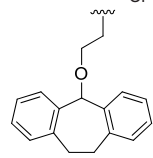
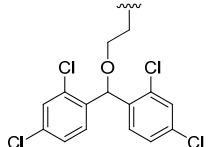
Removal of the 3-chloro (**16c**) or substitution of the 4-chloro with a phenyl (**16d**) in the 1-(3,4-dichloro-phenyl)-ethanone moiety in N1 of compound **16b** is allowed without any dramatic change in the affinity at CXCR3.

Compounds **16e-i**, having various substituents at N1 position of the imidazole ring, all revealed low affinity values suggesting that a proper substitution at the N1 position is responsible for the interaction with the receptor. Compounds like **16f** and **16i** with a more rigid structure are generally slightly more tolerated than more flexible compounds such as **16e**, **16g** and **16k**. For the tricyclic analogues (**16f**, **16i**) the removal of the 3-chloro substituent (**16i**) in the 1-(3,4-dichloro-phenyl)-ethanone moiety at N3 of compound **16f** led to a small drop in affinity. However a deeper SAR study of the substituent at N3 would better clarify its role for the affinity at CXCR3. The imidazolium derivative **16h** bearing a flexible polar substituent at N1 has a comparable affinity to compound **16i**. A complete removal of a substituent (**16j**) at N1 of the imidazole ring led to a dramatic decrease in the affinity. Also, compound **16l** having a benzyl acetamide substituent showed a poor affinity, once again underscoring the importance of a proper substitution at N1 for the affinity.

Imidazolium compounds as CXCR3 ligands

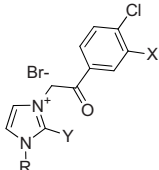
Table 1. pK_i values of the imidazolium analogues as determined by the displacement of [¹²⁵I]CXCL10 binding to the human CXCR3 receptor.

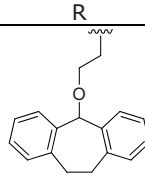
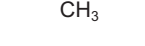
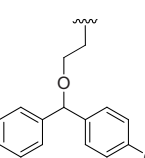
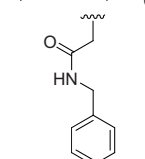
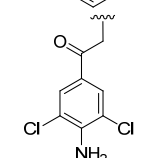
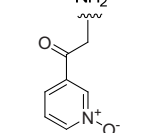


compd	X	Y	R	pK _i [#]
VUF 10085	-	-	-	7.39 ± 0.08 ¹⁹
16a VUF 10131	Cl	CH ₃		5.81 ± 0.10
16b VUF 10132	Cl	H		6.35 ± 0.03
16c VUF 10616	Cl	H		6.25 ± 0.01 ^{##}
16d VUF 10617	Cl	H		6.33 ± 0.01 ^{##}
16e VUF 10133	Cl	H		4.98 ± 0.10
16f VUF 10134	Cl	H		5.36 ± 0.03
16g VUF 10141	Cl	H		4.83 ± 0.05

[#]The binding experiments were carried out on cell membranes fractions from HEK-293 cells stably expressing the human CXCR3 receptor. The compounds were tested for their ability to displace [¹²⁵I]CXCL10 binding. The values are represented as the mean ± S.E.M. of at least three independent experiments.

^{##}Tested twice

Table 1. p*K_i* values of the imidazolium analogues as determined by the displacement of [¹²⁵I]CXCL10 binding to the human CXCR3 receptor.


compd	X	Y	R	p <i>K_i</i> [#]
16i VUF 10205	H	H		5.02 ± 0.14
16j VUF10713	Cl	H		4.35 ± 0.33 ^{##}
16k VUF 10618	Cl	H		4.86 ± 0.06 ^{##}
16l VUF 10611	Cl	H		4.29 ± 0.12 ^{##}
16m VUF 10612	Cl	H		6.79 ± 0.05 ^{##}
16n VUF 10639	Cl	H		4.57 ± 0.11 ^{##}

[#]The binding experiments were carried out on cell membranes fractions from HEK-293 cells stably expressing the human CXCR3 receptor. The compounds were tested for their ability to displace [¹²⁵I]CXCL10 binding. The values are represented as the mean ± S.E.M. of at least three independent experiments.

^{##}Tested twice.

Interestingly, the replacement of the 1-(3,4-dichloro-phenyl)-ethanone moiety in the N1 of **16b** by a 1-(4-amino-3,5-dichloro-phenyl)-ethanone unit (**16m**) afforded the most active compound in this series. It has a three times higher affinity value for CXCR3 ($pK_i = 6.79$) than the reference compound **16b**. The compound bears an aniline flanked by two chlorine atoms. Future SAR studies could address the elucidation of the exact roles of these three functional groups.

Last, compound **16n** bearing an N-oxide substituent showed a loss of affinity suggesting that a pyridine-N-oxide is not necessarily a preferred CXCR3 moiety.

Conclusions

In this study, we used a modeling approach with the aim to identify CXCR3 ligands that are structurally different from the ones already known. Using the 3*H*-pyrido[2,3-*d*]pyrimidin-4-one scaffold as starting point we developed a pharmacophore model and subsequently screened our *in-house* database. We combined the information obtained from the screening exercise with data extracted from patent literature. As such, we were able to obtain a series of permanently charged imidazolium derivatives that has been tested for binding affinity by displacement of [¹²⁵I]CXCL10. Compound **16m** ($pK_i=6.79$) has been identified as the most potent compound in this series, approximately three times better than the reference compound **16b**. It may represent an interesting tool compound for future CXCR3 research.

Experimental section

Pharmacophore Model

In an attempt to find a new scaffold for CXCR3 antagonism, a 3D pharmacophore model was developed using the MOE software. The "Pharmacophore from a single active molecules" approach has been chosen and VUF 10085 has been used as starting point being the most active molecule known at the time of the study ($pK_i = 7.39$)¹⁹. As source for new small molecules our *in-house* (BS/GBR) database was screened.

General synthetic

The solvents were dried according to standard procedures. All the reactions were performed under an atmosphere of dry nitrogen. ¹H NMR and ¹³C spectra were recorded on a Bruker AC-200 (200 MHz) spectrometer. Melting points were measured on an Electrothermal IA 9200 apparatus.

Building blocks

Building blocks **19a**, **19j** and **17a,b** were commercially available (Sigma-Aldrich). The synthesis of **17c** has been described by others.³⁰ Compounds **1**, **8**, **15** and **19h,k,l,m** belong to our in-house database. The structures of all these building blocks are depicted in **Figure 5**.

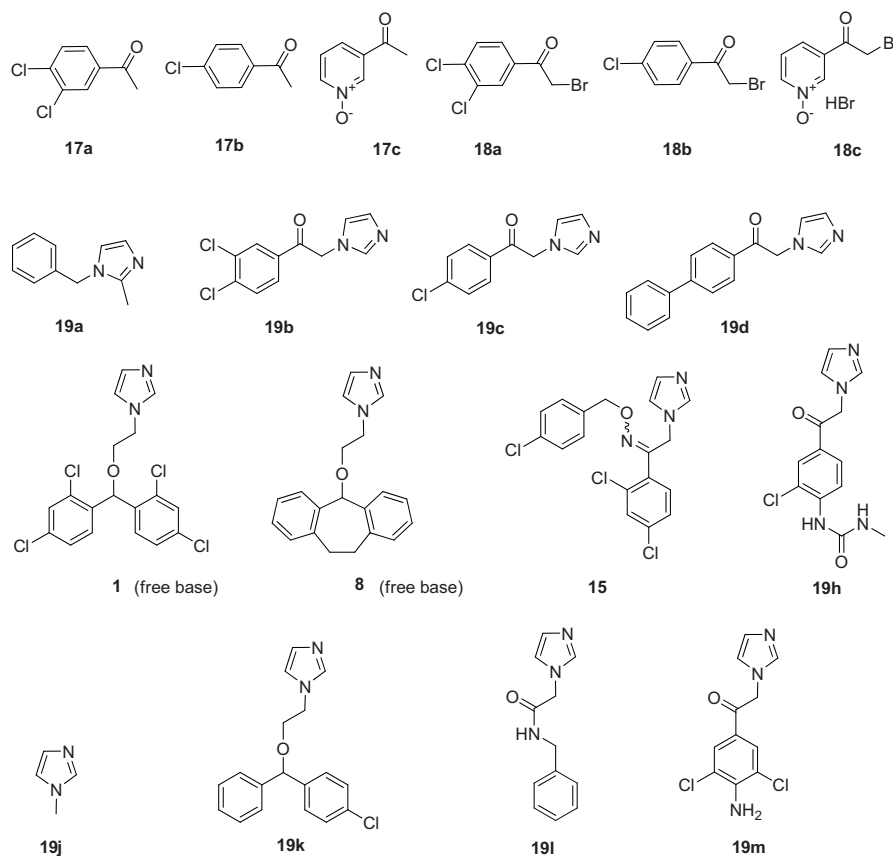


Figure 5. Building blocks structures.

2-Bromo-1-(3,4-dichlorophenyl)-ethanone (18a)

To a stirred solution of 1-(3,4-dichlorophenyl)-ethanone **17a** (10.00 g, 59.2 mmol) in acetic acid (100 mL) a solution of bromine (2.71 mL, 59.2 mmol) in acetic acid (30 mL) was added dropwise at 20-25 °C. After 6 hrs the mixture was poured in water (250 mL) and stirred overnight at rt. The biphasic solution was diluted in ether (150 mL) and the organic layer separated from water and washed again (3×200mL). The organic phases were dried over sodium sulphate and concentrated to afford **18a** as a green oil. Yield:

13.28 g (84%). ^1H NMR (CDCl_3) δ : 4.33 (s, 2H), 7.42-7.64 (m, 1H), 7.70-7.83 (m, 1H), 8.03 (s, 1H).

2-Bromo-1-(4-chloro-phenyl)-ethanone (18b)

Analogous to the preparation of **18a**, using 1-(4-chloro-phenyl)-ethanone **17b** (8.40 mL, 64.7 mmol). Yield: 7.80 g (78%). ^1H NMR (CDCl_3) δ : 4.40 (s, 2H), 7.25-7.44 (m, 2H), 7.73-7.90 (m, 2H).

3-(2-Bromoacetyl)pyridine 1-oxide hydrobromide (18c)

Bromine (0.21 mL, 4.08 mmol) was added to a solution of acetylpyridine N-oxide **17c** (0.56 g, 4.08 mmol) in CHCl_3 (10 mL).³⁰ The resulting mixture was gently refluxed under argon for 1h. The precipitate was filtered off, washed several times with diethylether and dried at rt. Yield: 0.75 g (62 %) as white solid. ^1H NMR (DMSO) δ : 5.0 (s, 2H), 7.7 (t, 1H), 8.0 (d, 1H), 8.5 (d, 1H), 8.8 (s, 1H).

1-(3,4-Dichloro-phenyl)-2-imidazol-1-yl-ethanone (19b)

Imidazole (0.13 g, 1.87 mmol) was dissolved in acetonitrile (50 mL). After 10 min, a solution of **18a** (0.50 g, 1.87 mmol) in acetonitrile (10 mL) was added dropwise. The mixture was stirred overnight at rt. A precipitate was formed and filtrated. The solution was concentrated, dissolved in dichlorometane (50 mL) basified with sodium bicarbonate saturated solution (50 mL) and extracted with dichlorometane (3×50mL). The organic layers were dried over sodium sulphate and concentrated. The crude material was purified by flash chromatography on silica gel eluting with ethanol/dichloromethane (1:9) to afford the desired compound as pale yellow solid. Yield: 0.15 g (31%). ^1H NMR (CDCl_3) δ : 5.30 (s, 2H), 6.89 (s, 1H), 7.10 (brs, 1H), 7.45 (brs, 1H), 7.50-7.82 (m, 2H), 7.99 (s, 1H).

1-(4-Chlorophenyl)-2-(1H-imidazol-1-yl) ethanone (19c)

This procedure was carried out analogously to the preparation of **19b** using 2-bromo-1-(4-chlorophenyl)ethanone **18b** (0.50 g, 2.14 mmol) and imidazole (0.15 g, 2.14 mmol). The product was obtained as a off white powder. Yield: 110 mg (23 %) ^1H NMR (CDCl_3) δ : 5.36 (s, 2H), 6.92 (s, 1H), 7.12 (s, 1H), 7.49 (d, 2H), 7.50 (s, 1H), 7.89 (d, 2H).

1-(Biphenyl-4-yl)-2-(1H-imidazol-1-yl) ethanone (19d)

This procedure was carried out analogously to the preparation of **19b**, using 2-bromo-4'-phenylacetophenone (0.44 g, 1.60 mmol) and imidazole (0.11g, 1.60 mmol). The product was obtained as a yellow powder. Yield: 148 mg (35 %); ^1H NMR (CDCl_3) δ : 5.42 (s, 2H), 6.96 (s, 1H), 7.40-7.65 (m, 7H), 7.73 (d, 2H), 8.03 (d, 2H)

3-Benzyl-1-[2-(3,4-dichloro-phenyl)-2-oxo-ethyl]-2-methyl-3H-imidazol-1-ium bromide (16a) VUF10131

Compound **18a** (0.20 g, 0.75 mmol) and 1-benzyl-2-methyl-1*H*-imidazole **19a** (0.13 g, 0.75 mmol) were stirred overnight at rt in acetonitrile (50 mL). The mixture was diluted with ether. The solid product was filtered, washed with ether and dried to afford **16a** as white solid. Yield: 0.23 g (85%). ¹H NMR (DMSO) δ: 2.56 (s, 3H), 5.54 (s, 2H), 6.03 (s, 2H), 7.24-7.55 (m, 5H), 7.60-7.63 (m, 1H), 7.82-7.90 (m, 1H), 7.92-8.07 (m, 2H), 8.33-8.35 (m, 1H). M.p. 240.6-241.8°C.

1,3-Bis-[2-(3,4-dichloro-phenyl)-2-oxo-ethyl]-3H-imidazol-1-ium bromide (16b) VUF10132

This procedure was carried out analogously to the preparation of **16a** using **19b** (0.19 g, 0.75 mmol) and **18a** (0.20 g, 0.75 mmol). Yield: 0.31 g (78%) of a white solid. ¹H NMR (DMSO) δ: 6.20 (s, 4H), 7.67-7.80 (m, 4H), 7.88-8.12 (m, 3H), 8.23-8.25 (m, 2H), 9.12 (s, 1H). ¹³C NMR (50 MHz, DMSO) δ: 54.67, 55.45, 119.92, 122.65, 127.70, 128.45, 130.15, 131.16, 131.26, 131.98, 132.34, 133.76, 137.83, 138.15, 188.55, 189.74. M.p. 238.2-239.6 °C.

(2-(4-Chlorophenyl)-2-oxoethyl)-1-(2-(3,4-dichlorophenyl)-2-oxoethyl)-1H-imidazol-3-ium bromide (16c) VUF10616

This procedure was carried out analogously to the preparation of **16a** using **19c** (0.10 g, 0.44 mmol) and **18a** (0.09 g, 0.35 mmol). The desired product was obtained as white solid. Yield: 0.14 g, (67 %) ; ¹H NMR (DMSO) δ: 6.14 (s, 4H), 7.75 (d, 2H), 7.77-8.11 (m, 6H), 8.31 (s, 1H), 9.06 (s, 1H); ¹³C NMR (50 MHz, DMSO) δ: 55.42, 55.47, 123.48, 123.62, 127.91, 129.05, 129.83, 131.29, 131.92, 132.24, 133.77, 136.98, 138.30, 139.15, 189.64, 190.22. M.p. 239.1-240.4°C.

3-(2-(Biphenyl-4-yl)-2-oxoethyl)-1-(2-(3,4-dichlorophenyl)-2-oxoethyl)-1H-imidazol-3-ium bromide (16d) VUF10617

This procedure was carried out analogously to the preparation of **16a** using **19d** (0.13 g, 0.50 mmol) and **18a** (0.11g, 0.40 mmol). The product **16d** was obtained as a white powder. Yield: 0.15 g (55 %); ¹H NMR (DMSO) δ: 6.16 (s, 2H), 6.20 (s, 2H), 7.46-8.33 (m, 14H), 9.09 (s, 1H); ¹³C NMR (50 MHz, DMSO): 55.48, 123.46, 123.67, 126.87, 126.95, 127.92, 128.68, 128.96, 129.85, 131.30, 131.91, 132.29, 133.78, 136.99, 138.28, 138.34, 145.47, 189.66, 190.62 M.p. 240.8-242.1°C.

3-[2-[(E)-4-Chloro-benzyloxyimino]-2-(2,4-dichloro-phenyl)-ethyl]-1-[2-(3,4-dichloro-phenyl)-2-oxo-ethyl]-3H-imidazol-1-ium bromide (16e) VUF10133

This procedure was performed analogously to the preparation of **16a** using **15** (0.24 g, 0.60 mmol) and **18a** (0.15 g, 0.60 mmol). The product **16e** was obtained as a white powder. Yield: 0.13 g (32%). ¹H NMR (DMSO) δ: 5.07 (s, 2H), 5.49 (s, 2H), 6.06 (s, 2H), 7.27-7.40 (m, 2H), 7.41-7.49 (m, 4H), 7.56-7.61 (m, 3H), 7.71-8.05 (m, 2H), 8.28-8.30 (m, 1H), 9.11 (s, 1H). M.p. 202.4-206.1°C.

1-[2-(3,4-Dichloro-phenyl)-2-oxo-ethyl]-3-[2-(10,11-dihydro-5H-dibenzo[a,d]cyclohepten-5-yloxy)-ethyl]-3H-imidazol-1-ium bromide (16f) VUF10134

This procedure was performed analogously to the preparation of **16a** using **8** free base (0.15 g, 0.49 mmol) and **18a** (0.13 g, 0.49 mmol). The product **16f** was obtained as a white solid. Yield: 0.23 g (83%). ¹H NMR (DMSO) δ: 2.80-3.08 (m, 2H), 3.10-3.22 (m, 2H), 3.62-3.83 (m, 2H), 4.53-4.67 (m, 2H), 5.60 (s, 1H), 6.05 (s, 2H), 7.18-7.32 (m, 8H), 7.69-8.01 (m, 4H), 8.31-8.32 (m, 1H), 9.11 (s, 1H). M.p. 200.2-201.5°C.

3-{2-[Bis-(2,4-dichloro-phenyl)-methoxy]-ethyl}-1-[2-(3,4-dichloro-phenyl)-2-oxo-ethyl]-3H-imidazol-1-ium bromide (16g) VUF10141

This procedure was performed analogously to the preparation of **16a** using **1** free base (0.16 g, 0.38 mmol) and **18a** (0.10 g, 0.38 mmol). The product **16g** was obtained as a white solid. Yield: 0.19 g (77%). ¹H NMR (DMSO) δ: 3.78-3.90 (m, 2H), 4.45-5.54 (m, 2H), 5.96 (s, 1H), 6.05 (s, 2H), 7.13-7.18 (m, 2H), 7.42-7.47 (m, 2H), 7.68-7.70 (m, 3H), 7.80-8.02 (m, 3H), 8.32 (s, 1H), 9.10 (s, 1H). M.p. 241.2-241.9°C.

3-{2-[3-Chloro-4-(3-methyl-ureido)-phenyl]-2-oxo-ethyl}-1-[2-(3,4-dichloro-phenyl)-2-oxo-ethyl]-3H-imidazol-1-ium bromide (16h) VUF10142

This procedure was performed analogously to the preparation of **16a** using **19h** (35 mg, 0.12 mmol) and **18a** (32 mg, 0.12 mmol). The compound **16h** was obtained as a white solid. Yield: 0.03g (48%)¹H NMR (DMSO) δ: 2.68-2.71 (m, 3H), 6.07 (s, 2H), 6.13 (s, 2H), 7.22-7.33 (m, 1H), 7.76-8.10 (m, 5H), 8.30-8.32 (m, 1H), 8.48-8.52 (m, 2H), 9.04 (s, 1H). M.p. 202.6-204.3°C.

1-[2-(4-Chloro-phenyl)-2-oxo-ethyl]-3-[2-(10,11-dihydro-5H-dibenzo[a,d]cyclohepten-5-yloxy)-ethyl]-3H-imidazol-1-ium; bromide (16i) VUF10205

This procedure was performed analogously to the preparation of **16a** using **8** free base (85 mg, 0.28 mmol) and **18b** (65 mg, 0.28 mmol). The compound **16i** was obtained as a

white solid. Yield: 0.13 g (85%). ¹H NMR (DMSO) δ: 2.50-3.18 (m, 2H), 3.34-3.40 (m, 2H), 3.71-3.81 (m, 2H), 4.51-4.57 (m, 2H), 5.61 (s, 1H), 6.06 (s, 2H), 7.18-7.29 (m, 2H), 7.69-7.85 (m, 5H), 7.89-8.11 (m, 2H), 9.12 (s, 1H). M.p. 201.2-201.8°C.

1-[2-(3,4-Dichloro-phenyl)-2-oxo-ethyl]-3-methyl-3H-imidazol-1-ium bromide (16j) VUF10713

This procedure was performed analogously to the preparation of **16a** using *N*-methyl imidazole **19j** (0.12 g, 1.49 mmol) and **18a** (0.40 g, 1.49 mmol). The product **16j** was obtained as red oil. Yield: 0.46 g (88%). ¹H NMR (DMSO) δ: 3.96 (s, 3H), 6.06 (s, 2H), 7.67-7.68 (m, 1H), 7.70-7.78 (m, 1H), 7.80-8.04 (m, 2H), 8.29-3.31 (m, 1H), 9.05 (s, 1H).

3-(2-(4-chlorophenyl) (phenyl) methoxy) -2- oxoethyl) -1- (2 -(3, 4-dichlorophenyl) -2-oxoethyl)- 1H-imidazol-3-ium bromide (16k) VUF10618

This procedure was performed analogously to the preparation of **16a** using **19k** (100 mg, 0.26 mmol) and **18a** (56 mg, 0.21 mmol). The product **16k** was obtained as yellow foam. Yield: 0.10 g (65 %); ¹H NMR (DMSO) δ: 8.0 (s, 1H), 7.9 (dd, 1H), 7.6 (s, 1H), 7.5 (d, 1H), 7.4 (s, 1H), 7.3 (m, 10H), 6.8 (s, 1H), 6.3 (s, 2H), 5.4 (dd, 2H).

1-(2-(benzylamino)-2-oxoethyl)-3-(2-(3,4-dichlorophenyl)-2-oxoethyl)-1H-imidazol-3-ium bromide (16l) VUF10611

This procedure was performed analogously to the preparation of **16a**, using **19l** (0.10 g, 0.46 mmol) and **18a** (100 mg, 0.37 mmol). The product **16l** was obtained as a white powder. Yield: 0.14 g (63 %) ¹H NMR (DMSO) δ: 4.35 (d, 2H), 5.20 (s, 2H), 6.11 (s, 2H), 7.26-7.39 (m, 5H), 7.70 (s, 1H), 7.81 (s, 1H), 7.92 (d, 1H), 7.99 (d, 1H), 8.30 (s, 1H), 9.02 (t, 1H), 9.10 (s, 1H); ¹³C NMR (50 MHz, DMSO) 42.26, 50.46, 55.32, 123.11, 123.49, 126.84, 127.24, 127.91, 128.14, 129.84, 131.28, 131.89, 133.74, 136.92, 138.28, 138.33, 164.66, 189.62. M.p. 204.9-206.8°C.

1-(2-(4-amino-3,5-dichlorophenyl)-2-oxoethyl)-3-(2-(3,4-dichlorophenyl)-2-oxoethyl)-1H-imidazol-3-ium bromide (16m) VUF10612

This procedure was performed analogously to the preparation of **16a**, using **19m** (0.10 g, 0.33 mmol) and **18a** (71 mg, 0.26 mmol). The product **16m** was obtained as a white powder. Yield: 0.12 g (68 %) ¹H NMR (DMSO) δ: 6.03 (s, 2H), 6.13 (s, 2H), 6.78 (s, 2H), 7.75 (s, 2H), 7.93-8.05 (m, 4H), 8.31 (s, 1H), 9.04 (s, 1H); ¹³C NMR (50 MHz, DMSO) 54.65, 55.43, 117.20, 121.62, 123.43, 123.59, 127.90, 128.34, 129.83, 131.29, 131.90, 133.76, 138.27, 146.35, 187.22, 189.64. M.p. 202.0-204.1°C.

3-(2-(3-(2-(3,4-dichlorophenyl)-2-oxoethyl)-1H-imidazol-3-ium-1-yl)acetyl)pyridine 1-oxide bromide (16n) VUF10639

Compound **18c** (50 mg, 0.17 mmol) was suspended in acetonitrile (10 mL) and N,N-diisopropylethylamine (0.03 mL, 0.17 mmol) was added to liberate the free N-oxide by stirring for 15 min at r.t. This gave a red solution. Intermediate **19b** (43 mg, 0.17 mmol) was added and the solution was stirred overnight at r.t. The desired product precipitated and was filtered to give a red powder (44 mg, 56 %). ¹H NMR (DMSO) δ: 6.0 (s, 2H), 6.1 (s, 2H), 7.6 - 7.8 (m, 3H), 7.8 - 8.0 (3H), 8.3 (s, 1H), 8.5 (d, 1H), 8.9 (s, 1H), 9.1 (s, 1H). ¹³C NMR (50 MHz, DMSO) 55.49, 55.60, 123.52, 123.62, 123.79, 126.90, 127.89, 129.81, 131.29, 131.92, 132.79, 133.75, 137.00, 138.15, 138.32, 142.81, 188.98, 189.57. M.p. 196.2 - 197.8 °C.

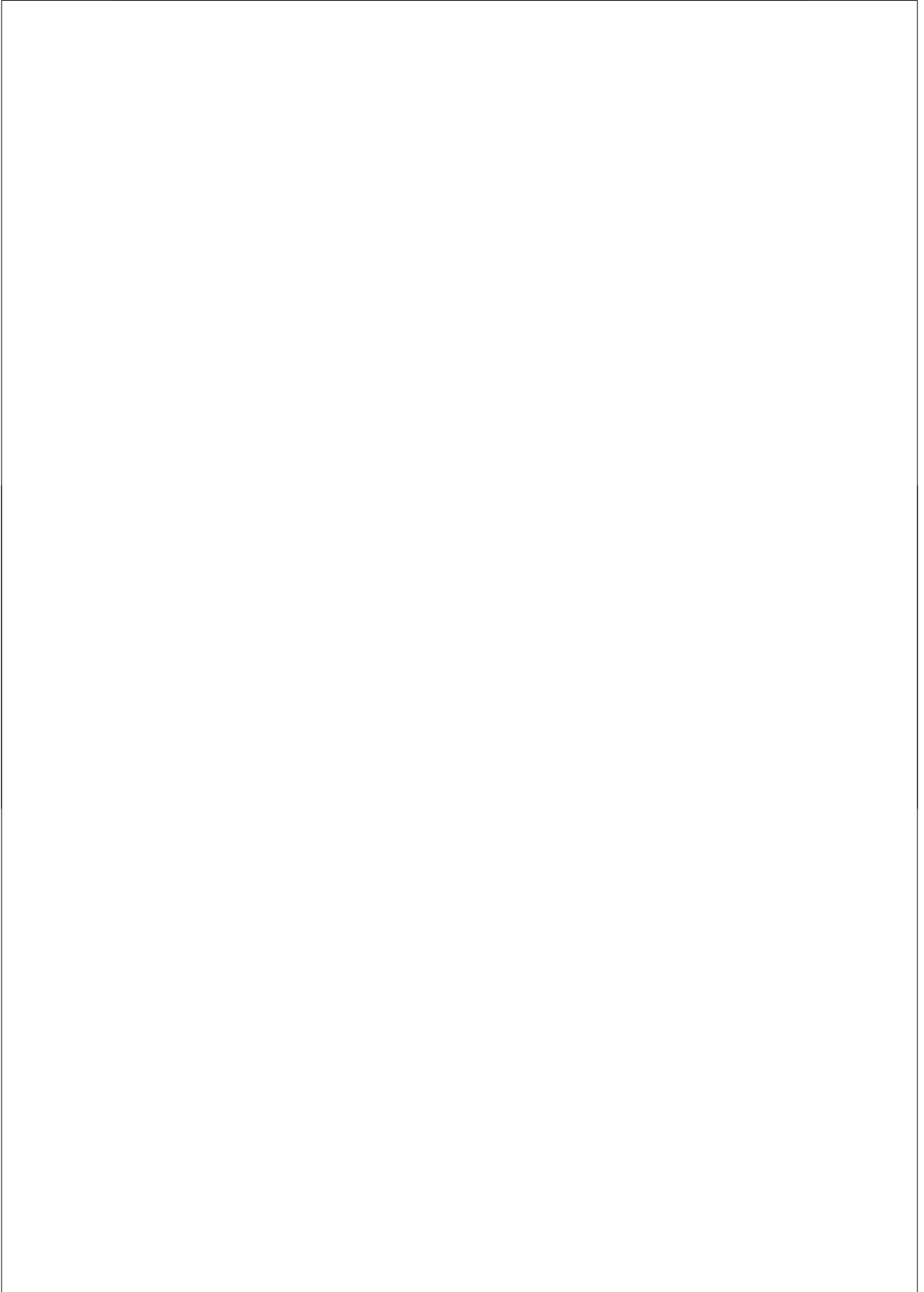
[¹²⁵I]CXCL10 binding to human CXCR3 receptor

Cell membranes from HEK293 cells stably expressing the human CXCR3 receptor were prepared as follows. Cells were washed with cold PBS, detached using cold PBS containing 1 mM EDTA and centrifuged twice at 1500 g for 10 min at 4 °C. The pellet was resuspended in cold membrane buffer (15 mM Tris pH 7.5, 1 mM EGTA, 0.3 mM EDTA, 2 mM MgCl₂) and homogenized by 10 strokes at 1100-1200 rpm using a Teflon-glass homogenizer. The membranes were subjected to two freeze thaw cycles using liquid nitrogen and centrifuged at 40,000 g for 25 min at 4 °C. The pellet was rinsed with cold Tris-sucrose buffer (20 mM Tris pH 7.4, 250 mM sucrose), resuspended in the same buffer and frozen in liquid nitrogen. Protein concentration was determined using a Bio-Rad protein assay. Membranes were incubated in 96 well plates in binding buffer (50 mM HEPES pH 7.4, 1 mM CaCl₂, 5 mM MgCl₂, 100 mM NaCl, 0.5% BSA) with approximately 50 pM ¹²⁵I-CXCL10 (PerkinElmer Life and Analytical Sciences, Boston, MA) and increasing concentrations of ligands for 2 h at RT. Subsequently, membranes were harvested via filtration through Unifilter GF/C plates (PerkinElmer Life and Analytical Sciences) pretreated with 1% polyethylenimine and washed three times with wash buffer (50 mM HEPES pH 7.4, 1 mM CaCl₂, 5 mM MgCl₂, 500 mM NaCl). Radioactivity was measured using a MicroBeta (PerkinElmer Life and Analytical Sciences) counter. Binding data were analyzed using Graphpad Prism.

References

- (1) Baggiolini, M.; Dewald, B.; Moser, B. Human chemokines: an update. *Annu. Rev. Immunol.*, **1997**, *15*, 675-705.
- (2) Fernandez, E. J.; Lolis, E. Structure, function, and inhibition of chemokines. *Annu Rev. Pharmacol. Toxicol.*, **2002**, *42*, 469-499.
- (3) Wuyts A, P. P., Lenaerts JP, Ben-Baruch A, Van Damme J, Wang JM. Wuyts A, Proost P, Lenaerts JP, Ben-Baruch A, Van Damme J, Wang JM. Differential usage of the CXC chemokine receptors 1 and 2 by interleukin-8, granulocyte chemotactic protein-2 and epithelial-cell-derived neutrophil attractant-78. *Eur. J. Biochem.*, **1998**, *255*, 67-73.
- (4) Qin, S.; Rottman, J. B.; Myers, P.; Kassam, N.; Weinblatt, M. et al. The chemokine receptors CXCR3 and CCR5 mark subsets of T cells associated with certain inflammatory reactions. *J. Clin. Invest.*, **1998**, *101*, 746-754.
- (5) Patel, D. D.; Zachariah, J. P.; Whichard, L. P. CXCR3 and CCR5 ligands in rheumatoid arthritis synovium. *Clin. Immunol.*, **2001**, *98*, 39-45.
- (6) Singh UP, V. C., Singh R, Lillard JW Jr. CXCR3 axis: role in inflammatory bowel disease and its therapeutic implication. *Endocr. Metab. Immune Disord, Drug Targets.* **2007**, *7*, 111-123.
- (7) Balashov, K. E.; Rottman, J. B.; Weiner, H. L.; Hancock, W. W. CCR5(+) and CXCR3(+) T cells are increased in multiple sclerosis and their ligands MIP-1alpha and IP-10 are expressed in demyelinating brain lesions. *Proc. Natl. Acad. Sci. USA*, **1999**, *96*, 6873-6878.
- (8) Hancock, W. W.; Lu, B.; Gao, W.; Csizmadia, V.; Faia, K. et al. Requirement of the chemokine receptor CXCR3 for acute allograft rejection. *J Exp Med* **2000**, *192*, 1515-1520.
- (9) Shields, P. L.; Morland, C. M.; Salmon, M.; Qin, S.; Hubscher, S. G. et al. Chemokine and chemokine receptor interactions provide a mechanism for selective T cell recruitment to specific liver compartments within hepatitis C-infected liver. *J. Immunol.*, **1999**, *163*, 6236-6243.
- (10) Mach, F.; Sauty, A.; Iarossi, A. S.; Sukhova, G. K.; Neote, K. et al. Differential expression of three T lymphocyte-activating CXC chemokines by human atheroma-associated cells. *J. Clin. Invest.*, **1999**, *104*, 1041-1050.
- (11) Tensen, C. P.; Flier, J.; Van Der Raaij-Helmer, E. M.; Sampat-Sardjoepersad, S.; Van Der Schors, R. C. et al. Human IP-9: A keratinocyte-derived high affinity CXC-chemokine ligand for the IP-10/Mig receptor (CXCR3). *J. Invest. Dermatol.*, **1999**, *112*, 716-722.
- (12) Flier, J.; Boorsma, D. M.; van Beek, P. J.; Nieboer, C.; Stoof, T. J. et al. Differential expression of CXCR3 targeting chemokines CXCL10, CXCL9, and CXCL11 in different types of skin inflammation. *J. Pathol.*, **2001**, *194*, 398-405.
- (13) Flier, J.; Boorsma, D. M.; Bruynzeel, D. P.; Van Beek, P. J.; Stoof, T. J. et al. The CXCR3 activating chemokines IP-10, Mig, and IP-9 are expressed in allergic but not in irritant patch test reactions. *J. Invest. Dermatol.*, **1999**, *113*, 574-578.
- (14) Saetta, M.; Mariani, M.; Panina-Bordignon, P.; Turato, G.; Buonsanti, C. et al. Increased expression of the chemokine receptor CXCR3 and its ligand CXCL10 in peripheral airways of smokers with chronic obstructive pulmonary disease. *Am. J. Respir. Crit. Care. Med.*, **2002**, *165*, 1404-1409.
- (15) Walsler, T. C.; Rifat, S.; Ma, X.; Kundu, N.; Ward, C.; Goloubeva, O.; Johnson, M. G.; Medina, J. C.; Collins, T. L.; Fulton, A. M. Antagonism of CXCR3 inhibits lung metastasis in a murine model of metastatic breast cancer. *Cancer Res.*, **2006**, *66*, 7701-7707.
- (16) Luster, A. D.; Leder, P. IP-10, a -C-X-C- chemokine, elicits a potent thymus-dependent antitumor response in vivo. *J. Exp. Med.*, **1993**, *178*, 1057-1065.
- (17) Hensbergen, P. J.; Wijnands, P. G.; Schreurs, M. W.; Scheper, R. J.; Willemze, R.; Tensen, C. P. The CXCR3 targeting chemokine CXCL11 has potent antitumor activity in vivo involving attraction of CD8+ T lymphocytes but not inhibition of angiogenesis. *J. Immunother.*, **2005**, *28*, 343-351.

- (18) Johnson, M. G., Li, A., Liu, J., Marcus, A. P., Huang, A. X., Medina, J. C. Abstracts of Papers. *231st National Meeting of the American Chemical Society, Atlanta, GA, 2006*.
- (19) Akashi, S.; Sho, M.; Kashizuka, H.; Hamada, K.; Ikeda, N. et al. A novel small-molecule compound targeting CCR5 and CXCR3 prevents acute and chronic allograft rejection. *Transplantation*, **2005**, *80*, 378-384.
- (20) Ondeyka, J. G.; Herath, K. B.; Jayasuriya, H.; Polishook, J. D.; Bills, G. F. et al. Discovery of structurally diverse natural product antagonists of chemokine receptor CXCR3. *Mol. Divers.*, **2005**, *9*, 123-129.
- (21) Cole, A. G.; Stroke, I. L.; Brescia, M. R.; Simhadri, S.; Zhang, J. J. et al. Identification and initial evaluation of 4-N-aryl-[1,4]diazepane ureas as potent CXCR3 antagonists. *Bioorg. Med. Chem. Lett.*, **2006**, *16*, 200-203.
- (22) Storelli, S.; Verzijl, D.; Al-Badie, J.; Elders, N.; Bosch, L.; Timmerman, H.; Smit, M.J.; De Esch, I.J.; Leurs, R. Synthesis and structure-activity relationships of 3H-quinazolin-4-ones and 3H-pyrido[2,3-d]pyrimidin-4-ones as CXCR3 receptor antagonists. *Arch. Pharm. (Weinheim)*, **2007**, *340*, 281-91
- (23) Allen, D. R., Bolt, A., Chapman, G.A., Knight, R.L., Meissner, J.W.G., Owen, D.A., Watson, R.J. Identification and structure-activity relationship of 1-aryl-3-piperidin-4-yl urea derivatives as CXCR3 receptor antagonists. *Bioorg. Med. Chem. Lett.*, **2007**, *17*, 697-701.
- (24) Axten, J. M., Foley, J.J., Kingsbury, W.D., Sarau, H.M. Imidazolium CXCR3 Inhibitors. *WO 03/101970 A1*, **2003**, 1-17.
- (25) Allen, D. R.; Bolt, A.; Chapman, G. A.; Knight, R. L.; Meissner, J. W. G.; Owen, D. A.; Watson, R. J. Identification and structure-activity relationships of 1-aryl-3-piperidin-4-yl-urea derivatives as CXCR3 receptor antagonists. *Bioorg. Med. Chem. Lett.*, **2007**, *17*, 697-701.
- (26) Gao, P.; Zhou, X. Y.; Yashiro-Ohtani, Y.; Yang, Y. F.; Sugimoto, N.; Ono, S.; Nakanishi, T.; Obika, S.; Imanishi, T.; Egawa, T.; Nagasawa, T.; Fujiwara, H.; Hamaoka, T. The unique target specificity of a nonpeptide chemokine receptor antagonist: selective blockade of two Th1 chemokine receptors CCR5 and CXCR3. *J. Leukocyte Biol.*, **2003**, *73*, 273-280.
- (27) De Kloe, G. E.; Bailey, D.; Leurs, R.; de Esch, I.J.P. Transforming fragments into candidates: small becomes big in medicinal chemistry. *Drug Discov. Today*, **2009**, *14*, 630-646.
- (28) Johnson, M. G. Presented at the *XIXth International Symposium on Medicinal Chemistry (Istanbul, Turkey), Aug 29 - Sep 2, 2006*.
- (29) Collins, T. L., Johnson, M.G., Ma, J., Medina, J.C., Miao, S., Schneider, M., Tonn, G.R. CXCR3 Antagonists. *WO 2004/075863 A2*, **2004**, 1-43.
- (30) Fujita, R., Watanabe, K., Ikeura, W., Ohtake, Y., Hongo, H., Harigaya, Y., Matsuzaki, H. Novel synthesis of tetrahydro-2(1H)-quinolones using Diels-Alder reactions of 1-arylsulfonyl-2(1H)-pyridones having an electronwithdrawing group. *Tetrahedron*, **2001**, *57*, 8841-8850.



Chapter 6

Non-competitive antagonism and inverse agonism as mechanism of action of non-peptidergic antagonists at primate and rodent CXCR3 chemokine receptors

Adapted from:

Dennis Verzijl, Stefania Storelli, Danny J. Scholten, Leontien Bosch, Todd A. Reinhart, Daniel N. Streblov, Cornelis P. Tensen, Carlos P. Fitzsimons, Guido J.R. Zaman, James E. Pease, Iwan J.P. de Esch, Martine J. Smit and Rob Leurs
J. Pharmacol. Exp. Ther., 2008, 325, 544 - 555

Abstract

The chemokine receptor CXCR3 is involved in various inflammatory diseases, such as rheumatoid arthritis, multiple sclerosis, psoriasis and allograft rejection in transplantation patients. The CXCR3 ligands CXCL9, CXCL10 and CXCL11 are expressed at sites of inflammation and attract CXCR3-bearing lymphocytes, thus contributing to the inflammatory process. Here, we characterize 5 non-peptidergic compounds of three different chemical classes that block the action of CXCL10 and CXCL11 at the human CXCR3, i.e. the 3H-pyrido[2,3-d]pyrimidin-4-one derivatives VUF10472/NBI-74330 and VUF10085/AMG 487, the 3H-quinazolin-4-one VUF5834, the imidazolium compound VUF10132 and the quaternary ammonium salt TAK-779. In order to understand the action of these CXCR3 antagonists in various animal models of disease, the compounds were also tested at rat and mouse CXCR3, as well as at CXCR3 from rhesus macaque, cloned and characterized for the first time in this study. Except for TAK-779, all compounds show slightly lower affinity for rodent CXCR3 than for primate CXCR3. Additionally, we have characterized the molecular mechanism of action of the various antagonists at the human CXCR3 receptor. All tested compounds act as noncompetitive antagonists at CXCR3. Moreover, this non-competitive behavior is accompanied by inverse agonistic properties of all 5 compounds as determined on an identified constitutively active mutant of CXCR3, CXCR3 N3.35A. Interestingly, all compounds except TAK-779 act as full inverse agonists at CXCR3 N3.35A. TAK-779 shows weak partial inverse agonism at CXCR3 N3.35A, and likely has a different mode of interaction with CXCR3 than the other two classes of small-molecule inverse agonists.

Introduction

Chemokines are secreted peptides that are important mediators in inflammation. They are classified into four families based on the number and position of conserved N-terminal cysteine residues, i.e. CC, CXC, CX₃C and XC chemokines.¹ Chemokines bind to a subset of G protein-coupled receptors (GPCRs) of class A, which are named based on their specific chemokine preferences.¹ The chemokine receptor CXCR3 is mainly expressed on activated Th1 cells, but also on B cells and natural killer cells.² CXCR3 is activated by the interferon-gamma-inducible chemokines CXCL9, CXCL10 and CXCL11, with CXCL11 having the highest affinity.^{3,4} Upon activation, CXCR3 activates *pertussis toxin*-sensitive G proteins of the G α_i class and mediates e.g. chemotaxis, calcium flux and activation of kinases such as p44/p42 MAPK and Akt.⁵

CXCR3 and its ligands are upregulated in a wide variety of inflammatory diseases, implying a role for CXCR3 in e.g. rheumatoid arthritis,² multiple sclerosis,⁶ transplant rejection,⁷ atherosclerosis⁸ and inflammatory skin diseases.⁹ The role of CXCR3 in cancer is two-fold: on one hand CXCR3 may be involved in the metastasis of CXCR3-expressing cancer cells,¹⁰ while on the other hand expression of CXCL10¹¹ or CXCL11¹² at tumor sites may attract CXCR3-expressing immune cells, that help control tumor growth and metastasis.

Several animal models have been developed for CXCR3, among which a murine model of metastatic breast cancer,¹⁰ a murine model of renal cell carcinoma (RENCA)¹³ and an arthritis model in Lewis rats.¹⁴ In a mouse rheumatoid arthritis model TAK-779, a small-molecule antagonist with affinity for CCR5, CCR2b and CXCR3, inhibits the development of arthritis by downregulating T cell migration, indicating that targeting chemokine receptors in models of inflammation is feasible and effective.¹⁵⁻¹⁷

Several classes of non-peptidergic compounds targeting CXCR3 have recently been described, including 4-*N*-aryl-[1,4]diazepane ureas,¹⁸ 1-aryl-3-piperidin-4-yl-urea derivatives,¹⁹ quinazolin-4-one and 3*H*-pyrido[2,3-*d*]pyrimidin-4-one derivatives²⁰⁻²³ and the above mentioned quaternary ammonium salt TAK-779.¹⁶ So far, no detailed information is available on the molecular mechanism of action of these antagonists at the CXCR3 receptor, despite the general notion that small-molecule ligands most likely will not have overlapping binding sites with the chemokines, which are supposed to bind mainly to the N-terminus and extracellular receptor loops.¹ Moreover, although most compounds have been tested on human CXCR3 using *in vitro* assays, little or no information on their affinity for CXCR3 of other species is available. Especially in view of rodent models of inflammatory diseases it is important to know the relative affinities of the compounds for the receptors of different species.

Here, we report on the molecular characterization of the 3*H*-pyrido[2,3-*d*]pyrimidin-4-one derivatives VUF10472 (NBI-74330)^{21,22} and VUF10085 (AMG 487)^{21,23}, the 3*H*-quinazolin-4-one VUF5834^{20,23} the imidazolium compound VUF10132²⁴ and the quaternary ammonium salt TAK-779¹⁵ at CXCR3 of human,³ rat²⁵ and mouse.²⁶ Additionally, CXCR3 from rhesus macaque was cloned, characterized and subjected to a detailed pharmacological analysis using the non-peptidergic compounds. Moreover, we constructed and characterized a constitutively active mutant (CAM) of CXCR3, which was used to further determine the inverse agonistic properties of the non-peptidergic ligands.

Methods

Materials. Dulbecco's modified Eagle's medium (DMEM) and trypsin were purchased from PAA Laboratories GmbH (Paschen, Austria), RPMI 1640 with glutamax-I and 25 mM HEPES, non essential amino acids, sodium pyruvate and 2-mercaptoethanol were from Sigma-Aldrich, penicillin and streptomycin were obtained from Cambrex, fetal bovine serum (FBS) was purchased from Integro B.V. (Dieren, The Netherlands), certified FBS was from Invitrogen. *myo*-[2-³H]inositol (10-20 Ci/mmol) was bought from GE Healthcare. [¹²⁵I]-CXCL10 (2200 Ci/mmol) and [¹²⁵I]-CXCL11 (2000 Ci/mmol) were obtained from PerkinElmer Life and Analytical Sciences. Chemokines were obtained from PeproTech (Rocky Hill, N.J.). TAK-779 was obtained from the NIH AIDS research and reference reagent program.

DNA constructs. The cDNA of human CXCR3 inserted in pcDNA3³ was amplified by PCR and inserted into pcDEF3 (a gift from Dr. Langer).

A cDNA containing the rhesus macaque (*Macaca mulatta*, GenBank accession number EU313340) CXCR3 open-reading frame was obtained from rhesus macaque peripheral blood mononuclear cells (PBMCs) stimulated overnight with phytohemagglutinin-P plus phorbol myristate acetate. Total RNA was extracted using Trizol (Life Technologies) and cDNA was generated by reverse transcription (RT) with avian myeloblastosis virus RT (Promega) and oligo(dT) primer. PCR was then performed with Taq polymerase (Promega) and primers TRCXCR3F2 (5'-AGCCCAGCCATGGTCCTTG-3') and TRCXCR3R2 (5'-CCTCACAAGCCCGAGTAGGA-3'). The resulting PCR product was spin-column purified (Qiagen) and ligated to pGEM-T vector (Promega). Subsequently the cDNA was subcloned into pcDEF3.

A cDNA containing the *rattus norvegicus* CXCR3 open-reading frame was cloned from an F344 heart allograft that was transplanted into a Lewis rat at 28 days post-transplantation.²⁷ Total RNA was prepared from 0.25 g of rat tissue using the Trizol

method. First strand cDNA was synthesized from 2 µg of total RNA using 1.0 µM oligo dT-T7 primer (GGCCAGTGAATTGTAATACGACTCACTATAGGG(A)₂₄) and 200 U Superscript III reverse transcriptase (Invitrogen). Doubled-stranded cDNA was generated by the addition of second strand buffer (Invitrogen) according to the manufacturer's protocol and purified by phenol/chloroform extraction. PCR was performed with Taq DNA polymerase and primers ratCXCR3Fwd: ATAGGATTCATGTACCTTGAGGTCAGTGAACGTCA and ratCXCR3Rev: ATAGAATTCTTACAAGCCCAAGTAGGAGGCCTCAGT. The resulting PCR fragment was cloned into pGEM-Teasy (Promega), and subcloned into pcDEF3. The cDNA of mouse CXCR3 was a kind gift from Dr. Luster²⁶ and was subcloned into pcDEF3. The chimeric G protein G_{α_{qi5}} (pcDNA1-HA-mG_{α_{qi5}}) was a gift from Dr. Conklin.²⁸ Other plasmids that were used are pcDNA3.1-CXCR1, pcDEF3-CXCR2, pcDNA3-CXCR4, pcDEF3-CCR1, pcDNA3.1-CCR2, pcDEF3-H₁, pCIneo-H₃(445).

Synthesis of non-peptidergic ligands. Synthesis of VUF5834,²⁰ VUF10472 and VUF10085²¹ has been described previously.

Synthesis of VUF10132 was adapted from the procedure described by Axten et al.²⁴ Briefly, 1-(3,4-dichloro-phenyl)-2-imidazol-1-yl-ethanone (0.19 g, 0.75 mmol) and 2-bromo-1-(3,4-dichloro-phenyl)-ethanone (0.20 g, 0.75 mmol) were stirred in acetonitrile (50 mL) overnight at rt. The mixture was diluted with ether. The solid product was filtered, washed with ether and dried to afford VUF10132 as white solid. Yield: 0.31 g (78%). ¹H NMR (DMSO) δ: 6.20 (s, 4H), 7.67-7.80 (m, 4H), 7.88-8.12 (m, 3H), 8.23-8.25 (m, 2H), 9.12 (s, 1H). ¹³C NMR (50 MHz, DMSO) δ: 54.67, 55.45, 119.92, 122.65, 127.70, 128.45, 130.15, 131.16, 131.26, 131.98, 132.34, 133.76, 137.83, 138.15, 188.55, 189.74. M.p. 238.2-239.6 °C.

Cell culture and transfection. HEK293T cells were grown at 5% CO₂ at 37 °C in Dulbecco's modified Eagle's medium (DMEM) supplemented with 10% fetal bovine serum, penicillin and streptomycin. HEK293T cells were transfected with 2.5 µg cDNA encoding CXCR3 supplemented with 2.5 µg pcDNA1-HA-mG_{α_{qi5}} (for PLC activation experiments and ELISA) or 2.5 µg pcDEF3 using linear polyethyleneimine (PEI) (MW 25,000; Polysciences Inc, Warrington, PA, USA). The total amount of DNA in gene-dosing experiments was kept constant at 5 µg by addition of pcDEF3. Briefly, a total of 5 µg DNA was diluted in 250 µl 150 mM NaCl. Subsequently 30 µg PEI in 250 µl 150 mM NaCl was added to the DNA solution and incubated for 10 min at RT. The mixture was added to adherent HEK293T cells in 100 mM tissue culture dishes. Next day, cells were trypsinized, resuspended into culture medium and plated in the appropriate poly-L-lysine (Sigma) coated assay plates. For membrane preparation, cells were harvested 48 h after transfection from the tissue culture dishes in which they were transfected.

Murine pre-B L1.2 cells were grown in RPMI 1640 medium with glutamax-I and 25 mM HEPES, supplemented with 10% heat-inactivated certified FBS, penicillin, streptomycin, glutamine, non-essential amino acids, 2-mercaptoethanol and sodium pyruvate. L1.2 cells were transfected with 10 µg per 20 million cells using a BioRad Gene Pulser II (330V and 975 µF) and grown in culture medium supplemented with 10 mM sodium butyrate.

Chemokine binding. Cell membrane fractions from transiently transfected HEK293T (CXCR3 and CXCR4) or COS-7 (CXCR2) cells were prepared as follows. Cells were washed with cold PBS, detached using cold PBS containing 1 mM EDTA and centrifuged at 1500 g for 10 min at 4 °C. Subsequently, cells were washed with PBS and centrifuged at 1500 g for 10 min at 4 °C. The pellet was resuspended in cold membrane buffer (15 mM Tris pH 7.5, 1 mM EGTA, 0.3 mM EDTA, 2 mM MgCl₂) and homogenized by 10 strokes at 1100-1200 rpm using a teflon-glass homogenizer and rotor. The membranes were subjected to two freeze thaw cycles using liquid nitrogen and centrifuged at 40,000 g for 25 min at 4 °C. The pellet was rinsed with cold Tris-sucrose buffer (20 mM Tris pH 7.4, 250 mM sucrose), resuspended in the same buffer and frozen in liquid nitrogen. Protein concentration was determined using a Bio-Rad protein assay. Membranes were incubated in 96 well plates in binding buffer (50 mM HEPES pH 7.4, 1 mM CaCl₂, 5 mM MgCl₂, 100 mM NaCl, 0.5% BSA for CXCR3 and CXCR4 radioligand binding assays and 50 mM Na₂/K-phosphate buffer, pH 7.4, 0.5% BSA for CXCR2 radioligand binding assay) with approximately 50 pM ¹²⁵I-chemokine and displacer for 2 h at RT. Subsequently, membranes were harvested via filtration through Unifilter GF/C plates (PerkinElmer Life and Analytical Sciences) pretreated with 1% polyethylenimine and washed three times with ice-cold wash buffer (50 mM HEPES pH 7.4, 1 mM CaCl₂, 5 mM MgCl₂, 500 mM NaCl for CXCR3 and CXCR4 and 50 mM Na₂/K-phosphate buffer, pH 7.4 for CXCR2). Radioactivity was measured using a MicroBeta (PerkinElmer Life and Analytical Sciences).

Histamine H₁ receptor binding. Cell homogenates from COS-7 cells transiently transfected with cDNA encoding the human histamine H₁ receptor were incubated with 7 nM [³H]-mepyramine and 10 µM CXCR3 antagonist in H₁ buffer (50 mM Na₂/K-phosphate buffer, pH 7.4) for 30 min at RT and harvested via filtration using ice-cold H₁ buffer as described above.

Phospholipase C activation. Twenty-four hours after transfection, HEK293T cells were labeled overnight in Earle's inositol-free minimal essential medium (Invitrogen) supplemented with 10% fetal bovine serum, penicillin and streptomycin and *myo*-[2-³H]inositol (1 µCi/ml). Cells were washed with InsP assay buffer (20 mM HEPES pH 7.4, 140 mM NaCl, 5 mM KCl, 1 mM MgSO₄, 1 mM CaCl₂, 10 mM glucose and 0.05% (w/v)

BSA) and incubated for 2 h in InsP assay buffer supplemented with 10 mM LiCl in the presence or absence of indicated ligands. The incubation was stopped by aspiration of the assay buffer and addition of ice-cold 10 mM formic acid. After incubation for 90 min at 4 °C, [³H]-InsP were isolated by anion-exchange chromatography (Dowex AG1-X8 columns, Bio-Rad) and counted by liquid scintillation.

Chemotaxis. Twenty-four h after transfection, chemotaxis of L1.2 cells towards CXCL10 (10 nM) was determined in the presence or absence of compounds, using 5 μM pore ChemoTx 96 well plates (Neuroprobe Inc, MD, USA). Briefly, ChemoTx plates were blocked using RPMI 1640 with glutamax-I and 25 mM Hepes supplemented with 1% (w/v) BSA. Chemokine and compound dilutions were made in RPMI 1640 with glutamax-I and 25 mM Hepes supplemented with 0.1% (w/v) BSA and added to the wells. L1.2 cells were added on top of the membrane and incubated for 5 h in a humidified chamber at 37 °C. The number of migrated cells per well was determined using a haemocytometer.

ELISA. Forty-eight hours after transfection, HEK293T cells were washed with TBS and fixed with 4% paraformaldehyde in PBS. After blocking with 1% skim milk in 0.1 M NaHCO₃ (pH 8.6), cells were incubated with mouse monoclonal anti-CXCR3 antibody (MAB160, R&D Systems, Inc) in TBS containing 0.1% BSA, washed three times with TBS and incubated with goat anti-mouse horseradish peroxidase-conjugated secondary antibody (Bio-Rad). Subsequently, cells were incubated with substrate buffer containing 2mM *o*-phenylenediamine (Sigma, St. Louis, Mo), 35 mM citric acid, 66 mM Na₂HPO₄, 0.015% H₂O₂ (pH 5.6). The reaction was stopped with 1 M H₂SO₄ and absorption at 490 nm was determined.

Data analysis. Nonlinear regression analysis of the data and calculation of K_d and K_i values was performed using Prism 4.03. The pK_b values in the PLC activation assay were calculated using the Cheng-Prusoff equation $pK_b = IC_{50} / (1+[agonist]/EC_{50})$.²⁹

Results

Non-peptidergic CXCR3 antagonists

A selection of CXCR3-targeting small-molecule antagonists from two different structural classes was synthesized as previously described and subjected to detailed pharmacological analysis, including the quinazolinone-derived 3*H*-pyrido[2,3-*d*]pyrimidin-4-one compounds VUF10472 (NBI-74330)^{21,22} and VUF10085 (AMG 487),^{21,23} the 3*H*-

quinazolin-4-one VUF5834,^{20,23} and the imidazolium compound VUF10132²⁴ (Fig. 1). The well described CCR5 antagonist TAK-779¹⁵ has been reported to show affinity for mouse CXCR3¹⁶ and was therefore included in our set of non-peptidergic ligands as well (Figure 1).

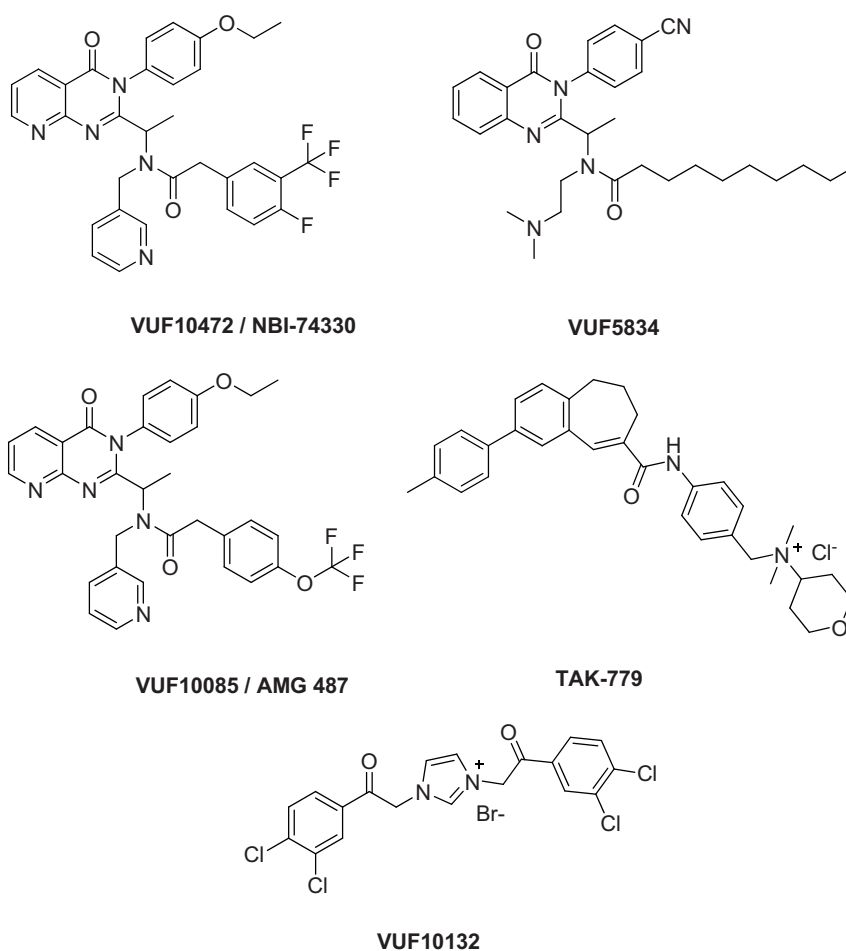


Figure 1. Structures of small non-peptidergic compounds targeting CXCR3. The structures of VUF10472 (NBI-74330; *N*-1*R*-[3-(4-ethoxy-phenyl)-4-oxo-3,4-dihydro-pyrido[2,3-*d*]pyrimidin-2-yl]-ethyl-*N*-pyridin-3-ylmethyl-2-(4-fluoro-3-trifluoromethyl-phenyl)-acetamide), VUF10085 (AMG 487; *N*-1*R*-[3-(4-ethoxy-phenyl)-4-oxo-3,4-dihydro-pyrido[2,3-*d*]pyrimidin-2-yl]-ethyl-*N*-pyridin-3-ylmethyl-2-(4-trifluoromethoxy-phenyl)-acetamide), VUF5834 (decanoic acid (1-[3-(4-cyano-phenyl)-4-oxo-3,4-dihydro-quinazolin-2-yl]-ethyl)-(2-dimethylamino-ethyl)-amide), VUF10132 (1,3-Bis-[2-(3,4-dichloro-phenyl)-2-oxo-ethyl]-3*H*-imidazol-1-ium bromide) and TAK-779 (*N,N*-dimethyl-*N*-[4-[[[2-(4-methylphenyl)-6,7-dihydro-5*H*-benzocyclohepten-8-yl]carbonyl]amino]benzyl] tetrahydro-2*H*-pyran-4-aminium chloride) are shown.

Characterization of human CXCR3

Binding studies were performed with radiolabeled CXCL10 and CXCL11 on membranes prepared from HEK293T cells transiently transfected with cDNA encoding human CXCR3.³ Homologous displacement of the radioligands with unlabeled chemokines resulted in pK_d values \pm SEM of 9.8 ± 0.1 for CXCL10 and 10.6 ± 0.1 for CXCL11 (Figure 2A, Table 1), in accordance with the values and rank-order for these chemokines reported in literature.^{4, 22}

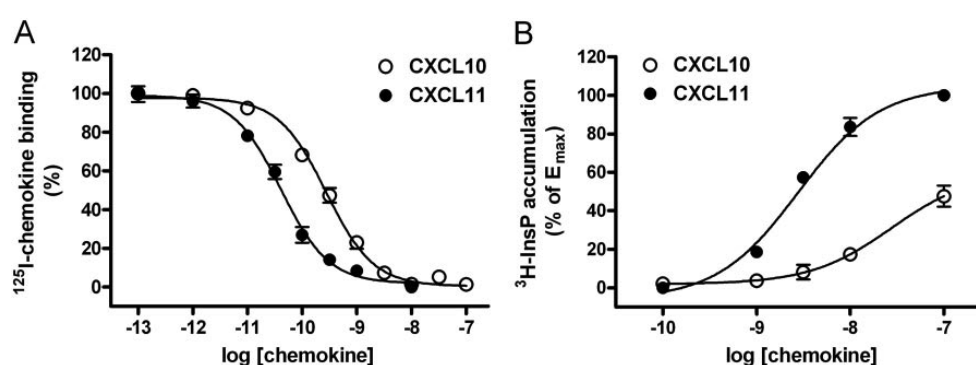


Figure 2. Characterization of human CXCR3. A) Homologous displacement binding at human CXCR3. Binding experiments were performed with approximately 50 pM ^{125}I -CXCL10 (\circ) or ^{125}I -CXCL11 (\bullet) and increasing concentrations of homologous unlabeled chemokine on membranes from HEK293T cells transfected with cDNA encoding human CXCR3. Data are presented as percentage of total binding. pK_d values for CXCL10 and CXCL11 were 9.8 ± 0.1 ($n=11$) and 10.6 ± 0.1 ($n=7$) respectively. **B)** Activation of PLC by human CXCR3. HEK293T cells were transfected with cDNA encoding human CXCR3 and $G\alpha_{q15}$. After 48 h, ^3H -InsP accumulation was determined in the presence of increasing concentrations of CXCL10 (\circ) or CXCL11 (\bullet). Data are presented as percentage of the maximal response obtained with CXCL11 (100 nM). pEC_{50} values for CXCL10 and CXCL11 were 7.5 ± 0.1 ($n=8$) and 8.5 ± 0.1 ($n=12$) respectively.

In HEK293 cells human CXCR3 does not couple efficiently to the phospholipase C (PLC)-inositolphosphates (InsP) pathway.²⁵ Therefore, CXCR3 was transiently co-transfected with cDNA encoding the chimeric G protein $G\alpha_{q15}$,²⁸ after which robust PLC activation could be observed upon stimulation with CXCL10 and CXCL11. Using this functional assay, pEC_{50} values of 7.5 ± 0.1 and 8.5 ± 0.1 were obtained for respectively CXCL10 and CXCL11 (Figure 2B, Table 1). CXCL10 acted as a partial agonist, with an intrinsic activity of 0.48 ± 0.8 compared to the full agonist CXCL11 (Figure 2B, $n=5$).

Characterization of rhesus macaque, rat and mouse CXCR3

Since the affinities of non-peptidergic ligands targeting chemokine receptors may differ among species, e.g. for TAK-779 at human and mouse CCR5^{15,16} and significant differences between the amino acid sequences of human and rodent CXCR3 are apparent (Figure 3), we set out to characterize CXCR3 of rhesus macaque, mouse and rat. CXCR3 of mouse²⁶ and rat²⁵ have previously been cloned and described. Here, we report the cloning and characterization of rhesus macaque CXCR3 from PBMCs (GenBank accession number EU313340, see experimental procedures). The deduced amino acid sequence of rhesus macaque CXCR3 was found to be 99% identical to human CXCR3. The Thr⁸³ residue in the first intracellular loop of human CXCR3 is Ala⁸³ in rhesus macaque CXCR3, and Val²⁵⁹ at position 6.39¹ in TM6 of human CXCR3 is Ala²⁵⁹ in rhesus macaque CXCR3 (Figure 3).

Table 1. Properties of chemokine ligands at CXCR3.

species	human CXCL10					
	pK _d	n	B _{max}	n	pEC ₅₀	n
human	9.8 ± 0.1	11	358 ± 53	6	7.5 ± 0.1	8
N3.35A	10.2 ± 0.2	4	327 ± 91	4	7.5 ± 0.0	2
rhesus	10.0 ± 0.1	3	163 ± 7	2	7.4 ± 0.1	3
rat	10.2 ± 0.2	7	631 ± 141	7	8.8 ± 0.1	3
mouse	10.1 ± 0.1	3	658 ± 127	3	8.3 ± 0.1	5

species	human CXCL11					
	pK _d	n	B _{max}	n	pEC ₅₀	n
human	10.6 ± 0.1	7	407 ± 126	4	8.5 ± 0.1	12
N3.35A	11.3 ± 0.3	3	564 ± 242	3	8.7 ± 0.1	4
rhesus	10.8 ± 0.3	3	255 ± 114	4	8.5 ± 0.1	3
rat	10.7 ± 0.2	4	1170 ± 644	3	9.5 ± 0.1	3
mouse	10.7 ± 0.3	4	1882 ± 858	4	9.2 ± 0.2	3

Shown are pK_d values and B_{max} values ± SEM for human CXCL10 and human CXCL11 at the various CXCR3, calculated from homologous radioligand binding experiments. pEC₅₀ values ± SEM were obtained using the PLC activation assay.

After expression in HEK293T cells, CXCR3 from rhesus, rat and mouse showed similar binding affinities for human CXCL10 and CXCL11 as human CXCR3 (Table 1). B_{max} values of rodent CXCR3 were increased compared to human CXCR3, approximately 2-fold higher for CXCL10 and 3 to 4-fold higher for CXCL11 (Table 1) when equal amounts of cDNA were transfected. The B_{max} for CXCL10 at rhesus CXCR3 was 2-fold lower than for human CXCR3, whereas human and rhesus CXCR3 had comparable B_{max} values for CXCL11 (Table 1). Rhesus CXCR3 stimulated PLC with similar maximum effect (E_{max}) and similar

EC₅₀ values for human CXCL10 and CXCL11 as human CXCR3 (Figure 4A and 4B, Table 1). In contrast, the rodent CXCR3 species had approximately 10-fold higher potencies and showed increased E_{max} for human CXCL10 compared to human CXCR3 (Figure 4A and 4B, Table 1). The E_{max} for human CXCL11 at rat CXCR3 was also increased compared to the effect of CXCL11 at CXCR3 of the other species (Figure 4B).

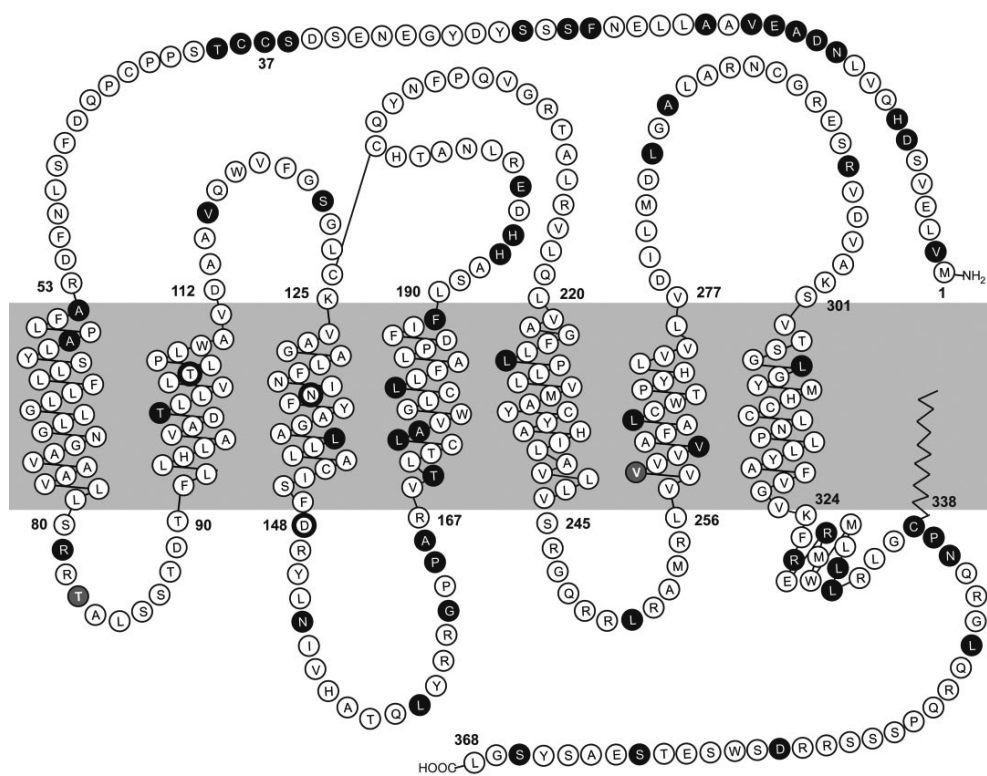


Figure 3. Snakeplot of CXCR3. Amino acids that were mutated in order to generate constitutively active mutants (T2.56, N3.35 and D3.49) are indicated as bold circled residues. Amino acids that differ between human and rhesus macaque CXCR3 (T⁸³ in intracellular loop 1 and V6.39 are both Ala in rhesus macaque CXCR3) are shown as grey circles. Residues which are different between primate and rodent (i.e. rat and/or mouse) CXCR3 are indicated as black circles. Human and rhesus macaque CXCR3 have an additional Cys (C³⁷) in their amino-terminus compared to rat and mouse CXCR3. Helix 8 at the membrane proximal part of the carboxy-terminus and potential palmitoylation of Cys³³⁸ are shown as well.

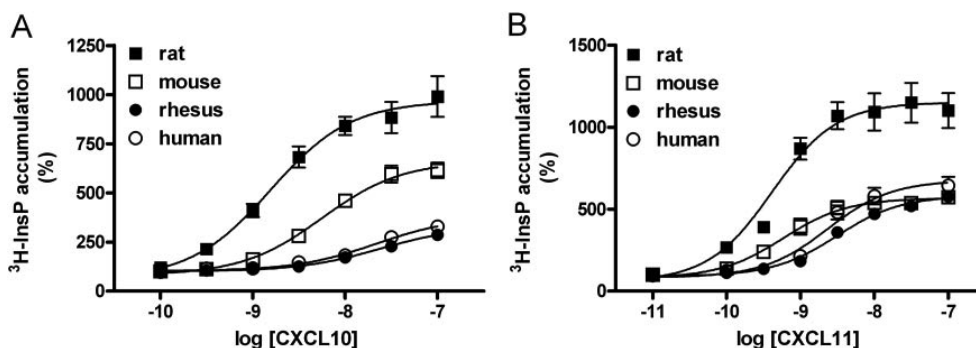


Figure 4. Activation of PLC by primate and rodent CXCR3. A) CXCL10-induced activation of PLC. HEK293T cells were transfected with cDNA encoding human, rhesus, rat or mouse CXCR3 and $G_{\alpha_{q15}}$. After 48 h, [3 H]-InsP accumulation was determined in the presence of increasing concentrations human CXCL10. pEC_{50} values for CXCL10 were 7.5 ± 0.1 (human CXCR3, $n=8$), 7.4 ± 0.1 (rhesus CXCR3, $n=3$), 8.8 ± 0.1 (rat CXCR3, $n=3$) and 8.3 ± 0.1 (mouse CXCR3, $n=5$). **B)** CXCL11-induced activation of PLC. HEK293T cells were transfected with cDNA encoding human, rhesus, rat or mouse CXCR3 and $G_{\alpha_{q15}}$. After 48 h, [3 H]-InsP accumulation was determined in the presence of increasing concentrations human CXCL11. pEC_{50} values for CXCL11 were 8.5 ± 0.1 (human CXCR3, $n=12$), 8.5 ± 0.1 (rhesus CXCR3, $n=3$), 9.5 ± 0.1 (rat CXCR3, $n=3$) and 9.2 ± 0.2 (mouse CXCR3, $n=3$). Data are presented per receptor as percentage of 3 H-InsP accumulation in the absence of chemokine.

Behavior of non-peptidergic compounds at CXCR3

The panel of non-peptidergic ligands inhibited [125 I]-CXCL10 binding to human CXCR3 with K_i values ranging between 4 nM for VUF10472 and 1.3 μ M for TAK-779 (Figure 5A and Table 2). VUF10085, VUF5834 and VUF10132 showed intermediate K_i values of 20 nM, 158 nM and 251 nM respectively (Figure 5A and Table 2). Subsequently, the ability of the small molecules to inhibit CXCL10-induced PLC activation through human CXCR3 was determined. All compounds reduced CXCL10-mediated (10-50 nM) PLC activation with K_b values ranging from 6 nM for VUF10472 to 800 nM for TAK-779 (Figure 5B, Table 2). A good correlation ($r^2 = 0.997$) was observed between the measured pK_i values and pK_b values determined against CXCL10 (Figure 5C). For the most potent compound, VUF10472, inhibition of CXCL11-induced (5 nM) PLC activation was also determined, resulting in a K_b value of 12.6 nM (Figure 5D). This value corresponds well to the value obtained against CXCL10 (Figure 5D and Table 2). Finally, the ability of the non-peptidergic ligands to inhibit chemotaxis was investigated. The murine pre-B cell line L1.2 was transiently transfected with cDNA encoding human CXCR3 and migration of cells towards CXCL10 in the presence or absence of VUF10085 and VUF5834 was determined. CXCR3-transfected L1.2 cells did not migrate in the absence of CXCL10,

whereas $10.3 \pm 0.8 \%$ ($n=3$) of the cells migrated to CXCL10 (10 nM) in the absence of inhibitors (Figure 5E, inset). Both compounds completely inhibited CXCL10-induced (10 nM) migration at a concentration of 10 μ M, with pIC_{50} values of 6.8 ± 0.2 ($n=2$) and 5.8 ± 0.1 ($n=3$) for VUF10085 and VUF5834 respectively (Figure 5E).

Next, the affinity of the non-peptidergic ligands for CXCR3 of the different species was determined using [125 I]-CXCL10. The pK_i values of the compounds tested at rhesus CXCR3 were identical to the values found for human CXCR3 (Table 2). Similarly, the affinities of the compounds tested at rat and mouse CXCR3 were identical to each other. However, VUF10472, VUF10085, VUF5834 and VUF10132 showed an approximately 4-fold lower affinity for the rodent CXCR3 (mouse and rat) compared to the primate CXCR3 (human and rhesus). Only for TAK-779 no difference in affinity between CXCR3 from the different species was observed.

Since the non-peptidergic compounds showed slightly lower affinity for rodent CXCR3 and the previous experiments were performed with human chemokines, we also determined the ability of the antagonists to inhibit mouse CXCL10-induced signaling at mouse CXCR3. The pEC_{50} of mouse CXCL10 at mouse CXCR3 (8.4 ± 0.1 , $n=3$) was comparable with the pEC_{50} of human CXCL10 at mouse CXCR3 (8.3 ± 0.1 , $n=5$). The different antagonists inhibited mouse CXCL10-induced activation of mouse CXCR3 (measured as PLC stimulation) with K_b values ranging from 4 nM for VUF10472 to 400 nM for TAK-779. The K_b values obtained under these conditions are within two-fold of the K_b values for inhibition of human CXCL10 at human CXCR3 (Figure 5F, Table 2).

In order to determine whether the antagonists show competitive or non-competitive behavior, a Schild analysis was performed. HEK293T cells expressing human CXCR3 and $G_{\alpha_{q15}}$ were incubated with increasing concentrations of CXCL10 (Figure 6A) or CXCL11 (Figure 6B) in the absence or presence of different concentrations of VUF10472. A decreased maximal effect combined with a rightward shift of the curves was observed in the presence of VUF10472, indicating non-competitive antagonist behavior. The mechanism of antagonism of the other classes of non-peptidergic ligands was investigated using only CXCL11. VUF10132 (Figure 6C) and TAK-779 (Figure 6D) both clearly showed non-competitive antagonistic behavior similar to that of VUF10472.

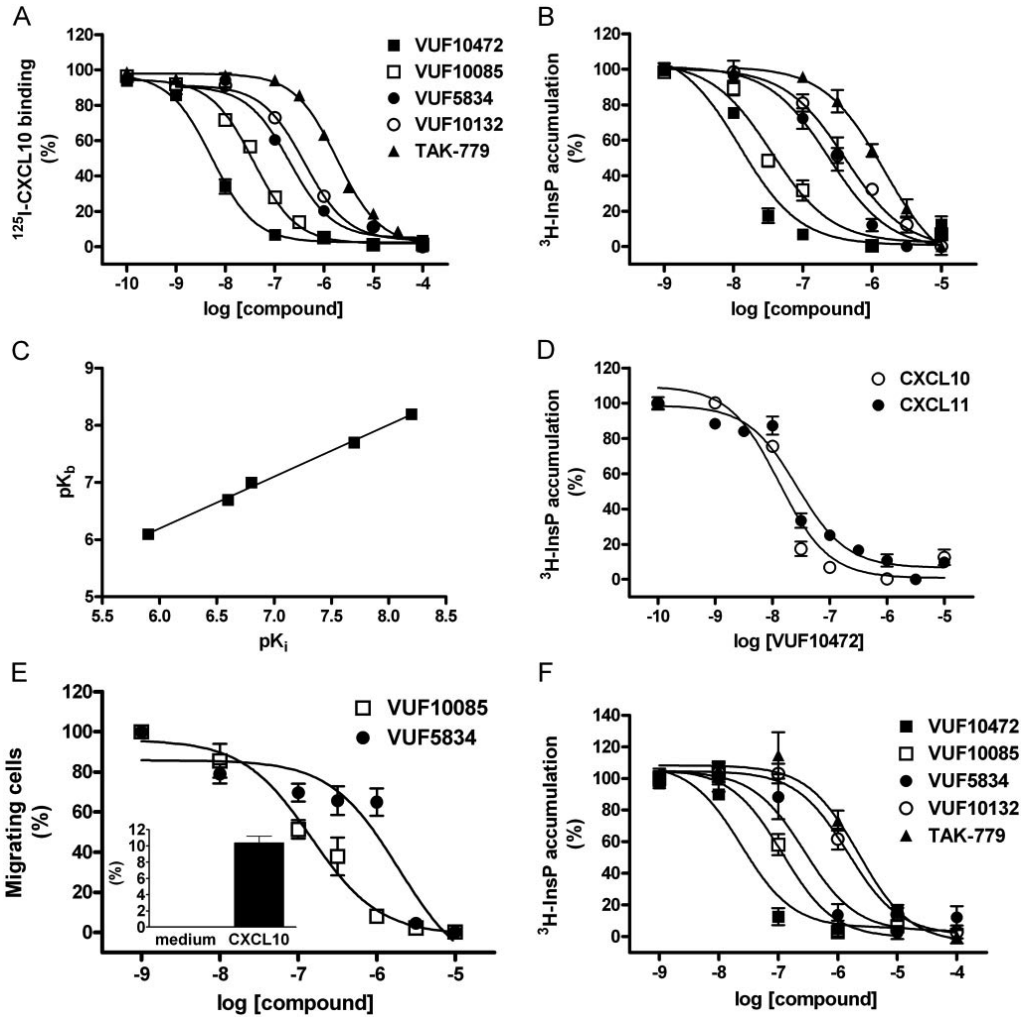


Figure 5. Characterization of small non-peptidergic compounds at human CXCR3

A) Displacement of ^{125}I -CXCL10. Binding experiments were performed with approximately 50 pM ^{125}I -CXCL10 and increasing concentrations of VUF10472 (■), VUF10085 (□), VUF5834 (●), VUF10132 (○) or TAK-779 (▲) on membranes from HEK293T cells transfected with cDNA encoding human CXCR3. Data are presented as percentage of total binding. pK_i values were 8.4 ± 0.1 (VUF10472, $n=7$), 7.7 ± 0.0 (VUF10085, $n=18$), 6.8 ± 0.1 (VUF5834, $n=3$), 6.6 ± 0.0 (VUF10132, $n=4$) and 5.9 ± 0.0 ($n=6$).

B) Inhibition of CXCL10-induced PLC activation. HEK293T cells were transfected with cDNA encoding human CXCR3 and $G_{\alpha_{q15}}$. After 48 h, CXCL10-induced (10-50 nM) ^3H -InsP accumulation was determined in the presence of increasing concentrations of VUF10472 (■), VUF10085 (□), VUF5834 (●), VUF10132 (○) or TAK-779 (▲). pK_b values were 8.2 ± 0.1 (VUF10472, $n=5$), 7.7 ± 0.1 (VUF10085, $n=9$), 7.0 ± 0.1 (VUF5834, $n=5$), 6.7 ± 0.1 (VUF10132, $n=5$) and 6.1 ± 0.1 (TAK-779, $n=4$).

C) Relationship between pK_i and pK_b of non-peptidergic ligands. pK_b values obtained using CXCL10 were plotted against pK_i values obtained against ^{125}I -CXCL10 ($r^2 = 0.997$).

D) Inhibition of CXCL11-induced PLC activation by VUF10472. HEK293T cells were transfected with cDNA encoding human CXCR3 and $G_{\alpha_{q15}}$. After 48 h, CXCL11-induced (5 nM) ^3H -InsP accumulation was determined in the presence of increasing concentrations of VUF10472 (●). The pK_b value of VUF10472 was 7.9 ± 0.0 ($n=3$). For comparison, inhibition of CXCL10-induced (50 nM) PLC activation by VUF10472 is shown as well (○). Data are represented as percentage stimulation in the absence of antagonist. pK_b values were calculated using the Cheng-Prusoff equation²⁹.

E) Inhibition of CXCL10-induced chemotaxis. L1.2 cells were transfected with cDNA encoding human CXCR3. After 24 h, inhibition of CXCL10-induced (10 nM) chemotaxis was determined. pIC_{50} values were 6.8 ± 0.2 (VUF10085, $n=2$) and 5.8 ± 0.1 (VUF5834, $n=3$). Data are presented as percentage of migrated cells in the absence of antagonist. Inset, CXCL10-induced chemotaxis of L1.2 cells. Data are presented as percentage of total L1.2 cells that migrated to CXCL10 (10 nM) in the absence of antagonist ($n=3$).

F) Inhibition of mouse CXCL10-induced PLC activation through mouse CXCR3. HEK293T cells were transfected with cDNA encoding mouse CXCR3 and $G_{\alpha_{q15}}$. After 48 h, mouse CXCL10-induced (20 nM) ^3H -InsP accumulation was determined in the presence of increasing concentrations of VUF10472 (■), VUF10085 (□), VUF5834 (●), VUF10132 (○) or TAK-779 (▲). pK_b values were 8.4 ± 0.1 (VUF10472, $n=4$), 7.7 ± 0.1 (VUF10085, $n=4$), 7.4 ± 0.2 (VUF5834, $n=3$), 6.6 ± 0.1 (VUF10132, $n=4$) and 6.4 ± 0.1 (TAK-779, $n=4$).

Table 2. Properties of small non-peptidergic compounds at CXCR3

	pK _i						pK _b						pIC ₅₀							
	human	n	N3.35A	n	rhesus	n	rat	n	mouse	n	hCXCR3	hCXCL10	n	mCXCR3	mCXCL10	n	hCXCR3	hCXCR3	N3.35A	n
VUF10472	8.4 ± 0.1	7	7.9 ± 0.2	3	8.4 ± 0.1	3	7.8 ± 0.0	3	7.9 ± 0.1	3	8.2 ± 0.1	3	8.4 ± 0.1	5	8.4 ± 0.1	4	8.1 ± 0.1	3		
VUF10085	7.7 ± 0.0	18	7.3 ± 0.1	3	7.5 ± 0.0	3	6.9 ± 0.1	10	7.0 ± 0.1	3	7.7 ± 0.1	3	7.7 ± 0.1	9	7.7 ± 0.1	4	8.0 ± 0.1	3		
VUF5834	6.8 ± 0.1	3	6.4 ± 0.0	3	6.8 ± 0.0	3	6.2 ± 0.1	6	6.2 ± 0.1	3	7.0 ± 0.1	3	7.4 ± 0.2	5	7.4 ± 0.2	3	7.3 ± 0.0	3		
VUF10132	6.6 ± 0.0	4	5.9 ± 0.1	3	6.6 ± 0.1	3	6.0 ± 0.1	6	6.0 ± 0.1	3	6.7 ± 0.1	3	6.6 ± 0.1	5	6.6 ± 0.1	4	6.6 ± 0.1	3		
TAK-779	5.9 ± 0.0	6	5.9 ± 0.0	3	5.9 ± 0.1	3	5.8 ± 0.0	6	5.9 ± 0.0	3	6.1 ± 0.1	3	6.4 ± 0.1	4	6.4 ± 0.1	4	5.9 ± 0.1	3		

pK_i values ± SEM were generated in heterologous radioligand binding experiments using human ¹²⁵I-CXCL10. pK_b values were obtained at human CXCR3 with human CXCL10 and at mouse CXCR3 with mouse CXCL10 in the PLC activation assay and pIC₅₀ values were generated using human CXCR3 N3.35A in the PLC activation assay.

Table 3. Selectivity of CXCR3 antagonists

	Inhibition of agonist-induced PLC activation (%)										Inhibition of specific binding (%)				
	CXCR3	CXCR1	CXCR2	CXCR4	CCR2	CCR1	CCR2	H ₁ R	H ₃ R	CXCR2	CXCR4	H ₁ R	CXCR2	CXCR4	H ₁ R
CXCL11	CXCL8	CXCL1	CXCL12	CCL5	CCL2	histamine	histamine	histamine	¹²⁵ I-CXCL8	¹²⁵ I-CXCL12	³ H-mepyramine	¹²⁵ I-CXCL8	¹²⁵ I-CXCL12	³ H-mepyramine	
VUF10472	103 ± 8	-19 ± 16	8 ± 1	-7 ± 5	-6 ± 7	11 ± 3	-12 ± 24	-14 ± 2	6 ± 15	17 ± 11	30 ± 13	17 ± 11	17 ± 11	30 ± 13	
VUF10085	100 ± 13	-7 ± 17	6 ± 2	1 ± 8	-3 ± 2	10 ± 4	-37 ± 11	-33 ± 14	-15 ± 3	18 ± 7	20 ± 10	18 ± 7	18 ± 7	20 ± 10	
VUF5834	67 ± 9	-7 ± 29	13 ± 3	-19 ± 5	-3 ± 13	-1 ± 4	11 ± 17	-35 ± 12	-13 ± 7	0 ± 7	28 ± 11	0 ± 7	0 ± 7	28 ± 11	
VUF10132	71 ± 6	-2 ± 10	-33 ± 5	24 ± 2	61 ± 4	-1 ± 11	0 ± 2	-3 ± 8	-21 ± 14	4 ± 12	30 ± 6	4 ± 12	4 ± 12	30 ± 6	
TAK-779	53 ± 4	-8 ± 25	-8 ± 4	-2 ± 16	-12 ± 4	95 ± 6	-10 ± 26	-3 ± 15	-12 ± 6	-9 ± 32	41 ± 7	-9 ± 32	-9 ± 32	41 ± 7	

HEK293T cells coexpressing indicated human GPCRs and Gα_{q/15} were stimulated with indicated chemokines (100 nM) or histamine (10 μM) in the presence of CXCR3 antagonists (10 μM). The percentage inhibition of agonist-induced PLC activation is shown. Experiments were performed in duplicate and repeated two (CXCR2) or three times. Radioligand binding studies were performed on membranes of HEK293T (CXCR4) or COS-7 cells (CXCR2 and histamine H₁ receptor). The percentage inhibition of specific radioligand binding by the CXCR3 antagonists (10 μM) is shown. Experiments were performed in triplicate and repeated two (CXCR2) or three times.

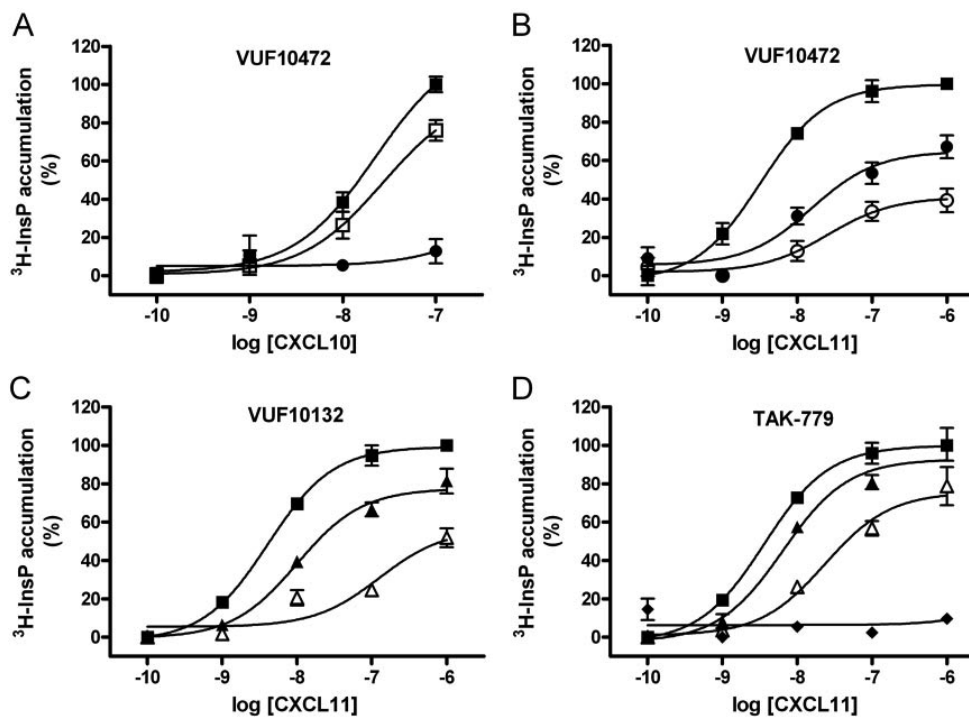


Figure 6. Non-competitive behavior of non-peptidergic compounds at human CXCR3. A) Schild analysis of VUF10472 using CXCL10 as agonist. HEK293T cells were transfected with cDNA encoding human CXCR3 and $G_{\alpha_{q15}}$. After 48 h, CXCL10-induced $^3\text{H-InsP}$ accumulation was determined in the absence (■) or in the presence of 10 nM (□) or 30 nM (●) VUF10472 (n=2-3). **B-D)** Schild analysis using CXCL11 as agonist. HEK293T cells were transfected with cDNA encoding human CXCR3 and $G_{\alpha_{q15}}$. After 48 h, CXCL11-induced $^3\text{H-InsP}$ accumulation was determined in the absence (■) or in the presence of 30 nM (●), 100 nM (○), 1 μM (▲), 10 μM (△) or 100 μM (◆) VUF10472 (Fig. 6B, n=6), VUF10132 (Fig. 6C, n=6) or TAK-779 (Fig. 6D, n=7). Data are presented as percentage of chemokine-induced (1 μM) stimulation in the absence of non-peptidergic ligand.

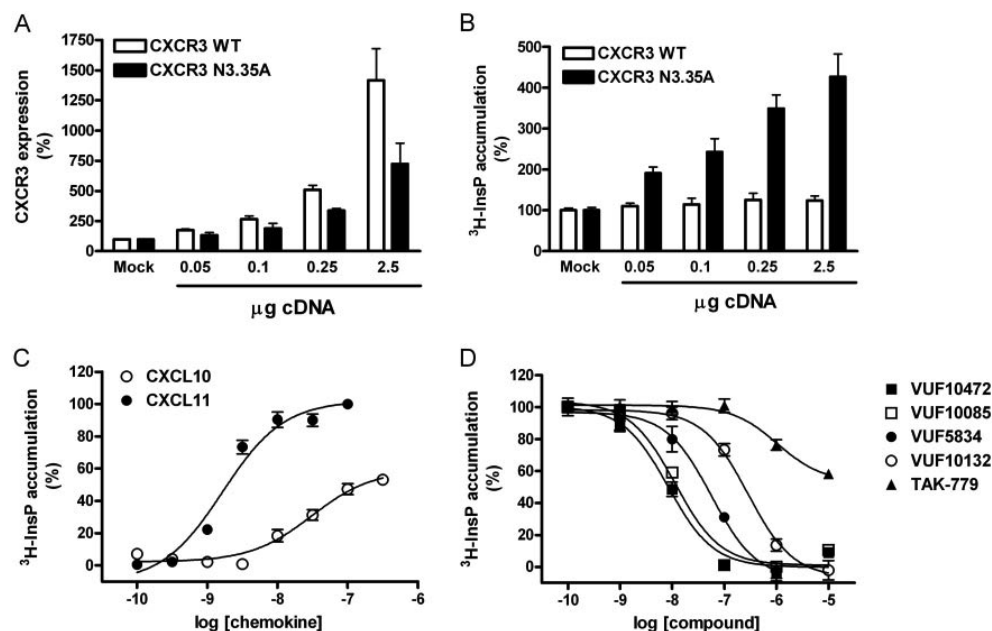


Fig. 7. Characterization of the constitutively active mutant CXCR3 N3.35A

A) Expression of CXCR3 WT and CXCR3 N3.35A. HEK293T cells were transfected with cDNA encoding $G_{\alpha_{q15}}$ and increasing amounts of cDNA encoding human CXCR3 WT or CXCR3 N3.35A. Mock cells were transfected with cDNA encoding $G_{\alpha_{q15}}$ and pcDEF3 empty vector. After 48 h, CXCR3 expression was determined in an ELISA assay. Data are presented as percentage signal obtained in mock-transfected cells ($n=2-3$).

B) Constitutive activity of CXCR3 N3.35A. HEK293T cells were transfected with cDNA encoding $G_{\alpha_{q15}}$ and increasing amounts of cDNA encoding human CXCR3 WT or CXCR3 N3.35A. Mock cells were transfected with cDNA encoding $G_{\alpha_{q15}}$ and pcDEF3 empty vector. After 48 h, $^3\text{H-InsP}$ accumulation was determined in the absence of chemokines. Data are presented as percentage $^3\text{H-InsP}$ in mock-transfected cells ($n=3$).

C) Chemokine-induced PLC activation by CXCR3 N3.35A. HEK293T cells were transfected with cDNA encoding CXCR3 N3.35A and $G_{\alpha_{q15}}$. After 48 h, $^3\text{H-InsP}$ accumulation was determined in the presence of increasing concentrations CXCL10 or CXCL11. $p\text{EC}_{50}$ values for CXCL10 and CXCL11 were 7.5 ± 0.0 ($n=2$) and 8.7 ± 0.1 ($n=4$) respectively. Data are presented as percentage of the maximal response obtained with CXCL11 (100 nM).

D) Inverse agonism at CXCR3 N3.35A. HEK293T cells were transfected with cDNA encoding CXCR3 N3.35A and $G_{\alpha_{q15}}$. After 48 h, $^3\text{H-InsP}$ accumulation was determined in the presence of increasing concentrations VUF10472 (■), VUF10085 (□), VUF5834 (●), VUF10132 (○) or TAK-779 (▲). $p\text{IC}_{50}$ values ($n=3$) were 8.1 ± 0.1 (VUF10472), 8.0 ± 0.1 (VUF10085), 7.3 ± 0.0 (VUF5834), 6.6 ± 0.1 (VUF10132) and 5.9 ± 0.1 (TAK-779). Data are presented as percentage of CXCR3 N3.35A-mediated constitutive $^3\text{H-InsP}$ accumulation.

Specificity of the non-peptidergic CXCR3 antagonists

The CXCR3 antagonists were tested against a small panel of chemokine and histamine receptors to determine their specificity. HEK293T cells expressing the different GPCRs were incubated with their respective agonists in the presence or absence of CXCR3 antagonists and activation of PLC was determined. The percentage inhibition of agonist-induced PLC activation by the CXCR3 antagonists is shown in Table 3. As expected, the CXCR3 antagonists (10 μ M) showed 50-100 % inhibition of CXCL11-induced (100 nM) PLC activation through CXCR3 and the CCR5/CCR2/CXCR3 antagonist TAK-779 inhibited CCL2-induced activation of CCR2 with 95%. Unexpectedly, VUF10132 inhibited CCL5-induced CCR1 activation with 61%, compared to 71% inhibition of CXCR3-mediated response. The other CXCR3 antagonists did not significantly inhibit the tested chemokine or histamine receptors (Table 3). Additionally, the compounds were tested in radioligand binding studies on membranes expressing CXCR2, CXCR4 or the histamine H₁ receptor. At the tested concentration (10 μ M), the CXCR3 antagonists typically inhibit [¹²⁵I]-CXCL10 binding to CXCR3 with 80-100% (Figure 5A). Besides TAK-779, which inhibited binding of [³H]-mepyramine to the histamine H₁ receptor with only 41% at 10 μ M, no significant inhibition of radioligand binding to CXCR2, CXCR4 or the H₁ receptor by the other CXCR3 antagonists was observed.

Non-peptidergic antagonists are inverse agonists at a constitutively active mutant of CXCR3

Inverse agonism has recently been shown to be an important molecular mechanism of action of small-molecule antagonists at a variety of GPCR family members.³⁰ Human chemokine receptors generally do not show high levels of constitutive activity. However, constitutively active chemokine receptor mutants have been described that signal in the absence of ligands. Examples are CXCR2 D3.49V,³¹ mutation of N3.35 of CXCR4,³² and mutation of T2.56 in CCR2 and CCR5.³³ To determine if the studied CXCR3 antagonists act as neutral antagonists or inverse agonists at CXCR3, analogous CAMs of CXCR3 were constructed (Figure 3). Upon expression of the CXCR3 mutants N3.35A, N3.35S and T2.56P significant constitutive activity was shown, whereas no constitutive activity was found for the CXCR3 D3.49V mutant (data not shown). In view of the signal to noise ratio we choose CXCR3 N3.35A for further characterization. Upon transfection of HEK293T cells with increasing amounts of cDNA encoding CXCR3 WT or CXCR3 N3.35A an increase in receptor expression was detected in ELISA experiments (Figure 7A). When similar amounts of cDNA were transfected, CXCR3 WT was expressed at higher levels

than CXCR3 N3.35A (Figure 7A). As expected, CXCR3 WT did not activate PLC in the absence of ligands (Figure 7B). Even though CXCR3 N3.35A was expressed at lower levels than CXCR3 WT, CXCR3 N3.35A showed a marked increase of PLC activation upon transfection of increasing amounts of cDNA (Figure 7B).

The affinities of CXCL10 (pK_d 10.2 ± 0.2) and CXCL11 (pK_d , 11.3 ± 0.3) for CXCR3 N3.35A were slightly higher than for CXCR3 WT (Table 1). CXCL10 and CXCL11 activated CXCR3 N3.35A over basal levels in a similar manner as CXCR3 WT, with pEC_{50} values of 7.5 ± 0.0 ($n=2$) and 8.7 ± 0.1 ($n=4$) respectively (Figure 7C, Table 1). Subsequently, the affinity of the antagonists at CXCR3 N3.35A was determined using [^{125}I]-CXCL10. The affinity of all compounds, except TAK-779, was slightly reduced for CXCR3 N3.35A compared to CXCR3 WT (Table 2). Finally, the effect of the antagonists on the constitutive activation of PLC was investigated. VUF10472, VUF10085, VUF5834 and VUF10132 all acted as full inverse agonists, with IC_{50} values ranging between 8 nM for VUF10472 and 251 nM for VUF10132 (Figure 7D, Table 2). In contrast, TAK-779 acted as a partial inverse agonist with an intrinsic activity of -0.42 ± 0.0 and an IC_{50} of 1.3 μ M ($n=3$) (Figure 7D, Table 2).

Discussion

CXCR3 has attracted considerable attention as a new drug target due to its involvement in a variety of serious disorders, including cancer,¹⁰ atherosclerosis,⁸ inflammatory disorders like rheumatoid arthritis,² skin diseases⁹ and transplant rejection.⁷ Following the recognition of CXCR3 as a potential attractive drug target, several small molecule CXCR3 antagonists have recently been identified.^{16,18-23} In this study, we have selected five non-peptidergic antagonists from three different structural classes and studied their mechanism of action at the human CXCR3. In addition, the interaction of these antagonists with human, rhesus macaque, rat and mouse CXCR3 was investigated.

All tested non-peptidergic antagonists inhibited CXCL10-induced activation of PLC with pK_b values that correlated very well with their affinity, with a rank order VUF10472 > VUF10085 > VUF5834 > VUF10132 > TAK-779 (Table 2). Subsequently, the mechanism of action of the antagonists was explored using Schild analysis. The dose-response curves for CXCL10 and CXCL11 did not reach the maximal response in the presence of VUF10472 (Figure 6), as has been previously shown by others for human and mouse CXCR3.^{22,34} Antagonists from other structural classes also decreased the maximum response of CXCL11, in a manner that follows the rank-order of their affinities. This indicates that all tested non-peptidergic antagonists behave as non-competitive antagonists for the PLC activation by the endogenous agonists of CXCR3.

Antagonists of GPCRs can be classified as neutral antagonists or (partial) inverse agonists.^{30,35} Although both antagonist classes are able to block an agonist-induced response by occupying the receptor, there is an ongoing debate about the exact clinical benefits or disadvantages of each class.³⁰ Treatment with inverse agonists may be beneficial when a constitutively active receptor underlies the pathogenesis. To date, there are no reports about constitutive activity of CXCR3 and there are only few examples of constitutive activity of chemokine receptors. Constitutive activity is a function of the relative stoichiometry of receptors and G proteins³⁵ and chemokine receptors, including CXCR3, are often upregulated under inflammatory conditions.^{1,36} Hence, under pathophysiological conditions constitutive activity of chemokine receptors might become apparent and therefore the use of inverse agonists beneficial. In order to study the relative efficacy of the non-peptidergic antagonists, we generated mutants of CXCR3, i.e. CXCR3 N3.35A, N3.35S, D3.39V and T2.56P, based on CAMs of chemokine receptors reported in literature.³¹⁻³³ All generated mutants, except for CXCR3 D3.49V with a mutation in the conserved DRY motif at the cytoplasmic end of TM3, displayed basal signaling. Mutation of the DRY motif of CXCR2 to VRY confers constitutive activity to CXCR2,³¹ while the same mutation for CXCR1³¹ or CCR5³⁷ did not result in constitutive activity. Conversely, mutation of the VRY motif to DRY in the highly constitutively active chemokine receptor ORF74 encoded by Kaposi's sarcoma-associated herpesvirus did not diminish its constitutive activity but even increased it.³⁸ Therefore, mutation of D3.49 to Val does not appear to be a universal switch for constitutive activity in chemokine receptors. In the same way, mutation of T2.56 in the conserved TXP motif resulted in a CAM for CXCR3 (this study), CCR5 and CCR2 but not for CCR1, CCR3, CCR4, CXCR2 and CXCR4.³³ Mutation of N3.35 in the N(L/F)Y motif in TM3 of CXC chemokine receptors resulted in CAMs for both CXCR3 (this study) and CXCR4.³² The non-peptidergic compounds acted as full inverse agonists at CXCR3 N3.35A, except for TAK-779, which only partially inhibited constitutive signaling at the highest concentration used (Figure 7D). Since VUF10132 and TAK-779 have similar affinities for CXCR3 N3.35A (Table 2), it appears that TAK-779 lacks certain structural features needed for full inverse agonism at CXCR3. Interestingly, TAK-779 acts as a full inverse agonist at CCR5.³⁷ As expected for a receptor in the active state,³⁵ the affinities of the agonists CXCL10 and CXCL11 for CXCR3 N3.35A were increased compared to CXCR3 WT (Table 1). The full inverse agonists VUF10472, VUF10085, VUF5834 and VUF10132, which are predicted to have a higher affinity for an inactive receptor conformation,³⁵ all showed reduced affinity for CXCR3 N3.35A compared to CXCR3 WT (Table 2). In contrast, the affinity of the weak partial inverse agonist TAK-779 did not change, indicating a different mode of interaction with CXCR3 compared to the other structural classes of compounds.

If antagonists are to be tested in animal models, detailed information on the interaction of the compound with the receptor of that specific species is required, since species differences may occur. We therefore tested the non-peptidergic antagonists on rhesus macaque CXCR3, which was cloned in this study, as well as on rat and mouse CXCR3. Human and rhesus macaque show 99% amino acid identity (Figure 3). Consistent with this high homology, no differences in affinity or potency of CXCL10 and CXCL11, or in the affinity of the non-peptidergic antagonists for the two receptors were found. Similarly, the protein sequences of rat and mouse CXCR3 are 96% identical and no significant differences in affinity of the endogenous agonists or the non-peptidergic compounds are observed between the CXCR3 of these rodent species. However, lower sequence identity is found when human and rhesus macaque CXCR3 are compared with rat and mouse CXCR3. Approximately 85% identity exists between the primate (human and rhesus macaque) and rodent (rat and mouse) species (Figure 3). Nevertheless, the affinities of CXCL10 and CXCL11 found for rodent CXCR3 were comparable to the affinities found for primate CXCR3 (Table 1). While the affinities of CXCL10 and CXCL11 were comparable, the affinities of VUF10472, VUF10084, VUF5834 and VUF101032 were only about 4-fold lower for rodent CXCR3 than for primate CXCR3 (Table 2). Also their pK_b values against hCXCL10/hCXCR3 and mCXCL10/mCXCR3 are comparable (Table 2, Figure 5B and 5F), indicating the usefulness of these compounds in mouse models. In contrast, the affinity of TAK-779 was equal for CXCR3 of all tested species, again indicating that TAK-779 interacts with CXCR3 in another manner than the other antagonists. TAK-779, developed as a CCR5 antagonist, has been thoroughly investigated because of its potential use as a HIV-entry inhibitor. TAK-779 shows high affinity for human CCR5 and to a lesser extent for human CCR2b.¹⁵ Furthermore, TAK-779 was reported to bind mouse CCR5, as well as mouse CXCR3.¹⁶ Remarkably, TAK-779 shows a more than 100-fold higher affinity for human CCR5 than for mouse CCR5.^{15,16} This species selectivity of TAK-779 for CCR5 is not observed for human and mouse CXCR3, which both bind TAK-779 with affinities around 1 μ M (Table 2). It appears that TAK-779 has nanomolar affinity for human CCR5 and micromolar affinity for human CXCR3, whereas it has only micromolar affinity for mouse CCR5 and mouse CXCR3. This should be kept in mind when analyzing and extrapolating data from rodent models, since at a certain effective concentration of TAK-779 different receptors will be occupied in humans and mice. While in mice the observed effects would likely be mediated by a combined blockage of CCR5 and CXCR3, in humans the effects of TAK-779 would be mostly through inhibition of CCR5 with low nanomolar affinity. The non-peptidergic CXCR3 antagonists investigated in this study only showed a 3 to 4-fold species selectivity for CXCR3 of primates versus rodents in radioligand binding studies, whereas no species difference was observed in functional studies. When testing for selectivity against a small panel of GPCRs, VUF10132 inhibited CCR1-mediated

signaling and should therefore be optimized with respect to its affinity and specificity for CXCR3. In contrast, we observed that VUF10472, VUF10085 and VUF5834 are selective for CXCR3 amongst the GPCRs in the tested panel. In line with our findings, VUF10472/NBI-74330 has previously been reported not to affect chemotactic responses by human H9 T-cell lymphoma cells in response to CXCL12 and CCL19 and not to interfere with calcium mobilization induced by lysophosphatidic acid or radioligand binding to several GPCRs.²²

Conclusions

In summary, we characterized representative examples of three classes of small non-peptidergic and non-competitive CXCR3 antagonists at CXCR3 of four different species, with VUF10472 being the most potent compound at human, rhesus, rat and mouse CXCR3. The observed selectivity profile and relatively small differences in affinity observed between human and rodent CXCR3 imply that VUF10472/NBI-74330, VUF10085/AMG 487 and VUF5834 are useful in rodent models of CXCR3-mediated pathogenesis. Interestingly, it was found that the non-peptidergic antagonists act as inverse agonists at a constitutively active CXCR3 mutant.

Acknowledgements

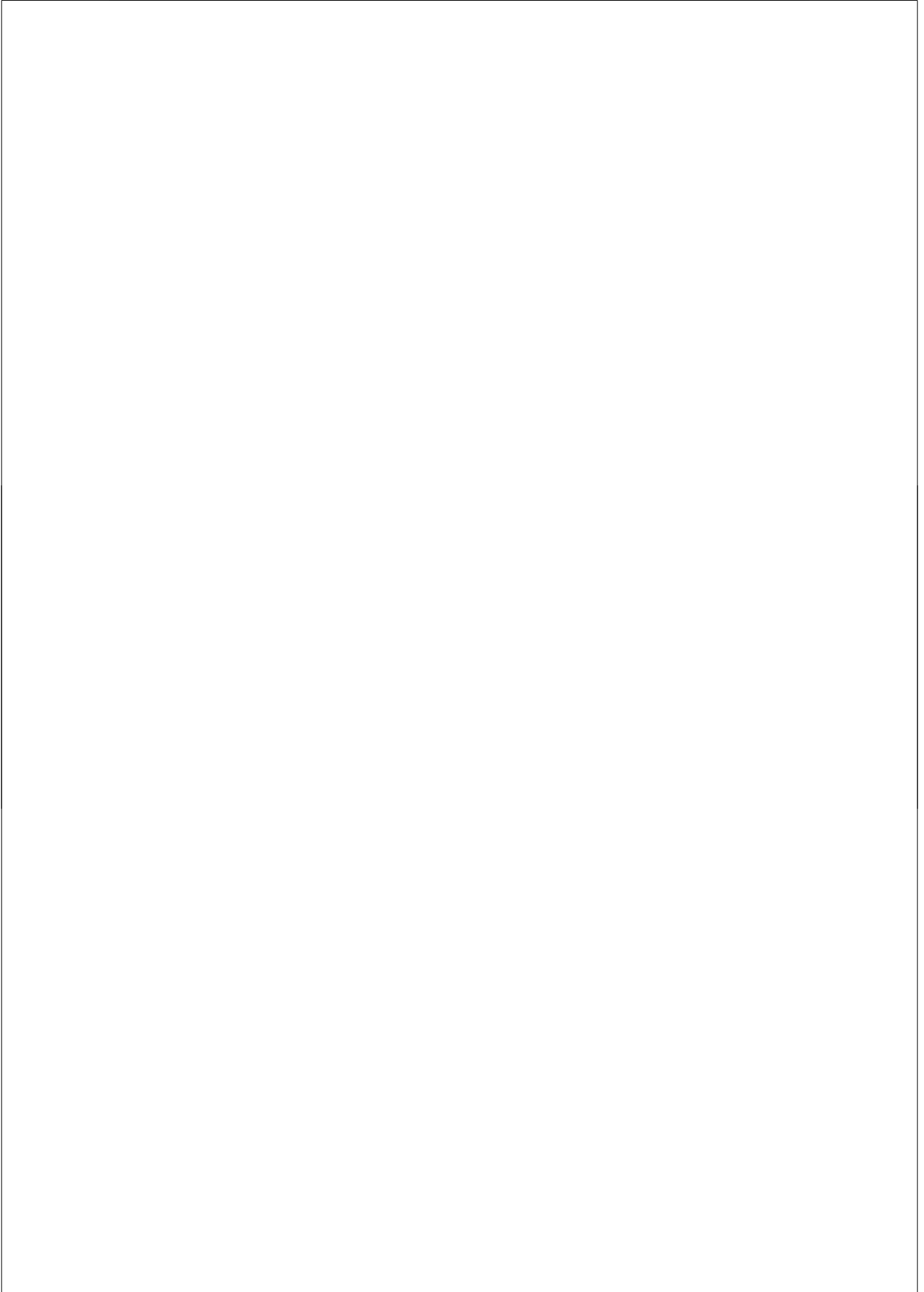
Kamonchanok Sansuk and Anne O. Watts (both from the Division of Medicinal Chemistry at the Vrije Universiteit Amsterdam) are thanked for their kind help with some of the experiments.

References

- (1) Murphy, P. M.; Baggiolini, M.; Charo, I. F.; Hebert, C. A.; Horuk, R.; Matsushima, K.; Miller, L. H.; Oppenheim, J. J.; Power, C. A. International union of pharmacology. XXII. Nomenclature for chemokine receptors. *Pharmacol. Rev.*, **2000**, *52*, 145-176.
- (2) Qin, S.; Rottman, J. B.; Myers, P.; Kassam, N.; Weinblatt, M.; Loetscher, M.; Koch, A. E.; Moser, B.; Mackay, C. R. The chemokine receptors CXCR3 and CCR5 mark subsets of T cells associated with certain inflammatory reactions. *J. Clin. Invest.*, **1998**, *101*, 746-754.
- (3) Loetscher, M.; Gerber, B.; Loetscher, P.; Jones, S. A.; Piali, L.; Clark-Lewis, I.; Baggiolini, M.; Moser, B. Chemokine receptor specific for IP10 and mig: structure, function, and expression in activated T-lymphocytes. *J. Exp. Med.*, **1996**, *184*, 963-969.
- (4) Cole, K. E.; Strick, C. A.; Paradis, T. J.; Ogborne, K. T.; Loetscher, M.; Gladue, R. P.; Lin, W.; Boyd, J. G.; Moser, B.; Wood, D. E.; Sahagan, B. G.; Neote, K. Interferon-inducible T cell alpha chemoattractant (I-TAC): a novel non-ELR CXC chemokine with potent activity on activated T cells through selective high affinity binding to CXCR3. *J. Exp. Med.*, **1998**, *187*, 2009-2021.
- (5) Smit, M. J.; Verdijk, P.; van der Raaij-Helmer, E. M.; Navis, M.; Hensbergen, P. J.; Leurs, R.; Tensen, C. P. CXCR3-mediated chemotaxis of human T cells is regulated by a Gi- and phospholipase C-dependent pathway and not via activation of MEK/p44/p42 MAPK nor Akt/PI-3 kinase. *Blood*, **2003**, *102*, 1959-1965.
- (6) Sorensen, T. L.; Tani, M.; Jensen, J.; Pierce, V.; Lucchinetti, C.; Folcik, V. A.; Qin, S.; Rottman, J.; Sellebjerg, F.; Strieter, R. M.; Frederiksen, J. L.; Ransohoff, R. M. Expression of specific chemokines and chemokine receptors in the central nervous system of multiple sclerosis patients. *J. Clin. Invest.*, **1999**, *103*, 807-815.
- (7) Hancock, W. W.; Lu, B.; Gao, W.; Csizmadia, V.; Faia, K.; King, J. A.; Smiley, S. T.; Ling, M.; Gerard, N. P.; Gerard, C. Requirement of the chemokine receptor CXCR3 for acute allograft rejection. *J. Exp. Med.*, **2000**, *192*, 1515-1520.
- (8) Mach, F.; Sauty, A.; Iarossi, A. S.; Sukhova, G. K.; Neote, K.; Libby, P.; Luster, A. D. Differential expression of three T lymphocyte-activating CXC chemokines by human atheroma-associated cells. *J. Clin. Invest.*, **1999**, *104*, 1041-1050.
- (9) Flier, J.; Boorsma, D. M.; van Beek, P. J.; Nieboer, C.; Stoof, T. J.; Willemze, R.; Tensen, C. P. Differential expression of CXCR3 targeting chemokines CXCL10, CXCL9, and CXCL11 in different types of skin inflammation. *J. Pathol.*, **2001**, *194*, 398-405.
- (10) Walser, T. C.; Rifat, S.; Ma, X.; Kundu, N.; Ward, C.; Goloubeva, O.; Johnson, M. G.; Medina, J. C.; Collins, T. L.; Fulton, A. M. Antagonism of CXCR3 inhibits lung metastasis in a murine model of metastatic breast cancer. *Cancer Res.*, **2006**, *66*, 7701-7707.
- (11) Luster, A. D.; Leder, P. IP-10, a -C-X-C- chemokine, elicits a potent thymus-dependent antitumor response in vivo. *J. Exp. Med.*, **1993**, *178*, 1057-1065.
- (12) Hensbergen, P. J.; Wijnands, P. G.; Schreurs, M. W.; Scheper, R. J.; Willemze, R.; Tensen, C. P. The CXCR3 targeting chemokine CXCL11 has potent antitumor activity in vivo involving attraction of CD8+ T lymphocytes but not inhibition of angiogenesis. *J. Immunother.*, **2005**, *28*, 343-351.
- (13) Pan, J.; Burdick, M. D.; Belperio, J. A.; Xue, Y. Y.; Gerard, C.; Sharma, S.; Dubinett, S. M.; Strieter, R. M. CXCR3/CXCR3 ligand biological axis impairs RENCA tumor growth by a mechanism of immunoangiostasis. *J. Immunol.*, **2006**, *176*, 1456-1464.
- (14) Salomon, I.; Netzer, N.; Wildbaum, G.; Schiff-Zuck, S.; Maor, G.; Karin, N. Targeting the function of IFN-gamma-inducible protein 10 suppresses ongoing adjuvant arthritis. *J. Immunol.*, **2002**, *169*, 2685-2693.
- (15) Baba, M.; Nishimura, O.; Kanzaki, N.; Okamoto, M.; Sawada, H.; Iizawa, Y.; Shiraiishi, M.; Aramaki, Y.; Okonogi, K.; Ogawa, Y.; Meguro, K.; Fujino, M. A

- small-molecule, nonpeptide CCR5 antagonist with highly potent and selective anti-HIV-1 activity. *Proc. Natl. Acad. Sci. USA*, **1999**, *96*, 5698-5703.
- (16) Gao, P.; Zhou, X. Y.; Yashiro-Ohtani, Y.; Yang, Y. F.; Sugimoto, N.; Ono, S.; Nakanishi, T.; Obika, S.; Imanishi, T.; Egawa, T.; Nagasawa, T.; Fujiwara, H.; Hamaoka, T. The unique target specificity of a nonpeptide chemokine receptor antagonist: selective blockade of two Th1 chemokine receptors CCR5 and CXCR3. *J. Leukoc. Biol.*, **2003**, *73*, 273-280.
- (17) Yang, Y. F.; Mukai, T.; Gao, P.; Yamaguchi, N.; Ono, S.; Iwaki, H.; Obika, S.; Imanishi, T.; Tsujimura, T.; Hamaoka, T.; Fujiwara, H. A non-peptide CCR5 antagonist inhibits collagen-induced arthritis by modulating T cell migration without affecting anti-collagen T cell responses. *Eur. J. Immunol.*, **2002**, *32*, 2124-2132.
- (18) Cole, A. G.; Stroke, I. L.; Brescia, M. R.; Simhadri, S.; Zhang, J. J.; Hussain, Z.; Snider, M.; Haskell, C.; Ribeiro, S.; Appell, K. C.; Henderson, I.; Webb, M. L. Identification and initial evaluation of 4-N-aryl-[1,4]diazepane ureas as potent CXCR3 antagonists. *Bioorg. Med. Chem. Lett.*, **2006**, *16*, 200-203.
- (19) Allen, D. R.; Bolt, A.; Chapman, G. A.; Knight, R. L.; Meissner, J. W.; Owen, D. A.; Watson, R. J. Identification and structure-activity relationships of 1-aryl-3-piperidin-4-yl-urea derivatives as CXCR3 receptor antagonists. *Bioorg. Med. Chem. Lett.*, **2007**, *17*, 697-701.
- (20) Storelli, S.; Verdijk, P.; Verzijl, D.; Timmerman, H.; van de Stolpe, A. C.; Tensen, C. P.; Smit, M. J.; De Esch, I. J.; Leurs, R. Synthesis and structure-activity relationship of 3-phenyl-3H-quinazolin-4-one derivatives as CXCR3 chemokine receptor antagonists. *Bioorg. Med. Chem. Lett.*, **2005**, *15*, 2910-2913.
- (21) Storelli, S.; Verzijl, D.; Al-Badie, J.; Elders, N.; Bosch, L.; Timmerman, H.; Smit, M. J.; De Esch, I. J.; Leurs, R. Synthesis and Structure-Activity Relationships of 3H-Quinazolin-4-ones and 3H-Pyrido[2,3-d]pyrimidin-4-ones as CXCR3 receptor antagonists. *Arch. Pharm. (Weinheim)*, **2007**, *340*, 281-291.
- (22) Heise, C. E.; Pahuja, A.; Hudson, S. C.; Mistry, M. S.; Putnam, A. L.; Gross, M. M.; Gottlieb, P. A.; Wade, W. S.; Kiankarimi, M.; Schwarz, D.; Crowe, P.; Zlotnik, A.; Alleva, D. G. Pharmacological characterization of CXC chemokine receptor 3 ligands and a small molecule antagonist. *J. Pharmacol. Exp. Ther.*, **2005**, *313*, 1263-1271.
- (23) Johnson, M.; Li, A. R.; Liu, J.; Fu, Z.; Zhu, L.; Miao, S.; Wang, X.; Xu, Q.; Huang, A.; Marcus, A.; Xu, F.; Ebsworth, K.; Sablan, E.; Danao, J.; Kumer, J.; Dairaghi, D.; Lawrence, C.; Sullivan, T.; Tonn, G.; Schall, T.; Collins, T.; Medina, J. Discovery and optimization of a series of quinazolinone-derived antagonists of CXCR3. *Bioorg. Med. Chem. Lett.*, **2007**, *17*, 3339-3343.
- (24) Axten, J. M.; J., F. J.; D., K. W.; Sarau, H. M. Imidazolium CXCR3 inhibitors (Smithkline Beecham Corporation) WO 03/101970 A1, **2003**.
- (25) Wang, X.; Li, X.; Schmidt, D. B.; Foley, J. J.; Barone, F. C.; Ames, R. S.; Sarau, H. M. Identification and molecular characterization of rat CXCR3: receptor expression and interferon-inducible protein-10 binding are increased in focal stroke. *Mol. Pharmacol.*, **2000**, *57*, 1190-1198.
- (26) Lu, B.; Humbles, A.; Bota, D.; Gerard, C.; Moser, B.; Soler, D.; Luster, A. D.; Gerard, N. P. Structure and function of the murine chemokine receptor CXCR3. *Eur. J. Immunol.*, **1999**, *29*, 3804-3812.
- (27) Streblov, D. N.; Kreklywich, C.; Yin, Q.; De La Melena, V. T.; Corless, C. L.; Smith, P. A.; Brakebill, C.; Cook, J. W.; Vink, C.; Bruggeman, C. A.; Nelson, J. A.; Orloff, S. L. Cytomegalovirus-mediated upregulation of chemokine expression correlates with the acceleration of chronic rejection in rat heart transplants. *J. Virol.*, **2003**, *77*, 2182-2194.
- (28) Coward, P.; Chan, S. D.; Wada, H. G.; Humphries, G. M.; Conklin, B. R. Chimeric G proteins allow a high-throughput signaling assay of Gi-coupled receptors. *Anal. Biochem.*, **1999**, *270*, 242-248.

- (29) Cheng, Y.; Prusoff, W. H. Relationship between the inhibition constant (K₁) and the concentration of inhibitor which causes 50 per cent inhibition (I₅₀) of an enzymatic reaction. *Biochem. Pharmacol.*, **1973**, *22*, 3099-3108.
- (30) Parra, S.; Bond, R. A. Inverse agonism: from curiosity to accepted dogma, but is it clinically relevant? *Curr. Opin. Pharmacol.*, **2007**, *7*, 146-50.
- (31) Burger, M.; Burger, J. A.; Hoch, R. C.; Oades, Z.; Takamori, H.; Schraufstatter, I. U. Point mutation causing constitutive signaling of CXCR2 leads to transforming activity similar to Kaposi's sarcoma herpesvirus-G protein-coupled receptor. *J. Immunol.*, **1999**, *163*, 2017-2022.
- (32) Zhang, W. B.; Navenot, J. M.; Haribabu, B.; Tamamura, H.; Hiramatu, K.; Omagari, A.; Pei, G.; Manfredi, J. P.; Fujii, N.; Broach, J. R.; Peiper, S. C. A point mutation that confers constitutive activity to CXCR4 reveals that T140 is an inverse agonist and that AMD3100 and ALX40-4C are weak partial agonists. *J. Biol. Chem.*, **2002**, *277*, 24515-24521.
- (33) Arias, D. A.; Navenot, J. M.; Zhang, W. B.; Broach, J.; Peiper, S. C. Constitutive activation of CCR5 and CCR2 induced by conformational changes in the conserved TXP motif in transmembrane helix 2. *J. Biol. Chem.*, **2003**, *278*, 36513-36521.
- (34) Jopling, L. A.; Watt, G. F.; Fisher, S.; Birch, H.; Coggon, S.; Christie, M. I. Analysis of the pharmacokinetic/pharmacodynamic relationship of a small molecule CXCR3 antagonist, NBI-74330, using a murine CXCR3 internalization assay. *Br. J. Pharmacol.*, **2007**, *152*, 1260-1271.
- (35) Kenakin, T. The classification of seven transmembrane receptors in recombinant expression systems. *Pharmacol. Rev.*, **1996**, *48*, 413-463.
- (36) Rabin, R. L.; Park, M. K.; Liao, F.; Swofford, R.; Stephany, D.; Farber, J. M. Chemokine receptor responses on T cells are achieved through regulation of both receptor expression and signaling. *J. Immunol.*, **1999**, *162*, 3840-3850.
- (37) Lagane, B.; Ballet, S.; Planchenault, T.; Balabanian, K.; Le Poul, E.; Blanpain, C.; Percherancier, Y.; Staropoli, I.; Vassart, G.; Oppermann, M.; Parmentier, M.; Bachelier, F. Mutation of the DRY motif reveals different structural requirements for the CC chemokine receptor 5-mediated signaling and receptor endocytosis. *Mol. Pharmacol.*, **2005**, *67*, 1966-1976.
- (38) Ho, H. H.; Ganeshalingam, N.; Rosenhouse-Dantsker, A.; Osman, R.; Gershengorn, M. C. Charged residues at the intracellular boundary of transmembrane helices 2 and 3 independently affect constitutive activity of Kaposi's sarcoma-associated herpesvirus G protein-coupled receptor. *J. Biol. Chem.*, **2001**, *276*, 1376-1382.
- (39) Ballesteros, J. A.; Weinstein, H. Integrated Methods for the Construction of Three Dimensional Models and Computational Probing of Structure-Function Relations in G-Protein Coupled Receptors. *Methods in Neuroscience*, **1995**, *25*, 366-428.



Chapter 7

Preliminary investigations into bivalent ligands for CXCR3

Abstract

The "bivalent ligand" approach can be used to probe dimers of GPCRs. Here, this approach is applied to the development of a new type of CXCR3 antagonists able to target possible CXCR3 dimers. Using the well known 3*H*-quinazolin-4-one and 3*H*-pyrido[2,3-*d*]pyrimidin-4-one CXCR3 antagonists **3a-b** and **4** as monomers, bivalent ligands with alkyl spacers have been synthesized. In comparison to **3a** and **3b** the bivalent analogues exhibit a decreased affinity and antagonistic activity at CXCR3 receptor. In the series of these bivalent analogue compounds, **1a** showed the highest affinity whereas **1b** showed the best antagonistic activity towards CXCR3. Owing to their interesting structures and pharmacological profiles, compounds **1a** and **1b** may be used as tools for CXCR3 dimerization studies.

Introduction

Chemokine receptors, like the majority of cell surface receptors, belong to the superfamily of G-protein coupled receptors. They exert their activity through coupling to a heterotrimeric G protein which can initiate second messenger signaling cascades.^{1,2} Although the classical literature routinely described GPCRs functioning as monomers signaling through downstream G-proteins in 1:1 stoichiometric ratio, in the last decade the focus has shifted to the concept of GPCRs existing and potentially functioning as dimers/oligomers^{3,4}. To date, several pharmacological studies as well as biochemical and biophysical techniques such as cross-linking,^{5,6} immunoprecipitation,^{7,8} bioluminescence^{9,10} or fluorescence resonance energy transfer (FRET) studies¹¹ have provided evidence for this new concept. Furthermore, in a study where infrared-laser atomic force microscopy was used to reveal the rhodopsin arrangement in the native disc membranes,¹² it has been shown that almost all rhodopsin molecules are present as rows of dimers. This appears consistent with the proposed dimeric form of GPCRs (Figure 1).

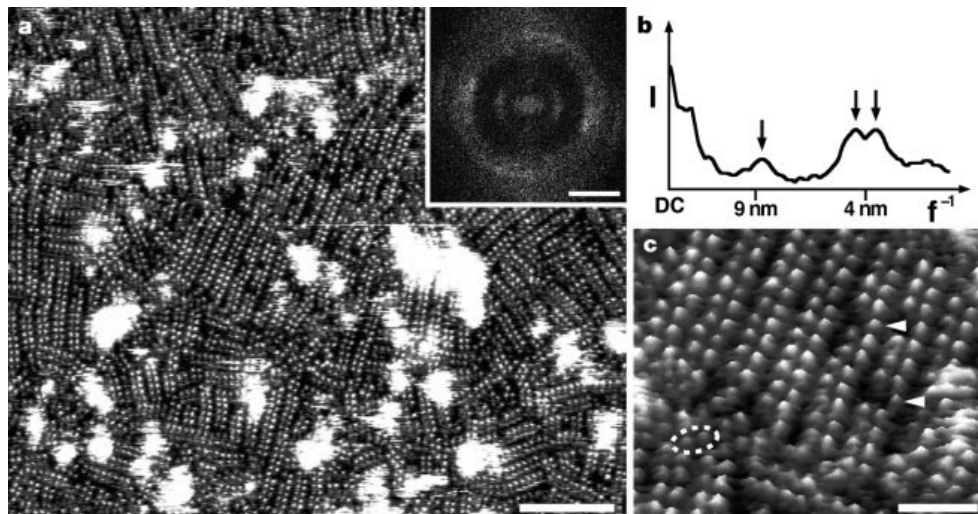


Figure 1. Organization and topography of the cytoplasmic surface of rhodopsin. **a**, Topograph obtained using atomic-force microscopy, showing the arrangement of rhodopsin dimers in the native disc membrane. **b**, Angularly averaged powder-diffraction pattern. **c**, Magnification of a region of the topograph in **a**, showing rows of rhodopsin dimers, as well as individual dimers (inside dashed ellipse) and occasional rhodopsin monomers (arrowheads). Adapted from Fotiadis et al.¹²

Interestingly, however, Whorton et al¹³ showed that when incorporating the β_2 -adrenergic receptor in a high-density lipoprotein particle system, there is the possibility that the minimal GPCR functional unit required for signaling is simply a monomer. In fact, in this setting, where the β_2 -adrenergic receptor was not able to dimerize, agonist

treatment induced a rapid guanine-nucleotide exchange in G proteins. Therefore it might be speculated that even if the GPCRs exist as dimers/oligomers, the dimerization/oligomerization plays only a marginal role in the G protein activation. Nonetheless, in general all these important findings on GPCR dimers may collectively represent the basis for new pharmacological mechanisms of action and for new molecular designs that address a better ligand selectivity coupled to a lower incidence of side effects.¹⁴ Based on whether two of the same type of GPCR bind or two different types, one can distinguish homodimers or heterodimers. Both types can in principle be targeted by bivalent ligands. Bivalent (dimeric) ligands are defined as molecules containing two pharmacological recognition units (pharmacophores) linked covalently by a connecting unit (spacer). Bivalent ligands are generally thought to interact first via univalent binding which is then followed by a binding of a second pharmacophore to a second recognition site on an adjacent receptor¹⁵. In principle, this double binding event can increase affinity and selectivity toward the targeted receptor(s). Thus, bivalent ligands may be more effective than the respective monomeric ligands and their use may open the door to future development of potent, selective GPCR drugs. Figure 2 shows a cartoon depicting a bivalent ligand binding to a GPCR heterodimer.

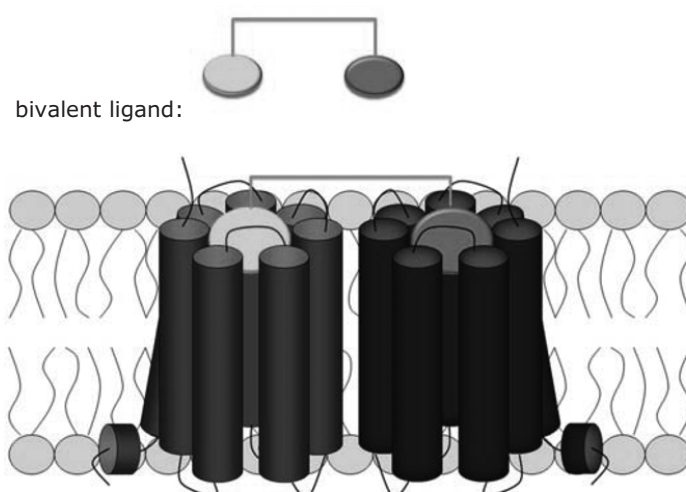


Figure 2. Example of a bivalent ligand binding to a GPCR heterodimer. Adapted from Filizola.¹⁶

Besides being novel entries into drugs, bivalent ligands are expected to be valuable molecular probes for the study of GPCR dimerization. Particularly, studies in the opioid receptor area have shown that bivalent ligands can exhibit enhanced affinity compared to their monomeric analogues depending on the type and length of the spacer.^{17,18} Moreover, in some studies the bivalent ligands showed improved selectivity for one of the receptor subtype over the others in the same family.¹⁹⁻²³ These studies provided indications for the existence of several types of opioid receptor dimers.

A few studies have shown that, like many GPCRs, some chemokines receptors are able to form homo- and heterodimers.²⁴⁻²⁷ Using different techniques such as the bioluminescence resonance energy transfer (BRET), homo- and heterodimerisation has been demonstrated for CCR2 and CCR5 receptors.²⁴⁻²⁶ Babcock et al used the BRET technique to show that CXCR4 is unable to heterodimerise with CCR5, but forms clusters (oligomers) of two or more CXCR4 monomers.²⁷

To date no evidence for CXCR3 homo- and/or heterodimerisation is available, nor are any specific studies on bivalent ligands for CXCR3 reported in the public domain. Interestingly, though, in the patent literature it has been claimed that certain aminoquinoline compounds, having the general structure shown in Figure 3, are effective in treating inflammatory and immuno diseases through their binding to CXCR3 receptors.²⁸ Also, a screen on natural binders turned up a dipyridinium salt (Figure 3, $IC_{50}=690$ nM) as a CXCR3-binding hit.²⁹ Both ligand classes bear some hallmarks of bivalent character, but neither study explicitly discusses receptor dimers as the targets. We were interested in studying whether bivalent analogues of known CXCR3 antagonists could increase the affinity for CXCR3 through a putative CXCR3 homodimer. Toward this end, some bivalent ligands derived from the validated CXCR3-pharmacophores of **3a** (VUF10085 / AMG 487), **3b** and **4**^{30,31} (Figure 4) were designed and tested for their affinity and activity towards CXCR3.

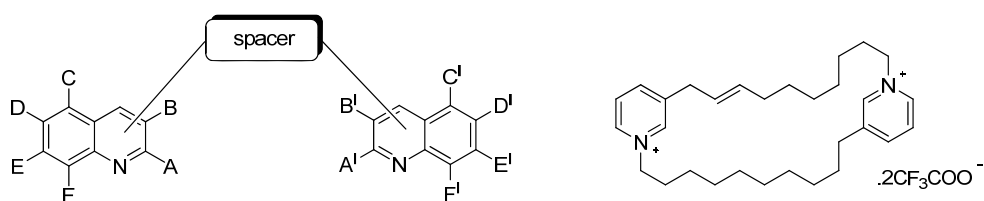


Figure 3. (Left) General structure of aminoquinoline compounds as reported by Lin.²⁸ (Right) A natural product found on a screen on CXCR3.²⁹

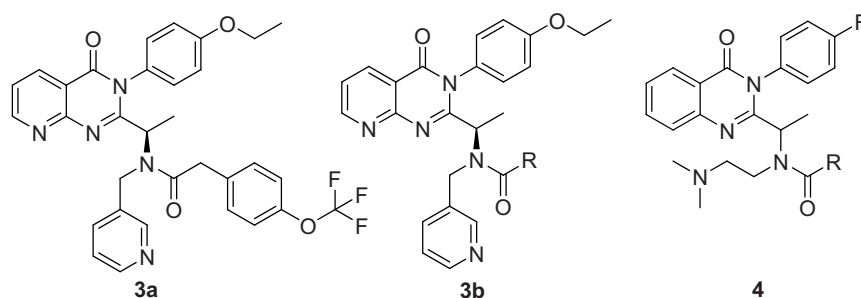


Figure 4. Structures of the reference compounds **3a-b** and **4**. R= nonyl

Chemistry

Synthetic pathways for compounds **3a-b** and **4** have been previously described^{30,31}. As depicted in Scheme 1 and 2, final compounds **1a-c** were obtained via alkylation of intermediates **5**^{30,31} and **6**³¹ with decanedioyl and dodecanedioyl dichloride, respectively. Incomplete conversion in the case of **1a-b** yielded **2a-b** in the same reaction and these compounds were also isolated. As outlined in Chapter 4, the used building blocks (e.g. **5**) were racemic and this will hold true for the final compounds in this chapter as well.

Pharmacology

The affinity for the human CXCR3 of all compounds was determined by displacement of [¹²⁵I]CXCL10 binding to membranes from HEK-293 cells stably expressing the human CXCR3 receptor. Functional activity was inspected by recording the effect of compounds on CXCL11-induced phospholipase C (PLC) activity. This was determined by measuring the production of [³H]-inositol phosphates ([³H]-IPx) in COS-7-CXCR3 cells.

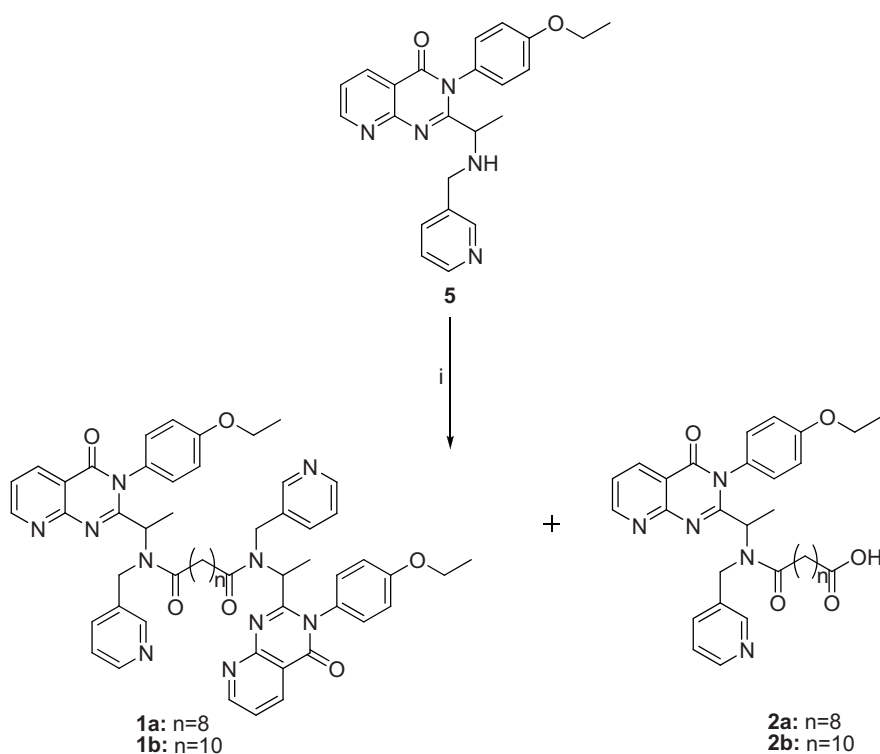
Results and discussion

In this study, the bivalent ligand approach was used in order to investigate the behavior of bivalent molecules at CXCR3 and to probe putative CXCR3 dimers. The pharmacophores of previously reported CXCR3 antagonists (**3a-b** and **4**) were selected as monomeric units on the basis of their affinities and antagonistic activities at human CXCR3 receptor.^{27,28}

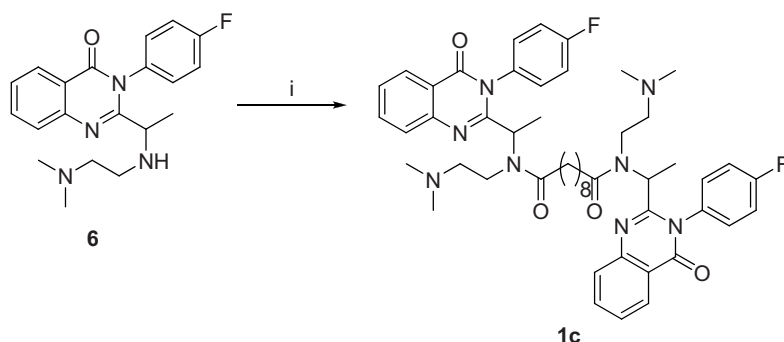
Bivalent ligands were designed as duplication of the aforementioned ligands by linking the two monomeric units with a spacer length of eight (**1a**, **1c**) or ten (**1b**) methylene

chains. The linkage of choice is an amide bond as this was already present in the parent compounds. Also, an alkyl spacer was selected because of its presence in reference compounds **3b** and **4**. The monomeric carboxylic products **2a** and **2b** were also tested for affinity and activities at human CXCR3. They function as important references to correct for any non-specific affinity effects induced by e.g. addition of extra bulk or hydrophobicity.

Scheme 1. Synthetic Pathway for compounds **1a-b** and **2a-b**



Reagents and conditions. (i) Decanedioyl dichloride (**a**-series, n=8) or dodecanedioyl dichloride (**b**-series, n=10), Et₃N, dioxane, rt, overnight.

Scheme 2. Synthetic Pathway for compound **1c**

Reagents and conditions. (i) Decanedioyl dichloride, Et₃N, dioxane, rt, overnight.

Table 1. pK_i and pIC₅₀ values for hCXCR3 of the compounds **1a-c**, **2a-b** and **3a-b** as determined by the displacement of [¹²⁵I]CXCL10 binding and by the inhibition of CXCL11-induced [³H]-IPx accumulation, respectively.

compound	pK _i ^a ([¹²⁵ I]CXCL10)	pIC ₅₀ ^b
1a (VUF10091)	5.86 ± 0.10	6.04 ± 0.07
1b (VUF10089)	5.71 ± 0.05	6.83 ± 0.09
1c (VUF10143)	5.15 ± 0.13	5.17 ^d
2a (VUF10092)	5.15 ± 0.18	4.92 ± 0.09
2b (VUF10090)	5.71 ± 0.13	5.61 ± 0.05
3a	7.46 ± 0.10	7.36 ± 0.02
3b	6.47 ± 0.09 ^c	nt ^e

^a The binding experiments were carried out on cell membranes fractions from HEK-293 cells stably expressing the human CXCR3 receptor. The compounds were tested for their ability to displace [¹²⁵I]CXCL10 binding. The values are represented as the mean ± S.E.M of at least three independent experiments.

^b Experiments were performed on COS-7 cells transfected with cDNA encoding human CXCR3 and Gα_{q15}. The compounds were tested for their ability to inhibit [³H]-IPx accumulation. Cells were stimulated with 10 nM CXCL11. The values are represented as the mean ± S.E.M of at least two independent experiments.

^c Data published.³⁰

^d Tested only one time.

^e Not tested.

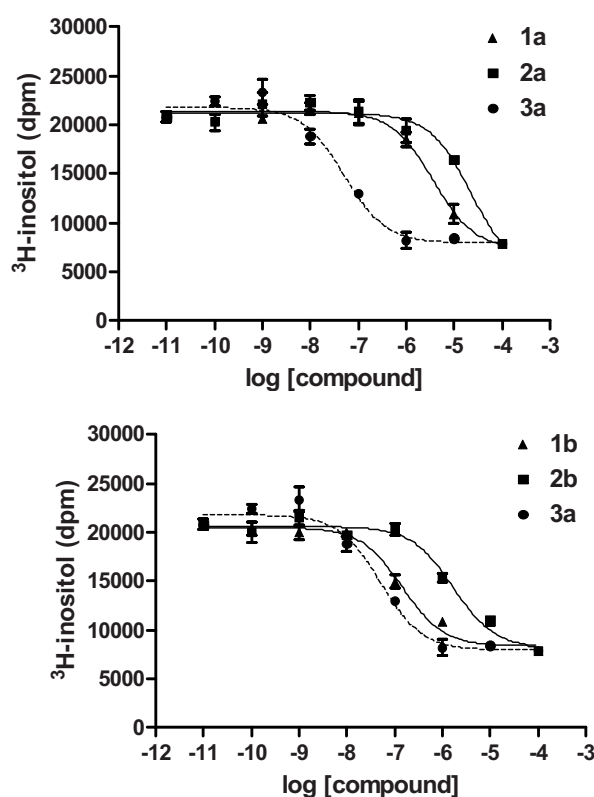


Figure 5. Effect of compounds **1a-b**, **2a-b** and **3a** on CXCR3-mediated PLC activity by CXCL11. PLC activity was measured by the production of [^3H]IPx from radioactively labeled inositol in COS-7-CXCR3.

Reference compounds **3a-b**, in accord to previous published data,^{30,31} showed the highest affinity values for CXCR3 (pK_i **3a** = 7.46 ± 0.10 , pK_i **3b** = 6.47 ± 0.09). In comparison to the reference compounds **3a** and **3b**, their bivalent analogues **1a-b** exhibit a decreased affinity and antagonistic activity at the human CXCR3 receptor (Table 1). Indeed, the bivalent analogues with eight (**1a**) or ten (**1b**) methylene units in the spacer display a dramatic decrease in affinities when compared to **3a**, and four (**1a**) and six (**1b**) times lower affinities when compared to **3b**. Compound **1a** is the best bivalent analogue in this small series, showing a pK_i value of 5.86.

The bivalent analogue of compound **4** (i.e. **1c**) showed a decrease in affinity confirming the importance of the 3*H*-pyrido[2,3-*d*]pyrimidin-4-one scaffold properly substituted with e.g. pyridin-3-ylmethyl and *p*-ethoxy-phenyl moieties for the affinity at CXCR3 (**4**: IC_{50} = 3.2 μM , see Chapter 3).

The monomeric carboxylic acid analogues (**2a-b**) of compounds **1a** and **1b** were also tested. Unexpectedly, **2b** has an affinity value equal to that of its bivalent analogue **1b**, whereas **2a** has a lower affinity compared to **1a**. This means that **1b** may display non-

specific binding effects resulting from e.g. addition of extra hydrophobic bulk by the spacer.

In order to inspect functional activity, the effect of compounds **1a-c**, **2a-b** and **3a** on CXCL11-induced PLC activity was determined (see Figure 5 for exemplary curves). All compounds showed the ability to inhibit the [³H]IPx accumulation. However, none of them was superior to **3a** ($pIC_{50} = 7.36 \pm 0.02$). Among the new compounds in the series, the best CXCR3 antagonistic activity is shown by the dimeric analogues (**1a-b**) especially when compared to their respective carboxylic monomeric analogues (**2a-b**). In fact, compounds **2a** and **2b** are more than ten times less potent than the bivalent counterparts (**1a**, **1b**). The decyl-bivalent ligand (**1b**) showed the best activity, four times lower than reference compound **3a** but six times higher than its analogue with an eight-methylene spacer (**1a**).

In general, most tested antagonists inhibited CXCL11-induced receptor activation with pIC_{50} values that qualitatively correlated with the measured affinity at CXCR3 (CXCL10). However, an apparent discrepancy in this trend can be observed when inspecting the affinity and activity of **1b** (e.g. in contrast to **1a**). The relevance of this is currently unclear.

Conclusions

In this first study on bivalent ligands for CXCR3, we identified two bivalent molecules (**1a-b**) displaying micromolar affinity and antagonistic activity towards the CXCR3 receptor. The discussed bivalent ligands may be used as tools for further investigations into possible CXCR3 dimers.

Experimental section

General

The solvents were dried according to standard procedures. All reactions were performed under an atmosphere of dry nitrogen. ¹H NMR spectra were recorded on a Bruker AC-200 (200 MHz) spectrometer. Flash column chromatography was carried out on J. T. Baker silica gel was used for flash chromatography. HPLC-MS analyses were conducted using a Shimadzu LC-8A preparative liquid chromatograph pump system with a Shimadzu SPD-10AV UV-Vis detector set at 254 nm, with the MS detection performed with a Shimadzu LCMS-2010 liquid chromatograph mass spectrometer. Conditions: Xbridge (C18) 5 μm column (100mm x 4.9 mm) with solvent A: 10% buffer pH 8- 90% H₂O; solvent B: 10%

aqueous buffer pH 8 - 90% acetonitrile (30% of B in A). The buffer pH 8 is prepared with ammonium bicarbonate in H₂O (0.4 % w/v) adjusted to pH=8 with ammonium hydroxide. The total run time was 20 min. The synthesis of intermediates **5** and **6** has been described elsewhere^{30,31}.

N¹,N¹⁰-bis(1-(3-(4-ethoxyphenyl)-4-oxo-3,4-dihydropyrido[2,3-d]pyrimidin-2-yl)ethyl)-N¹,N¹⁰-bis(pyridin-3-ylmethyl)decanediamide (1a) and **10-((1-(3-(4-ethoxyphenyl)-4-oxo-3,4-dihydropyrido[2,3-d]pyrimidin-2-yl)ethyl)(pyridin-3-ylmethyl)amino)-10-oxodecanoic acid (2a)**

To a solution of compound **5** (0.12 g, 0.30 mmol) in 1,4-dioxane (20 mL), triethylamine (0.04 mL, 0.30 mmol) was added. After 30 min, decanedioyl dichloride (0.03 mL, 0.15 mmol) was added. The solution was stirred overnight. HPLC-MS analysis on the crude material revealed two compounds corresponding to **1a** (*t_R* = min 7.40) and **2a** (*t_R* = min, 4.53) which were isolated by flash column chromatography with butanol/acetic acid/water (14:5:1). This afforded **1a** (0.03 g, 21%) and **2a** (0.02 g, 23%) as pale yellow oils.

1a: ¹H NMR (CDCl₃) δ: 0.82-1.57 (m, 12H), 1.57-1.98 (m, 8H), 2.05-2.44 (m, 2H), 3.92-4.31 (m, 4.02H), 4.83-2.29 (m, 3.8H), 6.51-7.19 (m, 9H), 7.30-7.68 (m, 5H), 8.16-8.51 (m, 6H), 8.88-8.97 (m, 2H) Peak splitting due to the presence of rotamers was observed. M/z = 485.5 [M+2/2]²⁺

2a: ¹H NMR (CDCl₃) δ: 0.87-1.21 (m, 21H), 2.12-2.36 (m, 4H), 4.06-4.41 (m, 2H), 5.03-5.34 (m, 2H), 7.01-7.24 (m, 3H), 7.46-7.71 (m, 4H), 8.22-8.58 (m, 3H), 8.96-9.01 (m, 1H). Peak splitting due to the presence of rotamers was observed. M/z = 586.2 [M+1]⁺.

N¹,N¹²-bis(1-(3-(4-ethoxyphenyl)-4-oxo-3,4-dihydropyrido[2,3-d]pyrimidin-2-yl)ethyl)-N¹,N¹²-bis(pyridin-3-ylmethyl)dodecanediamide (1b) and **12-((1-(3-(4-ethoxyphenyl)-4-oxo-3,4-dihydropyrido[2,3-d]pyrimidin-2-yl)ethyl)(pyridin-3-ylmethyl)amino)-12-oxododecanoic acid (2b)**

To a solution of compound **5** (0.36 g, 0.91 mmol) in 1,4-dioxane (20 mL), triethylamine (0.13 mL, 0.91 mmol) was added. After 30 min, dodecanedioyl dichloride (0.11 mL, 0.46 mmol) was added. The solution was stirred overnight. HPLC-MS analysis on the crude material revealed two compounds corresponding to **1b** (*t_R* = min 10.38) and **2b** (*t_R* = min 7.53) which were isolated by flash column chromatography with butanol/acetic acid/water (14:5:1). This afforded **1b** (0.01 g, 24%) and **2b** (0.04 g, 14%) as pale yellow oils.

1b: ¹H NMR (CDCl₃) δ: 0.82-1.63 (m, 30 H), 1.98-2.19 (m, 2H), 2.18-2.42 (m, 2H), 3.91-4.41 (m, 3.7H), 4.72- 5.11 (m, 4.3H) 6.50-7.22 (m, 8H), 7.40-7.71 (m, 6H), 8.12-

8.60 (m, 6H), 8.90-9.11 (m, 2H). Peak splitting due to the presence of rotamers was observed. $M/z = 499.5 [M+2/2]^{2+}$.

2b: ^1H NMR (CDCl_3) δ : 0.88-1.25 (m, 25H), 2.14-2.35 (m, 4H), 4.05-4.41 (m, 2.2H), 5.01-5.36 (m, 1.8H), 7.02-7.24 (m, 3H), 7.45-7.68 (m, 4H), 8.27-8.61 (m, 3H), 8.98-9.01 (m, 1H). Peak splitting due to the presence of rotamers was observed. $M/z = 614.3 [M+1]^+$

$\text{N}^1, \text{N}^{10}$ -bis(2-(dimethylamino)ethyl)- $\text{N}^1, \text{N}^{10}$ -bis(1-(3-(4-fluorophenyl)-4-oxo-3,4-dihydroquinazolin-2-yl)ethyl)decanediamide (1c)

Compound **6** (0.35 g, 1 mmol) and triethylamine (0.14 mL, 1 mmol) were dissolved in 1,4-dioxane (10 mL). After 30 min, decanedioyl dichloride (0.10 mL, 0.5 mmol) was added and the solution was stirred overnight. The residue was dissolved in dichloromethane (30 mL) and washed with saturated aqueous Na_2CO_3 solution (30 mL), then twice with water (50 mL). The organic phases were dried over anhydrous Na_2SO_4 , filtered and evaporated. The crude material was purified by flash chromatography on silica gel eluting with ethyl acetate/methanol (9:1) to afford the desired compound (0.09 g, 21%) as white solid. ^1H NMR (CDCl_3) δ : 0.88-1.70 (m, 22H), 1.91-2.64 (m, 16H), 3.21-3.59 (m, 4H), 4.73 (q, 0.6H), 5.21 (q, 1.4H), 6.99-7.81 (m, 14.5H), 7.89-8.31 (m, 1.5H). Peak splitting due to the presence of rotamers was observed.

Pharmacology

Radioligand binding assay

HEK293-CXCR3 cells were grown at 5% CO_2 at 37°C in Dulbecco's modified Eagle's medium supplemented with 10% fetal bovine serum, 250 mg/mL G-418, 50 IU of penicillin per mL, and 50 mg of streptomycin per mL. These cells were seeded in poly-L-Lysine-coated 48-well plates. After 24h, binding was performed on whole cells for 4h at 4°C using approximately 70 pM [^{125}I]-labelled CXCL10 (Perkin Elmer Life Science, Boston, USA) in binding buffer (50 mM HEPES [pH 7.4], 1 mM CaCl_2 , 5 mM MgCl_2 , 0.5% BSA) containing increasing concentrations of the indicated compounds. After incubation, cells were washed three times with ice-cold binding buffer supplemented with 0.5 M NaCl. Subsequently, cells were lysed and counted in a Wallac Compugamma counter.

[³H]Inositol phosphate production

COS-7 cells were transfected with CXCR3 and G_{q15} chimeric protein.³² 24 h after transfection cells were labeled overnight in inositol free medium (modified Eagle's medium with Earle's salts) supplemented with 2 mM L-glutamine, L-cysteine, L-leucine, L-methionine, L-arginine, glucose, 0.2% bovine serum albumin, and 2 μCi/mL *myo*-[2-³H]inositol (Amersham Pharmacia Biotech, Roosendaal, The Netherlands). Subsequently, the labeling medium was aspirated, cells were washed for 10 min with Dulbecco's modified Eagle's medium containing 25 mM HEPES (pH 7.4) and 20 mM LiCl. Cells were preincubated for 10 minutes with/or without the indicated compounds and incubated for 2 h in the same medium in the absence or presence of 10 nM CXCL11 or 30 nM CXCL10. The incubation was stopped by aspiration of the medium and addition of cold 10 mM formic acid. After 90 min of incubation on ice, inositol phosphates were isolated by anion exchange chromatography (Dowex AG1-X8 columns, Bio-Rad) and counted by liquid scintillation.

References

- (1) Marinissen, M.J.; Gutkind, J.S. G-protein-coupled receptors and signaling networks: emerging paradigms. *Trends. Pharmacol. Sci.*, **2001**, *22*, 368-376.
- (2) Zawarynski, P.; Tallerico, T.; Seeman, P.; Lee, S.P.; O'Dowd, B.F.; George, S.R. Dopamine D2 receptor dimers in human and rat brain. *FEBS Lett.*, **1998**, *441*, 383-386.
- (3) Milligan, G. G protein-coupled receptor dimerization: function and ligand pharmacology. *Mol. Pharmacol.*, **2004**, *66*, 1-7.
- (4) Milligan, G. G protein-coupled receptor dimerisation: molecular basis and relevance to function. *Biochim. Biophys. Acta*, **2007**, *1768*, 825-835.
- (5) Rodríguez-Frade, J.M.; Vila-Coro, A.J.; de Ana, A.M.; Albar, J.P.; Martínez, A.C.; Mellado, M. The chemokine monocyte chemoattractant protein-1 induces functional responses through dimerization of its receptor CCR2. *Proc. Natl. Acad. Sci. USA*, **1999**, *96*, 3628-3633.
- (6) Jordan, B.A.; Trapaidze, N.; Gomes, I.; Nivarthi, R.; Devi, L.A. Oligomerization of opioid receptors with beta 2-adrenergic receptors: a role in trafficking and mitogen-activated protein kinase activation. *Proc. Natl. Acad. Sci. USA*, **2001**, *98*, 343.
- (7) Nimchinsky, E.A.; Hof, P.R.; Janssen, W.G.; Morrison, J.H.; Schmauss, C. Expression of dopamine D3 receptor dimers and tetramers in brain and in transfected cells. *J. Biol. Chem.*, **1997**, *272*, 29229-29237.
- (8) Mercier, J.F.; Salahpour, A.; Angers, S.; Breit, A.; Bouvier, M. Quantitative assessment of beta 1- and beta 2-adrenergic receptor homo- and heterodimerization by bioluminescence resonance energy transfer. *J. Biol. Chem.*, **2002**, *277*, 44925-44931.
- (9) Angers, S.; Salahpour, A.; Joly, E.; Hilairret, S.; Chelsky, D, Dennis.; M, Bouvier, M. Detection of beta 2-adrenergic receptor dimerization in living cells using bioluminescence resonance energy transfer (BRET). *Proc. Natl. Acad. Sci USA*, **2000**, *97*, 3684-3689.
- (10) Cornea, A.; Janovick, J.A.; Maya-Núñez, G.; Conn, P.M. Gonadotropin-releasing hormone receptor microaggregation. Rate monitored by fluorescence resonance energy transfer. *J. Biol. Chem.*, **2001**, *276*, 2153-2158.
- (11) Patel, R.C.; Kumar, U.; Lamb, D.C.; Eid, J.S.; Rocheville, M.; Grant, M.; Rani, A.; Hazlett, T.; Patel, S.C.; Gratton, E.; Patel, Y.C. Ligand binding to somatostatin receptors induces receptor-specific oligomer formation in live cells. *Proc. Natl. Acad. Sci. USA*, **2002**, *99*, 3294-3299.
- (12) Fotiadis, D.; Liang, Y.; Filipek, S.; Saperstein, D.A.; Engel, A.; Palczewski, K. Atomic-force microscopy: Rhodopsin dimers in native disc membranes. *Nature*, **2003**, *421*, 127-128.
- (13) Whorton, M.R.; Bokoch, M.P.; Rasmussen, S.G.; Huang, B.; Zare, R.N.; Kobilka, B.; Sunahara, R.K. A monomeric G protein-coupled receptor isolated in a high-density lipoprotein particle efficiently activates its G protein. *Proc. Natl. Acad. Sci. USA*, **2007**, *104*, 7682-7687.
- (14) Milligan, G.; Kostenis, E. Heterotrimeric G-proteins: a short history. *Br. J. Pharmacol.*, **2006**, *147* (Suppl 1): S46-S55.
- (15) Portoghese, P.S.; Ronsisvalle, G.; Larson, D.L.; Yim, C.B.; Sayre, L.M.; Takemori, A.E. Opioid agonist and antagonist bivalent ligands as receptor probes. *Life. Sci.*, **1982**, *31*, 1283-1286.
- (16) Filizola M. Increasingly accurate dynamic molecular models of G-protein coupled receptor oligomers: Panacea or Pandora's box for novel drug discovery?, *Life Sci.*, **2009**, doi:10.1016/j.lfs.2009.05.004
- (17) Erez, M.; Takemori, A.E.; Portoghese, P.S. Narcotic antagonistic potency of bivalent ligands which contain beta-naltrexamine. Evidence for bridging between proximal recognition sites. *J. Med. Chem.*, **1982**, *7*, 847-849.

- (18) Bruysters, M.; Pertz, H.H.; Teunissen, A.; Bakker, R.A.; Gillard, M.; Chatelain, P.; Schunack, W.; Timmerman, H.; Leurs, R. Mutational analysis of the histamine H1-receptor binding pocket of histaprodifens. *Eur. J. Pharmacol.*, **2004**, *487*, 55-63.
- (19) Portoghese, P.S.; Larson, D.L.; Sayre, L.M.; Yim, C.B.; Ronsisvalle, G.; Tam, S.W.; Takemori, A.E. Opioid agonist and antagonist bivalent ligands. The relationship between spacer length and selectivity at multiple opioid receptors. *J. Med. Chem.*, **1986**, *10*, 1855-1861.
- (20) Portoghese, P.S. Bivalent ligands and the message-address concept in the design of selective opioid receptor antagonists. *Trends Pharmacol. Sci.*, **1989**, *6*, 230-235.
- (21) Lalchandani, S.G.; Lei, L.; Zheng, W.; Suni, M.M.; Moore, B.M.; Liggett S.B.; Miller D.D.; Feller D.R. Yohimbine dimers exhibiting selectivity for the human alpha 2C-adrenoceptor subtype. *J. Pharmacol. Exp. Ther.*, **2002**, *303*, 979-984.
- (22) Neumeyer, J.L.; Zhang, A.; Xiong, W.; Gu, X.H.; Hilbert, J.E.; Knapp, B.I.; Negus, S.S.; Mello, N.K.; Bidlack, J.M. Design and synthesis of novel dimeric morphinan ligands for kappa and micro opioid receptors. *J. Med. Chem.*, **2003**, *46*, 5162-5170.
- (23) Larraya, C.; Guillard, J.; Renard, P.; Audinot, V.; Boutin, J.A.; Delagrangue, P.; Bennejean, C.; Viaud-Massuard, M.C. Preparation of 4-azaindole and 7-azaindole dimers with a bisalkoxyalkyl spacer in order to preferentially target melatonin MT1 receptors over melatonin MT2 receptors. *Eur. J. Med. Chem.*, **2004**, *39*, 515-526.
- (24) Mellado, M.; Rodriguez-Frade, J.M.; Vila-Coro, A.J.; Fernandez, S.; Martin de Ana, A.; Jones, D.R.. Chemokine receptor homo- or heterodimerization activates distinct signaling pathways. *Embo J.*, **2001**, *20*, 2497-2507.
- (25) Huttenrauch, F.; Nitzki, A.; Lin, F.T.; Honing, S.; Oppermann, M. Beta-arrestin binding to CC chemokine receptor 5 requires multiple C-terminal receptor phosphorylation sites and involves a conserved Asp-Arg-Tyr sequence motif. *J. Biol. Chem.*, **2002**, *277*, 30769-30777.
- (26) Issafras, H.; Angers, S.; Bulenger, S.; Blanpain, C.; Parmentier, M.; Labbe-Jullie, C. Constitutive agonist-independent CCR5 oligomerization and antibody-mediated clustering occurring at physiological levels of receptors. *J. Biol. Chem.*, **2002**, *277*, 34666-34673.
- (27) Babcock, G.J.; Farzan, M.; Sodroski, J. Ligand-independent dimerization of CXCR4, a principal HIV-1 coreceptor. *J. Biol. Chem.*, **2003**, *278*, 3378-3385.
- (28) Lin, C.; Liu, J.; Chang, C.; Chen, S.; Xiang, Y.; Cheng, P. Aminoquinoline compounds WO2004091485, **2004**.
- (29) Ondeyka, J.G.; Herath, K.B.; Jayasuriya, H.; Polishook, J.D.; Bills, G.F.; Dombrowski, A.W.; Mojena, M.; Koch, G.; Di Salvo, J.; De Martino, J.; Guan, Z.; Nanakorn, W.; Morenberg, C.M.; Balick, M.J.; Stevenson, D.W.; Slattery, M.; Borris, R.P.; Singh, S.B. Discovery of structurally diverse natural product antagonists of chemokine receptor CXCR3. *Mol. Diversity*, **2005**, *9*, 123-129.
- (30) Storelli, S.; Verzijl, D.; Al-Badie, J.; Elders, N.; Bosch, L.; Timmerman, H.; Smit, M.J. De Esch, I.J.P.; Leurs, R. Synthesis and structure-activity relationships of 3H-quinazolin-4-ones and 3H-pyrido[2,3-d]pyrimidin-4-ones as CXCR3 receptor antagonists. *Arch. Pharm. (Weinheim)*, **2007**, *340*, 281-291.
- (31) Storelli, S.; Verdijk, P.; Verzijl, D.; Timmerman, H.; van de Stolpe, A.C.; Tensen, C.P.; Smit, M.J.; De Esch, I.J.P.; Leurs, R. Synthesis and structure-activity relationship of 3-phenyl-3H-quinazolin-4-one derivatives as CXCR3 chemokine receptor antagonists. *Bioorg. Med. Chem. Lett.*, **2005**, *15*, 2910-2913.
- (32) Coward, P., Chan, S.D., Wada, H.G., Humphries, G.M., Conklin, B.R. Chimeric G proteins allow a high-throughput signaling assay of Gi-coupled receptors. *Anal. Biochem.*, **1999**, *270*, 242-248.

Summary

Design, synthesis and pharmacological evaluation of non-peptidergic ligands for the human CXCR3 receptor

The CXCR3 receptor belongs to the class of chemokine receptors, themselves the endogenous receptors for chemokine proteins and part of the superfamily of G protein-coupled receptors (GPCRs). CXCR3 is thought to be involved in various diseases. Based on expression studies or knock-out models, CXCR3 has been shown to play a role in many inflammatory conditions, such as multiple sclerosis, rheumatoid arthritis and psoriasis. Much attention was also devoted to CXCR3 as a key factor in the rejection of donor organs after transplantation, although some controversy has emerged here in the last few years. Furthermore, CXCR3 appears to be involved in metastasis of melanoma and colon cancer cells to the lymph nodes and in metastasis of breast cancer cells to the lung. All this has led to CXCR3 being recognized as an interesting pharmacological target with potential therapeutic relevance. Toward this end, CXCR3 antagonists are believed to represent a means to capitalize on this therapeutic promise.

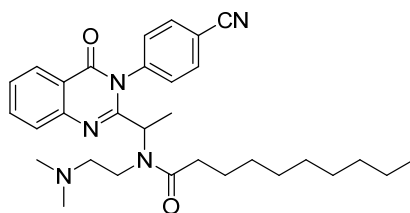
The goal of the research described in this thesis was the development of various types of CXCR3 antagonists and the identification of structural requirements for antagonism at the human CXCR3 receptor. The thesis focuses on the design, synthesis and pharmacological evaluation of small non-peptidergic ligands for CXCR3.

A review on small non-peptidergic CXCR3 ligands is presented in Chapter 1, in which the status concerning the medicinal chemistry on CXCR3 is described. It is shown how publications on CXCR3 antagonists did not start to emerge until ~2006. The current set of CXCR3 antagonist classes display high chemical variability. However, only one compound (AMG 487) is known to have progressed to Phase II clinical trials where it showed a lack of efficacy, probably due to pharmacokinetic problems.

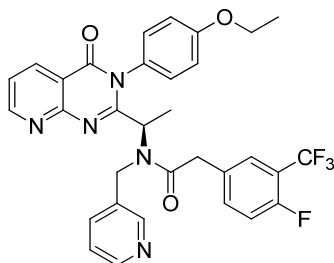
The aim of the thesis is described in Chapter 2. The synthesis and pharmacological evaluation of novel ligands for CXCR3 can provide key information for better understanding the molecular features necessary for affinity and activity on CXCR3. This in turn will lead to a better understanding of ligand-receptor interactions and therefore to

Summary

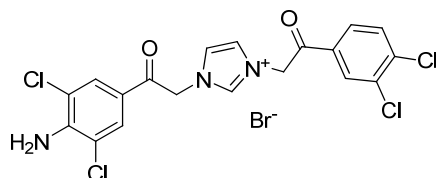
new insights and ideas for the generation of novel classes of CXCR3 ligands. This overall goal was pursued using medicinal chemistry approaches initiated from various angles. These are addressed in the different chapters.



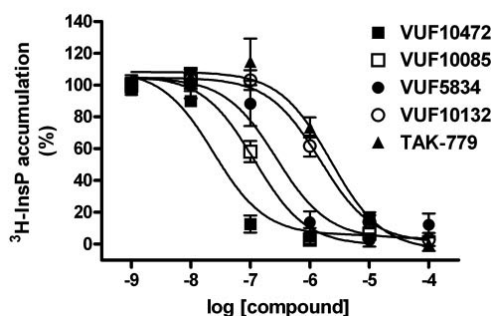
In Chapter 3, the synthesis and structure-activity relationships of a series of 3-phenyl-3*H*-quinazolin-4-one derivatives are described. In this work, a compound reported in a patent was selected and SAR explorations involved removing the decanoyl chain and inspecting different 4-phenyl ring substituents. This approach enabled the identification of a compound (VUF 5834) which showed submicromolar affinity for CXCR3. Moreover, this compound effectively inhibits CXCR3-mediated IP₃ production and calcium mobilization in cells expressing the human CXCR3. It also abrogates CXCR3-mediated actin polymerization and chemotaxis of human T cells. Therefore, it represents a valuable tool for future lead optimization programs.



Deeper inspection of the active ligand described in Chapter 3 (VUF 5834) was pursued. Chapter 4 provides a detailed SAR-study of the 3*H*-quinazolin-4-one and 3*H*-pyrido[2,3-*d*]pyrimidin-4-one series of CXCR3 antagonists, which allows linking VUF 5834 to the known AMG 487 antagonist. These studies revealed the importance of the (4-fluoro-3-(trifluoromethyl)phenyl)acetyl and the 3-methylene-pyridine moieties in achieving high affinity. The superior affinities of AMG 487 and NBI-74330 were confirmed to be in the nanomolar range, therefore reinstating these compounds as valuable tools for targeting CXCR3 in various therapeutic areas.

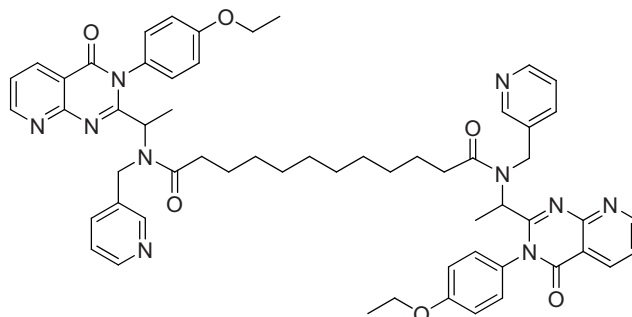


Chapter 5 presents the results of a search for novel scaffolds using a pharmacophore model. Based on this model, the *in-house* database was screened. Unfortunately this approach did not identify any compound with encouraging affinity. However, a close inspection of the compounds possessing some affinity allowed the identification of the imidazole core as a common feature. The similarity of these imidazole compounds to some imidazolium derivatives from a patent application by Smithkline Beecham was observed. Based on this, the two compound classes were merged which led to a series of new imidazolium derivatives with CXCR3 affinity. The best compound of this series showed a submicromolar affinity for CXCR3 and bore an interesting dichloroaniline-unit.



The molecular mechanism of action of diverse small molecule antagonists at the CXCR3 receptor is addressed in Chapter 6. Five different non-peptidergic molecules, belonging to three different chemical classes including the ones described in Chapters 3-5, were used. The ligands were tested at rat and mouse CXCR3 as well as at CXCR3 from rhesus macaque. Except for TAK-779, all compounds display slightly lower affinity for rodent CXCR3 than for primate CXCR3. Additionally, the molecular mechanism of action of the various antagonists at the human CXCR3 receptor has been characterized, revealing that all tested compounds act as noncompetitive antagonists at CXCR3. Moreover, all compounds except one (TAK-779) showed inverse agonistic properties at a constitutively active mutant of CXCR3. This suggests a different mode of interaction at CXCR3 for some classes of compounds.

Summary



Chapter 7 deals with the first studies on “bivalent ligands” for CXCR3. This approach is based on linking two CXCR3 pharmacophores with the goal of targeting putative CXCR3 dimers. This has the potential to afford more efficacious and selective ligands. Using the 3*H*-quinazolin-4-one and 3*H*-pyrido[2,3-*d*]pyrimidin-4-one scaffolds described in Chapters 3 and 4, bivalent counterparts with amido-alkyl spacers were synthesized. This resulted in two bivalent molecules displaying micromolar affinity and antagonistic activity toward the CXCR3 receptor. The compounds in this chapter can be used as tools for further investigations into possible CXCR3 dimers.

Taken together, this thesis describes the design and synthesis of small non-peptidergic ligands for CXCR3 by means of several conceptually different approaches, such as lead optimization, library screening, molecular design techniques and the use of ‘bivalent ligands’. The obtained ligands have provided more insights in the structural requirements that are important for binding and functional activity at CXCR3. Ultimately this knowledge will be helpful to develop compounds with an improved activity and selectivity profile at CXCR3.

Samenvatting

Ontwerp, synthese en farmacologische evaluatie van non-peptiderge liganden voor de menselijke CXCR3 receptor

De CXCR3 receptor behoort tot de klasse van chemokine receptoren. Deze fungeren als de endogene receptoren voor chemokine signaaleiwitten en maken deel uit van de superfamilie van G eiwit-gekoppelde receptoren (GPCRs). CXCR3 lijkt bij verscheidene ziektes betrokken te zijn. Op basis van expressiestudies en/of knock-out modellen is bijvoorbeeld aangetoond dat CXCR3 een rol speelt bij vele ontstekingsgerelateerde aandoeningen zoals multiple sclerose, rheumatoïde artritis and psoriasis. Ook heeft CXCR3 de aandacht getrokken door een mogelijke sleutelrol in de afstoting van donororganen door het lichaam. CXCR3 lijkt ook betrokken te zijn bij de metastase van huid- en darm-kankercellen naar de lymfeknopen en bij de metastase van borstkankercellen naar de longen. Dit heeft alles heeft ertoe geleid dat CXCR3 inmiddels wordt gezien als een farmacologisch interessant eiwit met duidelijke therapeutische relevantie. De ontwikkeling van CXCR3 blokkers (antagonisten) is één van de manieren om deze relevantie verder te bestuderen en hopelijk waar te maken.

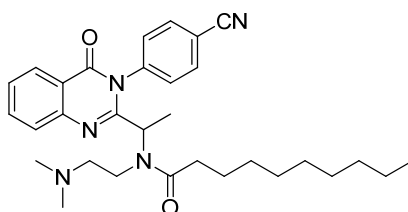
Het doel van het onderzoek dat beschreven staat in dit proefschrift is de ontwikkeling van verscheidene klassen van CXCR3 antagonisten en het identificeren van de moleculaire elementen die vereist zijn voor antagonisme op CXCR3. Het werk in dit proefschrift is in het bijzonder toegespitst op het ontwerpen, synthetiseren en farmacologisch evalueren van kleine, non-peptiderge liganden voor CXCR3.

Hoofdstuk 1 beschrijft in het algemeen de medicinale chemie op de CXCR3 receptor en verschaft daarbij een overzicht van reeds bestaande non-peptiderge CXCR3 liganden. Het laat zien dat publicaties over CXCR3 liganden pas rond 2006 hun intrede deden. Getoond wordt hoe de reeds bekende klassen een grote variëteit aan chemische structuren aan de dag leggen. Toch is het zo dat, voor zover bekend, pas één verbinding (AMG487) het stadium van klinische studies heeft gehaald. Helaas viel deze verbinding in Fase 2 klinisch onderzoek af door gebrek aan effectiviteit. Men vermoedt dat farmacokinetische problemen hieraan ten grondslag kunnen liggen.

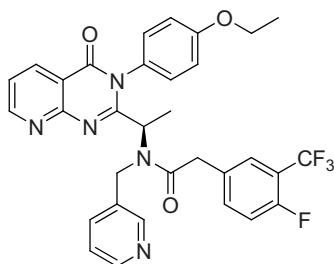
Samenvatting

In Hoofdstuk 2 wordt het doel van dit proefschrift in meer detail beschreven. De beoogde synthese en farmacologische evaluatie van nieuwe liganden voor de CXCR3 receptor zal belangrijke informatie verschaffen over de moleculaire elementen die benodigd zijn voor affiniteit en activiteit op CXCR3. Dit zal weer leiden tot een beter begrip van de interacties die CXCR3 liganden aangaan met CXCR3 en tot optimaal beargumenteerde voorstellen voor nieuwe klassen van antagonisten.

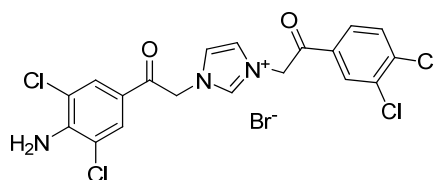
In het proefschrift wordt het algemene doel benaderd vanuit verschillende invalshoeken, zoals te lezen is in de verschillende hoofdstukken.



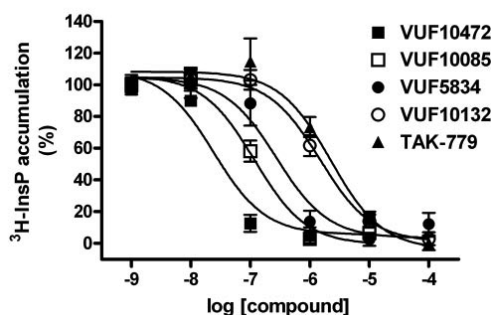
Hoofdstuk 3 behandelt de synthese en structuur-activiteits relaties (SAR) van een serie 3*H*-quinazolin-4-on derivaten. Een 3*H*-quinazolin-4-on dat gerapporteerd was in een octrooi werd gekozen als geschikt uitgangspunt. Vervolgens werden SAR studies uitgevoerd waarin de rollen van de decanoyl groep en phenyl substituenten verder bekeken werden. Deze studies leidden uiteindelijk tot de verbinding VUF5834 die submicromolaire affiniteit vertoont voor CXCR3. De verbinding is ook in staat om effectief CXCR3-geïnduceerde productie van IP₃ alsmede calcium mobilisatie te remmen in cellen die de menselijke CXCR3 receptor tot expressie brengen. Ook bleek dat de stof polymerisatie van actine en de chemotaxis van menselijke T cellen reduceert. Bij beide processen speelt CXCR3 een belangrijke rol. Geconcludeerd kan worden dat VUF5834 een waardevolle lead is voor verdere studies.



Hoofdstuk 4 beschrijft een gedetailleerde SAR studie van twee klassen CXCR3 antagonisten, namelijk die van de 3H-quinazolin-4-onen (e.g. VUF5834, Hoofdstuk 3) en die van de 3H-pyrido[2,3-d]pyrimidin-4-onen (waarvan AMG 487 een voorbeeld is). De SAR resultaten voor beide klassen werden in detail met elkaar vergeleken hetgeen resulteerde in een aantal gemeenschappelijke SAR trends. Zo bleek dat de (4-fluoro-3-(trifluoromethyl)phenyl)acetyl en de 3-methylene-pyridine elementen in beide klassen belangrijk zijn om hoge affiniteit voor CXCR3 te bewerkstelligen. Deze studies bevestigden ook dat AMG 487 en NBI-74330 heel effectieve CXCR3 antagonisten zijn en dat het gebruik van deze twee als sleutelverbindingen in CXCR3 onderzoek dus gerechtvaardigd is.

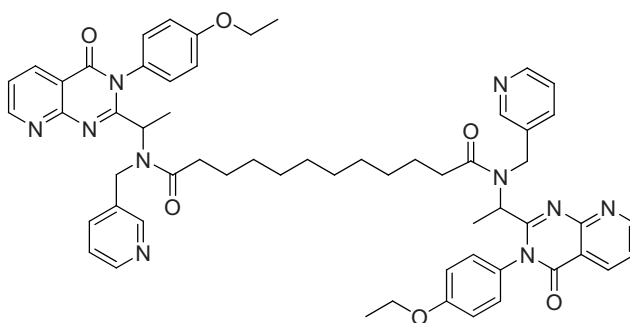


In Hoofdstuk 5 wordt een aanpak beschreven waarbij een farmacofoor model als de basis fungeerde voor het screenen van een in-house database. Helaas leidde dit vooralsnog niet tot nieuwe hits met hoge affiniteit. Wel werd opgemerkt dat veel van de matige hits een imidazool groep als gemeenschappelijk structurelement bezaten en dat deze imidazool overeenkomsten vertoonde met een geotrooieerde klasse antagonisten, namelijk die van imidazolium zouten. Uitgaande van deze interessante overeenkomst werd besloten om de structuren van de gevonden matige hits en die van de geotrooieerde stoffen te combineren tot een nieuw chemotype imidazolium zouten. De beste verbinding uit deze nieuwe klasse bevatte een opmerkelijk dichloroaniline-element en vertoonde submicromolaire affiniteit voor CXCR3.



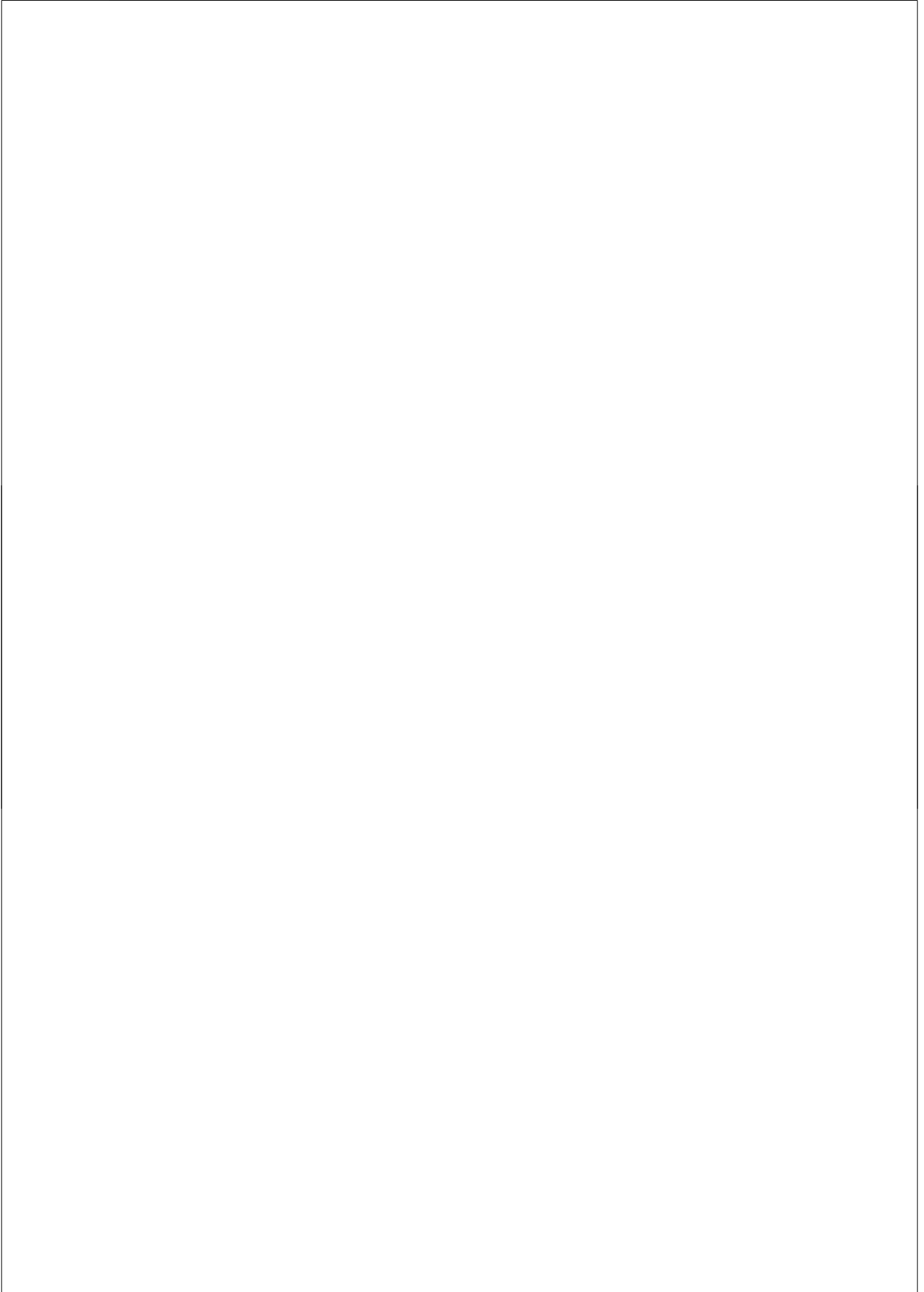
Samenvatting

Het moleculaire werkingsmechanisme van diverse kleine CXCR3 antagonisten wordt behandeld in Hoofdstuk 6. Vijf verschillende non-peptidische liganden uit drie verschillende klassen (inclusief diegene die in Hoofdstukken 3-5 zijn beschreven) zijn hierbij in detail bestudeerd. De liganden werden getest op rCXCR3 en mCXCR3 maar ook op CXCR3 van rhesus macaque. Met uitzondering van TAK-779 vertoonden alle verbindingen een ietwat lagere affiniteit voor CXCR3 van knaagdieren dan voor CXCR3 van primaten. Ook werd het moleculaire werkingsmechanisme van de stoffen op menselijk CXCR3 bekeken. Hieruit volgde dat alle verbindingen fungeren als non-competitieve antagonisten. Ook bleek dat, met uitzondering van TAK-779, de verbindingen zich als inverse agonisten gedroegen op een constitutief actieve CXCR3 mutant. De verkregen resultaten suggereren dat verschillende klassen CXCR3 antagonisten verschillende werkingsmechanismen op CXCR3 kunnen hebben.



Hoofdstuk 7 beschrijft verkennende studies naar het gebruik van "bivalente" liganden voor CXCR3. In deze aanpak worden twee bekende farmacoforen verbonden door een moleculaire linker. Het idee hierachter is dat, als CXCR3 uit dimeren zou bestaan, bivalente liganden efficiënt beide receptoren van zo'n dimeer kunnen binden. In het algemeen kan dit leiden tot efficiëntere en selectievere liganden. Gebaseerd op de 3H-quinazolin-4-on and 3H-pyrido[2,3-d]pyrimidin-4-on chemotypes beschreven in Hoofdstukken 3 en 4 werd een aantal bivalente liganden gemaakt met amido-alkyl linkers. Farmacologische studies lieten zien dat twee van de gemaakte bivalente liganden micromolaire affiniteit voor CXCR3 bezaten en zich als antagonisten gedroegen in een functionele test. Deze twee liganden zijn dan ook geschikt voor vervolgstudies gericht op mogelijke CXCR3 dimeren.

Het gehele proefschrift in ogenschouw nemend kan gezien worden dat het ontwerpen en synthetiseren van non-peptidische CXCR3 liganden is nagestreefd vanuit verschillende invalshoeken. Er is bijvoorbeeld gebruik gemaakt van lead optimalisatie, library screening, moleculaire modellering en bivalente liganden. De verkregen CXCR3 liganden verschaffen nieuwe inzichten in de moleculaire structuurelementen die belangrijk zijn voor binding en activiteit op CXCR3. Deze kennis zal uiteindelijk bijdragen aan de verdere ontwikkeling van liganden voor CXCR3.



Acknowledgments

I would like to express here my sincere thank to all people that have contributed to this work in different ways.

First of all my gratitude goes to my promoters prof. dr. Henk Timmerman and prof. dr. Rob Leurs for being so welcoming and giving me the opportunity to run my PhD project in the Pharmacochimistry Department at Vrije Universiteit in Amsterdam. This experience would not have ever started without prof. dr. Carlo Melchiorre who made the first contact with his "Dutch colleagues" and without the precious advices from Anna Minarini and Vincenzo Tumiatti. I am also grateful to dr. Iwan de Esch for being my co-supervisor, following my work and especially for his suggestions and support in the computational chemistry aspects. I feel deeply indebted to dr. Maikel Wijtmans for the thorough review of the full thesis and for coordinating the many aspects related to the thesis submissions to the reading committee.

Medicinal chemistry is multidisciplinary by definition, therefore many colleagues deserve to be recognized for their contributions and fruitful discussions. Dr. Martine Smith and Dennis Verzijl for their help and support with the pharmacological aspects addressed in this PhD thesis, dr. Franciscus de kanter for special NMR measurements, Mark Verheij and Elwin Jansen for helping with some LCMS measurements and organic chemistry.

The constructive and enjoyable atmosphere I worked in was possible thanks to the many colleagues and students: Marinella, Ruengwit, Janneke, Andrea, Maikel, Nalan, Gardien, Mark, Federico, Jawad, Jaime, Sjef, Sarina, Leontien, Elwin, Cindy, Rogier, Ewald, Atilla, Carlos, Silvina, Dennis, David, Jane, Civianny, Jib and so many others.

My family deserves a mention here for having been really supportive during these years. And of course to all friends and people I have met, with whom I have shared my private life and I will not be able to remember all: Marinella and Calina my *paraninphen* and friends since the beginning of this adventure; then in a random order: Silvia, Desiree, Xheni, Jane, Nicola, Alvise, Cristian, Marinella C., Irene, Wenona, Alois, Sara, Diego, Fetze, Wolf, Elena, Sergio, Marina, Luca, Alessandro, Alberto, Chiara, Mark, Stefano, Gaia, Vittorio, Marilena... Thank you for your friendship!

